MECHANOTRANSDUCTION IN ENGINEERED CARTILAGINOUS TISSUES: IN VITRO OSCILLATORY TENSILE LOADING

A Dissertation
Presented to
The Academic Faculty

By

Eric James Vanderploeg

In Partial Fulfillment
Of the Requirements for the Degree
Doctor of Philosophy in Mechanical Engineering

Georgia Institute of Technology

August 2006

MECHANOTRANSDUCTION IN ENGINEERED CARTILAGINOUS TISSUES: IN VITRO OSCILLATORY TENSILE LOADING

Approved by:

Dr. Marc E. Levenston, Chair
School of Mechanical Engineering
Georgia Institute of Technology

Dr. Andrés J. García
School of Mechanical Engineering
Georgia Institute of Technology

Dr. Michelle C. LaPlaca
Department of Biomedical Engineering
Georgia Institute of Technology

Dr. Robert M. Nerem
School of Mechanical Engineering
Georgia Institute of Technology

Dr. Harish Radhakrishna
Senior Scientist
The Coca-Cola Company

Date Approved: May 2, 2006

TEN·SION (tĕn’shən)

noun. Middle French or Latin.

The act or action of **stretching** or the condition or degree of being stretched to stiffness

Either of two *balancing forces* causing or tending to cause extension

Inner striving, unrest, or imbalance often with physiological indication of emotion

- Merriam-Webster dictionary

ACKNOWLEGEMENTS

Scientific research is a collaborative effort and dissertation research is certainly no exception. In addition to the names that may appear on a publication, those that made direct scientific contributions to a project, there are numerous others who contribute in perhaps less tangible but equally important ways. There are many people falling into each of these categories to whom I am indebted. Without them I would not have been able to reach this point.

First, thank you to Marc Levenston, my thesis advisor throughout my graduate school career. He convinced me that I didn't really want to spend any more time enduring cold Michigan winters and that Georgia Tech was a good place to be – he was right on both counts. He has been incredibly supportive through this process; available when needed, but never stifling. I appreciated his willingness to let me try things that I thought would be interesting as well as his direction when he knew those things were wild goose chases and snipe hunts. Marc has truly fulfilled the role of mentor in every sense of the word.

I also want to thank the members of my dissertation reading committee, Drs. Andrés García, Robert Nerem, Michelle LaPlaca, and Harish Radhakrishna. Each of these people contributed to the success of this project with their scientific input, challenging questions, and moral support. Additionally, none of this work would have been possible without funds for supplies and stipends, and therefore I would like to acknowledge the National Institutes of Health (NIDCR DE014463 and NIAMS AR048253 and AR052861), the National Science Foundation Graduate Fellowship

Program, the Georgia Tech/Emory Center for the Engineering of Living Tissues (GTEC) as part of the National Science Foundation ERC program, and the ARCS Foundation.

Kyle French and John Graham from the school of Mechanical Engineering as well as Jim McEntee from JM Machining also deserve recognition for their hard work in helping to design and build the Oscillatory Tensile Loading Device. Without their expertise in electronics and machining many technical aspects of this project would not have been possible.

During graduate school, I have had the honor and privilege to work with some of the most intelligent and talented people I have ever met. Many thanks go to Topher Hunter, who first taught me how to pipette (among other things), and seemed to have unlimited patience as I bungled through my first year in the lab. My experience at Georgia Tech will forever be linked to Stacy Imler and Janna Mouw. They welcomed me into the lab and made me feel like a part of the team immediately. Sharing two offices and a lab with them taught me the meaning of drama, but their friendship and willingness to always lend a hand made it so worth it. I also want to thank Ashley Palmer, Onyi Irrechukwu, John Connelly, and Christopher Wilson for their help, ideas, and for making this a really great place to come to work. I especially want to acknowledge Chris for all his help running Western Blots in the final months and always being willing to brainstorm and work through ideas as the final pieces of this project were coming together. Finally, to friends and colleagues in Wing 2D, to adversaries and colleagues in Wing 1D, and to the members of the All Conference Team, you have helped make this experience memorable in so many ways that I can't (and probably shouldn't) list them all here.

My parents, Jim and Sandy Vanderploeg, taught me at an early age the value of education and in many ways it was following their example that has led me here. Their unwavering support, along with that of my younger brother Kent, has been a constant source of strength throughout this process. Without their love, guidance, and encouragement I would not have become the person I am today.

Finally, I wish to thank Shannon Stott. She has been here since the beginning, both encouraging me and challenging me, celebrating in the victories and consoling in the defeats. Whether it was NSF fellowship essays, qualifying exams, frustrating experiments, or conclusion chapters, she has been there pushing me to excel and telling me that I could do it. Over the years she has helped make me a better scientist and a better person. I cannot imagine a life without her.

Thank you.

TABLE OF CONTENTS

LIST OF TABLES

LIST OF FIGURES

LIST OF ABBREVIATIONS

ACA	ε-aminocaproic acid
ADAM-TS4	A disintigrin and metalloproteinase with thrombospondin-4 motifs
-TS5	thrombospondin-5 motifs
ANOVA	Anaysis of variance
BMSCs	Bone marrow stromal cells
CS	Chondroitin sulfate
DMEM	Dulbeccos's Modified Eagle Medium
DMSO	Dimethyl sulfoxide
DNA	Deoxyribonucleic acid
DS	Dermatin sulfate
ECM	Extracellular matrix
ELISA	Enzyme-linked immunosorbent assay
G1, G2, G3	Globular domains of aggrecan core protein
GAG	Glycosaminoglycan
GAPDH	Glyceraldehyde-3-phosphate dehydrogenase
HPLC	High pressure liquid chromatography
KS	Keratin sulfate
OA	Osteoarthritis
PBS	Phosphate buffered saline
PG	Proteoglycan
PRG4	Proteoglycan-4
RNA	Ribonucleic acid
RT-PCR	Reverse-transcription polymerase chain reaction
sGAG	Sulfated glycosaminoglycan

SUMMARY

Disease and degeneration of articular cartilage and fibrocartilage tissues severely compromise the quality of life for millions of people. Although current surgical repair techniques can address symptoms in the short term, they do not adequately treat degenerative joint diseases such as osteoarthritis. Thus, novel tissue engineering strategies may be necessary to combat disease progression and repair or replace damaged tissue. Both articular cartilage and the meniscal fibrocartilage in the knee joint are subjected to a complex mechanical environment consisting of compressive, shear, and tensile forces. Therefore, engineered replacement tissues must be both mechanically and biologically competent to function after implantation. The goal of this work was to investigate the effects of oscillatory tensile loading on three dimensional engineered cartilaginous tissues in an effort to elucidate important aspects of chondrocyte and fibrochondrocyte mechanobiology.

To investigate the metabolic responses of articular chondrocytes and meniscal fibrochondrocytes to oscillatory tensile loading, various protocols were used to identify stimulatory parameters. Several days of continuously applied tensile loading inhibited extracellular matrix metabolism, whereas short durations and intermittently applied loading could stimulate matrix production. Subpopulations of chondrocytes, separated based on their zonal origin within the tissue, differentially responded to tensile loading. Proteoglycan synthesis was enhanced in superficial zone cells, but the molecular structure of these molecules was not affected. In contrast, neither total proteoglycan nor protein synthesis levels of middle and deep zone chondrocytes were substantially affected by

tensile loading; however, the sizes of these new matrix molecules were altered. Up to 14 days of intermittently applied oscillatory tensile loading induced modest increases in construct mechanical properties, but longer durations adversely affected these mechanical properties and increased degradative enzyme activity. These results provide insights into cartilage and fibrocartilage mechanobiology by elucidating cellular responses to tensile mechanical stimulation, which previously had not been widely explored for these tissues. Understanding the role that mechanical stimuli such as tension can play in the generation of engineered cartilaginous tissues will further the goal of developing successful treatment strategies for degenerative joint diseases.

CHAPTER 1

INTRODUCTION

1.1 Motivation

Diarthrodial joints rely on a complex interplay of diverse tissues to maintain proper function. If one or more of these tissues (*e.g.* articular cartilage, meniscus, ligament, or tendon) is damaged due to an acute injury or chronic degradation, the homeostatic balance of the entire joint can be disrupted. One potential consequence of this imbalance is osteoarthritis, a degenerative joint disease characterized by thinning of the articular cartilage, joint pain, and loss of mobility that affects millions of Americans costing over $60 billion annually[1]. In addition to direct trauma or degradation of the articular cartilage, incidences of osteoarthritis have been shown to increase following injury to the menisci[2]. This may be in part because tears to the inner region of the meniscus, which is highly avascular, often fail to adequately heal and the joint biomechanics of the knee are adversely altered[3]. One potential solution to this clinical problem is promoting meniscal repair via tissue engineering strategies[4]. A key component to successful meniscus or articular cartilage tissue engineering is to develop an understanding of the role that mechanical loading can play in tissue development, maintenance, and repair. During normal physiologic joint loading, the meniscus experiences compressive stresses in the inner region but predominately circumferential tensile stresses in the outer region. Thus, investigating cellular responses to tensile forces

could provide useful insights for tissue engineering ultimately leading to improved repair strategies.

1.2 Research Objectives

The overall goal of this dissertation research was to explore the effects of tissue appropriate mechanical stimulation, namely tensile loading, on fibrochondrocytes from the meniscus of the knee. The effects of tensile loading on articular chondrocytes were of interest, both for comparison to the fibrochondrocyte response and as an independent investigation into how these cells would respond to mechanical stimulation that may less prominent in normal physiology but potentially important in some cases. In addition to these goals the distribution and organization of extracellular matrix (ECM) molecules in the meniscus were examined in an effort to better understand the spatial relationship between various components. At its heart, this work aimed to contribute to the overall understanding of how cells from both articular cartilage and fibrocartilage respond to mechanical stimulation, furthering efforts to develop tissue engineered repair strategies.

Driving these goals was the central hypothesis that tensile mechanical stimulation could be used to modulate the extracellular matrix synthesis of meniscal fibrochondrocytes and articular chondrocytes in three dimensional hydrogel construct culture. This hypothesis was refined into three major components and specific aims were set forth to address each question posed by the hypotheses.

Hypothesis I: Continuously applied oscillatory tensile loading will inhibit meniscal fibrochondrocyte and articular chondrocyte matrix synthesis. However, short durations

of continuous oscillatory tensile loading (≤ 24 hours) as well as intermittently applied oscillatory tensile loading will promote matrix synthesis.

Specific Aim I: Determine the responses of meniscal fibrochondrocytes as well as articular chondrocytes seeded in fibrin hydrogel constructs to various protocols of oscillatory tensile loading.

To investigate the effects of oscillatory tensile loading on chondrocytes and fibrochondrocytes, studies evaluating a wide variety of cellular responses using several different loading conditions were conducted. Initial studies focused on using continuous oscillatory tensile loading (1.0 Hz, 5% ± 5% amplitude) for three consecutive days. Subsequent studies, primarily using only articular chondrocytes, examined the effects of shorter duration loading protocols, such as comparing 24, 48, and 72 hours of continuous loading. Additionally, changes in matrix molecule gene expression levels were investigated using short loading durations (≤ 8 hours). Finally, using the results of these studies as well as information from the literature as guides, intermittent oscillatory tensile loading protocols consisting of repeated load/rest cycles were used to evaluate chondrocyte cellular responses.

Hypothesis II: Cells isolated from distinct zones of articular cartilage and meniscal fibrocartilage will respond in a zone-dependent manner to intermittently applied oscillatory tensile loading.

Specific Aim II: Investigate the effects of intermittent oscillatory tensile loading on subpopulations of articular chondrocytes from the superficial, middle, and deep regions

of articular cartilage as well as subpopulations of meniscal fibrochondrocytes from the inner and outer regions of the meniscus.

Heterogeneous cell populations reside within both articular cartilage and the meniscus, and recently a careful elucidation of potential differences in these cell populations has been of increasing interest. Since cells from different phenotypic populations may behave differently during *in vitro* culture and in response to mechanical loading, several studies were undertaken to investigate the zone-dependent cellular responses of articular chondrocytes and meniscal fibrochondrocytes. Articular chondrocytes were separated in three groups according to their origin in the tissue: superficial zone, middle zone, and deep zone. ECM synthesis, cellular proliferation, and cell morphology were evaluated at various time points in fibrin hydrogel constructs. Additionally, an intermittent protocol was used to evaluate potential zone-dependent responses to oscillatory tensile loading. Finally, fibrochondrocytes from the meniscus were separated into inner zone and outer zone subpopulations and subjected to the same intermittent oscillatory tensile loading protocol.

Hypothesis III: Extended *in vitro* culture of fibrin hydrogel constructs seeded with articular chondrocytes in combination with intermittent oscillatory tensile loading will stimulate extracellular matrix production yielding constructs with enhanced tensile and compressive mechanical properties.

Specific Aim III: Determine the effects of extended durations of intermittent oscillatory tensile loading on the extracellular matrix accumulation and mechanical properties of articular chondrocyte seeded tissue engineered hydrogel constructs.

Although to date cartilage tissue engineering strategies have failed to produce tissue replacements with mechanical properties equivalent to the native tissue, significant enhancement of construct mechanical properties has been achieved using extended *in vitro* culture times coupled with mechanical stimulation[5]. Therefore, an initial study was undertaken to evaluate the changes in the tensile mechanical properties of fibrin hydrogel constructs over extended durations of free swelling culture. Hydrogel constructs were allowed to culture *in vitro* for up to 27 days and the dynamic tensile properties of the constructs were tested at various points over the course of the study. In a subsequent study, hydrogel constructs were cultured in free swelling conditions for 7 days and then subjected to intermittently applied oscillatory tensile loading for up to an additional 21 days. The dynamic tensile mechanical properties over a three decade frequency sweep of strain rates were measured every 7 days. Additionally, cylindrical cores of each construct were tested in unconfined compression at a quasi-equilibrium state. Finally, changes in ECM accumulation and degradation were evaluated in an effort to correlate the structural contents of the hydrogel constructs with their mechanical properties.

1.3 Significance and Contribution

The studies performed for this dissertation provide insights into the responses of meniscal fibrochondrocytes to a tissue appropriate loading mode, oscillatory tension, in a three dimensional *in vitro* culture system. Additionally, using hydrogel constructs seeded with articular chondrocytes allowed for not only a direct comparison to a more well characterized cell type, but also aided in understanding how chondrocytes respond to mechanical forces that are not necessary a major component of their native environment.

However, additional rationale exists for investigating the articular chondrocyte response to oscillatory tension, because tensile strains are found along the articular surface and may become more prevalent in articular cartilage following a traumatic injury that disrupts the otherwise smooth joint surface or even after surgical intervention where a softer material is used to repair damaged cartilage tissue.

Although the studies presented here certainly add to the knowledge base of this biological system, they also contribute in the broader context of tissue engineering and regenerative medicine in a more tangible way. Rigorous therapeutic strategies to treat cartilage and fibrocartilage damage require an understanding of the cellular processes occurring during physiologically relevant mechanical stimulation. Knowledge of the structure and organization of native tissue provides clues to mechanisms involved in mechanotransduction as well as establishes design parameters for developing tissue engineered constructs. Studying the responses to shorter durations of mechanical stimulation yields insights into how specific loading scenarios could be used to manipulate cellular behavior. Additionally, studying construct development over extended periods of *in vitro* culture is important for refining techniques used to create replacement or repair tissues.

CHAPTER 2

BACKGROUND AND LITERATURE REVIEW

2.1 Articular Cartilage

Articular cartilage is a complex tissue that lines the ends of long bones in articulating joints providing compressive resistance and excellent frictional properties during joint motion[6]. The structure and organization of the macromolecular components of articular cartilage convey unique mechanical and biological characteristics to the tissue, often yielding an entire lifetime of normal function[7].

2.1.1 Articular Cartilage Composition and Structure

Articular cartilage possesses four major constituents: water, collagens, proteoglycans, and cells. Similar to many soft tissues, cartilage is highly hydrated with water comprising approximately 75% of the total tissue mass. Collagens account for 10-20% of the tissue mass while proteoglycans contribute another 5-10%. The primary collagen in articular cartilage is type II collagen, which accounts for up to 90% of the total collagen content. Other collagens such as types VI, IX, X, and XI have also been found in articular cartilage. The main proteoglycan in articular cartilage is the large aggregating chondroitin sulfate proteoglycan also known simply as *aggrecan*. Additionally, smaller proteoglycans such as decorin, biglycan, fibromodulin, and perlecan are also present. Smaller amounts of a variety of other non-collagenous proteins constitute the remaining portion of the articular cartilage extracellular matrix. In

addition, adult articular cartilage is predominantly avascular[7], which may contribute to the inadequate healing response typically seen following injury or disease.

The Collagen Network

Although organizational patterns of the collagen network are not apparent under visible light, detailed observations are possible with electron microscopy. Type II collagen, the dominant collagen protein in articular cartilage, is a triple helical molecule containing three identical α_1(II) chains that can interact with adjacent molecules to form larger fibrils up to 120 nm in diameter[6]. Near the articular surface, the collagen fibers are densely packed and primarily oriented parallel to the surface. This organizational pattern gives the surface zone of articular cartilage greater tensile stiffness compared to deeper regions in the tissue, which is thought to be a functional adaptation to the shear and tensile forces induced at the joint surface during articulation[8-10]. Deeper within the tissue, collagen content decreases, but the diameter of the fibrils increases[6,7]. Additionally, collagen fibers in the midsubstance of the tissue are more randomly oriented. The deepest regions of non-calcified cartilage contain the largest diameter collagen fibrils, which are oriented perpendicular to the articular surface passing through the tidemark and into the calcified cartilage below. This highly organized collagen network conveys tensile stiffness to articular cartilage, providing mechanical characteristics that vary through the tissue depth and are well suited for the stress environment that develops during joint loading.

Proteoglycan Organization

Proteoglycans (PGs) are molecules possessing a protein core with at least one attached glycosaminoglycan (GAG) side chain. The GAG side chains are long,

unbranched polysaccharides consisting of repeating disaccharide units each with a negatively charged group, often sulfate[11,12]. Hyaluronic acid (HA), chondroitin sulfate (CS), keratin sulfate (KS), and dermatin sulfate (DS) are the major GAGs found in human articular cartilage[13-15]. As noted above, aggrecan is the most prominent PG found in articular cartilage. Newly synthesized, intact aggrecan consists of a long core protein with a globular domain (G1) at its N-terminal, a short inter-globular domain, a second globular domain (G2), a long region with up to several hundred GAG molecules, and finally a third globular domain (G3) at the C-terminal (Figure 2.1).

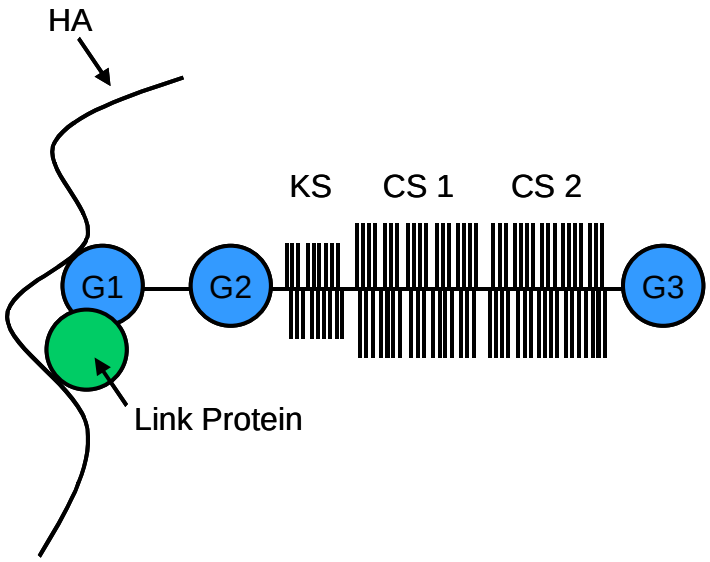

Figure 2.1 Molecular structure of aggrecan shown attached to a hyaluronic acid (HA) backbone and stabilized by link protein. Aggrecan consists of the core protein, three globular domains (G1, G2, G3), a keratin sulfate (KS) rich region, and two chondroitin sulfate (CS1 and CS2) rich glycosaminoglycan regions.

Aggrecan molecules bind to hyaluronic acid (HA) via the G1 domain, and this interaction is stabilized by link protein. The HA backbone is found in various lengths from several hundred to more than 10,000 nanometers with larger aggregates having as many as 300 attached aggrecan molecules[16,17]. GAG chains contain negatively charged sulfate groups, and it is these sulfated glycosaminoglycans (sGAG) that give aggrecan molecules their functional properties. Since the sGAGs have a high anionic charge, they both repel each other as well as attract water molecules. The result is an influx of water into the tissue causing swelling. However, the aggrecan molecules are entangled with the collagen network, restricting expansion and thereby inducing a swelling pressure within the tissue. The compressive mechanical properties of cartilage result from this swelling pressure. Additionally, the swelling pressure maintains tension on the collagen network.

As with the collagen network, aggrecan is not uniformly distributed throughout articular cartilage. Aggrecan concentration is lowest near the surface of the tissue[18], but smaller PGs such as decorin and biglycan are most abundant in this region[6,18-20]. The concentration of aggrecan increases through the middle and deep zones of articular cartilage, but is lower in the region containing calcified cartilage. This inhomogenous distribution of aggrecan has functional consequences, as evidenced by experiments demonstrating that the compressive mechanical properties vary through the tissue depth[21].

2.1.2 Cells of the Articular Cartilage: Chondrocytes

Articular cartilage is populated with a single cell type, the chondrocyte, which synthesizes and maintains the complex architecture of extracellular matrix molecules within the tissue. Although all cells in articular cartilage are referred to as chondrocytes,

differences in cellular morphology, gene expression profiles, and extracellular matrix synthesis exist throughout the tissue depth. Near the superficial zone, chondrocytes are primarily flat or oblong in shape and align parallel to the joint surface[7]. Chondrocytes further from the surface have a spherical shape and are larger than superficial zone cells (Figure 2.2). In the cartilage deep zone, chondrocytes tend to be arranged in vertical columns as the tissue transitions to calcified cartilage[22]. Overall, the cell density and metabolic activity in articular cartilage is low compared with many other tissues (~35 x 10^6 cells/cm^3)[7]. Cell density also varies with tissue depth, being highest in the superficial zone and lowest deeper within the tissue.

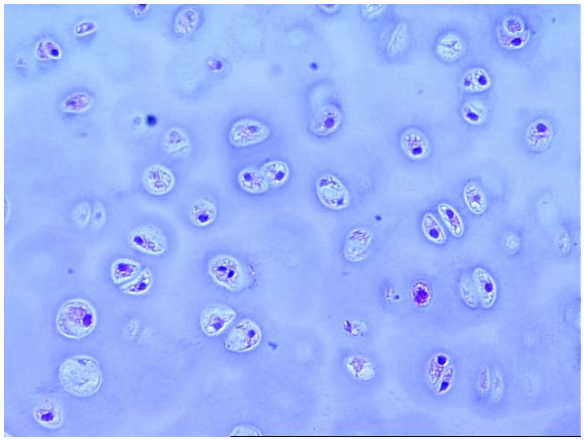

Figure 2.2 Hematoxylin and Eosin (H&E) stain of the middle zone of immature bovine articular cartilage. Cell nuclei are dark blue and cartilage matrix is lighter blue.

The composition of the matrix molecules surrounding chondrocytes also is dependent on tissue depth. Proteoglycan-4 (PRG4), also known as superficial zone protein or lubricin, is only found along the tissue surface and surrounding chondrocytes

in the superficial zone[23]. Type VI collagen is found in the pericellular matrix in nearly all chondrocytes in adult cartilage as a fine filamentous network[24] that interacts with the small proteoglycan decorin[25]. Chondrocytes residing in the deepest zone, the calcified cartilage, synthesize type X collagen and can calcify the extracellular matrix[6].

The depth dependent compositional differences seen in articular cartilage are due, at least partially, to metabolic specialization of the chondrocytes resident in each tissue zone[26]. Only chondrocytes from the superficial zone synthesize PRG4 *in situ*[23], and this characteristic was conserved during both *in vitro* monolayer culture and three dimensional construct culture for up to 9 days[27]. However, multiple passages of monolayer culture eliminated differences in PRG4 gene expression in chondrocyte subpopulations[28]. Consistent with PG synthesis rates *in situ*[22] and the overall PG distribution found in articular cartilage, chondrocytes isolated from the deep zone synthesize more extracellular matrix PGs than cells from the superficial zone during two or three dimensional *in vitro* culture[26,29]. Gene expression profiles for freshly isolated chondrocytes from these distinct zones also exhibit a similar pattern[28,30].

2.1.3 Pathology of Articular Cartilage

Although many individuals go their entire lives without persistent symptoms of joint pain or stiffness, it is estimated that virtually all elderly adults exhibit some level of cartilage degradation. In fact, aggrecan molecules in elderly, but otherwise healthy, cartilage tissue exhibit extensive processing such that numerous aggrecan fragments but very little full length, intact aggrecan (structure shown in Figure 2.1) are found in the tissue[31]. Many joint diseases are characterized by inflammation and irritation of articulating joints, broadly classified as *arthritis*. The most prevalent of all joint disease

is osteoarthritis (OA), which compromises the quality of life for over 20 million Americans[1]. OA is characterized by progressive joint pain, loss of joint mobility, radiologically apparent joint space thinning, as well as fibrillation and degeneration of the articular cartilage. The incidence of OA greatly increases with age[32,33], joint injury[34,35], and excessive joint loading[36-39]. The majority of cases of OA develop in the absence of an identified acute cause and rarely occur in individuals under 40 years of age. However, incidents of injury, hereditary abnormalities, and developmental or metabolic disorders can lead to the development of OA at a much younger age[1]. Relatively little is known regarding specific mechanisms involved in the progression of OA from mild joint pain to a debilitating lack of mobility.

Following joint injury, osteoarthritis may be initiated by seemingly minor damage to the articular cartilage surface. Mechanical disruption of the surface not only damages nearby chondrocytes, but also affects the frictional and wear properties of the joint during articulation. Hence, small asymptomatic fissures or cracks can become significant over time due to repetitive wear on the compromised surface. Concomitant with macroscopic tissue damage is a loss of functional proteoglycan matrix molecules following injury[40,41]. As a result of the decreased concentration of PGs in the cartilage matrix, the water content in the tissue increases leading to a loss of mechanical integrity. As the articular cartilage become softer, greater stresses are transferred to the subchondral bone further altering the joint biomechanics and exacerbating the problem[42]. More severe injuries can create full thickness cartilage lesions resulting in immediate symptoms and more rapid degradation of the surrounding tissue. Ultimately, progressive OA can lead to a total loss of articular cartilage function, bone on bone contact, and severe joint pain.

Although many treatment options are available for patients suffering from various stages of osteoarthritis, none of them actually cure the disease. Several treatments, however, do improve patient symptoms and may slow the progression of OA. Minor damage to the articular surface can be treated with arthroscopic lavage and debridement, a process involving the removal of torn pieces of cartilage to reduce mechanical symptoms[43]. This technique may have short term mechanical benefits, but does not alter pain or functional levels in patients with arthritic knees[44]. Injuries penetrating the entire cartilage depth into the subchondral bone are known to fill with fibrocartilage repair tissue presumably due to the access to blood and reparative cells in the underlying bone marrow[45]. The technique of arthroscopic microfracture[46] attempts to initiate this healing process by penetrating the subchondral bone in a controlled manner to induce bleeding into full thickness cartilage defects. The microfracture technique has proven to be useful in younger patients with traumatic injuries rather than chronic cartilage degradation, but the newly synthesized repair tissue typically does not completely fill the defect site and is mechanically inferior to the surrounding tissue[47].

More invasive repair techniques may be necessary in cases of severe injury or after less complicated treatments have failed. Osteochondral autograft or allograft procedures involve removing a full thickness cylindrical core from a non-load bearing region of cartilage (or from a cadaveric donor) and transplanting it into the defect site[48,49]. However, complications from these procedures can arise from donor site morbidity and failure of the graft to integrate with the surrounding tissue. Additionally, great care must be taken to properly size the graft as even small mismatches in diameter or height can severely compromise the success of the procedure[50]. An additional method called

autologous chondrocyte implantation (or transplantation) is based on a similar strategy except that chondrocytes are isolated from excised tissue and expanded in two dimensional *in vitro* culture[51]. The expanded chondrocytes are then implanted into the cartilage defect site as a cell slurry, covered with a periosteal flap, and sealed with fibrin glue. The newly implanted cells can then adhere to the surrounding cartilage and form a repair tissue. Like the osteochondral autograft procedure, autologous chondrocyte implantation can cause donor site morbidity; however, patients generally do report improvements and a reduction in pain symptoms following autologous chondrocyte implantation[47]. Additionally, one randomized prospective study found significant improvements in healing following autologous chondrocyte implantation compared with osteochondral autograft procedures[52].

The final option for patients with severe OA is total joint replacement. This procedure is extremely invasive, but highly effective for alleviating pain and restoring joint mobility. Total joint replacement remains the best treatment option for elderly patients with debilitating OA. However, these replacements will typically only last 10-15 years before a revision surgery is required due to implant loosening or wear. Therefore total joint replacement does not represent an attractive option for younger patients who expect to outlive their implants. Thus, an unmet clinical need remains for younger patients (*i.e.* < 65 years old) who develop osteoarthritis following traumatic injury or articular cartilage degradation. Ideally, intervention strategies would be successful in halting the progression of OA and restoring normal joint function in these patients before painful and difficult to treat cartilage lesions develop.

Tissue engineering represents an exciting opportunity for improving the treatment options in cartilage repair. Tissue engineering "is an interdisciplinary field that applies the principles of engineering and life sciences toward the development of biological substitutes that restore, maintain, or improve tissue function"[53,54]. Many of the shortcomings of the cartilage repair techniques described above may, in fact, be overcome using tissue engineering approaches. Cartilage tissue engineering strategies seek to replace or repair damaged cartilage tissue with biological materials thereby relieving pain and restoring joint function.

2.2 Fibrocartilage Tissues

Fibrocartilage tissues are found in many joints throughout the body, most prominently the knee, the temporomandibular joint, and the vertebral joints. The regions in tendons that wrap around bones or are located near bone insertion sites are also considered fibrocartilage[55]. Fibrocartilage tissues typically experience a combination of compressive and tensile forces during joint motion and are composed of extracellular matrix molecules well suited for this complex mechanical environment. Structurally and compositionally, fibrocartilage tissues lie somewhere between articular cartilage and other connective tissues such as tendon or ligament. These tissues are rich in highly organized collagen fibers, but also contain significant quantities of both large and small proteoglycan molecules.

In many ways, fibrocartilage tissues play mechanical supporting roles by protecting the adjacent articular cartilage or bone from excessive loading and by contributing to the overall joint stability. The two menisci of the knee joint certainly

fulfill these roles and will be the primary focus of the remaining discussion on fibrocartilage tissues. The menisci are semilunar tissues situated between the femoral condyles and the tibial plateau in the knee joint. The pair is instrumental in load transmission, bearing 50-70% of the total load during normal joint motion[56,57]. Additionally, the menisci absorb shock during impact loading and also participate in joint lubrication[58]. As knowledge of the mechanics, structure, and biology of the menisci has increased in the past half century, recognition of their importance in maintaining normal knee joint biomechanics and function has also increased.

2.2.1 Composition and Structure of the Knee Menisci

The knee meniscus is highly hydrated with approximately 70% of its total mass being water[58]. The primary extracellular matrix component in the meniscus is collagen, which accounts for over 70% of the solid mass of the tissue[59]. Several collagen types including I, II, III, V, and VI are found in the meniscus, but type I collagen is by far the most prominent, comprising 98% of the total collagen content[58]. Proteoglycans are found in the meniscus at much lower concentrations (1-3% of the total mass) than in articular cartilage[57-59]. Both the large chondroitin sulfate proteoglycan, aggrecan, and smaller dermatin sulfate proteoglycans such as decorin and biglycan can be found in the meniscus. Vascularity in the meniscus decreases with age until only the outer 10-30% of the periphery remains highly vascularized in adulthood[60,61].

<u>The Collagen Network</u>

Large bundles of type I collagen constitute the vast majority of the extracellular matrix in the meniscus. Type I collagen is a triple helical molecule with two identical

α_1(I) chains and one α_2(I) chain[59] that can form long microfibrils and aggregate laterally to form relatively large diameter fibrils. In all tissues, collagen fibers play a significant role in resisting tensile forces. The collagen fibers in the meniscus are primarily oriented circumferentially, parallel with the outer periphery of the tissue. This structure can readily be seen with simple chromatic staining and a light microscope (Figure 2.3). Additionally, there are smaller, radially oriented fibers both along the surfaces of the tissue and disbursed through the midsbustance[58,62,63]. The inner zone of the meniscus also contains smaller, more randomly oriented collagen fibers with a higher proportion of type II collagen.

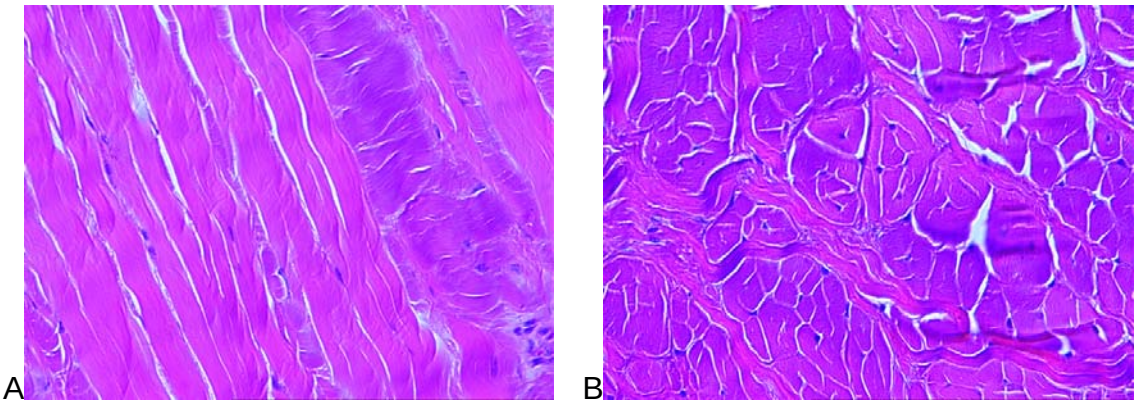

Figure 2.3 Hematoxylin and Eosin (H&E) stain of the midsubstance of immature bovine meniscus tissue. Cell nuclei are dark blue and fibrocartilage matrix is pink/purple. (A) Large, parallel collagen fibers dominate the structure of the meniscus. (B) Cross-section of collagen fibers depicting the network of large bundles (perpendicular to image plane) interspersed with smaller connecting fibers (in image plane).

This highly organized structure in the meniscus is particularly well suited to its mechanical environment. During joint loading, the menisci are displaced radially by the

femoral condyles due to their wedge-like shapes. However, because the menisci are attached to the underlying bone on the tibia at both the anterior and posterior horns, this displacement induces large circumferentially oriented tensile hoop stresses in the outer region of the tissues[57,58]. The effect of this load distributing phenomenon is that the large compressive forces in the knee resulting from normal joint motion are translated to circumferential tensile forces alleviating the adjacent articular cartilage from bearing much of the direct load.

Other collagen types are also found in the menisci, but their functions are not clearly understood. Type II collagen has been found primarily in the inner, avascular regions of the meniscus, and it appears to colocalize with the larger type I collagen fibers and concentrate around the radially oriented "tie" fibers in the midsubstance of the tissue[60,64]. Type VI collagen is also found in the meniscus in fairly significant quantities (~ 2% of the dry mass[65]), primarily located in the interterritorial regions of the matrix[60]. The function of type VI collagen in the meniscus is not well understood, but has been suggested to act as an intermolecular adhesion protein and a cell attachment protein. Our findings regarding type VI collagen in the meniscus will be discussed in more detail in the following chapter.

Proteoglycan Distribution

The proteoglycan content in the meniscus significantly lower than in articular cartilage, however, the structures of the large chondroitin sulfate proteoglycans (*i.e.* aggrecan) found in both tissues are similar[66,67]. Additionally, a larger proportion of PGs with dermatin sulfate GAGs are present in the meniscus compared with articular cartilage[68]. The distribution of PGs, especially aggrecan, within the meniscus varies

throughout the tissue. In adult porcine menisci, approximately 8% of the dry mass of the inner region is comprised of GAGs, whereas only 2% of the total dry mass in the outer region is GAG[69]. The dermatin sulfate PGs, namely decorin and biglycan, are more uniformly distributed throughout the meniscal extracellular matrix. This inhomogenous PG distribution in the meniscus correlates well with the mechanical environment of different regions of the tissue. As discussed above, aggrecan molecules carry the compressive loads in cartilage tissues through the interactions of the GAG side chains with interstitial water. Compressive loads are known to be highest in the inner region of the meniscus, and thus higher aggrecan content may represent a functional adaptation to the local mechanical environment[58,69].

2.2.2 Cells of the Meniscus: Fibrochondrocytes

The cells resident in meniscal fibrocartilage tissues exhibit characteristics of both fibroblasts and chondrocytes, and have therefore been designated as *fibrochondrocytes*. These cells, however, are not a homogeneous population with uniform phenotype[70,71]. Two distinct populations, one more proliferative and the other with higher matrix synthesis potential were identified in monolayer cultures and could be preferentially stimulated with different culture medium supplements[72]. Early work using light and electron microscopy revealed that cells near the superficial regions of the meniscus (*i.e.* near the articular surface) were predominantly elongated and oval in shape, whereas cells deeper in the tissue were rounded with numerous filamentous projections emanating from the cell body[60,73].

More recently, detailed immunohistochemical localization suggested that four distinct fibrochondrocyte subpopulations are present in adult rabbit menisci[74]. Cells near

the tibial and femoral surfaces of the inner tip were classified as fusiform and lacked any cytoplasmic projections. Fibrochondrocytes in the midsubstance of the inner region were found to be rounded and chondrocyte-like in appearance. In the middle and outer zones two fibrochondrocyte populations were identified each with rounded cell bodies, but increasingly more elaborate cytoplasmic projections extending in multiple directions. Clear regional delineations for the different subpopulations were not found, but instead these morphological changes developed gradually. These distinct, yet related, subpopulations of fibrochondrocytes synthesize and assemble the diverse extracellular matrix structure found in meniscal fibrocartilage. These specialized morphological characteristics may indicate the ability of cellular subpopulations to sense, respond, and maintain their local matrix environment[74].

2.2.3 Pathology of the Meniscus

Damage to the menisci of the knee can occur concurrently with traumatic injuries to the anterior cruciate ligament, but is also found in the absence of other signs of joint damage[2,75,76]. Additionally, non-traumatic meniscal tears can occur in patients with degenerate menisci suffering from osteoarthritis in the adjacent cartilage tissues[3]. Meniscal tears restricted to the outer vascular region of the tissue have the potential to heal without the need for surgical intervention, but tears penetrating the avascular inner region do not heal autonomously[3,77,78]. Traditionally, torn menisci were fully or partially excised with little attempt to preserve meniscal function. However, as the importance of the meniscus in maintaining normal knee joint function has become better understood, efforts have increased to develop novel surgical repair techniques[57,79].

Injury or disease in the meniscus, itself, is not necessarily the primary clinical concern, but rather the secondary impact on the neighboring articular cartilage. Full or partial meniscectomy following injury often results in the early onset of osteoarthritis[2,80,81]. This process is not completely understood, but the higher incidence of articular cartilage degeneration is at least partially due to a dramatic change in knee biomechanics in the absence of a competent meniscus. Without the meniscus bearing the majority of load in the knee joint, the underlying articular cartilage is exposed to significantly larger compressive forces. This may induce direct mechanical damage to the cartilage, which then can initiate the progression of OA. Additionally, compressive overloads can induce the upregulation of catabolic cytokines that cause secondary tissue damage and initiate a biochemical cascade leading to OA[82]. Meniscal allograft transplantation following total meniscectomy can be successful in alleviating pain symptoms and slowing articular cartilage degradation, however substantial disability in joint function often remains[83]. Additionally, the potential for disease transmission and a limited donor supply remain complicating factors for allograft transplantation.

Tears in the avascular region of the meniscus often are not candidates for surgical intervention using currently available techniques[79], and even surgically repaired injuries can heal with mechanically inferior tissue and may be susceptible to re-injury[84]. Therefore, opportunities exist for tissue engineering strategies to improve the prospects for meniscal repair.

2.3 Engineering Cartilaginous Tissues

Investigations into the potential to engineer replacement tissues for damaged articular cartilage began in the early 1990's[85,86]. Since this time, scientific efforts have grown immensely with hundreds of research studies currently being published on various aspects of cartilage and fibrocartilage tissue engineering each year. The fundamental goal of this field is to create a biologically based, mechanically stable replacement for damaged cartilage or fibrocartilage that will reduce pain, restore joint function, and halt or slow the progression of osteoarthritis. Many different techniques have been employed to stimulate the development of engineered cartilaginous tissues, including two and three dimensional *in vitro* cell culture, mechanical conditioning, and biochemical stimulation. Although much progress has been made in recent years, a clinically successful cartilage or fibrocartilage tissue replacement remains out of reach.

2.3.1 *In Vitro* Cell Culture

A fundamental principle in tissue engineering is the ability to stimulate the development of a new tissue outside the body that can later be implanted into a patient. Unlike some cell types such as fibroblasts or endothelial cells, chondrocytes quickly lose their phenotype when cultured in two dimensional monolayers[28,87]. Therefore, rapid and extensive expansion of a chondrocyte population is not possible without compromising some cartilage specific cell behaviors, namely the production of the extracellular matrix molecules aggrecan and type II collagen. However, chondrocytes do posses the ability to redifferentiate following expansion in two dimensional culture if placed in a proper three dimensional environment[88]. Therefore, many cartilage tissue engineering efforts have involved using three dimensional scaffolds to preserve the chondrocytic phenotype[89-93].

Although culturing chondrocytes in this way will preserve their phenotype and yields a cartilage-like tissue construct, neither the native structure nor mechanical characteristics of cartilage are adequately reproduced.

Fibrochondrocytes in two dimensional monolayer cultures and may retain their phenotype to a greater extent than chondrocytes over short times in culture[72,94-96]. Limited data are available on the behavior of fibrochondrocytes in three dimensional *in vitro* culture, however, many of the principles and techniques used for articular chondrocyte culture have been applied to fibrochondrocytes[96-99].

2.3.2 Exogenous Stimuli

Several forms of exogenous stimuli have been used in an effort to generate more functionally competent cartilage and fibrocartilage tissue engineered constructs. Additionally, assessing cellular responses to these stimuli in three dimensional *in vitro* culture provides insights into fundamental cell behaviors that may be crucial for tissue engineering strategies to be successful. Some of the earliest work using exogenous stimuli for cartilage tissue engineering demonstrated that dynamic mechanical compression could enhance chondrocyte extracellular matrix synthesis in agarose constructs[100]. Additionally, short bouts of dynamic compression applied for several weeks significantly improve the mechanical characteristics of agarose constructs seeded with articular chondrocytes[5]. Dynamic shear loading can stimulate chondrocyte extracellular matrix synthesis in cartilage explants[101] and in scaffold-free tissue engineered constructs[102]. In addition to direct mechanical stimulation, fluid induced shear stress improves the biochemical and mechanical characteristics of engineered cartilage tissues[103-106].

The effects of mechanical stimulation on fibrochondrocytes have not been widely studied in three dimensional culture. However, static compression has been shown to modulate intervetebral disk fibrochondrocyte gene expression in alginate beads[107] as well as inhibit fibrochondrocyte extracellular matrix synthesis in tissue explants[108]. Compression of fibrochondrocytes in two dimensional monolayer cultures has also been shown to influence gene expression of meniscal fibrochondrocytes[109]. Interestingly, cyclic tensile strain on two dimensional cultures of fibrochondrocytes from the temporomandibular joint disk has anti-catabolic effects at both the gene expression and protein synthesis levels[110,111].

In addition to direct or indirect mechanical stimulation, biochemical factors have also been used to stimulate chondrocytes and fibrochondrocytes during *in vitro* culture. Growth factors such as transforming growth factor-β (TGF-β), insulin like growth factor (IGF), basic fibroblast growth factor (bFGF), and platelet derived growth factor (PDGF) can stimulate chondrocyte and fibrochondrocyte extracellular matrix synthesis *in vitro*. Other types of stimulation such as using low oxygen concentration in the culture environment also improve the characteristics of engineered cartilage tissues[112-114]. Combinations of mechanical and biochemical stimuli are also being increasingly employed to further enhance development of engineered cartilaginous tissues[108,115-117].

2.3.3 A Role for Tensile Loading

Many forms of mechanical stimulation have been used in an effort to engineer cartilaginous tissue replacements. Mechanical tension, however, has not been widely explored as a means to modulate chondrocyte or fibrochondrocyte extracellular matrix biosynthesis or stimulate the development of engineered cartilaginous tissues. Although

cartilage and fibrocartilage tissues may not be directly loaded in tension, several scenarios exist where these tissues are subjected to a tensile mechanical environment.

In healthy fibrocartilage, normal compressive joint loading induces significant tensile stress in specific regions of these tissues due to their anchorage in the joint, anatomical shape, and ultrastructural organization. For example, the menisci in the knee joint develop circumferential tensile hoop stresses in the outer region of the tissue during normal loading[57,58,118]. Similarly, tensile stress develops near the upper boundary of the temporomandibular joint disc under normal conditions[119]. Thus, any engineered replacement tissue implanted into a defect site or used as a tissue substitute would experience a similar tensile mechanical environment. Understanding the role of tensile loading and deformation in tissue development, maintenance, and repair may therefore be crucial to understanding how repair or replacement tissues will perform in an *in vivo* fibrocartilage environment.

Although tension is not typically a major component in the *in vivo* mechanical environment, tensile strains are found in normal articular cartilage as well. Compressive joint loading will induce some local tensile strain in transverse directions throughout the tissue due to the Poisson effect. Additionally, tension is a more significant part of the local mechanical environment near the articular surface. During articulation, a combination of compressive and shear forces are imparted to the cartilage surface, which induces local tensile strains[58]. Traumatic injury or arthritic degradation may cause cracking or tearing of the joint surface. Compressive loading of this damaged region could result in high stress concentrations near injury sites also leading to the development of significant tensile strains. This dramatic change in the local mechanical environment

may then cause further degeneration and disease progression. Alternatively, many cartilage tissue engineering repair strategies involve inserting a relatively soft engineered construct into a defect site. Since the surrounding cartilage tissue is stiffer than the repair tissue, a region with a substantial material property mismatch would result around the implant. During functional loading, the repair and native tissues will deform to different degrees thereby potentially inducing tensile strains. This local tensile mechanical environment could influence how the repair tissue matures and integrates with the surrounding tissue.

The use of mechanical tension for cartilage or fibrocartilage tissue engineering provides opportunities to investigate potentially unique characteristics of the cells resident in these tissues that may not be possible with other modes of mechanical stimulation. Understanding how these cells respond to mechanical tension in a well controlled *in vitro* environment may offer insights into the development, maturation, and integration of implanted tissue engineered constructs. In addition, mechanical tensile stimulation may be useful for generating constructs with anisotropic material properties or matrix organization similar to those found in native tissue and potentially important for successful repair. The series of studies presented in this dissertation focuses on understanding the effects of tensile loading on chondrocytes and fibrochondrocytes during *in vitro* culture. Elucidating how these cells may respond to a tensile mechanical environment will provide valuable and novel contributions to the field of cartilage and fibrocartilage tissue engineering.

CHAPTER 3

CHARACTERIZATION OF THE DISTRIBUTION AND ORGANIZATION OF EXTRACELLULAR MATRIX MOLECULES IN THE BOVINE MENSICUS

3.1 Introduction

Although tears restricted to the avascular midsubstance of the semilunar menisci of the knee have long been known to inadequately heal[77], these tissues have only more recently been recognized to play important functions in the joint[57]. The discovery that the predominant structural components of the menisci differ from those of hyaline or elastic cartilages[59] provided further distinctions. Although great strides have been made towards elucidating meniscal structure, organization, and function; research on the meniscus remains in its infancy compared with articular cartilage, bone, and many other tissues.

Recently, the structure and orientation of collagen fibrils in the menicus[62] as well as regional variations in meniscal cell morphology[74] have been shown in great detail. Additionally, the organization of specific extracellular matrix molecules, such as types I and II collagen, aggrecan, and other small proteoglycans has been elucidated to varying degrees of detail in several species[64,120-123]. Each of these studies further revealed the complexities of meniscal structure and the organization of its extracellular matrix. Types I and II collagen were found to co-localize in an intricate network in stark contrast to the diffuse type II collagen staining seen in articular cartilage[64]. This finding raised interesting questions of how diverse matrix molecules may interact to form a more complex and functionally competent tissue.

As stated previously and discussed in more depth in the preceding chapter, injuries to the avascular inner region of the meniscus often fail to adequately heal, and although surgical techniques have been constantly improving, many meniscal tears remain unsuitable for surgical repair[79]. In recent years meniscal tissue engineering research has garnered increasing attention and may eventually be able to fulfill this unmet clinical need. Gaining a more complete understanding of the intricacies of meniscal structure will aid in the pursuit of successful tissue engineering repair strategies. Using detailed imaging analyses of meniscal microarchitecture, potential design templates for scaffolding materials as well as benchmark criteria for *in vitro* tissue regeneration can be developed.

Several studies were undertaken to histologically evaluate the distribution and organization of a variety of extracellular matrix molecules in the bovine meniscus. Initially, types I, II, and VI collagen as well as aggrecan were independently imaged using fluorescence immunohistochemical techniques. However, to truly appreciate the potential interplay between these matrix molecules, multiple collagen types were also visualized simultaneously.

3.2 Materials and Methods

3.2.1 Meniscal Tissue Harvest and Processing

Intact immature bovine stifle joints were obtained from an abattoir and aseptically disarticulated. The lateral and medial menisci were excised from the joint and transferred to sterile PBS that had been supplemented with antibiotic/antimycotic (see Appendix D for formulation). Using a sterile scalpel, several 2-3 mm slices were cut from each

meniscus in two different orientations: radial cross-sections and circumferential cross-sections (Figure 3.1). The radial cross-sections would allow for end-on imaging of the primary collagen network in the menisci, whereas circumferential cross-sections would provide views along the main axis of these fibers. Two fixation and processing treatments were subsequently used to prepare meniscal tissue slices for imaging. They were designated "formalin fixed" and "fixed-frozen."

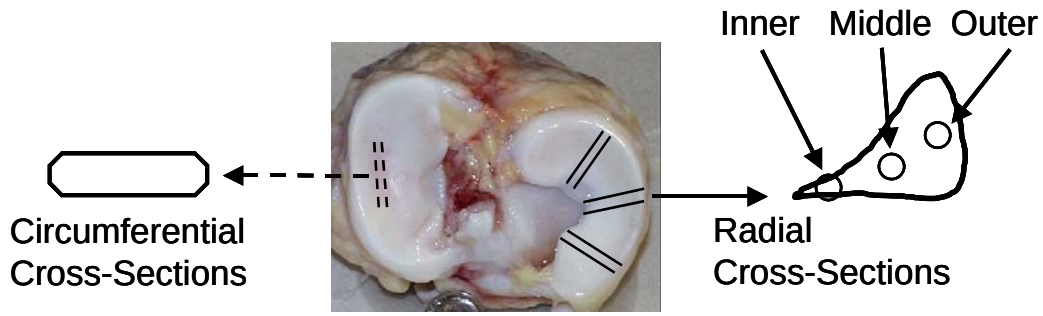

Figure 3.1 Schematic of meniscus cross-section preparation for imaging analysis

Formalin-Fixed Tissue

Tissue slices to be used for the imaging of individual extracellular matrix molecules were processed using the formalin-fixed protocol. Slices were transferred to 50 mL conical tubes and 10% neutral buffered formalin was added until all tissue was submerged. Tubes were maintained at 4°C for 3-4 days to allow for complete fixation of the tissue. Formalin was then removed and tissue slices were washed several times with PBS before being stored in fresh PBS at 4°C. Meniscus slices were affixed to the freezing stage of a Microm sledge microtome with a small amount of Tissue-Tek O.C.T.

compound and sectioned to 50 μm. Sections were then washed in PBS and carefully transferred to 1.5 mL microcentrifuge tubes. All subsequent processing and immuno-staining was performed in the microcentrifuge tubes.

Antigen retrieval was accomplished using 0.25% trypsin in PBS for 30 minutes at 37°C. Tissue slices were then treated with 1% Triton X for 20 minutes at 37°C and blocked against non-specific interactions using 2% normal goat serum for 10 minutes at room temperature. Several PBS washes were performed between each of the above processing steps.

Fixed-Frozen Tissue

Tissue slices to be used for simultaneous imaging of multiple extracellular matrix molecules were processed using the fixed-frozen protocol. After being cut from the intact menisci, tissue slices were transferred to 50 mL conical tubes and 10% neutral buffered formalin was added until all tissue was submerged. Tubes were maintained at 4°C for only 4 - 6 hours to allow for preliminary fixation of the tissue, but not extensive crosslinking. Formalin was then removed and replaced with a solution of 30% sucrose, and tubes were maintained at 4°C overnight. Tissue slices were then transferred to appropriately sized cryomolds and covered in Tissue-Tek O.C.T. compound. Finally, tissue slices were rapidly frozen using liquid nitrogen cooled isopentane and stored at -80°C until sectioning. Frozen tissue blocks were sectioned using a Microm Cryo-Star HM 560MV cryostat to 7 μm, carefully transferred to SuperFrost plus microscope slides, and stored at -80°C.

Immediately prior to immuno-staining, slides were removed from the -80°C freezer and allowed to dry at room temperature for 20 minutes. Sections were then fixed

with acetone for 5 minutes at room temperature in a chemical fume hood. Finally, sections were allowed to dry for at least 5 minutes and then rehydrated in PBS. Slides were transferred to Thermo Shandon Sequenza Slide racks and washed several times with PBS. Sections were treated with 0.1% Triton X for 15 minutes at room temperature and antigen retrieval was accomplished using 0.5% trypsin for 10 minutes at 37°C. Blocking of non-specific interactions was achieved by incubating sections for 1 hour at room temperature in PBS supplemented with 1% bovine serum albumin (BSA), 0.1% gelatin, 0.05% Tween-20, and 2% normal goat serum. Three washes with PBS were performed between each of the above processing steps.

3.2.2 Meniscus Tissue Immuno-Staining

Thick sections (50 μm) in microcentrifuge tubes were incubated overnight at 4°C with solutions of PBS plus 2% normal goat serum containing antibodies against either types I, II, or VI collagen or aggrecan. Primary antibodies were either raised against or had confirmed cross reactivity with bovine proteins. All primary antibodies were used at a 1:50 dilution; additional information can be found in Appendix D. According to information from the manufacturer, the primary antibodies against collagen molecules had been affinity purified and verified not to exhibit cross reactivity with other collagen subtypes. Sections were washed twice with PBS and again blocked with 2% normal goat serum for 10 minutes at room temperature. Fluorescently conjugated secondary antibodies appropriately matched to the primary antibodies for species and immunoglobulin subtype were diluted 1:100 in PBS. Sections were incubated with the secondary antibody solutions for 2-3 hours at 4°C before being thoroughly washed in PBS and mounted on microscope slides using aqueous gel mounting medium. Primary

antibody solutions also contained AlexFluor 546-phalloidin to label F-actin cytoskeletal proteins and secondary antibody solutions contained 0.1 μg/mL Hoechst 33258 to label DNA.

Fixed-frozen sections were incubated for 1 hour at room temperature in the Sequenza staining racks with solutions of PBS plus 1.0% BSA and 0.1% gelatin containing combinations of primary antibodies raised against types I, II, or VI collagen. The antibody against type I collagen was raised in a different species (mouse) than the antibodies against the other collagen molecules (rabbit) and therefore could be used in combination with either type II or VI collagen antibodies (see Appendix D). Dilutions of 1:100 were used for all primary antibodies. Appropriate combinations of fluorescently conjugated secondary antibodies were diluted 1:100 in PBS, added to the Sequenza racks, and maintained for 1 hour at room temperature. Finally, DAPI was used to counterstain nuclei and coverslips were mounted on the slides using aqueous gel mounting medium. As before, several PBS washes were performed between each of the above staining steps.

Negative controls were performed either by omitting primary antibodies from the immuno-staining solutions (formalin fixed tissue) or by substituting non-immune mouse and rabbit IgG molecules for primary antibodies (fixed-frozen tissue).

3.2.3 Extracellular Matrix Molecule Imaging

Thick sections (50 μm) were imaged using laser scanning confocal microscopy. An argon laser was used to excite green fluorescent molecules at 488 nm, a helium-neon laser was used to excite red fluorescent molecules at 543 nm, and an argon laser was used to excite blue fluorescent molecules at 364 nm. Zeiss LSM 510 software was used to collect and process images.

Thin, fixed-frozen sections were imaged using epifluorescence microscopy with a mercury lamp providing excitation for all fluorescent molecules. Individual filter cubes were used to view blue, green, and red fluorescence signals. Images for each fluorescence channel were captured individually with Q-Pro software and later combined using Adobe Photoshop. Images for all samples were obtained using identical exposure time settings for the digital camera.

All images presented here were obtained from medial menisci. However, images from lateral menisci typically revealed similar extracellular matrix molecule structure, organization, and distribution. Although some differences in biosynthesis have been found between fibrochondrocytes from medial and lateral menisci[99,124], an in depth structural comparison between them was beyond the scope of these studies.

3.3 Results

Variations in meniscal fibrochondrocyte actin cytoskeletal morphology throughout the tissue were clearly evident in the radial cross-sections and were similar to the vimentin structure previously reported in rabbit mensici[74]. The innermost zone of the meniscus contained predominantly rounded or oblong shaped cells with peripheral F-actin filaments, but cells exhibiting cytoskeletal projections were typically not seen (Figure 3.2A). Fibrochondrocytes containing extensive cytoskeletal projections and a more stellate morphology were increasingly found in the middle and outer regions of the meniscus (Figure 3.2B,C). Cells in the middle zone often maintained a rounded cell body with concentrated F-actin around the perimeter and typically had two or three small cytoskeletal projections consisting of well organized F-actin filaments. However, cells in

the outermost region typically possessed a less well defined cell body that had little associated F-actin. These cells contained numerous cytoskeletal projections extending in three dimensions and were characterized by punctuate F-actin staining. The morphological transition evident in fibrochondrocytes was in stark contrast to that seen in articular cartilage (Figure 3.3). In agreement with published reports[7], articular chondrocytes were found to exhibit morphological changes with distance from the tissue surface, transitioning from a flattened morphology aligned parallel to the surface to a spheroidal morphology of increasing size, but cells were always rounded or oblong and cytoskeletal projections were not evident.

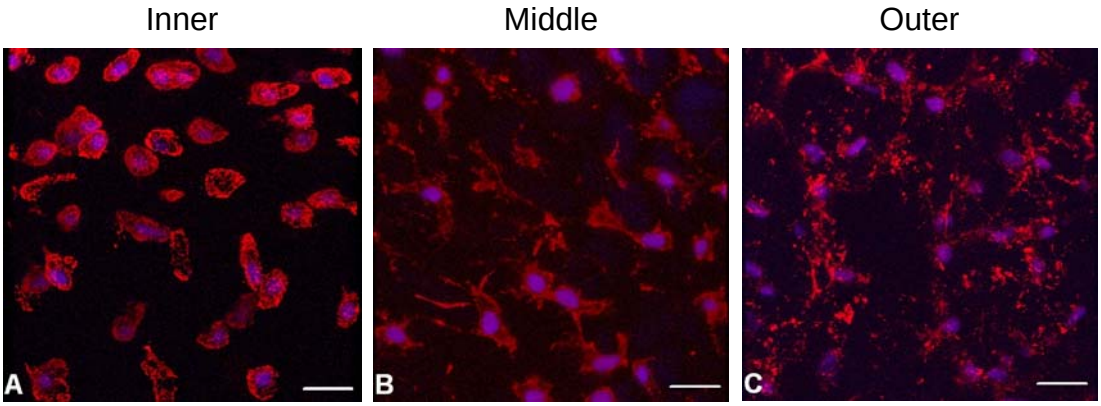

Figure 3.2 Meniscal fibrochondrocyte cell morphology transitioned from round in the inner zone to stellate in the outer zone. Red is F-actin, blue is DNA, scale bars are 20μm.

Images shown in Figure 3.2 are composites of many planar images representing a tissue thickness of 20 – 40 μm. Because cellular projections were often perpendicular to the plane of the sections, these three-dimensional images provided unique insights into

the fibrochondrocyte cell morphology that would not have been readily apparent using thin slices of tissue and conventional fluorescence microscopy.

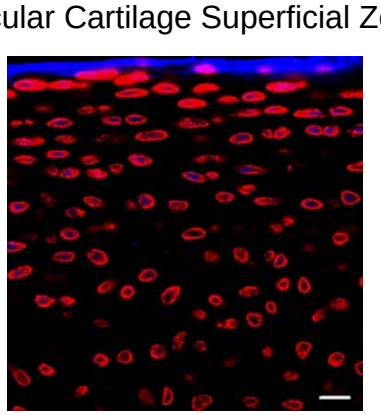

Figure 3.3 Articular chondrocyte cell morphology was flattened at the surface but round deeper within the tissue. Red is F-actin, blue is DNA and also designates the tissue surface at the top of the image, scale bar is 20 μm.

Confocal microscope images of extracellular matrix molecules in the immature bovine meniscus revealed several interesting structural and organizational features of the tissue. The intensity of staining for the G1 domain of aggrecan was found to decrease over radial cross-sections of the tissue. Aggrecan staining in the inner region was dense with additional localization in the pericellular matrix contributing to a semi-organized network interconnecting neighboring cells (Figure 3.4A). Staining intensity for aggrecan was lower in the middle zone and lower still in the outer zone (Figure 3.4B,C). Aggrecan in the outer zone was found in an organized network that appeared to both surround large fiber bundles and subdivide them into smaller compartments.

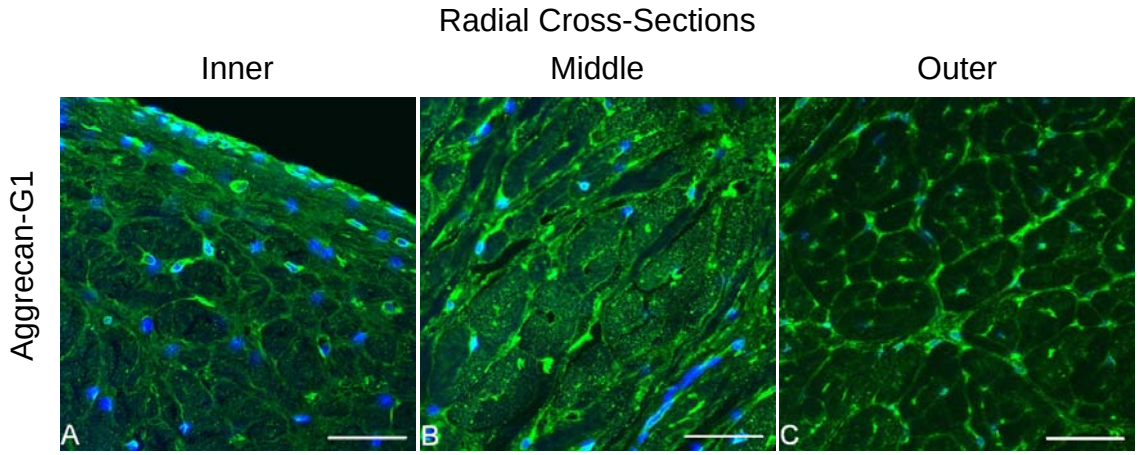

Figure 3.4 Confocal microscope images of aggrecan distribution and organization in three zones of radial cross-sections of medial menisci. Green is the G1 domain of aggrecan, blue is DNA, and scale bars are 50 μm.

The organization of collagen molecules was also found to vary throughout radial cross-sections of the meniscus and several differences among specific collagen types was also noted. Staining for type I collagen was diffuse in the inner zone, but appeared highly organized in the middle and outer zones (Figure 3.5A-C). Large fiber bundles perpendicular to the plane of the images were seen in both the middle and outer zones. Additionally, somewhat smaller fibers oriented parallel to the image plane (referred to as radial tie fibers[63,64]) were positive for type I collagen. Fibrochondrocytes in the middle and outer zones were most often found at the junctions of the collagen fiber network as well as along the radially oriented tie fibers.

Type II collagen staining was found in a similar pattern to that seen for type I collagen (Figure 3.5D-F). The inner zone exhibited diffuse, mostly unorganized type II collagen, although more intense staining was found pericellularly as well as near the

tissue surface. The middle and outer zones, however, contained a highly organized network of fibers. Although staining seemed to be more intense in the inner zone, type II collagen was found throughout the cross-section of the meniscus up to the outermost rim.

Some interesting distinctions between type VI collagen staining and the other collagen molecules studied were evident (Figure 3.5G-I). First, type VI collagen seemed to be more organized in the inner region compared with the other collagens. Intense staining was seen surrounding cells, similar to that found in articular cartilage (not shown), but type VI collagen also appeared to be organized in the interstitial areas between cells. Discrete fibers of varying sizes were clearly evident and often branched between multiple cells. Overall, the organization of type VI collagen staining in the middle and outer regions was similar to that seen for types I and II collagen, but a finer meshwork of fibers was found. Type VI collagen was clearly organized into larger bundles perpendicular to the image plane, but was also more often found in the intrabundular space compared with the other collagens. The presence of type VI collagen in the space within the larger collagen fiber bundles was a consistent and potentially a functionally important distinction from types I or II collagen. Additionally, very intense staining for type VI collagen was seen in the radial tie fibers in the middle and outer tissue zones. Negative controls lacking primary antibodies exhibited very little signal in all cases.

As discussed above, fibrochondrocyte cell morphology varied over the meniscal cross-sections, a feature that was also evident in sections stained for type VI collagen (Figure 3.5G-I). In contrast to the other extracellular matrix molecules examined in this study, regardless of the tissue zone, type VI collagen was found in the pericellular matrix

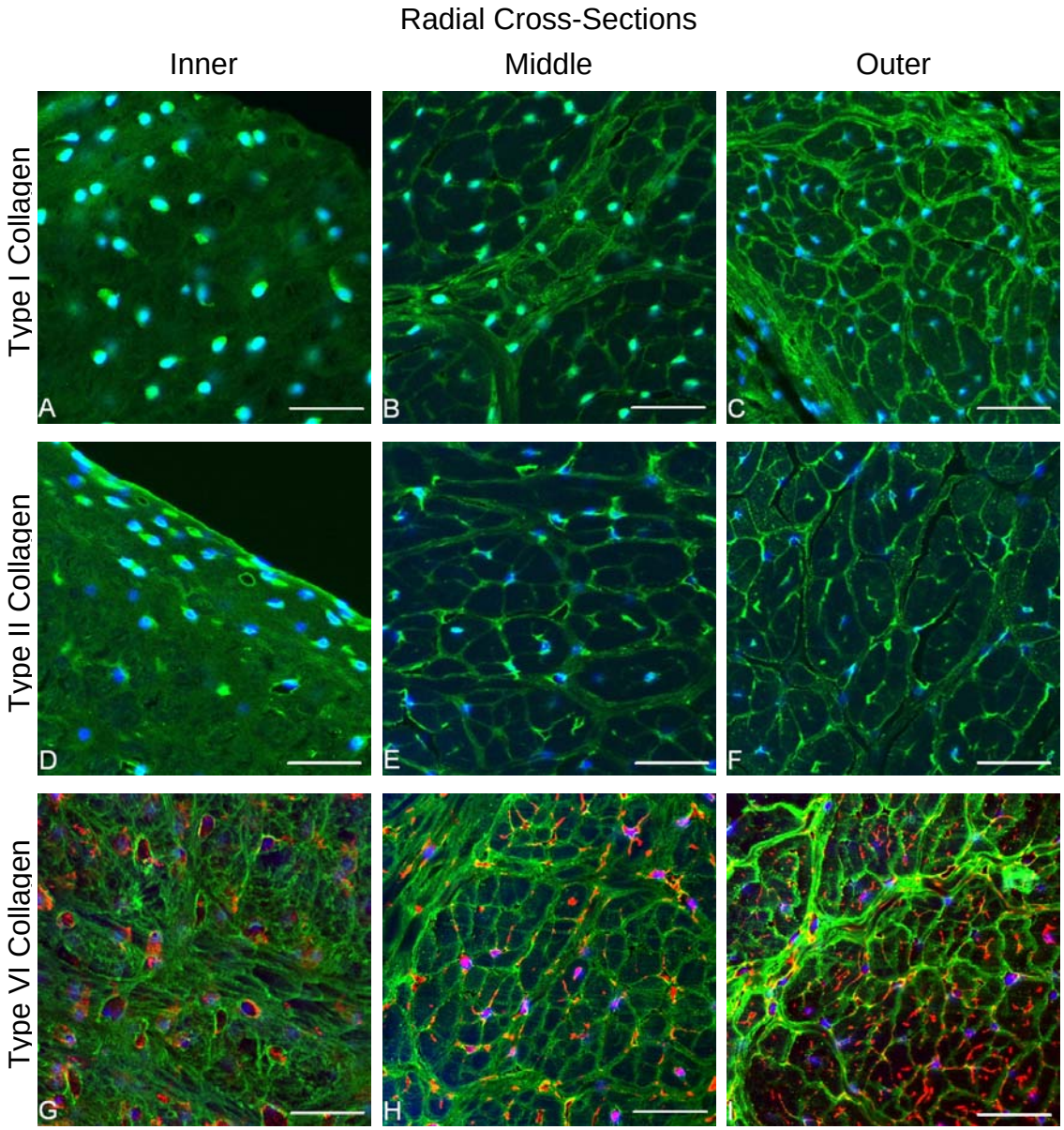

Figure 3.5 Confocal microscope images of collagen organization in three zones of radial cross-sections of medial menisci. Green is the indicated collagen molecule, blue is DNA, and red is the F-actin cytoskeleton (type VI collagen images only). Scale bars are 50 μm.

immediately surrounding the resident fibrochondrocytes. In the middle and outer zones, cytoskeletal projections, evidenced by F-actin staining, were found to colocalize with and often oriented along the type VI collagen network. Since the overall organization in the middle and outer zones was similar among all three collagen molecules imaged, cellular projections could be seen oriented along types I and II collagen as well. However, this feature was most prominent in the sections stained for type VI collagen, perhaps due to the finer type VI collagen network. In fact, if the green fluorescence channel showing the collagen network was turned off, leaving only the channels showing the actin cytoskeleton and DNA visible, the organized network in the middle and outer zones of the tissue could still be detected based solely on the location and orientation of the resident fibrochondrocytes.

Images of the collagen extracellular matrix from circumferential cross-sections (see Figure 3.1 for details on tissue sample orientation) revealed further distinctions in meniscal collagen organization. Large, circumferentially oriented fibers, parallel to the image plane in this view, stained heavily for type I collagen (Figure 3.6A); whereas smaller, similarly oriented fibers stained positive for types II and VI collagen (Figure 3.6B,C). These smaller fibers were spread out, typically with 10 – 20 μm spacing between areas of more intense staining. The relative fiber sizes and spacing of the three collagen molecules imaged suggested that the large circumferential type I collagen fiber bundles are surrounded or even lined by smaller type II and VI collagen fibers. Cell bodies were typically only found in areas that stained positively for type II or type VI collagen, often being completely surrounded. This finding indicated that fibrochondrocytes may directly interact with types II or VI collagen *in situ*.

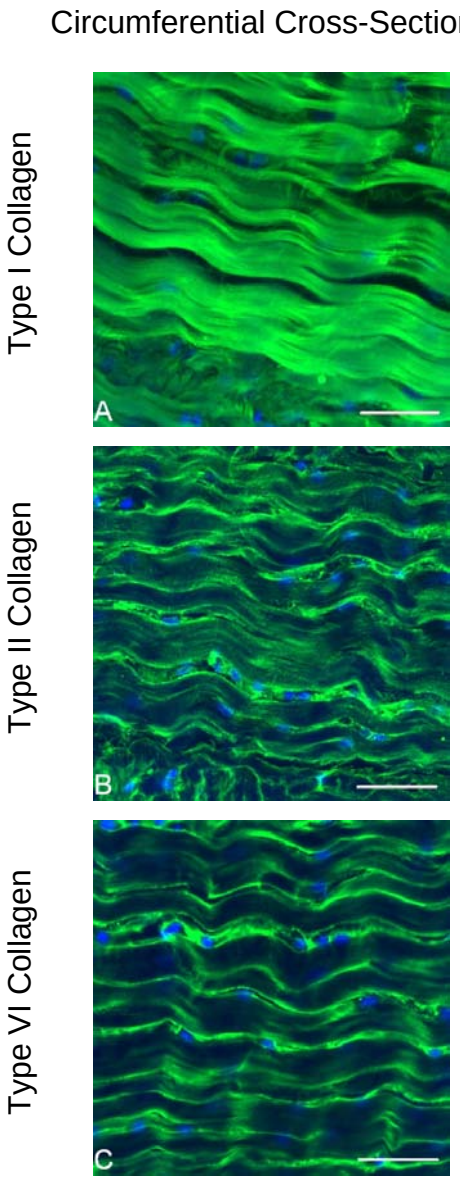

Figure 3.6 Confocal microscope images of collagen organization in circumferential cross-sections of medial menisci. Tissue slices used for these images were taken from the outer zone of the meniscus. Green is the indicated collagen molecule and blue is DNA. Scale bars are 50 μm.

Fixed-frozen meniscus sections simultaneously immuno-stained for multiple collagen molecule types exhibited similar patterns for the individual collagen types as the sections described above. Images from the co-stained sections, however, provided additional insights into the relative locations of the three collagen molecules. Sections co-stained for types I and II collagen produced images very similar to those reported by Kambic and McDevitt[64] (data not shown). Colocalizaion of types I and II collagen was most striking in the outer zone, because type I collagen was fairly diffuse in the inner zone. The outer zone contained large fiber bundles that stained positively for both collagen types as well as radial tie fibers, which stained somewhat diffusely for type I collagen, but more discretely for type II collagen. From the combined images it was clear that type II collagen appeared nearly everywhere that type I collagen was present. In addition, type II collagen tended to stain more intensely than type I collagen in the finer network of fibers that existed between larger circumferentially oriented fiber bundles.

Sections co-stained for types I and VI collagen also yielded striking images that provided interesting insights into the spatial relationship of these two molecules (Figure 3.7 and Figure 3.8). Images of the inner zone again showed an intricate network of type VI collagen but diffuse staining for type I collagen (Figure 3.7A,B). The combined images indicated that there was some degree of colocalization throughout the tissue section, most likely due to the diffuse nature of type I collagen (Figure 3.7C). Additionally, areas surrounding cells evidenced increased staining intensity for both matrix molecules and therefore a greater degree of colocalization was seen in these areas.

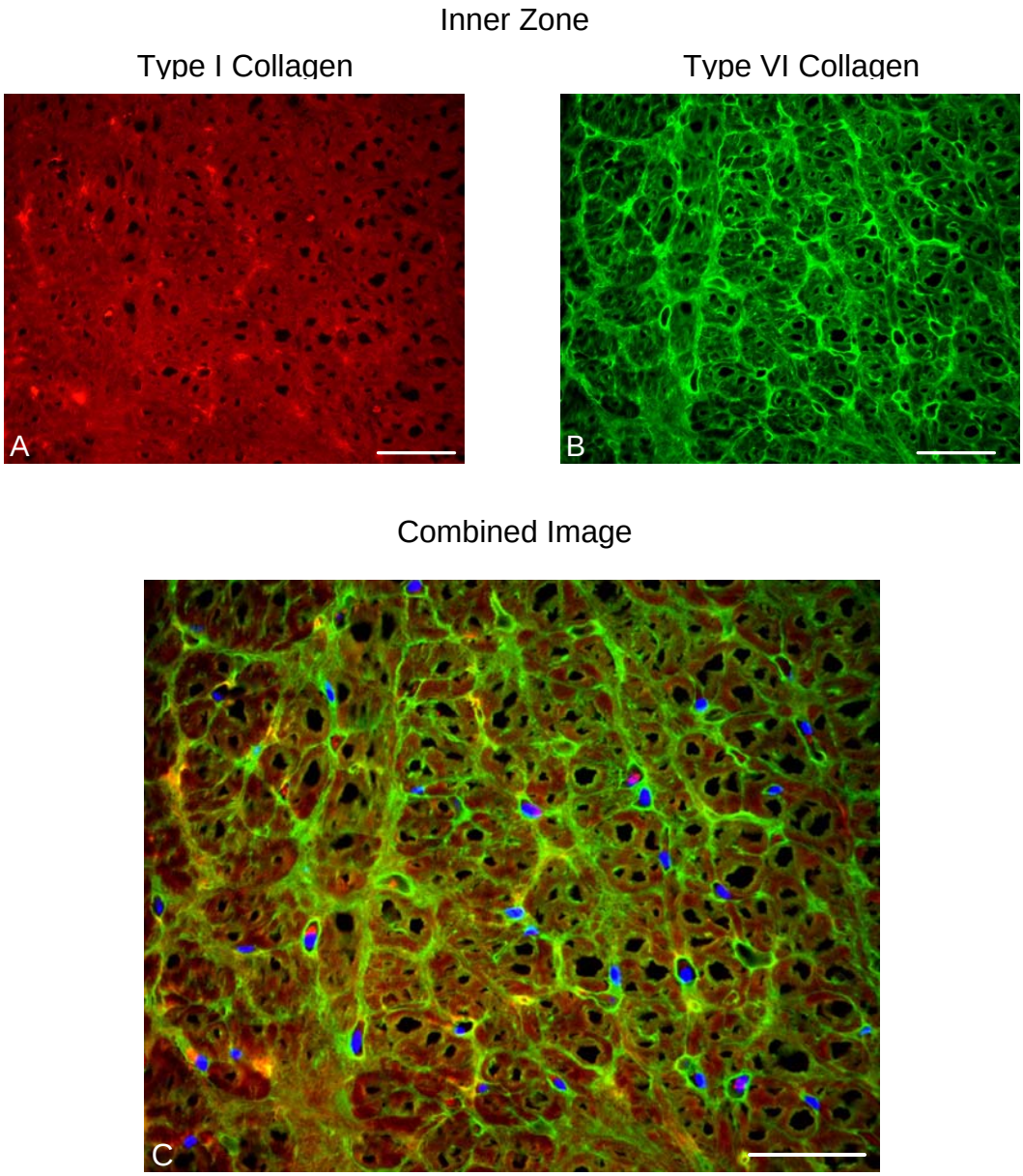

Figure 3.7 Colocalization of types I and VI collagen in the inner zone of the medial meniscus. (A) and (B) are individual images of type I and type VI collagen, respectively, and (C) is the overlay of these two images plus the blue fluorescence channel. Red is type I collagen, green is type VI collagen, and blue is DNA. Areas of yellow indicate colocalization of types I and VI collagen in (C). Scale bars are 50 μm.

In the outer zone, types I and VI collagen were predominately found to colocalize along large fiber bundles (Figure 3.8C). Careful inspection of the images revealed that these large fiber bundles stained positive for type I collagen across their entire thickness, whereas type VI collagen staining was most intense at the periphery. This observation indicated that type VI collagen lines the outside of the larger type I collagen bundles. Interestingly, in the outer zone less colocalization was found in the area immediately surrounding the cells than what was seen in the inner zone. The pericellular matrix in the outer zone nearly always stained intensely for type VI collagen, but not necessarily for type I collagen. Additionally, intense colocalization was found at fiber junctions, especially where multiple large fibers came together. Negative controls using non-immune IgG molecules in place of primary antibodies exhibited minimal signal for all tissue zones and sections imaged.

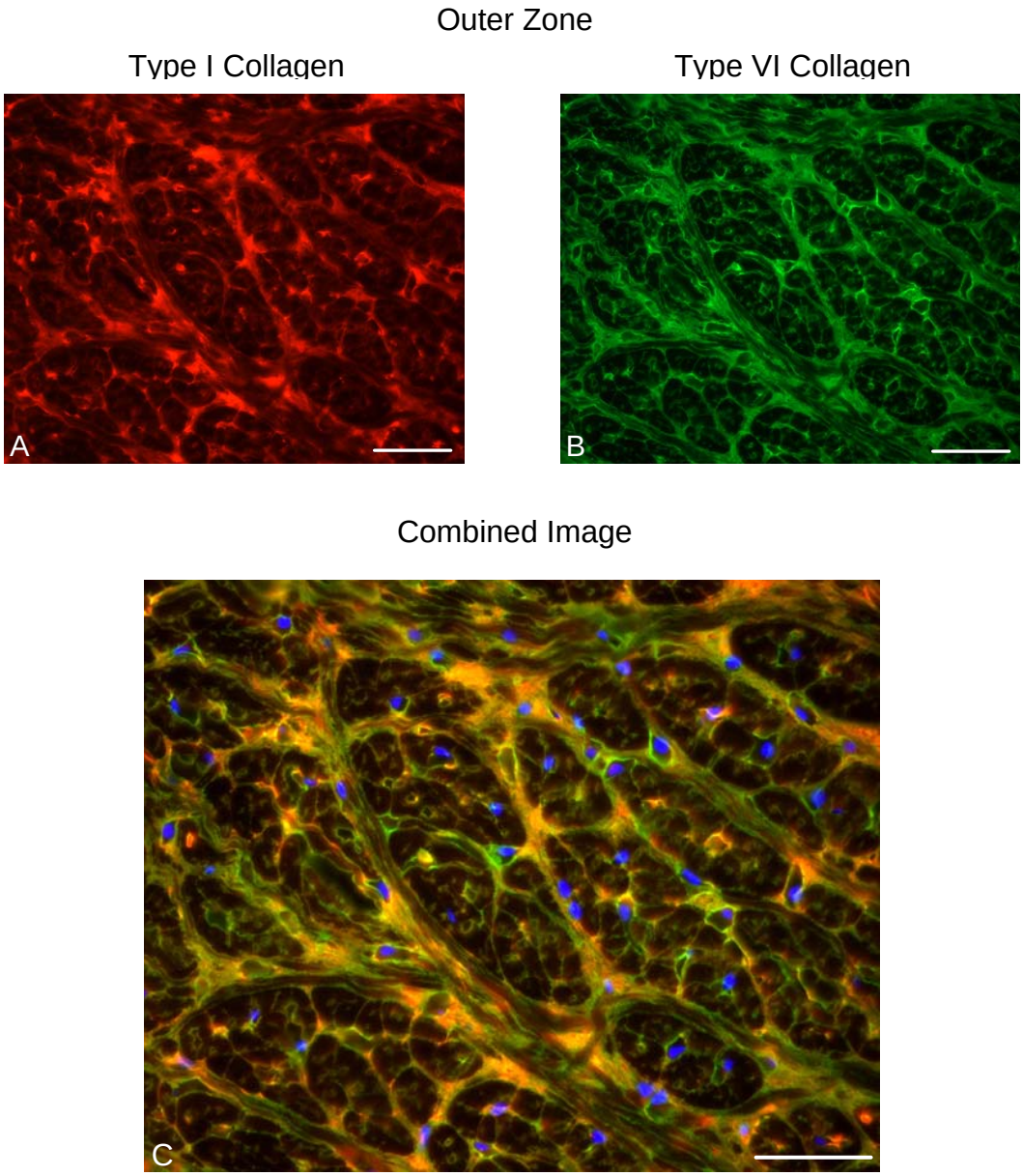

Figure 3.8 Colocalization of types I and VI collagen in the outer zone of the medial meniscus. (A) and (B) are individual images of type I and type VI collagen, respectively, and (C) is the overlay of these two images plus the blue fluorescence channel. Red is type I collagen, green is type VI collagen, and blue is DNA. Areas of yellow indicate colocalization of types I and VI collagen in (C). Scale bars are 50 μm.

3.4 Discussion

Not long ago it was believed that the menisci were nothing more than evolutionary remnants of perhaps muscle or other musculoskeletal tissues. However, a mounting body of evidence has shown that the menisci play a critical role in knee joint biomechanics[56,125-127] and their full or partial removal adversely affects the neighboring articular cartilage, often leading to osteoarthritis[2,80]. The matrix composition and ultrastructure of the menisci give these tissues mechanical characteristics that are well adapted to performing their biomechanical role in the body[57]. In particular, the large circumferentially oriented collagen fibers in the outer regions of the meniscus seem well suited for supporting the tensile hoop stress that develops in this region during joint loading[62]. In addition to correlating meniscal mechanical properties with the organizational features of primary matrix constituents, efforts to further elucidate and understand the functional roles of less abundant extracellular matrix molecules have been ongoing[60,69,128,129]. Although many different extracellular matrix molecules have been identified in the meniscus, there remains a limited understanding of how these molecules may relate to and interact with one another. Thus, the goal of the studies presented in this chapter was to investigate the structural complexities of bovine meniscal tissue and explore the spatial relationships that exist between various extracellular matrix molecules.

The images of immunolocalized extracellular matrix molecules in the immature bovine meniscus described in this chapter provided a detailed view of meniscal ultrastructure and matrix organization. Immunolocalization patterns for types I and II collagen were consistent with a recently published report[64]. Type I collagen was found to

be diffuse in the inner zone of medial menisci, but organized into large circumferentially oriented bundles in the middle and outer zones. Additionally, radially directed tie fibers were found throughout the middle and outer regions and stained diffusely for type I collagen. The inner zone contained type II collagen that seemed to be somewhat more organized with significant staining immediately surrounding cells, especially those near the surfaces of the tissue. The middle and outer zones exhibited highly organized type II collagen fibers in patterns similar to those seen for type I collagen. Additionally, images from the circumferential cross-sections reinforced the observation that the type II collagen fibers seemed to surround the larger type I fibers in the outer zone of the meniscus.

An interesting difference between the results of our studies and those of Kambic and McDevitt[64] was that we found positive staining for type II collagen well into the outer region of the immature bovine meniscus, whereas they reported an abrupt loss of type II collagen signal in the outer zone of mature canine menisci. This loss of type II collagen staining coincided with the vascularized region of the meniscus, approximately 10-12% of the length of the tissue cross-sections. Although some decline in type II collagen staining intensity in the outer zone was found in our studies, it was both subtle and gradual. Additionally, we found vascular structures, evidenced by circular or oblong clusters of cells staining heavily for F-actin filaments, in the midsubstance of the immature tissue. No attempt was made to quantify this observation, but it was clear that the region containing blood vessels was greater than 10-12% of the cross-section length. The difference seen in the degree of vascularization and potentially in the type II collagen distribution was likely due to the different ages of the tissue investigated, as the meniscus

is known to become less vascularized with age[61]. A careful comparison of meniscal tissue from various aged animals of the same species correlating vascular structures with a lack of matrix molecules typically found in hyaline cartilage (*i.e.* type II collagen and aggrecan) could test this hypothesis and provide insights into meniscal structure and developmental patterns.

A preliminary study of this kind was performed in our laboratory with bovine menisci of several ages (4 weeks, 8 weeks, and 2-3 years old). Type II collagen staining was decreased in the outer region of 8 week old animals compared to 4 week old animals, although similar structural features were evident in menisci of both ages. Additionally, the 2-3 year old menisci had greatly reduced staining for type II collagen in all regions, indicating age-related changes in type II collagen that may have affected the accessibility of the epitope recognized by our primary antibody. However, neither the distribution nor organization of type VI collagen was dramatically affected by age. This preliminary study suggested that some components of the extracellular matrix in the bovine meniscus may be affected by aging; however, further work is necessary before more definitive conclusions can be drawn.

Staining for the G1 domain of aggrecan was intense, but lacked extensive organization in the inner zone of the meniscus. However, aggrecan in the middle and outer zones was organized in a highly ordered network, but stained at progressively lower intensities. The distribution of aggrecan found in our studies was consistent with reports describing the proteoglycan distribution and aggrecan gene expression profiles in different zones of the meniscus[64,69,120]. Another study investigating the distribution of a number of matrix molecules, including aggrecan, in ovine menisci of varying ages

showed a similar aggrecan distribution in young animals (2 and 7 days old), but a uniform aggrecan distribution over meniscal cross-sections from older animals (1.5 and 10 years old)[122]. However, images of the same specimens stained with toluidine blue, which reacts with all anionic proteoglycans, exhibited areas of lower staining intensity in the middle and outer tissue zones regardless of animal age. This difference could be due to a loss of heavily sulfated glycosaminoglycan chains known to occur in fibrocartilage and articular cartilage with age[130,131], but retention of the hyaluronic acid binding region of aggrecan, the target of the primary antibody. However, our studies in immature bovines as well as those of Valiyaveettil *et al.*[120] in skeletally mature canines used primary antibodies directed against a similar region of aggrecan. In both cases the staining intensity for aggrecan was lower in the outer zone of the meniscus. Therefore, perhaps the differences found in aggrecan distribution were the result of inter species variation or even differential binding characteristics of the antibodies used. Taken together, our data and the published studies cited above indicated that the inner zone of meniscal tissue contains relatively high levels of aggrecan regardless of species or age, whereas the outer zone may contain decreased amounts of aggrecan, which is organized into an interconnected network.

The observed spatial distribution for types I and II collagen and aggrecan in our studies was consistent with proposed structure-function relationships of the meniscus where compressive forces that develop in the inner zone are primarily resisted by proteoglycans, and large circumferential tensile forces that develop in the outer zones are resisted by collagen fibers. Although the role for aggrecan in the inner zone of the meniscus seems clear, its function in the outer zone is less well established. An emerging

related hypothesis is that proteoglycans in the fibrocartilaginous regions of tendons serve to provide some compressive stiffness as well as separate and allow collagen fibers to slide relative to one another during deformation[132]. Aggrecan as well as the small leucine rich proteoglycan decorin have be identified in tendons in remarkably similar patterns to those shown here for meniscus[132-134]. The organized network of aggrecan we observed in the outer region of the meniscus, which seemed to localize at the periphery of large, circumferentially oriented type I collagen fiber bundles, could serve a similar role in meniscal tissue.

Type VI collagen is ubiquitous in connective tissues, and has been identified in meniscus and other fibrocartilages[60,65,135]. Naumann *et al.*[123] described weak type VI collagen staining in the matrix and moderate staining in cellular and pericellular regions of rabbit menisci; however the images were taken at low magnification and detailed spatial and organizational analyses was not performed. Additionally, it has been reported that type VI collagen is located primarily in the interterritorial regions of the meniscus matrix[60]. In our studies, type VI collagen was immunolocalized in areas immediately surrounding cells as well as in an interconnected network throughout cross-sections of the tissue. To our knowledge these are the most detailed images of type VI collagen in the meniscus to have been presented. In addition, the cytoskeletal projections of fibrochondrocytes located in the middle and outer zones of the tissue were often oriented along and colocalized with type VI collagen. These cells were predominately found at fiber junctions and bifurcations, but could also be seen along the radial tie fibers. Finally, images of circumferential cross-sections revealed thin type VI collagen fibers spaced in

such a way that indicated they were located at the periphery of the larger type I collagen fibers.

Both articular chondrocytes[136] and meniscal fibrochondrocytes[137] have been shown to directly attach to type VI collagen *in vitro*, and type VI collagen has been shown to interact with a number of extracellular matrix molecules[25,138]. Thus, this protein may provide a functional link between cells and the extracellular matrix. Our investigations supported this hypothesis. The images presented in this chapter strongly suggest that the pericellular matrix, and thus the local cellular microenvironment, is rich in type VI collagen throughout the meniscus. Types I and II collagen were also found in the pericellular matrix, but not as consistently as type VI collagen. These findings have a number of implications for fibrocartilage and potentially articular cartilage tissue engineering.

Many outcome measures for cartilage and fibrocartilage tissue engineering focus on major matrix components (*i.e.* types I and II collagen and aggregating proteoglycans), which are most responsible for the mechanical integrity of these engineered tissues. However, the images presented in our studies suggest that these matrix molecules may not be the most prominent in areas directly surrounding cells in the meniscus. The native microenvironment of a fibrochondrocyte may consist mostly of type VI collagen, and thus when attempting to recreate an extracellular matrix in an engineered tissue it may be equally important to promote the development of an appropriate pericellular matrix. Therefore, a successful tissue engineered fibrocartilage replacement may not only need a highly organized network of oriented collagen fibers, but also a pericellular matrix rich in

type VI collagen providing a mechanical and cell signaling environment similar to native tissue.

In addition to strong pericellular staining, type VI collagen was found in an intricate network of fibers colocalized around the periphery of large type I collagen fiber bundles. This structural hierarchy is similar to that seen in tendon fibrocartilages[132,135], and may have functional implications for the meniscus during normal joint loading, degradation, and repair. It is not clear what role type VI collagen plays in the meniscus, however images from our studies suggest several possibilities. Since type VI collagen is known to interact with hyaluronan[138] and small proteoglycans[25], it may participate in the organization of these proteoglycans at the surface of type I collagen fibers. An organized proteoglycan network surrounding the collagen fiber bundles, as discussed above, could both provide structural support during compressive loading as well as facilitate collagen sliding during tensile loading. Type VI collagen may also function as a cell attachment protein in the meniscus, and the sheath-like organization surrounding the larger type I collagen fibers could be a product of cellular matrix synthesis and migration during tissue development or provide an ongoing means of cellular migration during tissue maintenance or repair.

The studies described in this chapter provided an in depth investigation of the structure, distribution, and organization of several extracellular matrix molecules in the immature bovine meniscus. Differential organization patterns were seen in the inner and outer zones of the meniscus for aggrecan and types I, II, and VI collagen. Additionally, the distribution of aggrecan was found to vary over cross-sections of the meniscus in a pattern consistent with typical proteoglycan contents found in each tissue zone. Images

of type VI collagen revealed a network of fibers organized around larger type I collagen fiber bundles that had not been previously described in detail. These studies add to the overall understanding of meniscus structure and its complexity. The ability to visualize the extracellular matrix organization in the meniscus using high magnification images produced using highly specific immunohistochemical techniques also provides insights into the potential function of these matrix molecules and how they may interact with one another. Finally, efforts to develop tissue engineered replacements for a damaged or diseased meniscus can be greatly enhanced by understanding the complexities of cell and extracellular matrix organization. The detailed images presented in this chapter could be used to develop a design template for tissue engineered scaffolds as well as to provide histological benchmarks for cellular and matrix organization in tissue engineered constructs.

CHAPTER 4

DESIGN AND VALIDATION OF A NOVEL BIOREACTOR: THE OSCILLATORY TENSILE LOADING DEVICE

4.1 Introduction

The ability to apply well-defined mechanical stimuli to cells and tissues has been pivotal in furthering the understanding of both the biomechanical properties and the mechanobiology of many biological systems. In addition to simply measuring the mechanical characteristics of these systems, much can be learned by stimulating (or suppressing) biological processes via alterations to the mechanical environment. Dozens, of different types of devices, often referred to as *bioreactors*, have been developed to apply a myriad of forces, displacements, or flows to cells and tissues. Some of these systems can be very simple, merely supplying a circulating supply of culture medium, whereas others can be quite complex, imparting well defined mechanical compression[139,140] or shear[101], uniform fluid induced shear stress[105], tightly controlled medium perfusion[141], or some combination of these.

For this thesis research, a bioreactor capable of applying oscillatory tensile displacements to tissue engineered constructs was necessary. Although bioreactors capable of applying tensile stretch to monolayer cultures[142] were commercially available, no comparable system for three-dimensional tissue or constructs existed. Thus, the design and development of a novel bioreactor device was required.

4.2 Design Considerations

Once the overall goal of designing a device capable of imparting oscillatory tensile loads to three dimensional tissue engineered constructs had been established, it was necessary to develop more specific design criteria. Although no commercially available bioreactor met this overall design goal, a review of the relevant literature was conducted to assess the advantages and disadvantages of a variety of bioreactors[143,144] and identify specific features that would ultimately guide system development. Initially, these criteria were fairly modest and can be summarized as three main specifications. The following criteria served as guides for the first generation oscillatory tensile loading system design (Figure 4.1A) and remained important for each successive generation of the system.

(1) The ability to deliver oscillatory tensile displacements of at least 10% strain at a frequency of at least 1.0 Hz

(2) The ability to culture tissue engineered constructs in individual wells, allowing for analysis of conditioned media and using radioactive precursor molecules to assess extracellular matrix synthesis, as well as the ability to culture multiple samples in parallel providing statistical power

(3) The ability for the entire system to fit within a standard tissue culture incubator without the need for modifications, such as custom ports for cabling or a drive mechanism

After the first generation system was built, tested, and used as a proof of concept for subjecting tissue engineered constructs to oscillatory tensile loading, more rigorous design criteria were developed. This process was incremental, as shown in Figure 4.1, but ultimately the following final design criteria were implemented in addition to those stated above.

(1) Closed loop position feedback with computer control and custom programming capability
(2) Generation of uniform strain fields across and along the constructs during loading
(3) Use of relatively small tissue engineered constructs (< 1.0 mL volume) and therefore smaller culture media requirements (< 2.0 mL volume)
(4) Increased sample capacity for greatly experimental flexibility
(5) Simple to assemble, use, and disassemble rapidly and repeatably
(6) Relatively low per unit material and component cost (< $5,000)

Upon completion of the final design a novel bioreactor device had been developed (Figure 4.1D), which met or exceeded all of the stated requirements. This device, in itself, represented a unique contribution to the field of tissue engineering and provided the opportunity for an experimental system that would have otherwise been impossible. The oscillatory tensile loading device was designed to be extremely versatile with respect to the loading protocol employed as well as the size of the constructs used in the device, and therefore could be implemented in a wide variety of applications.

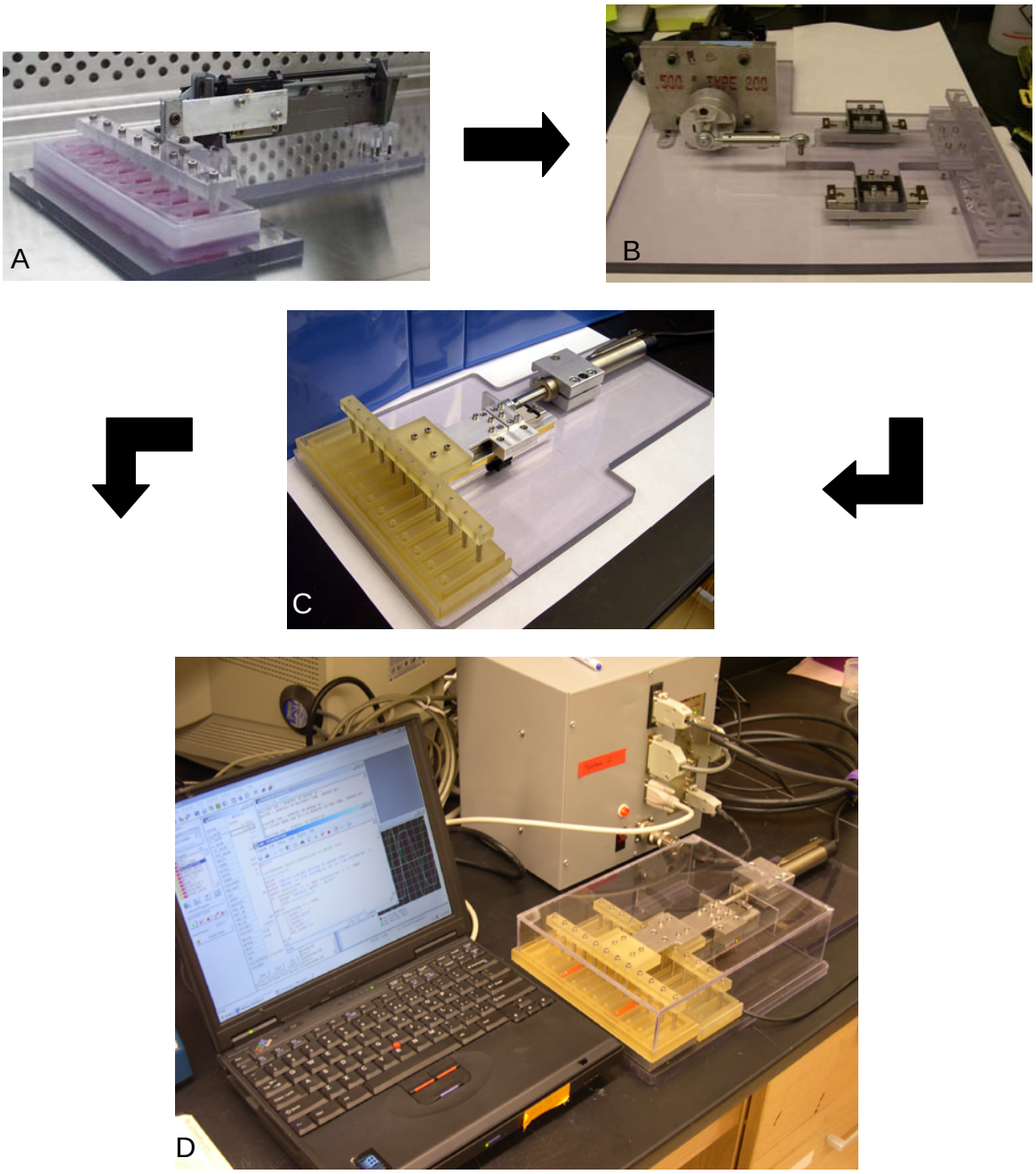

Figure 4.1 The design evolution of the oscillatory tensile loading device. (A) Initial device design satisfying preliminary design requirements. (B) Subsequent device design. (C) Penultimate device design. (D) Final device design meeting all design criteria shown with the control box and accompanying computer.

4.3 The Oscillatory Tensile Loading Device

The final design for the oscillatory tensile loading device (Figure 4.2) can be broken down into four essential components: (1) the linear motor, (2) the linear slide bearing, optical encoder, and interface adapters, (3) the mobile "tension rake" pieces, and (4) the stationary culture chambers. Additionally, a control unit is required, which houses the power supplies, amplifier, and controller for the device and interfaces with a computer. Engineering drawings for all parts of the device as well as a detailed list of the components can be found in Appendix A. Additionally, the operating instructions and the source code for the programs used during operation can be found in Appendix A.

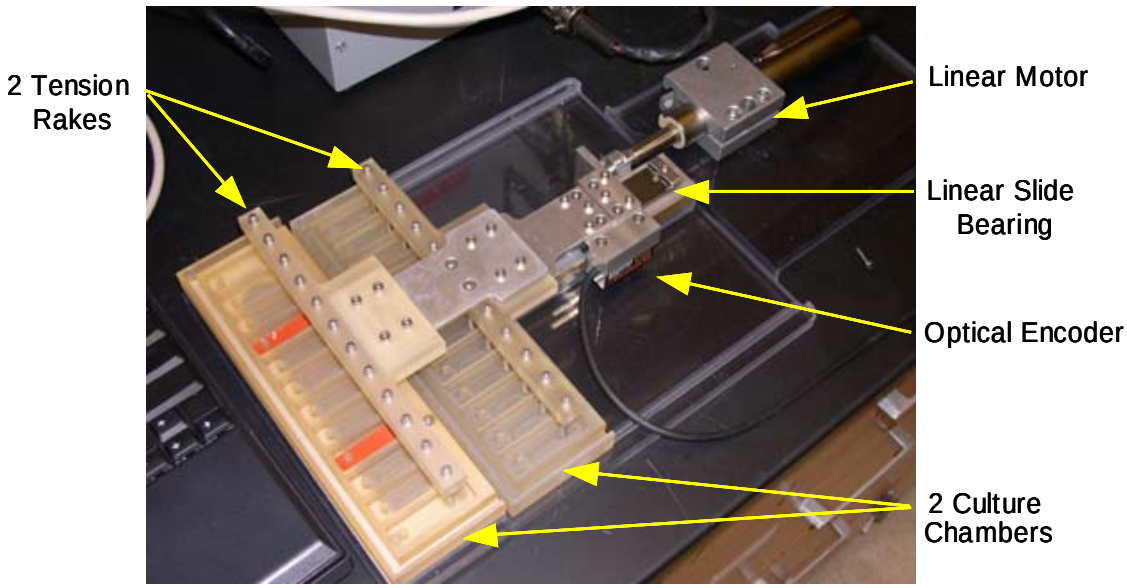

Figure 4.2 Final design of the oscillatory tensile loading device

The linear motor is mounted toward the rear of the polycarbonate base plate via a heat sink block. This method of attachment is preferred because it not only firmly connects the motor with the rest of the system, but also provides optimal heat dissipation away from the motor and guarantees maximum performance. A misalignment coupling is used to interface the motor with the linear slide bearing. This coupling assures that small inaccuracies in the position of the motor or slide bearing do not damage the motor or reduce overall device performance.

The linear slide bearing consists of a stainless steel rail interfaced with a block containing two rows of stainless steel ball bearings and is mounted on an aluminum block such that the motor can be connected at the appropriate height. The block on the linear slide bearing is fitted with three additional aluminum adapter pieces. The first adapter piece connects to the misalignment coupling and consequently the linear motor. The second adapter piece connects to the optical encoder and allows the encoder to read the position scale on the side of the aluminum spacer block. The optical encoder has a precision of 0.5 μm allowing for accurate position feedback to the controller. The final adapter piece interfaces with the mobile tension rake and ultimately enables the transfer of motion from the motor to the tissue engineering constructs.

The body of each mobile tension rake is made from polysulfone, chosen for its resistance to corrosion in humid environments and when in contact with saline based solutions. Twelve 4.0 mm diameter x 25 mm long stainless steel pins fit into the long, narrow end of the tension rake and are held in place with short 4-40 stainless steel socket head cap screws. Opposite the pins in the tension rake is a wide, shallow slot that loosely fits over the interface adapter, attaching the tension rake to the linear slide bearing. A

second tension rake can be attached using an additional aluminum interface adapter in a similar fashion (see Figure A.3 in Appendix A for a schematic of the tension rake).

The final essential component used with the oscillatory tensile loading device is the stationary culture chamber, which is also made from polysulfone. Two culture chambers can be used simultaneously in the device. Each culture chamber has twelve rectangular wells uniformly spaced over the length of the chamber. On one end of each well is a fixed 4mm diameter peg while on the other end is a 4.75 mm wide by 8.0 mm long slot. The culture chambers attach to the base plate such that the pins on the tension rakes align with slots in each well. The primary culture chamber is attached directly to the base plate, whereas the secondary culture chamber is raised approximately 12 mm by an aluminum spacer plate. Finally, the culture chambers, tension rakes, and linear slide bearing assembly can be covered with a polycarbonate shield to maintain sterility when transferring the device from the tissue culture hood to the incubator.

4.4 Hydrogel Constructs Used with the Oscillatory Tensile Loading Device

Developing a system to study the effects of oscillatory tension on cells within in a three dimensional hydrogel matrix also required careful design of tissue engineered constructs. Thus, in parallel with the oscillatory tensile loading device, constructs with a unique geometry and device interface features were developed. One of the important design criteria for the final system was that uniform strain fields would be generated across the width and down the length of the constructs. Early construct designs were oval in shape and consisted entirely of the fibrin hydrogel, but finite element modeling of this

design predicted highly non-uniform strain fields.[145] Therefore, a new construct design was implemented to address this concern (Figure 4.3).

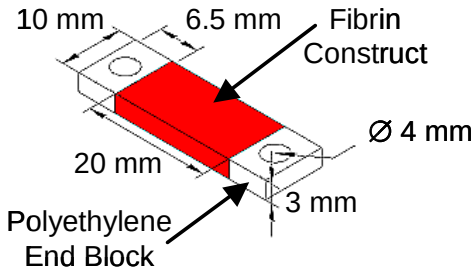

Figure 4.3 Fibrin construct used with the oscillatory tensile loading device.

The hydrogel material used in all studies presented in this dissertation was fibrin, the primary protein in blood clots. Fibrin spontaneously assembles when the enzyme thrombin cleaves 4 specific Arg-Gly peptide bonds on the molecule fibrinogen[146]. Globular domains on fibrinogen molecules possess binding sites specific to the amino acid sequence revealed by this enzymatic cleavage. Upon hydrolysis, the exposed peptide groups bind with the globular domains of adjacent fibrin monomers in a process called fibrilogenesis. Many fibrin monomers come together to form large, linear arrays. This fibrin structure is stabilized via amide bonds that form between side chains of the monomers in a reaction catalyzed by transglutaminase, also known as clotting factor XIIIa. Fibrin clots can be dissociated by plasmin, a serine protease that cleaves fibrin in its central α-helical coiled coil region[147].

Fibrin has been extensively used as a tissue engineering scaffold for a wide variety of cell types[148-151], including chondrocytes[140,152-154] and fibrochondrocytes[97]. The mechanical characteristics of fibrin hydrogels made them particularly attractive for the studies conducted for this dissertation. Fibrin hydrogels have viscoelastic properties in both tension and compression, and perhaps most importantly are highly extensible unlike some other hydrogel scaffolds, such as agarose. Additionally, chondrocytes[152], smooth muscle cells[148], and fibroblasts[155] have all been shown to exhibit increased levels of extracellular matrix synthesis when cultured in hydrogels composed of fibrin as opposed to type I collagen. Finally, many cells types can bind to fibrin or other adhesion molecules known to associate with fibrin (such as fibronectin) via integrin receptors[156,157] allowing for direct mechanotransduction between the hydrogel and the embedded cells. Hydrogels, such as alginate and many poly(ethylene glycol) based scaffolds, do not possess cellular binding sites. Therefore, fibrin was a favorable choice because forces generated during oscillatory tensile loading could be directly transmitted to cells embedded within the fibrin matrix.

A key design feature of the hydrogel construct was the polyethylene end blocks located at either end of the rectangular constructs. These end blocks were cut from porous polyethylene sheets with an average pore size of 15 – 45 μm and an average porosity of 50% (Porex, POR-4898). Additionally, the polyethylene sheets had been treated with a surfactant making the material hydrophilic. Rectangular end blocks (10 mm x 6.5 mm x 3 mm) were cut and a centered 4 mm diameter hole was punched in the blocks using a custom designed set of tools (see Appendix A). Finished end blocks were loaded into custom polycarbonate molds and the assembly could be sterilized via

autoclaving prior to construct preparation. Since the smooth polycarbonate surface of the molds was hydrophobic and the polyethylene end blocks were hydrophilic, the fibrin solution readily flowed into the pore space in the end blocks creating a hydrogel construct that was well integrated with the end blocks. Presumably, as the fibrin formed a gel-like matrix it not only bonded to the polyethylene due to the hydrophilic treatment, but the polymerizing fibers also became entangled in the pores of the end blocks. These hybrid fibrin-polyethylene constructs could then be used in the oscillatory tensile loading device.

To position the constructs in the loading device, the hole in one end block was placed over the peg in a well in the stationary culture chamber. Up to twelve constructs could be placed into each culture chamber. Then, a pin on the tension rake was inserted into each hole in the end block attached to the opposite end of the construct (Figure 4.2). After all constructs and the tension rake were in place, culture medium could be added to each well in the chambers. This mechanism for interfacing the constructs with the device allowed for well controlled displacements to be applied to the constructs by commanding the motor to move the tension rake to a desired position.

4.5 Validation of the Oscillatory Tensile Loading Device and Hydrogel Constructs

The final step in the development of the oscillatory tensile loading device was validating that the system was, in fact, meeting the specified design criteria. Four areas were determined to be important in the validation of the system: (1) the actual motion profile of the device, (2) the local strain fields generated in the hydrogel constructs, (3) the mechanical characteristics of the hydrogel constructs, and (4) the ability to maintain living chondrocytes in the three-dimensional hydrogel constructs during loading.

4.5.1 Motion Profile Validation

The final motion profile of the oscillatory tensile loading device was highly dependent on the servo loop PID tuning parameters assigned to the system controllers. It was determined that an accurate position profile could best be maintained by programming the controller for the linear motor (LinMot, Appendix A.1) in "force control mode" as opposed to "velocity control mode." Thus the LinMot controller could be tuned by setting appropriate values for the current amplifier gain and current offset, but addition parameters were not required. However, the tuning parameters for the system controller (Trio, Appendix A.1) had to be carefully selected to produce an optimal motion profile. In addition to the conventional PID parameters (Proportional gain, Integral gain, and Derivative gain), two additional parameters were incorporated into the Trio controller operation (Output Velocity gain and Velocity Feed Forward gain). Using these five parameters, the oscillatory tensile loading device was tuned to achieve an acceptable motion profile when operating at frequencies and displacements appropriate for this system. The values for each of these parameters can be found in Appendix A.

The Trio system controller had the ability to store and export values for many different parameters, such as the demanded position, the measured position, and the following error. Therefore to assess the motion profile of the oscillatory tensile loading device during a typical cycle, these three parameters were stored and exported for analysis. The demanded position, measured position, and following error for the motion profile used in this thesis research (1.0 Hz frequency, 2.0 mm peak-to-peak amplitude sine wave) is shown in Figure 4.4. Given the limitations of tuning any closed loop servo system, especially one with the dynamic demands of the oscillatory tensile loading

device, it was determined that the system met the design requirements of maintaining a consistent, repeatable motion profile.

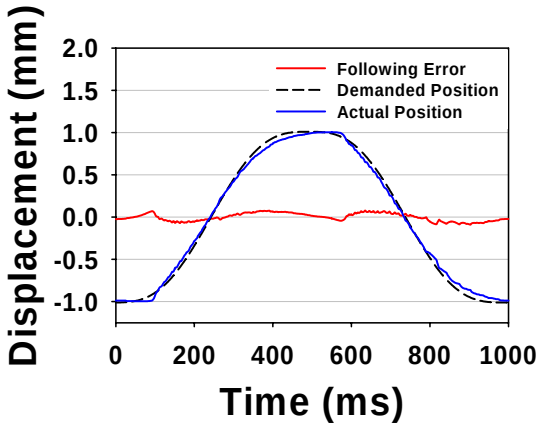

Figure 4.4 Sine wave motion profile for the oscillatory tensile loading device at 1.0Hz and 2mm peak-to-peak amplitude

4.5.2 Hydrogel Construct Strain Field Validation

To ensure that cells seeded throughout the hydrogel constructs were being subjected to similar levels of deformation, it was necessary to evaluate the local strain fields that developed during construct stretching. Although incorporating the polyethylene end blocks into the construct design should have eliminated much of the "end effects" and thus the non-uniform strain field associated with the interface between the constructs and the oscillatory tensile loading device, it was important to verify this assumption.

A poroelastic finite element model (Abaqus 6.3-3) had been developed to predict the strain fields, fluid velocities, and fluid pressures for the original construct design[145], and was adapted for the new construct design and geometry. The fibrin portion of the construct was modeled as brick elements and given an isotropic elastic modulus of 22 kPa[158], a Poisson's ratio of 0.3, and a permeability of $5x10^{-10}$ $m^4/N*sec$[159]. Since the polyethylene end blocks could be considered rigid in comparison to the fibrin hydrogel, they were not included in the model, and the elements at the hydrogel-end block interface were assigned uniform, rigid displacements. Deformation to the hydrogel construct was applied using 50 equal time steps up to a total displacement of 50%. Due to symmetry considerations, only 1/8 of the hydrogel construct was required for the model, and displacements were held at zero across the planes of symmetry. The FE model predicted that the logarithmic strain (true strain) in the axial direction (Y-direction) was highly uniform throughout the construct (Figure 4.5C). Areas near the interface between the fibrin construct and the end blocks tended to have slightly lower strain magnitudes than the bulk of the construct, but this non-uniformity only persisted a short distance. Additionally, in the bulk of the construct the model predicted strains that were approximately 90-93% of the displacement (*e.g.* a 10.0% displacement produced a 9.32% strain in the bulk of the construct).

Local strain fields in the hydrogel constructs were also verified experimentally. Constructs were cast using 50 mg/mL fibrinogen and 50 U/mL thrombin, and during polymerization small, tracking beads were placed in triad patterns on the surface of the constructs. No additional adhesive was necessary to attach the beads to the constructs. After approximately 18 hours in DMEM plus 10% FBS, constructs were stretched at

0.2mm/sec up to a total displacement of 50% while digital video images were recorded (Figure 4.5A). The video images were analyzed with Matrox 2.0 software and the position of each bead was obtained relative to a stationary point in the test configuration. Local Green's strains (E_{ij}) were calculated from the changes in the positions of the beads using large deformation strain theory with the following equations.

$$E_{ij} = \frac{1}{2}\left[F_{ji} \bullet F_{ij}\right] - I \qquad (1)$$

$$\text{where} \quad F_{ij} = \begin{bmatrix} x_1' x_2' & x_1' x_3' \\ y_1' y_2' & y_1' y_3' \end{bmatrix} \bullet \begin{bmatrix} x_1 x_2 & x_1 x_3 \\ y_1 y_2 & y_1 y_3 \end{bmatrix}^{-1} \qquad (2)$$

$$\text{and} \quad I = \begin{bmatrix} 1 & 0 \\ 0 & 1 \end{bmatrix} \qquad (3)$$

Finally, position information for nodes from the finite element model that corresponded to the locations of the tracking beads in the experimental analysis was extracted and used to calculate theoretical local Green's strain in the same way. Comparison of the experimental and theoretical local Green's strains showed a close match, especially at lower values of deformation (Figure 4.5B). Taken together, the finite element model and the experimental strain analysis indicated that the strain fields generated in the hydrogel constructs during loading were highly uniform and could be predicted reasonably well for a variety of applied deformation. Thus, the design criteria of having a uniform strain field throughout the construct had been satisfied.

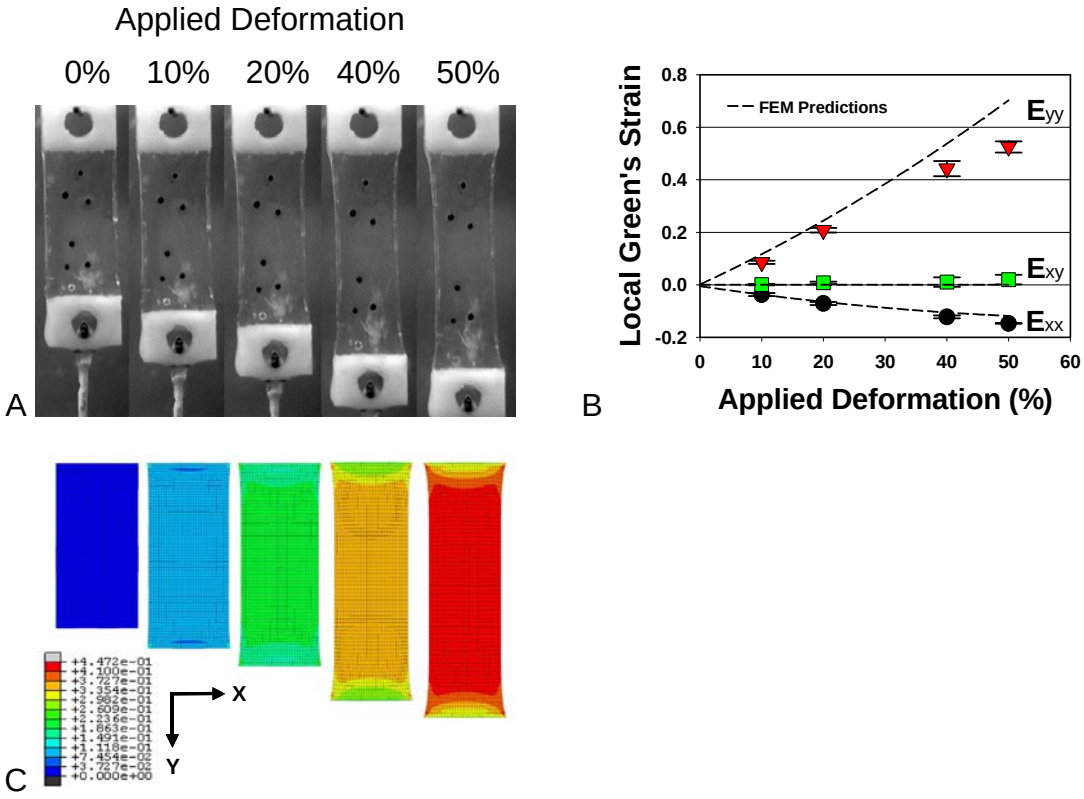

Figure 4.5 Experimental and theoretical validation of the strain field within fibrin constructs during loading. (A) Snapshots from video images during construct stretching showing tracking beads. (B) Calculated experiment and theoretical Green's strains correlated well, especially at low values of deformation. (C) FEM results indicated a uniform strain field throughout the construct.

4.5.3 Hydrogel Construct Mechanical Characterization

In addition to validating the strain fields generated during loading in the hydrogel constructs, it was important to characterize their mechanical behavior. Therefore, hydrogel constructs were cast and allowed to incubate in DMEM plus 10% FBS overnight as before. Using an EnduraTEC ELF-3200 testing frame, constructs were subjected to several mechanical testing protocols designed to evaluate construct strength and durability in tension (Figure 4.6A).

The first series of constructs were subjected to 10 sinusoidal preconditioning cycles at 0.1 Hz, 5% ± 5% amplitude, followed by a frequency sweep over three decades (0.1 Hz, 1.0 Hz, and 10 Hz) at 10% ± 5% amplitude. The constructs were then returned to 0% strain and allowed to equilibrate for 60 seconds. Finally, a tensile ramp at 0.1 mm/sec was preformed up to 60% displacement (Figure 4.6B). The hydrogel constructs exhibited a fairly linear stress-strain relationship after an initial "toe-in" region, and constructs cast in different batches and tested on different days yielded highly consistent results. The elastic modulus of the constructs was calculated using the linear region of the stress-strain curve and found to be 26 kPa – 30 kPa. The tensile ramp test was intended to be a failure test, but most constructs did not fail at displacements up to 60%, which was the limit of travel of the mechanical testing frame.

Additional constructs were similarly treated and then tested using a larger number of cycles. The sinusoidal tests were performed at 1.0 Hz, 10% ± 5% amplitude for a total of 500 cycles. The loads generated during this test closely followed the sinusoidal displacement (Figure 4.6C), and the stress-strain loading and unloading behavior did not vary significantly over time (Figure 4.6D). The results of this series of mechanical

tension tests indicated that the new hydrogel construct design possessed sufficient mechanical integrity for use with the oscillatory tensile loading device. Additionally, these tests showed that the tensile mechanical properties of the hydrogel constructs could be readily measured, an important improvement over earlier construct designs.

4.5.4 Chondrocyte Viability in the Hydrogel Constructs

The final necessary component in validating the oscillatory tensile loading device and the hydrogel constructs was to ensure that chondrocytes would remain viable when seeded in the constructs and during loading. Hydrogel constructs (50 mg/mL fibrin, 50U/mL thrombin) were seeded with 5 x 10^6 chondrocytes/mL and allowed to culture in free swelling conditions for five days in serum supplemented DMEM. Constructs were placed in the stationary culture chamber, interfaced with the tension rake, and loaded continuously with a 1.0 Hz frequency, 5% ± 5% amplitude sine wave for 24 hours. Parallel constructs held at 0% displacement served as unloaded controls. Following loading constructs were washed in PBS, incubated at 37°C with a vital dye solution containing 4μM calcein-AM and 4μM ethidium homodimer for 90 minutes, and finally washed again in PBS. Constructs were then imaged using laser scanning confocal microscopy to determine the viability of chondrocytes. In a separate study, constructs were seeded as described above, cultured in free swelling conditions for seven days, and subjected to 18 hours of the same loading protocol. Immediately following loading, portions of these constructs were fixed in 10% neutral buffered formalin for 30 minutes at 4°C and washed in PBS. Constructs were then incubated with AlexFluor 546 conjugated phalloidin and Hoechst dye to label F-actin filaments and DNA, respectively, and imaged using confocal microscopy.

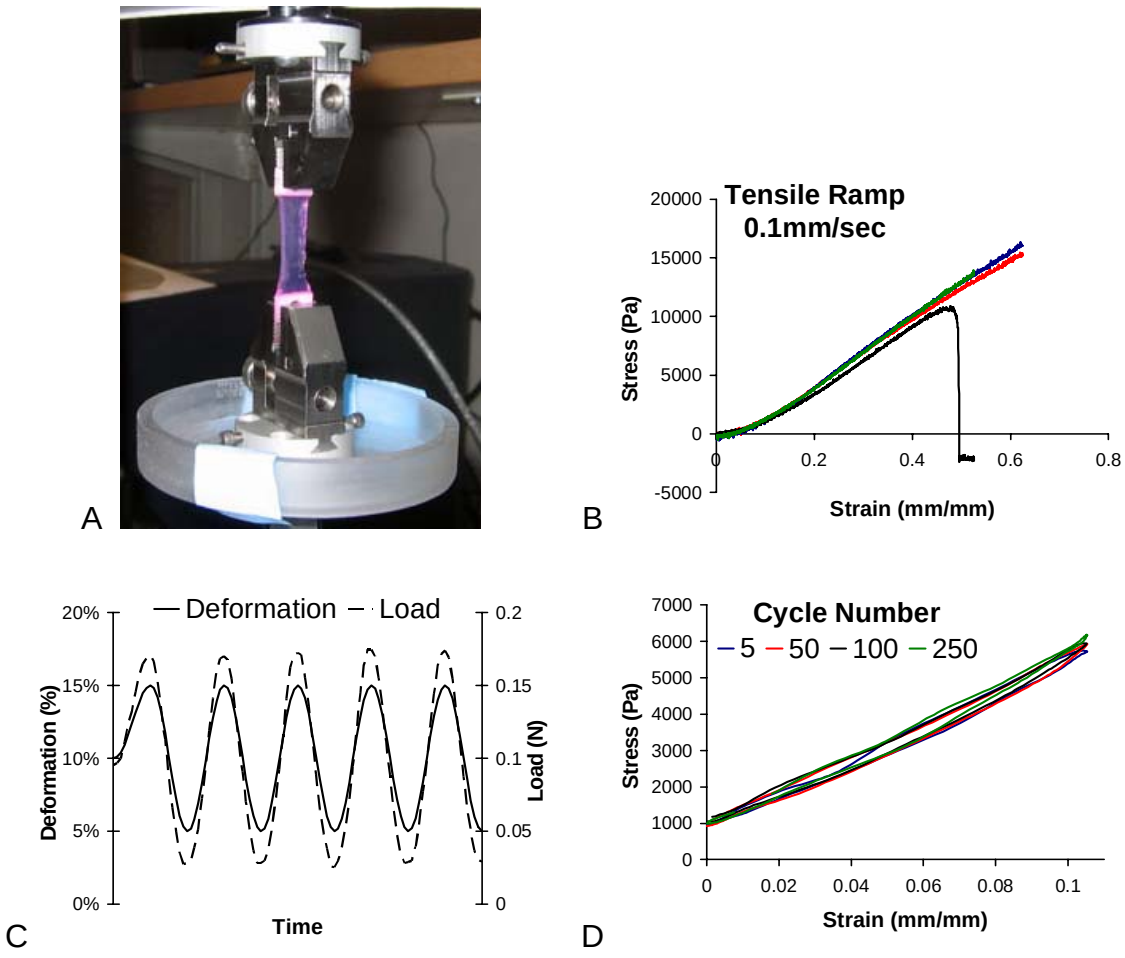

Figure 4.6 Mechanical characterization of hydrogel constructs. (A) Construct in the test frame. (B) Stress-strain data for several constructs during a 0.1 mm/sec tensile ramp. (C) Actuator position and load generated during 1.0 Hz frequency, 10% ± 5% amplitude sine waves. (D) Stress-strain data for a representative construct at various points in a cyclic fatigue test (1.0 Hz frequency, 10% ± 5% amplitude sine wave).

Images from this analysis indicated that chondrocyte viability was high in the hydrogel constructs regardless of loading condition (Figure 4.7A,B). In these images, larger, green areas defined the cytoplasm of live cells, while smaller, red areas revealed the DNA of dead cells. Additionally, chondrocytes near the interface between the hydrogel and the end blocks, indicated by the white line, as well as chondrocytes resident within the pore space of the end blocks remained viable (Figure 4.7C). Finally, images of chondrocyte F-actin (red) and DNA (blue) revealed cells with a round morphology, peripheral F-actin, and evidence of cell division (Figure 4.7D). Analysis of this series of images provided strong evidence that chondrocytes would remain viable and maintain an appropriate morphology during culture in the hydrogel constructs. The observation that chondrocytes also were viable near and within the polyethylene end blocks additionally suggested that the polyethylene did not create a locally toxic environment. Therefore, the final validation requirement of maintaining cell viability for the oscillatory tensile loading device was achieved.

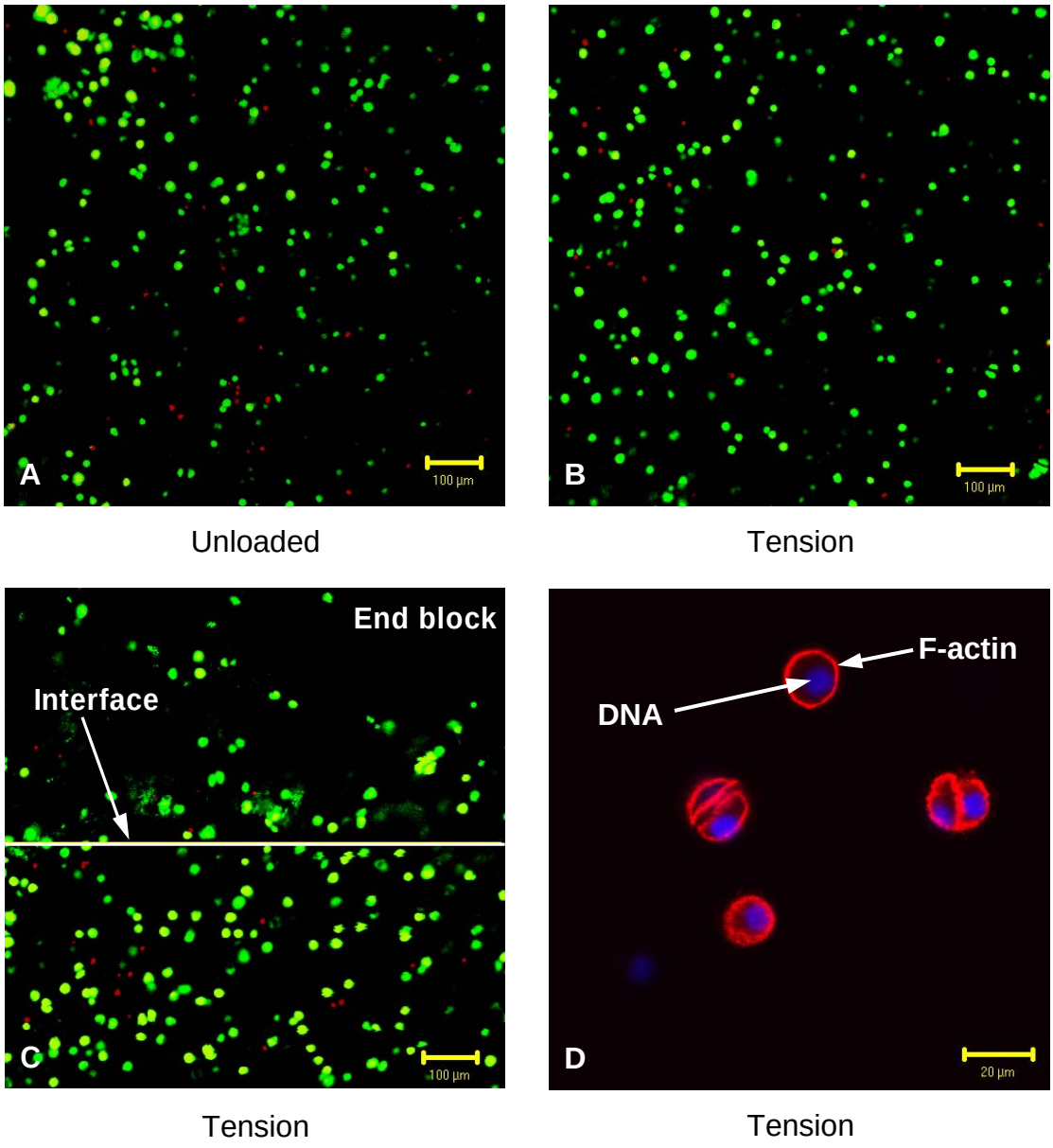

Figure 4.7 Viability of chondrocytes in hydrogel constructs. (A) Unloaded construct. (B) Construct subjected to oscillatory tensile loading. (C) Construct subjected to oscillatory tensile loading; white line indicates hydrogel-end block interface. (D) Construct subjected to oscillatory tensile loading. Scale bars in A, B, and C are 100 µm. Scale bar in D is 20 µm.

4.6 Conclusions

The development of the oscillatory tensile loading device was crucial to the success of this thesis research. Although designing the system was an iterative process, the design criteria set forth in this chapter were always used to make judgments regarding specific improvements that would be made. Through this process of design, evaluation, and redesign, a novel device was created that specifically addressed many of the limitations of existing tensile loading bioreactors. The oscillatory tensile loading device represents a unique contribution to the fields of biomechanics, bioreactor development, and mechanobiology, without which much of the work presented in this dissertation, would have been impossible.

CHAPTER 5

SUSTAINED AND INTERMITTENT SHORT TERM OSCILLATORY TENSILE LOADING OF ENGINEERED CARTILAGINOUS TISSUES

5.1 Introduction

Several different modes of mechanical stimulation have been extensively used to influence the behavior of articular chondrocytes or meniscal fibrochondrocytes during *in vitro* culture. Static compression can inhibit extracellular matrix synthesis in tissue explants from both articular cartilage[139] and meniscal fibrocartilage[108], whereas dynamic compression[139,160,161] and dynamic tissue shear[101] stimulate matrix synthesis. Similar effects have been found for articular chondrocytes seeded into three-dimensional tissue engineered scaffolds[5,100,162,163]. In contrast, mechanical tension has not been widely used as a means to modulate chondrocyte metabolism.

As discussed in Chapter 2, tensile strains are not a dominant component of the mechanical environment in articular cartilage, but do occur during normal joint loading. Specifically, the superficial zone of the tissue is subjected to a combination of shear and tensile forces due to the compressive and sliding motions inherent during articulation. Additionally, following injury to the joint surface or after a repair procedure, tensile strains may become more prominent due to discontinuities in the cartilage extracellular matrix. In contrast, tension is a significant component of the mechanical environment in normal fibrocartilage. During normal joint loading significant tensile stresses develop in specific regions of these tissues due to their location and anchorage in the joint,

anatomical shape, and ultrastructural organization. The mechanical environments of the menisci in the knee joint as well as the temporomandibular joint disc contain significant tensile components during normal loading. Therefore, understanding the role of tensile loading and deformation in tissue development, maintenance, and repair is important for successfully developing and implementing repair strategies for both fibrocartilage and articular cartilage tissues.

The overall goal of the studies presented in this chapter was to determine how oscillatory tensile loading affects articular chondrocytes and meniscal fibrochondrocytes in three-dimensional fibrin hydrogel culture. Studies varying the preculture time before loading were conducted to determine if the accumulation of a newly synthesized extracellular matrix would affect chondrocyte responses to tensile loading. The effects of various total loading durations initiated following a set preculture time were also evaluated. Additionally, sustained versus intermittently applied oscillatory tensile loading was investigated in an effort to identify protocols that could be used to stimulate extracellular matrix synthesis in developing tissue engineered constructs cultured *in vitro*. Based on preliminary work in our laboratory, we hypothesized that longer durations of continuously applied oscillatory tensile loading would inhibit extracellular matrix synthesis and accumulation, but shorter durations of continuous loading as well as longer periods of intermittently applied loading could promote matrix synthesis and deposition.

5.2 Materials and Methods

5.2.1 Tissue Harvest and Cell Isolation

Full thickness articular cartilage was aseptically harvested from the femoropatellar groove and femoral condyles of 2-4 week old bovine stifle joints. Tissue samples included the intact articular surface, but the deepest layers that may have included calcified cartilage were avoided. Throughout the harvest procedure, PBS supplemented with antibiotic/antimycotic was used to prevent tissue dehydration. Cartilage tissue was minced and articular chondrocytes were enzymatically isolated using 0.2% collagenase in antibiotic supplemented high glucose DMEM for approximately 40 hours at 37°C with gentle agitation. Meniscal fibrochondrocytes were isolated from the entire medial and lateral menisci of the same animals. Following excision from the joint and mincing, the tissue was soaked in 0.25% trypsin in PBS for 1 hour at 4°C. The trypsin solution was removed and tissue was transferred to a 37°C incubator for an additional hour. Finally, cells were isolated using 0.4% collagenase in antibiotic supplemented high glucose DMEM for approximately 40 hours at 37°C with gentle agitation.

Following tissue digestion, cell solutions were filtered through a sterile 74μm mesh, washed with PBS, concentrated with centrifugation for 10 minutes at 400 x g, and counted using a Coulter Multisizer II (preculture duration study) or a Coulter ViCell XR (all other studies). Finally, cells were cryopreserved at a concentration of 15e6 cells/mL in DMEM + 20% FBS + 10% DMSO by cooling the cell solution 1°C per minute to -80°C. Vials were then transferred to liquid nitrogen for storage. Note that chondrocytes

used in the final intermittent loading study (see section 5.2.6) were seeded into the fibrin hydrogel constructs directly after isolation to simplify the construct seeding procedure as well as maximize cell viability, which is inevitably reduced by cryopreservation.

5.2.2 Fibrin Hydrogel Construct Seeding

The preculture duration study used an early design of the oscillatory tensile loading device (Figure 4.1A) and oval-shaped fibrin hydrogel constructs[164]. All other studies utilized the closed-loop, computer controlled design of the oscillatory tensile loading device (Figure 4.1C,D) and rectangular fibrin hydrogel constructs (Figure 4.3). The cell density, fibrin and thrombin concentrations, and culture medium supplements, however, were identical for all studies described.

Cells were rapidly thawed, re-counted, and then seeded at a density of 5e6 cells/mL into fibrin hydrogel constructs using custom polycarbonate molds. As stated above, cells used in the final intermittent loading study were seeded into constructs immediately after isolation from the tissue. Fibrinogen was dissolved in DMEM at a concentration of 100 mg/mL in a 37°C water bath and briefly centrifuged to remove bubbles that had formed in the solution. An appropriate volume of cells suspended in DMEM was combined with FBS and ε-aminocaproic acid (ACA). The fibrinogen solution was then added to the cell/DMEM/FBS/ACA solution. A small volume of thrombin (~800 U/mL in 40 mM $CaCl_2$) was added to each well in the polycarbonate molds. Finally, the cell/fibrinogen solution was added to the molds, and the fibrin hydrogel constructs were incubated for 90 minutes at 37°C to allow for thorough gelation. The final concentrations of all components in the constructs are summarized in Table 5.1.

Table 5.1 Fibrin hydrogel construct composition

Component	Final Concentration
Chondrocytes or Fibrochondrocytes	5e6 cells/mL
FBS	10% v/v
ACA	2 mg/mL
Fibrin	50 mg/mL
Thrombin	50 U/mL
High glucose DMEM	~ 85% v/v

After constructs were fully formed, they were removed from the molds and transferred to 8-well rectangular tissue culture plates. Fully supplemented culture medium (Table 5.2) was added to each well and the culture plates were maintained in a 5% CO_2 incubator at 37°C. Culture medium was changed every 2 days, and in some cases aliquots were stored at -20°C for later analysis.

ACA acts as an inhibitor of fibrinolysis, stabilizing the constructs and preventing premature fibrin degradation[148]. This inhibitor is widely used clinically as a clot stabilizer to prevent fibrinolytic bleeding as well as to stabilize fibrin sealants. ACA has been used *in vitro* for fibrin constructs containing dorsal root ganglia[149], smooth muscle cells[148], and articular chondrocytes[140]. The moderate levels of ACA used in these studies prevent fibrin degradation with no apparent effects on chondrocyte metabolism for up to 40 days in culture (unpublished observations from our laboratory).

Table 5.2 Fully supplemented culture medium formulation

Component	Concentration
FBS	10% v/v
ACA	2 mg/mL
Non-essential amino acids	10 mM
HEPES buffer	10 mM
Ascorbic acid	50 mg/mL
L-proline*	0.4 mM
Gentamicin	50 μg/mL
Fungizone	0.25 μg/mL
High glucose DMEM	~85% v/v

* L-proline only added to the culture medium used in experiments with radiolabeled precursor molecules

5.2.3 Preculture Duration Study

Fibrin hydrogel constructs used in the preculture duration study were precultured for either 1, 7, or 14 days. A detailed schematic describing all of the loading protocols used in this chapter is shown in Figure 5.1 after section 5.2.6. Once the constructs had been transferred to the oscillatory tensile loading device, one hole in each construct was positioned over the stationary pin in the tensile loading chamber. When all constructs were positioned in the chamber, the mobile pins on the tension rake were inserted into the second hole on the opposite side of each construct. This procedure is described in more detail in Chapter 4.

Constructs in this study were subjected to 68 hours of continuous oscillatory tensile loading at a frequency of 1.0 Hz and 5% ± 5% sinusoidal displacement. These values for frequency and displacement were consistent with stimuli previously applied to fibroblasts in collagen gels[143,165] in an effort to impart physiologically relevant levels of deformation. Unloaded constructs served as controls in each group. During the final 20 hours of culture, the medium was additionally supplemented with 10 μCi/mL L-[5-^{3}H]-proline and 5 μCi/mL of ^{35}S-sodium sulfate. In cartilaginous tissues these radiolabled precursor molecules are incorporated into newly synthesized proteins (primarily collagens) and proteoglycans, respectively, and their incorporation rates can therefore be used as indicators of extracellular matrix production. The sample size for this study was 6 constructs per loading group per preculture duration.

5.2.4 Sustained Loading Duration Study

Based on results from the previous study, all constructs in the sustained loading duration study were precultured for a total of 7 days after seeding. For the first 6 days of culture the constructs were kept in the 8-well culture plates, as described above, with medium changed every 2 days. On the 6th day, constructs were transferred to either the unloaded or tensile culture chambers, positioned on the stationary pins in the chambers, and returned to the incubator. The following day the culture medium was changed in all wells and the tension culture chambers were interfaced with the oscillatory tensile loading device. Fresh culture medium was added to each well and oscillatory tensile loading was begun. As described in Chapter 4, the entire oscillatory tensile loading device and the unloaded culture chambers were placed inside an incubator held at 37 °C

and 5% CO_2. Note that the culture medium used during the application of loading in this study and all subsequent studies was not supplemented with gentamicin or Fungizone.

Fibrin hydrogel constructs in the sustained loading duration study were subjected to continuously applied oscillatory tensile loading for 24, 48, or 72 hours. Culture medium was replaced every day, and during the final 24 hours of culture for each group ^{3}H-proline and ^{35}S-sulfate were added to the culture medium as described above. As discussed in the previous chapter, the axial strains generated in the rectangular constructs closely matched the percentage displacements applied by the oscillatory tensile loading device (Figure 4.5). In contrast, the maximum axial strain generated in the oval constructs used in preculture duration study described above was approximately half of the applied displacement (*i.e.* a 10% displacement produced a maximum strain of ~5%)[145]. Therefore, a sinusoidal displacement of 1.0 Hz and 5% (2.5% ± 2.5%) amplitude was used for this study so as to yield a maximum strain in the hydrogel consistent with previous work. The sample size for this study was 6 constructs per loading group per loading duration.

5.2.5 Short Term Loading Study

Fibrin hydrogel constructs in the short term loading study were precultured for either 1 or 4 days in 8-well rectangular culture plates using the supplemented culture medium described previously (Table 5.2). After the prescribed preculture period, constructs were transferred to either the unloaded or tension culture chambers, fresh culture medium was added to each well, and oscillatory tensile loading was begun immediately. Constructs were loaded continuously for 1, 4 or 8 hours with a 1.0 Hz,

2.5% ± 2.5% amplitude sinusoidal displacement. The sample size for this study was 5-6 constructs per group.

Immediately following loading, constructs were removed from the culture chambers, the polyethylene end blocks were removed, and portions of the fibrin hydrogel constructs were transferred to RNase/DNase free microcentrifuge tubes. 300 μL of RLT lysis buffer (Qiagen RNeasy kit) supplemented with 10 μL/mL β-mercaptoethanol was added to each tube. The tubes were heated to 60°C for 10 minutes and vortexed periodically. Finally, samples were stored at -80°C until RNA extraction and further processing for gene expression profiles were performed.

The α-helical coiled coil region of fibrin contains numerous disulfide bonds that contribute to the structural integrity of the hydrogel. The addition of β-mercaptoethanol to the cell lysis buffer, in addition to inhibiting enzyme activity, facilitates solubilization of the fibrin hydrogels by disassociating these bonds. Therefore, the extraction of RNA from the hydrogels is more consistent and efficient than what can be obtained via mechanical disruption techniques, such as biopulverization with liquid nitrogen cooling or passing the hydrogel through a small bore syringe needle.

Isolation of RNA from the constructs was achieved using modifications to the TriSpin method[166,167] followed by the Qiagen RNeasy RNA isolation procedure. Total RNA was quantified and equal amounts were reversed transcribed to cDNA using the Promega Reverse Transcription System. Custom primers for bovine type II collagen, aggrecan, and type I collagen (see Table 6.1) were used to amplify cDNA, and SYBR green was used to measure the amplification in real time on an ABI Prism Sequence Detector 7700. Detailed protocols for these processes are available in Appendix C.

Known quantities of cDNA spanning 4-6 orders of magnitude for each gene were run in parallel to serve as standards.

5.2.6 Intermittent Loading Study

All constructs in the intermittent loading study were precultured for a total of 7 days and were transferred to the unloaded or tension culture chambers on the 6^{th} day of preculture, as described above. The initial experiment in this study used the 1.0 Hz, 2.5% ± 2.5% amplitude loading protocol that was also described above. However, constructs in this experiment were subjected to intermittent bouts of this loading protocol. The first intermittent loading protocol consisted of 3 hours of oscillatory tensile loading followed by 3 hours of recovery where constructs were held at 0% displacement. The cycle was repeated 4 times per day. This protocol was referred to as "3 Hour." The second intermittent loading protocol was dubbed "12 Hour" and consisted of 12 hours of oscillatory tensile loading followed by 12 hours of recovery at 0% displacement. These intermittent protocols were repeated for 3 consecutive days with the culture medium being changed every day during the final hour of the last recovery period each day. During the final 24 hours of culture for each group, ^{3}H-proline and ^{35}S-sulfate were added to the culture medium as described above.

The second experiment in the intermittent loading study used the same two loading protocols, but the amplitude of the sinusoidal displacement was increased to 10% (5% ± 5%). The intermittent protocols were then applied for either 3 or 7 consecutive days and culture medium was again changed every day as before. During the final 24 hours of culture for each group, ^{3}H-proline and ^{35}S-sulfate were again added to the

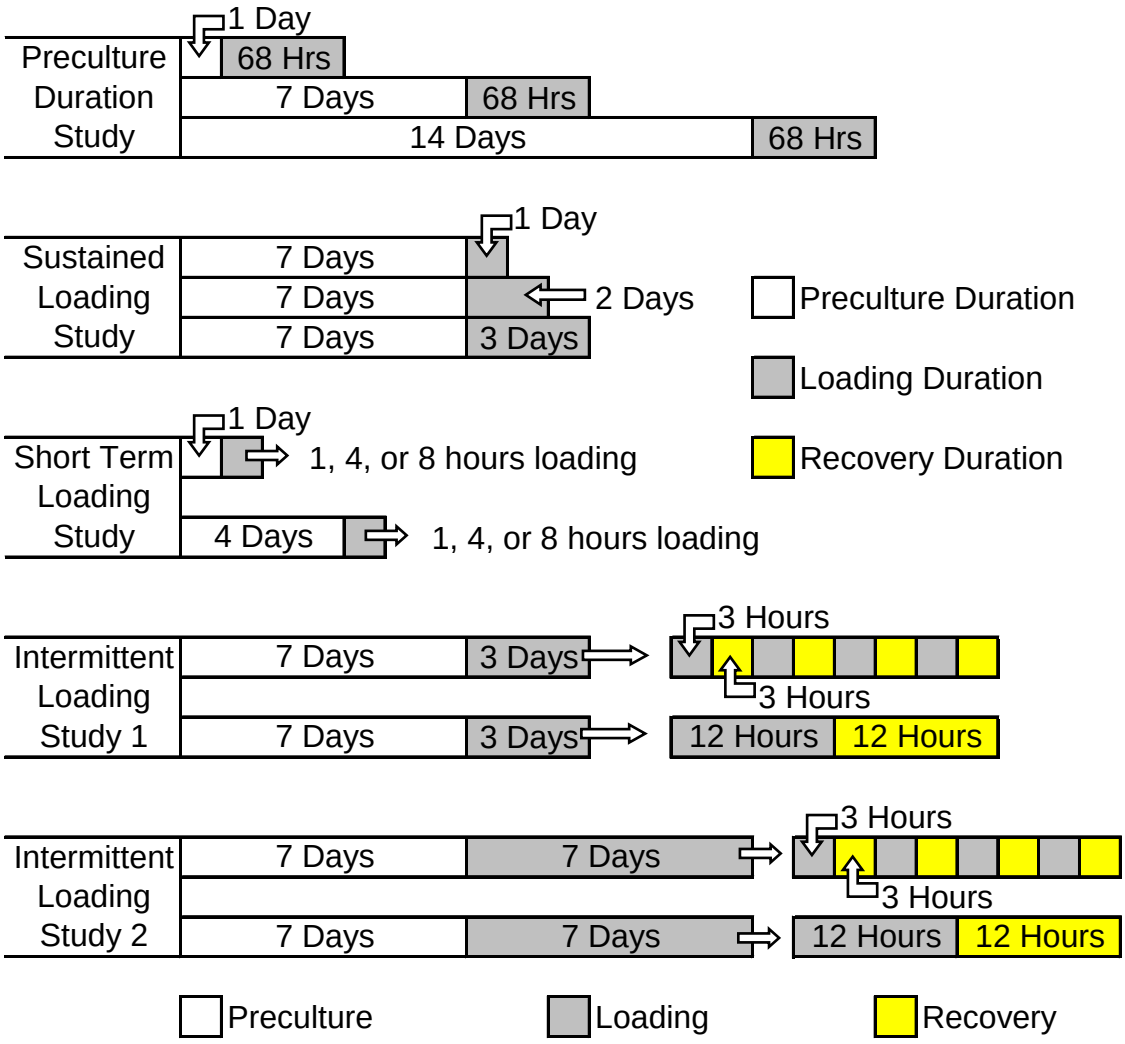

Figure 5.1 Schematic of protocols used in the oscillatory tensile loading studies.

culture medium. The sample size for both experiments in this study was 6 constructs per group.

5.2.7 Biochemical Composition Analyses

The cellular and biochemical contents of the fibrin hydrogel constructs used in all studies presented in this chapter, with the exception of the short term loading study, were assessed via well established techniques. At the conclusion of the loading period in each study, constructs were removed from the culture chambers and the polyethylene end blocks were removed. Oval-shaped constructs from the preculture duration study did not have end blocks, but only the central portions of these constructs were used in subsequent analyses. Constructs were then transferred to 8-well rectangular culture plates containing PBS supplemented with 0.8 mM L-proline and 1.0 mM sodium sulfate. Constructs were washed in this solution at 4°C for approximately 2 hours, and the wash solution was replaced every 30 minutes. This wash period was necessary to remove any ^{3}H-proline or ^{35}S-sulfate in the constructs that had not been incorporated into protein or proteoglycan macromolecules.

Following the wash procedure, total mass was measured and the constructs were frozen at -20°C. Constructs were then lyophilized to dryness and solid mass was measured. Proteinase K (≥ 0.25 mg/mL) in 100 mM ammonium acetate was used to solubilize constructs prior to further analysis. The digests were analyzed for ^{3}H and ^{35}S incorporation using liquid scintillation counting, DNA content using the Hoechst 33258 dye assay[168], and sulfated glycosaminoglycan (sGAG) content using the 1,9-DMMB dye binding assay[169]. sGAG released to the culture medium was also assessed with the DMMB dye assay for some studies.

5.2.8 Dynamic Tensile Testing

An additional set of fibrin hydrogel constructs was cultured in parallel with the final experiment of the intermittent loading study. The culture medium for these constructs was not supplemented with radiolabeled precursor molecules so that their mechanical properties could be assessed without risk of contaminating the mechanical testing equipment with radioactive material. Following the loading period for this experiment (either 3 or 7 days), constructs designated for mechanical testing were removed from the culture chambers, transferred to 8-well rectangular culture plates, and maintained in sterile PBS at 37°C for several hours until testing. Custom designed interface pieces (see Appendix B) were used with an EnduraTEC ELF 3200 mechanical testing frame to assess the dynamic tensile properties of these constructs.

Prior to testing, the length and thickness of each construct were measured using a digital Vernier caliper. At the beginning of each test, a small tensile preload (~ 0.01 N) was applied to the construct. Next, 5 preconditioning cycles were performed from 0-5% strain at 0.1 mm/sec followed by a slow (0.1 mm/sec) linear ramp to 10% total strain. This position was held for 60 seconds before constructs were returned to the starting position and allowed to equilibrate for several minutes. Constructs were then stretched until a preload of 0.01 N was achieved and this position was designated as the new start position. A 0.1 mm/sec ramp was again performed to 10% strain and then constructs were held at this position for 2 minutes to allow for stress relaxation. A dynamic frequency sweep over 3 decades was performed using a sinusoidal wave of 10% ± 1.5%. All tensile mechanical tests were performed at room temperature without supplemental hydration. A module accompanying the control software for the ELF 3200 was used to

perform FFT analysis on load and displacement data acquired during the dynamic frequency sweep. The sample size of this portion of the study was 4-6 constructs per group.

5.2.9 Statistical Analyses

All studies described in this chapter were analyzed using a general linear model and Tukey's test for post-hoc comparisons. Data are presented throughout as the mean ± the standard error of the mean with significance at $p < 0.05$. Models included all factors, including the interaction terms between factors, for which the significance criterion was met and are described in detail below. Analysis for the preculture duration study (Section 5.3.1) used a multifactor model with preculture time and loading as factors. Data from the loading duration study (Section 5.3.2) were analyzed as a single factor model (loading) with each loading duration group treated separately. In the short term loading study (Section 5.3.3) comparisons between preculture times were made using a two factor model (preculture time and loading duration), and comparisons between loading groups were made using a single factor model (loading). Similarly, data from the intermittent loading study (Section 5.3.4) were analyzed with a two factor model (loading and loading duration) when comparing the 3 day versus 7 day loading durations, but with a single factor model (loading) when comparing the unloaded and tension groups for each loading protocol. Finally, data for total sGAG synthesis (Section 5.3.4) was analyzed with a multifactor model (loading and loading duration).

5.3 Results

5.3.1 Preculture Duration Study*

The objective of the preculture duration study was to investigate the effects of various preculture times before beginning 68 hours of continuous oscillatory tensile loading. Constructs containing either articular chondrocytes or meniscal fibrochondrocytes were used in this study. Note that this study was performed using an early design of the oscillatory tensile loading device (Figure 4.1A) and used oval-shaped constructs consisting entirely of the fibrin hydrogel matrix. The fibrin hydrogel constructs containing fibrochondrocytes that were precultured for 14 days had contracted beyond a geometry that could be accommodated by the oscillatory tensile loading device; therefore, only data from the 1 and 7 day preculture groups were collected for the fibrochondrocyte constructs. Over extended periods of culture, constructs containing chondrocytes also exhibit some contraction, but this did not occur within the 14 days of preculture used in this study.

The DNA content of chondrocyte constructs from the preculture duration study increased with time in culture ($p < 0.001$) and was additionally increased by sustained oscillatory tensile loading (Figure 5.2A, $p < 0.007$). In contrast, the DNA content of fibrochondrocyte constructs decreased with time in culture ($p < 0.003$) and was further decreased with tensile loading (Figure 5.2B, $p < 0.05$).

---

* Material presented in Section 5.3.1 was reprinted from the Journal of Biomechanics, 37, Vanderploeg, Imler, Brodkin, Garcia, and Levenston, "Oscillatory tensile loading differentially modulates matrix metabolism and cytoskeletal organization in chondrocytes and fibrochondtrocytes," 1941-52, Copyright (2004) with permission from Elsevier.

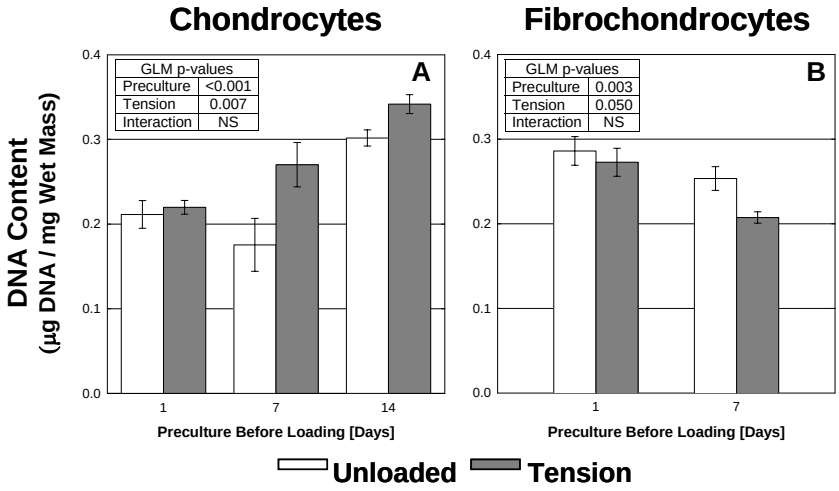

Figure 5.2 DNA contents for fibrin hydrogel constructs from the preculture duration study containing (A) chondrocytes or (B) fibrochondrocytes. Inset tables indicate results from two-factor general linear model analysis for statistical significance.

Sulfated glycosaminoglycan (sGAG) accumulation increased with time in culture for hydrogel constructs containing both cell types (Figure 5.3A,B, $p < 0.001$). Tensile loading did not significantly affect sGAG content in chondrocyte constructs, but did significantly reduce sGAG accumulation in fibrochondrocyte constructs for each preculture time investigated (Figure 5.3B, $p < 0.015$). Note that data for construct DNA and sGAG contents were presented as normalized to construct wet mass and DNA content, respectively, but analysis of non-normalized data yielded equivalent results.

Although biosynthesis rates, indicated by ^{3}H-proline and ^{35}S-sulfate incorporation, typically varied with preculture duration for constructs containing both cell types, these difference did not indicate any overall trends (Figure 5.3C-F). Therefore, the discussion of results from these analyses will be focused on differences found at each preculture time in response to the application of oscillatory tensile loading. ^{3}H-proline

incorporation, indicative of total protein production, was inhibited by tensile loading in the chondrocyte constructs precultured for 7 days (Figure 5.3C, $p < 0.001$), but was not significantly altered by loading in any other group. In contrast, ^{35}S-sulfate incorporation, indicative of proteoglycan synthesis, was inhibited by tensile loading at all preculture times in the chondrocyte constructs (Figure 5.3E, $p < 0.001$), but only after 1 day of preculture in the fibrochondrocyte constructs (Figure 5.3F, $p < 0.05$). Taken together these data suggested that 68 hours of sustained oscillatory tensile loading generally inhibited extracellular matrix synthesis in constructs containing either chondrocytes or fibrochondrocytes. Additionally, this tensile loading protocol promoted cellular proliferation in articular chondrocytes, but not in meniscal fibrochondrocytes.

5.3.2 Sustained Loading Duration Study

In the sustained loading duration study, the differential effects of subjecting fibrin hydrogel constructs containing articular chondrocytes to either 24, 48, or 72 hours of continuous oscillatory tensile loading were investigated. This study and all subsequent studies used the final design of the oscillatory tensile loading device in combination with the rectangular fibrin hydrogel constructs discussed in Chapter 4. A sinusoidal displacement of 1.0 Hz and 5% (2.5% ± 2.5%) was used for the remaining studies described in this chapter, unless otherwise noted.

The DNA content of fibrin hydrogel constructs was similar for all three loading durations investigated. However, consistent with the preculture duration study presented above, 72 hours of continuous oscillatory tensile loading led to a significant increase in construct DNA content (Figure 5.4A, $p < 0.05$). Construct sGAG accumulation was not

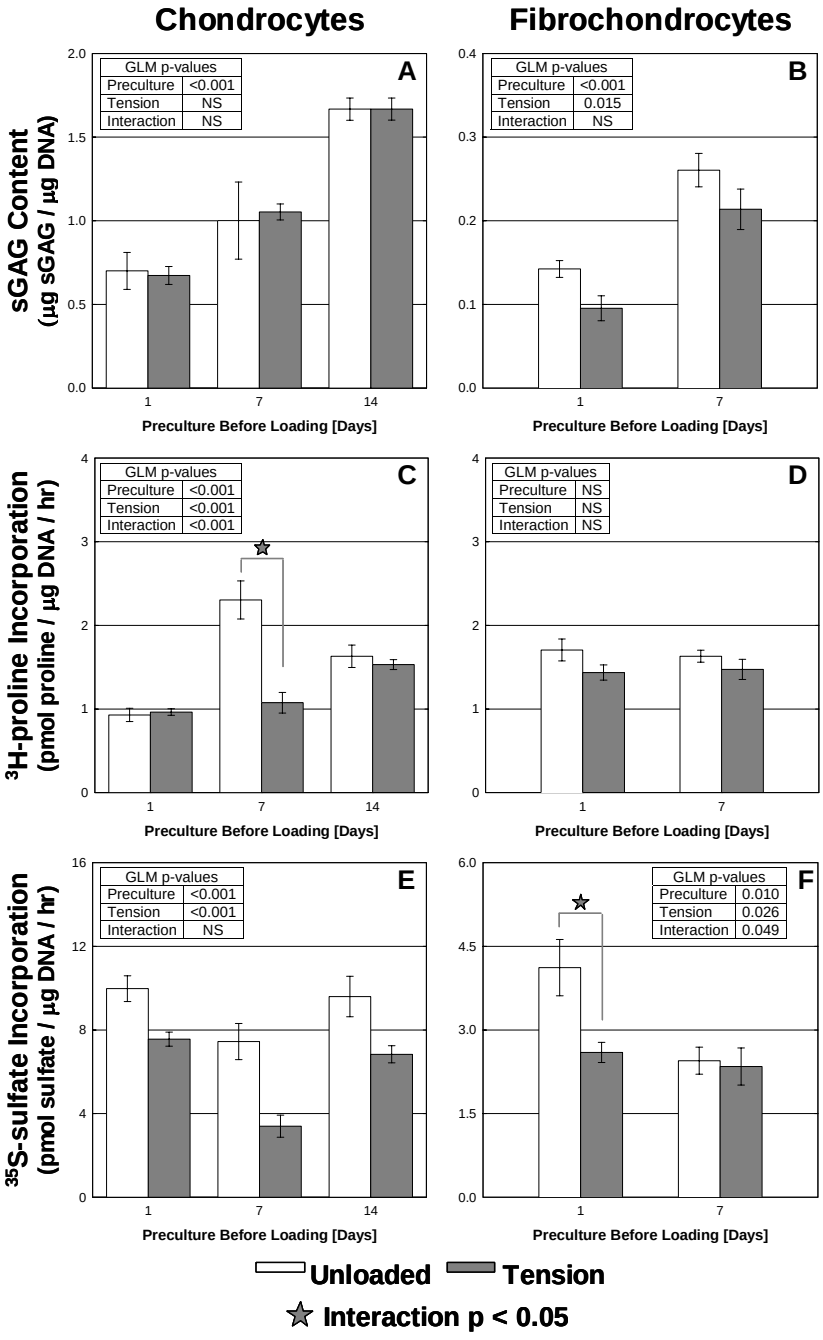

Figure 5.3 Biochemical analyses of the preculture duration study. The left column contains data from chondrocyte constructs: (A) sGAG content, (C) ^{3}H-proline incorporation, and (E) ^{35}S-sulfate incorporation. The right column contains data from fibrochondtocyte constructs: (B) sGAG content, (D) ^{3}H-proline incorporation, and (F) ^{35}S-sulfate incorporation. Inset tables indicate results from statistical analyses, and in cases with a significant interaction term, stars indicate the preculture durations for which the effect of tension was significant (Tukey's test, $p < 0.05$).

significantly affected by 24 or 48 hours of continuous oscillatory tensile loading, but sGAG accumulation was significantly reduced after 72 hours of loading (Figure 5.4B, $p < 0.02$). Trends in biosynthesis were consistent for both the ^{3}H-proline and ^{35}S-sulfate incorporation in response to various durations of sustained oscillatory tensile loading, although statistical significance was only found for ^{35}S-sulfate incorporation (Figure 5.4C,D). Specifically, 72 hours of loading significantly inhibited ^{35}S-sulfate incorporation ($p < 0.01$). Overall, these results were consistent with previous observations in our laboratory that longer periods of sustained oscillatory tensile loading tended to inhibit extracellular matrix synthesis and accumulation whereas this effect was less pronounced or even reversed when using shorter durations of tensile loading[164]. These findings led to the hypothesis that shorter tensile loading durations may stimulate chondrocyte matrix synthesis and were the impetus for the remaining studies presented in this chapter.

5.3.3 Short Term Loading Study

The objective of the short term loading study was to elucidate the potential effects of short durations of oscillatory tensile loading on chondrocyte gene expression. Fibrin hydrogel constructs were precultured for either 1 or 4 days and then subjected to tensile loading for either 1, 4, or 8 hours. Matrix molecule gene expression levels were chosen as the primary outcome measure in this study because extracellular matrix synthesis would be small and potential differences between treatment groups would most likely be undetectable on the time scales used.

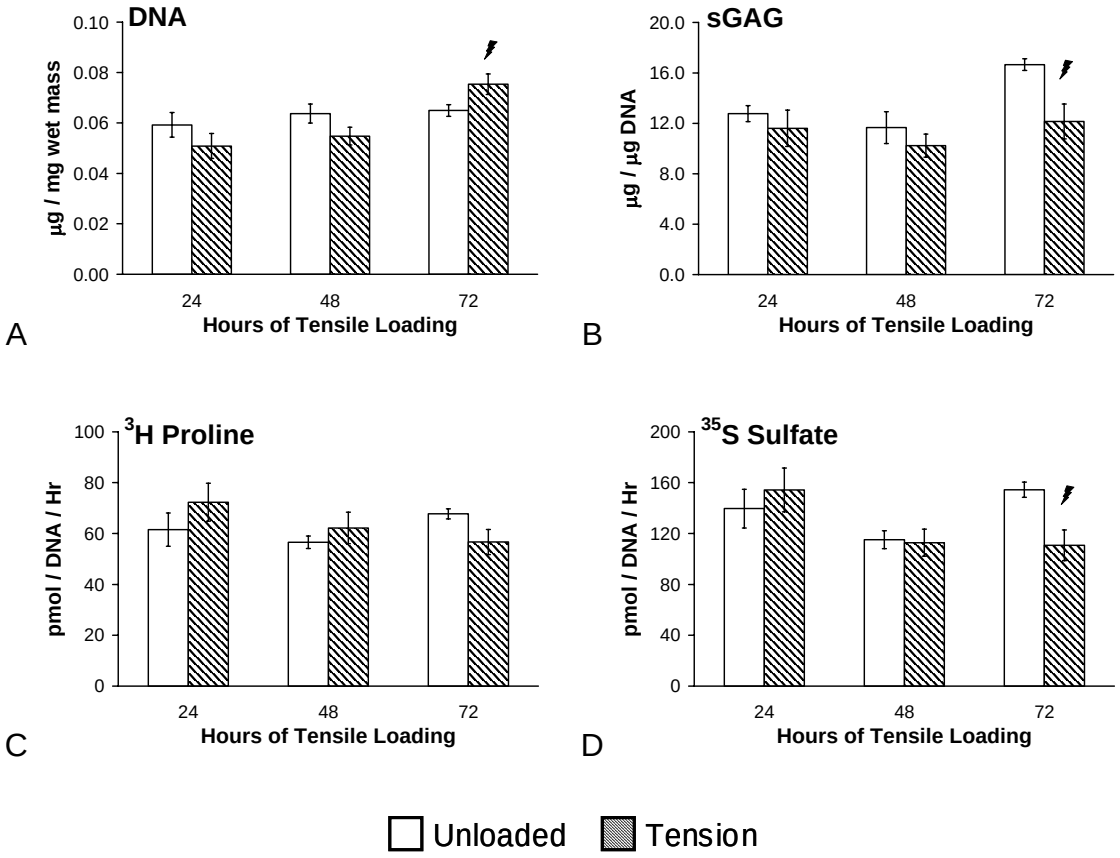

Figure 5.4 Biochemical analyses of fibrin hydrogel constructs subjected to various durations of sustained oscillatory tensile loading. All constructs were precultured for 7 days and then subjected to continuous oscillatory tensile loading for the lengths of time shown. ↯ indicates tension significantly different from unloaded.

Gene expression for both collagen types assessed (types I and II) was higher in constructs precultured for 4 days compared to those with only a 1 day preculture, but this effect was only statistically significant for the 1 and 4 hour loading groups (Figure 5.5A,B,E,F, $p < 0.001$). Additionally, aggrecan gene expression levels were higher after 4 days of preculture only in the 1 hour loading group (Figure 5.5C,D, $p < 0.011$). In contrast, aggrecan gene expression levels were found to be lower after 4 days of preculture for the 8 hour loading group (Figure 5.5C,D, $p < 0.05$). The constructs used for the 8 hour loading groups were seeded separately from those used for the 1 or 4 hour loading groups, which may account for the differences seen between these loading duration groups.

The effect of oscillatory tensile loading was found to be statistically significant only in three cases: aggrecan expression was decreased in the 1 day preculture group after 1 hour of tensile loading (Figure 5.5C, $p < 0.005$), type I collagen expression was increased in the 1 day preculture group after 4 hours of tensile loading (Figure 5.5E inset, $p < 0.022$), and type I collagen expression was decreased in the 4 day preculture group after 8 hours of tensile loading (Figure 5.5F, $p < 0.021$). Although these differences were statistically significant, none of the changes induced by tensile loading represented more than a 1.5 fold change in gene expression level and therefore were not considered to be functionally relevant. In contrast, the increases with preculture time seen in the gene expression levels of types I and II collagen ranged between 2 and 12 fold.

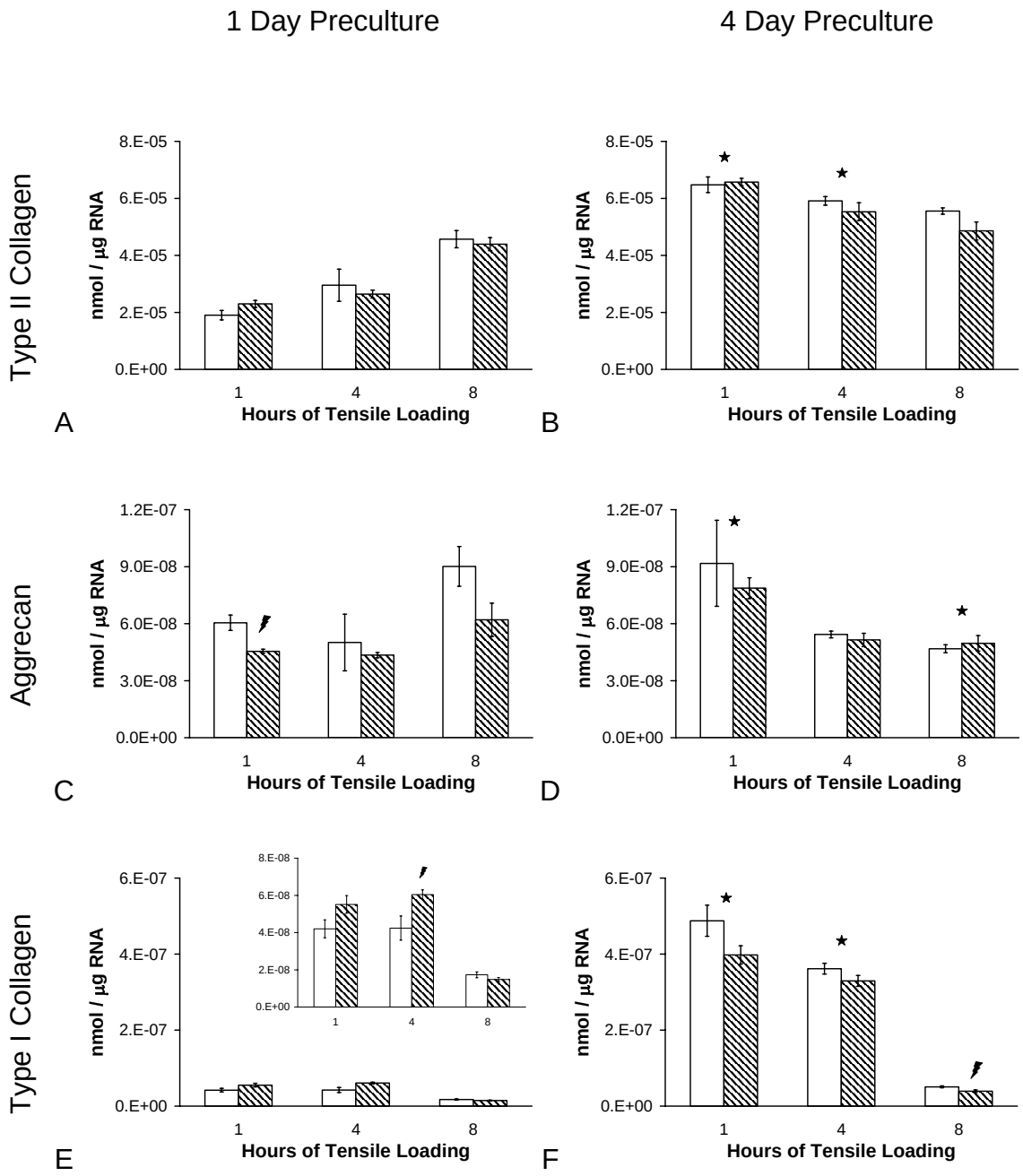

Figure 5.5 Gene expression profiles for chondrocytes in fibrin hydrogel constructs exposed to short durations of oscillatory tensile loading. (A,B) Type II collagen, (C,D) Aggrecan, and (E,F) Type I collagen. The left column shows constructs precultured for 1 day before loading, while the right column shows constructs precultured for 4 days before loading. The inset figure in (E) is a rescaled version of the primary figure in (E) to provide more detail. ★ indicates 4 day preculture significantly different from 1 day preculture. ↯ indicates tension significantly different from unloaded.

Two additional independent studies investigating other short term loading durations were also performed and yielded consistent results for matrix molecule gene expression levels as the study described here. Strong changes in gene expression levels were not found for either 2 or 6 hours of tensile loading after 4 days of preculture, or for 6 or 18 hours of tensile loading after 7 days of preculture compared to unloaded controls. The results of these studies indicated that collagen gene expression increased with time in culture for chondrocytes in fibrin hydrogel constructs, but overall matrix molecule gene expression was not sensitive to oscillatory tensile loading for the conditions chosen for these studies. These results favored using a longer preculture time in future studies. Additionally, it was hypothesized that repeated bouts of short durations of loading may be necessary to induce more substantial changes in the chondrocyte response to oscillatory tensile loading.

5.3.4 Intermittent Loading Study

The goal of the intermittent loading study was to investigate how various protocols of intermittently applied oscillatory tensile loading modulated chondrocyte extracellular matrix synthesis. Additionally, the mechanical characteristics and matrix molecule accumulation of fibrin hydrogel constructs were explored. Two intermittent loading protocols, selected based on results from earlier studies in our laboratory as well as relevant published reports on chondrocyte responses to intermittent mechanical loading[170,171], were used in each of two independent studies. Chondrocyte seeded fibrin hydrogel constructs were precultured for 7 days and then subjected to either the "3 Hour" protocol that consisted of 3 hours of tensile loading followed by 3 hours of recovery and

repeated 4 times each day or the "12 Hour" protocol that consisted of 12 hours of tensile loading followed by 12 hours of recovery and repeated once per day.

Neither DNA content (Figure 5.6A) nor sGAG accumulation (Figure 5.6B) was significantly affected by either intermittent loading protocol when applied for 3 consecutive days. The "3 Hour" intermittent oscillatory tensile loading protocol inhibited both ^{3}H-proline and ^{35}S-sulfate incorporation during the final day of 3 consecutive days of application (Figure 5.6C,D, $p < 0.005$). In contrast, the "12 Hour" protocol did not significantly affect ^{3}H-proline incorporation, but did significantly increase ^{35}S-sulfate incorporation during the final day of loading (Figure 5.6D, $p < 0.015$).

The hydrogel constructs used for each loading protocol were seeded separately from the same batch of cryogenically frozen chondrocytes. Note that both the DNA and sGAG contents of constructs from the "12 Hour" group are substantially lower than for constructs from the "3 Hour" group. These differences may be the result of different initial cell seeding densities, although every effort was made to maintain uniformity between seedings. Hence, it is difficult to make strong comparisons between the different loading protocols. However, each loading protocol was performed with an independent control group and therefore comparisons between the "Unloaded" and "Tension" groups for each protocol are valid.

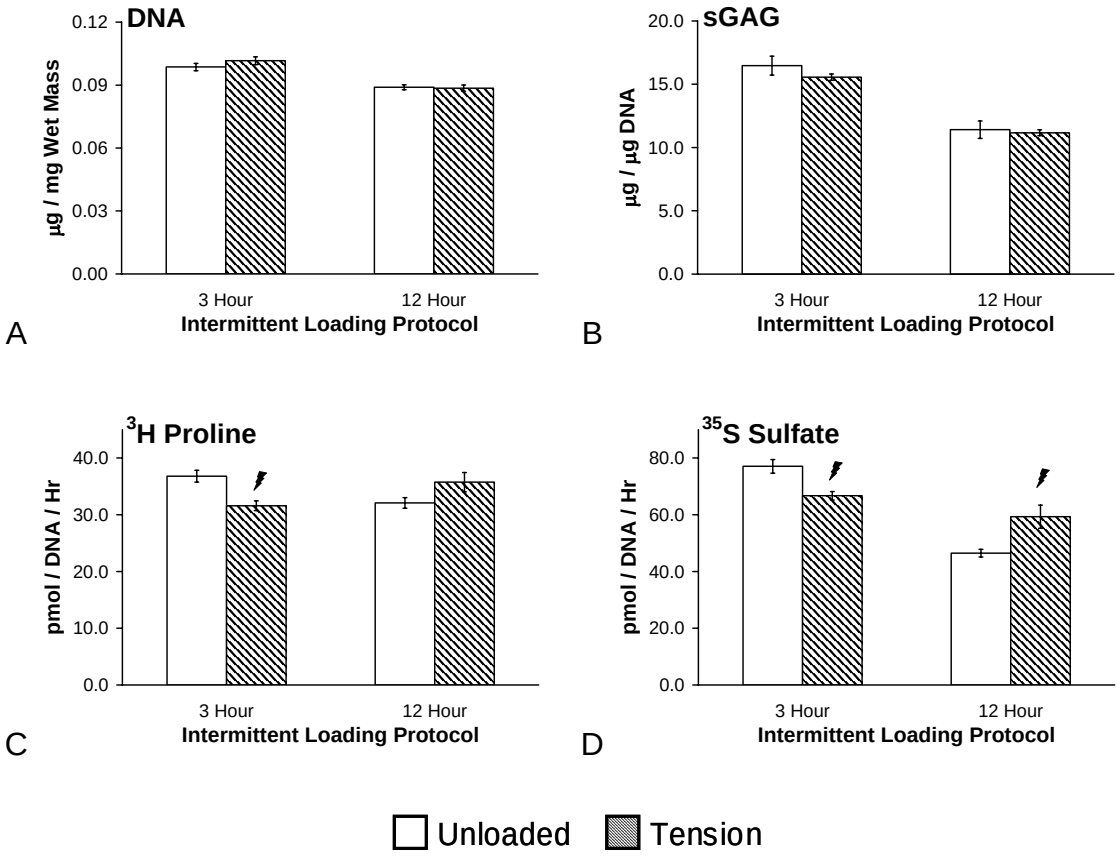

Figure 5.6 Biochemical analyses of fibrin hydrogel constructs subjected to protocols of intermittent oscillatory tensile loading. "3 Hour" = 3 hours of loading followed by 3 hours recovery, repeated 4 times per day. "12 Hour" = 12 hours of loading followed by 12 hours recovery, repeated once per day. ↯ indicates tension significantly different from unloaded.

A second study was performed to assess the effects of the same two intermittent oscillatory tensile loading protocols ("3 Hour" or "12 Hour"), but for longer durations. All constructs were precultured for 7 days and then the intermittent loading protocols were applied for either 3 or 7 consecutive days. Additionally, the amplitude of the sinusoidal displacement was increased to 10% (5% ± 5%). Both the extracellular matrix synthesis and the tensile mechanical properties of the hydrogel constructs were evaluated in this study.

The DNA content in constructs in the 7 day loading groups was higher than those in the 3 day loading groups ($p < 0.001$), but no significant differences were found in response to either intermittent loading protocol (Figure 5.7A). Constructs in the 7 day loading groups had similarly accumulated more sGAG compared to constructs in the 3 day loading groups (Figure 5.7B, $p < 0.005$). Additionally, the sGAG content of constructs subjected to 3 days of either intermittent tensile loading protocol was significantly lower compared to unloaded controls ($p < 0.05$).

Results for biosynthesis levels in the hydrogel constructs indicated that both ^{3}H-proline and ^{35}S-sulfate incorporation during the final day of loading were decreased in the 7 day loading groups compared to the 3 day loading groups (Figure 5.7C,D, $p < 0.001$). However, no significant differences were seen between the unloaded controls and constructs subjected to either intermittent loading protocol for either loading duration.

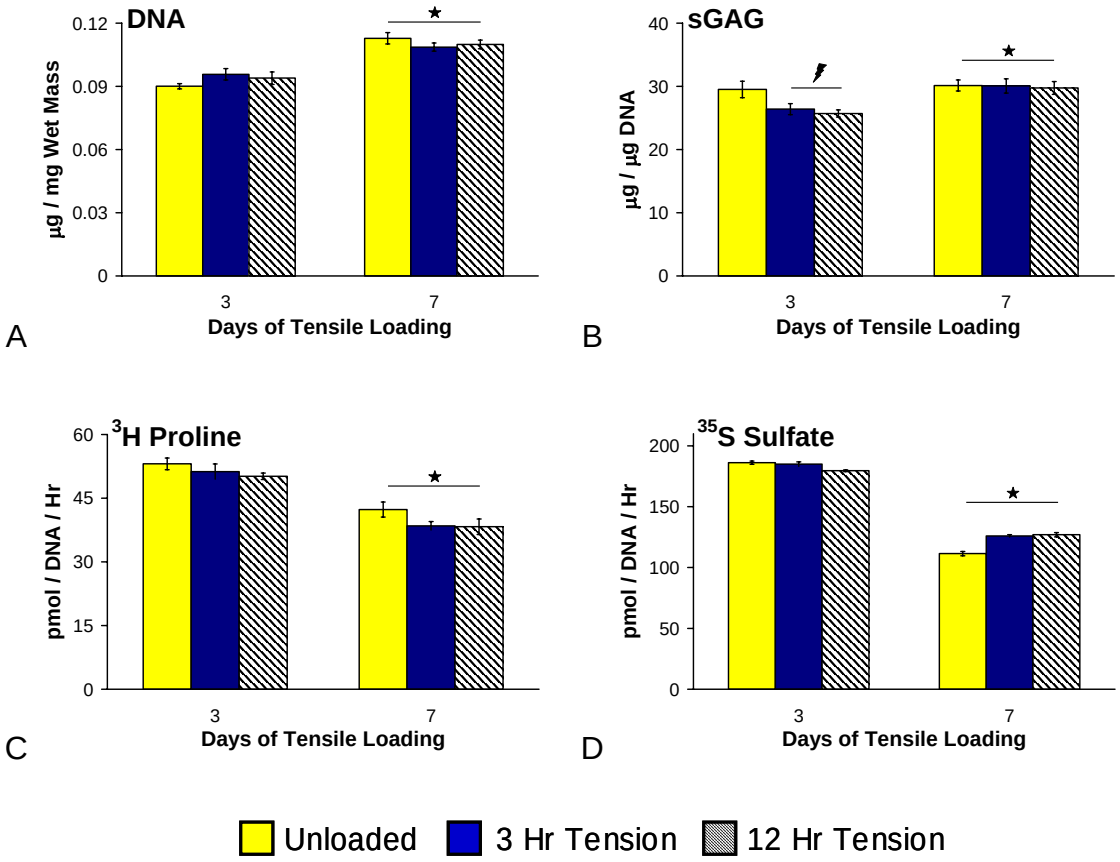

Figure 5.7 Biochemical analyses of fibrin hydrogel constructs subjected to intermittent oscillatory tensile loading for two different durations. "3 Hr Tension" = 3 hours of loading followed by 3 hours recovery, repeated 4 times per day. "12 Hr Tension" = 12 hours of loading followed by 12 hours recovery, repeated once per day. ★ indicates 7 days of loading significantly different from 3 days of loading. ↯ indicates tension significantly different from unloaded.

The amount of sGAG released to the culture medium was also measured throughout this study. Both intermittent tensile loading protocols induced an increase in sGAG release to the medium compared with unloaded controls at each loading duration investigated (Figure 5.8, $p < 0.015$). Interestingly, after 3 days of loading there was no difference in the total sGAG produced (retained in construct + released to medium) by either tensile loading group compared with the unloaded controls. However, after 7 days of loading total sGAG production in both intermittent loading groups was higher compared to unloaded controls ($p < 0.015$). Therefore, this study suggested that longer durations of intermittent oscillatory tensile loading stimulated extracellular matrix production, but reduced the retention of these newly synthesized matrix molecules in the constructs.

The dynamic moduli of constructs in the 7 day loading groups were significantly higher compared to constructs in the 3 day loading groups (Figure 5.9, $p < 0.001$). Additionally, constructs from both 3 and 7 day loading groups had a significantly higher dynamic modulus compared with constructs only allowed to culture for 1 day total (Figure 5.9, dashed line, $p < 0.001$). No differences in mechanical properties were seen between the unloaded controls and constructs subjected to either loading protocol.

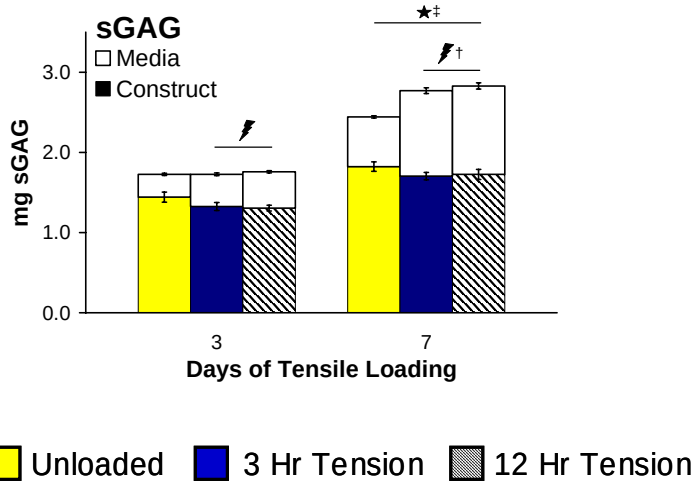

Figure 5.8 Total sGAG produced by chondrocytes in fibrin hydrogel constructs subjected to intermittent oscillatory tensile loading. "3 Hr Tension" = 3 hours of loading followed by 3 hours recovery, repeated 4 times per day. "12 Hr Tension" = 12 hours of loading followed by 12 hours recovery, repeated once per day. Colored bars represent sGAG retained in the constructs, while open bars represent sGAG released to the culture medium. ★ indicates media sGAG for 7 days of loading significantly different from 3 days of loading. ‡ indicates total sGAG (construct + media) for 7 days of loading significantly different from 3 days of loading. ↯ indicates media sGAG for tension significantly different from unloaded. † indicates total sGAG (construct + media) for tension significantly different from unloaded.

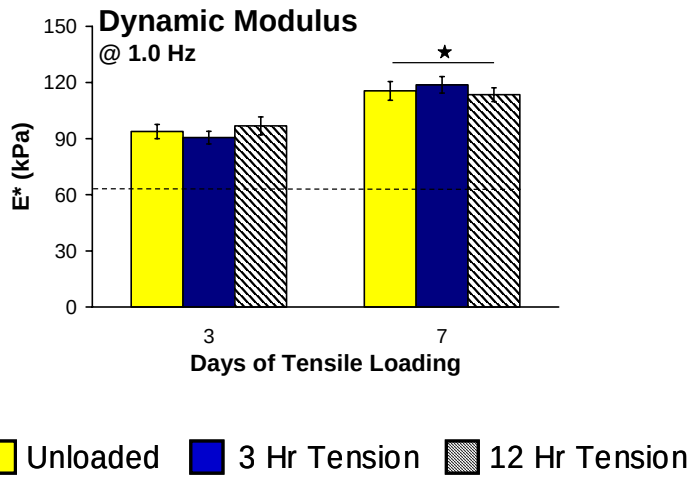

Figure 5.9 Mechanical characterization of fibrin hydrogel constructs subjected to intermittent oscillatory tensile loading for two different durations. "3 Hr Tension" = 3 hours of loading followed by 3 hours recovery, repeated 4 times per day. "12 Hr Tension" = 12 hours of loading followed by 12 hours recovery, repeated once per day. Dashed line indicates mean value for constructs tested 1 day after seeding. ★ indicates 7 days of loading significantly different from 3 days of loading.

5.4 Discussion

The studies described in this chapter explored the effects of various oscillatory tensile loading protocols on articular chondrocytes or meniscal fibrochondrocytes seeded in three dimensional fibrin hydrogel constructs. The objective of these efforts was to identify tensile loading regimes that modulated cellular proliferation and extracellular matrix biosynthesis in specific ways and ideally to establish an optimal protocol that could be used to stimulate the development of engineered cartilaginous tissues.

The initial preculture duration study indicated that 68 hours of continuous oscillatory tensile loading inhibited extracellular matrix synthesis in both articular chondrocytes and meniscal fibrochondrocytes for many of the preculture durations

investigated. This result was notable because several published reports have shown that other modes of dynamic mechanical stimulation, such as unconfined compression[100,139,160,172] and shear[101,102,116], stimulated extracellular matrix synthesis in both tissue explants and cell seeded constructs. These different responses to tension versus compression or shear could potentially be due to the different loading modes, and thus chondrocytes and fibrochondrocytes may respond fundamentally differently to tension. However, each of the reports referenced above used shorter total loading durations (*i.e.* 24 hours) or short bouts of dynamic loading that were repeatedly applied. Thus, the differing trends in matrix synthesis may, in fact, be the result of using shorter term versus prolonged mechanical stimulation.

This hypothesis was tested in the sustained loading duration study described in this chapter. Consistent with previous results, 72 hours of sustained oscillatory tensile loading was found to increase construct DNA content and decrease chondrocyte extracellular matrix synthesis. However, these trends were not seen in constructs subjected to only 24 or 48 hours of sustained loading. These observations were consistent with a previously published report from our laboratory describing decreases in extracellular matrix accumulation and mechanical properties following 10 and 20 days of dynamic compression in chondrocyte seeded fibrin constructs[140]. Additionally, many researchers have shown that short term continuous dynamic compression or long term application of intermittent dynamic compression increased chondrocyte matrix synthesis in several different scaffold systems[5,100,162,173].

Since tensile mechanical stimulation has not been widely explored as a means to influence chondrocyte or fibrochondrocyte behavior in culture, few published reports

were available for direct comparison. However, cyclic tensile loading of human dermal fibroblasts in three dimensional collagen[143,165] and fibrin[174] constructs has been shown to increase construct mechanical properties. Additionally, Seliktar et al.[165] demonstrated that 4 days of cyclic tensile strain enhanced construct mechanical properties, but prolonged exposure to strain had adverse effects due to increases in protease activity. Taken together, the results from our studies and the published reports referenced above supported the hypothesis that longer durations of oscillatory tensile loading can inhibit chondrocyte extracellular matrix production and accumulation, whereas shorter durations may stimulate matrix production and have the potential to enhance engineered cartilaginous tissues.

In an effort to identify specific effects of brief periods of oscillatory tensile loading on chondrocyte gene expression, several short term loading studies were performed. Although collagen gene expression levels were found to increase with time in culture, consistent and substantial changes in matrix molecule gene expression were not found in response to oscillatory tensile loading. A recently published study investigating the effects of cyclic tensile loading on chondrocytes in alginate hydrogels reported increases in gene expression levels for several extracellular matrix molecules, including collagen types I and II and lubricin[171]. Tensile loading was applied in this report for 3 hours per day for 3 consecutive days, based on previous findings indicating that biosynthesis was increased when loading was applied for several consecutive days compared to a single application of loading[175]. Hence, several repetitions of the 1, 4, and 8 hour tensile loading bouts used in our studies may have resulted in more dramatic differences in response to loading. However, in our studies the scaffold material used

was fibrin, whereas in the above cited report alginate was used. Presumably, tensile loading may influence gene expression levels via various mechanotransduction pathways, which are likely to depend on the local cellular mechanical environment and hence the scaffold system. As discussed in Chapter 4, fibrin possesses numerous binding sites that can facilitate direct cell attachment, but an alginate hydrogel is essentially inert and does not contain cellular binding domains. This difference in cellular attachment mechanisms could significantly influence the mechanotranduction characteristics between the two scaffold systems. Additionally, other scaffold differences such as ion concentration, porosity, and mechanical stiffness may also exist. Thus, the expectation that the modulation of matrix molecule gene expression found in one system will directly translate to another scaffold system is not well founded.

Finally, dynamic mechanical loading may not substantially regulate chondrocyte matrix metabolism at the level of gene transcription, as has been recently postulated for fibrin hydrogels[176] as well as suggested for cartilage tissue explants[177]. Rather than influencing gene transcription in our system, tensile loading may have had a more significant effect on post-translation modifications of extracellular matrix molecules influencing their assembly, distribution, and retention in the construct. Additionally, mechanical loading may have altered mRNA stability or functionality but not necessarily total transcription levels.

The series of intermittent loading studies described in this chapter investigated how the chondrocyte response to oscillatory tensile loading might be enhanced by using repeated bouts of shorter loading durations. The “3 Hour” intermittent protocol, which consisted of 3 hours of loading followed by 3 hours of recovery repeated 4 times per day,

was found to inhibit both ^{3}H-proline and ^{35}S-sulfate incorporation during the final day of a 3 day loading period. In contrast, the "12 Hour" protocol, consisting of 12 hours of loading followed by 12 hours of recovery repeated once per day, enhanced ^{35}S-sulfate incorporation during the final day of a 3 day loading period. These results were consistent with Chowdhury *et al.*[170], who found that a similar 12 hour dynamic compression loading protocol maximally stimulated ^{35}S-sulfate incorporation in chondrocyte seeded agarose constructs compared to protocols using shorter loading/recovery cycles.

The amplitude of tensile displacement was then increased to a 5% ± 5% sinusoid (as opposed to 2.5% ± 2.5% as in previous studies) and the intermittent oscillatory tensile loading study was repeated for either 3 or 7 consecutive days of loading. Interestingly, no changes in ^{3}H-proline and ^{35}S-sulfate incorporation were found in response to either tensile loading protocol under these conditions. However, both protocols increased the amount of sGAG released to the culture medium compared with the unloaded controls. Furthermore, the total sGAG produced, the sum of that retained in the constructs and released to the culture medium, was increased by both loading protocols after 7 days of application compared to unloaded controls, but no differences were seen after only 3 days of loading. Hence, intermittent oscillatory tensile loading applied for 7 days increased overall glycosaminoglycan production, but also increased the amount of these newly synthesized molecules released from the constructs. This finding was intriguing because it demonstrated that oscillatory tensile loading stimulated matrix production, but the fibrin hydrogel constructs were not able to effectively retain this new matrix. Therefore, a balance may exist between enhancing extracellular matrix production via mechanical

stimulation and achieving adequate retention such that sufficient construct maturation can occur. By optimizing the loading protocol to maximize matrix production using the least amount of loading time and enhance matrix retention by using the longest duration of recovery time, an ideal balance between synthesis and retention may be possible to achieve. Attempts at such an optimization have been made using dynamic mechanical compression with some success[173,178], but performing comparable studies with oscillatory tensile loading was beyond the scope of this dissertation.

The dynamic tensile properties of the fibrin hydrogel constructs were measured after 3 and 7 days of intermittent oscillatory tensile loading. Mirroring the biochemical contents, the constructs subjected to 7 days of loading (14 days of total culture) were significantly stiffer than those only subjected to 3 days of loading (10 days total culture). Both groups were stiffer than control constructs only cultured for 1 day before testing. Additionally, no differences in the dynamic tensile modulus of the constructs were seen in response to either loading protocol. Although this initially seemed like a null result, it provided valuable information regarding our fibrin hydrogel construct system. This study demonstrated that up to 7 days of intermittent tensile loading did not induce significant scaffold degradation or contraction. The fibrin scaffold provides the bulk of the mechanical integrity in these constructs, and therefore damage, either directly from stretching or from cell-mediated degradation, could undermine the utility of this system for studying the development of engineered cartilage tissues. Additionally, 21 days of dynamic compression was necessary before increases in the mechanical properties and extracellular matrix accumulation of chondrocyte seeded agarose hydrogels were

apparent[5]; thus similar increases in our system would not have been expected after only 7 days of loading.

Based on the results from all of the studies presented in this chapter, the "12 Hour" intermittent oscillatory tensile loading protocol was selected for the remainder of the work in this dissertation. This protocol consisted of 12 hours loading at a frequency of 1.0 Hz and a sinusoidal displacement of 5% ± 5% followed by 12 hours of recovery at 0% displacement.

The overall objective of all the studies presented in this chapter was to gain a better understanding of how articular chondrocytes and meniscal fibrochondrocytes would respond to oscillatory tensile loading and how various regimes of tensile loading could be used to modulate cellular processes in specific ways. Although several of these studies demonstrated that oscillatory tension could influence chondrocyte metabolism, often these changes in response to loading were subtle. This observation was not unique to our studies as many of the published reports cited throughout this dissertation described differences between treatment groups of 20% or less, which is not uncommon with three dimensional engineered tissues. However, the inhomogeneity of the cell population isolated from full thickness articular cartilage tissue may have also contributed to these results. Chondrocyte morphology and phenotype are known to be dependent on their origin within the tissue[7]. Many of the specific differences were discussed in Chapter 2, and it has been repeatedly shown that chondrocytes isolated from different zones of the tissue maintain at least some of these distinctions during *in vitro* culture[26,29,179-183]. Therefore, chondrocytes derived from different zones within the tissue may respond to oscillatory tensile loading in distinct ways, but these potential differences

could have been "diluted out" in our hydrogel constructs that contained a mixed population of cells.

The series of studies presented in this chapter represent a unique contribution to the field of cartilage tissue engineering and provide insights into how oscillatory tensile loading modulates chondrocyte and fibrchodrocyte behavior *in vitro*. Longer durations of continuous oscillatory tension generally inhibited extracellular matrix synthesis in both cell types, but this effect was not found for shorter loading times. Additionally, applying tensile loading intermittently was found to stimulate matrix synthesis, but also to induce increased levels of the newly synthesized matrix molecules to be released into the culture medium. Understanding how articular chondrocytes respond to altered mechanical loading environments, such as tension, may offer valuable insights into how better to manipulate tissue engineered cartilage constructs *in vitro*. Similarly, using tensile loading to modulate meniscal fibrochondrocyte metabolism could prove useful for developing fibrocartilage repair tissues. Ultimately, understanding more completely how various loading environments can affect cell behavior may prove crucial to understanding how cartilage and fibrocartilage tissues develop, are maintained, and can be repaired.

CHAPTER 6

DIFFERENTIAL RESPONSES OF ZONE-SPECIFIC CHONDROCYTES AND FIBROCHONDROCYES TO OSCILLATORY TENSILE LOADING

6.1 Introduction

Articular cartilage is a stratified tissue with well characterized depth-dependent patterns of cellular morphology[7], extracellular matrix ultrastructure[184], and mechanical characteristics[21]. Chondrocytes from the superficial zone have a flattened morphology and align parallel to the joint surface, whereas cells from deeper within the tissue possess a more spherical morphology[7]. Collagen content is most dense in the superficial region where the fibers are aligned parallel to the joint surface, whereas proteoglycan content is highest in the middle and deep regions[6,184]. Some zone-specific phenotypic differences in chondrocytes are lost after periods of two-dimensional *in vitro* culture[28,29], however some differences, especially in regard to extracellular matrix synthesis, seem to be more inherent and are retained in both two-dimensional and three-dimensional cultures[26,29]. Recreating this inhomogeneous composition of cartilage to some degree may be necessary for cartilage tissue engineering strategies to be successful. Therefore, several recent attempts have been made to create tissue engineered cartilage constructs with a stratified or zonal organization[180,182]. Additionally, subpopulations of chondrocytes originating from distinct tissue zones have been shown to differentially respond to mechanical compressive loading[181].

Similarly, as discussed in detail in Chapter 3, the extracellular matrix ultrastructure, as well as cellular phenotype and morphology vary by zone in the meniscus[58]. Fibrochondrocytes from the inner region of the meniscus tend to resemble articular chondrocytes, whereas cells found in the outer region have a more fibroblastic, stellate morphology[74]. Previous work in our laboratory has also demonstrated differences in the gene expression profiles, extracellular matrix synthesis rates, and response to static compression between cells from different meniscal zones[124].

Although several studies investigating three-dimensional culture of zone-specific chondrocytes have been published[180-182], these studies used scaffold materials that do not enable direct cell-matrix interactions, such as poly(ethylene glycol) derivatives, alginate, and agarose. The fibrin hydrogel construct system used in our current studies, however, does allow for direct cellular interaction with the surrounding matrix and therefore the cellular environment may be quite different from that of the more inert scaffolds. Hence initial studies were designed to investigate the ability of fibrin hydrogels to preserve zonal differences in chondrocyte phenotype. Subsequently, the effects of intermittent oscillatory tensile loading on zone-specific chondrocytes in fibrin hydrogel constructs were explored. An intermittent tensile loading protocol developed in earlier studies and described in Chapter 5 was chosen for the current investigation. Finally, an identical loading study was performed using zone-specific meniscal fibrochondrocytes from either the inner or outer region of the tissue.

Based upon available information regarding zone-specific chondrocytes as well as our own experimental findings with zone-specific meniscal fibrochondrocytes, we hypothesized that cells from distinct zones of articular cartilage and the meniscus would

differentially respond to oscillatory tensile loading. Since the surface of articular cartilage experiences some tensile strain *in vivo*, we believed that chondrocytes from the superficial zone would exhibit a more dramatic response to oscillatory tensile loading compared to chondrocytes from deeper in the tissue. Additionally, the subtle effects of oscillatory tensile loading seen in previous studies using cells pooled from all tissue regions may be the result of zone dependent responses to loading. Therefore investigating the effects of oscillatory tensile loading on separate subpopulations of chondrocytes and fibrochondrocytes may better elucidate specific inherent cellular responses.

6.2 Materials and Methods

6.2.1 Tissue Harvest and Cell Isolation

Articular chondrocytes and meniscal fibrochondrocytes were obtained from immature bovine stifle joints as described previously, but special harvest procedures were required to separate the tissues into distinctive zones. The intact femoral-patellar groove and femoral condyles were aseptically removed using a small hand saw. Rectangular osteochondral blocks (3-4 mm per side) were then cut from the tissue such that at least two sides were perpendicular to the surface. The tissue blocks were thoroughly rinsed in PBS supplemented with antibiotic/antimycotic before being divided into discrete zones using a sledge microtome. The top 250 μm was taken as the superficial zone, tissue ranging from 500 - 1000 μm from the surface was taken as the middle zone, and tissue 1250 - 2000 μm from the surface was taken as the deep zone (Figure 6.1). Tissue from

the deep zone never included regions of calcified cartilage. The overall thickness of the tissue blocks varied slightly with location in the joint (*i.e.* blocks from the central region of the femoropatellar groove were thicker than blocks from the femoral condyles). This procedure was developed based on information available in the literature[27,180] as well as several pilot studies conducted in our laboratory. Tissue slices from the discrete zones were pooled and chondrocytes were enzymatically isolated using 0.2% collagenase in DMEM supplemented with antibiotics for approximately 20 hours. The cell suspensions were then passed through a sterile 74 μm mesh, washed, and concentrated via several centrifugation steps. Cell counts and viability for each zonal group were determined using a Beckman Coulter Vi-Cell XR and cell size was determined using a Beckman Coulter Multisizer III. Finally, chondrocytes from each zone were suspended in fresh DMEM and seeded into either cylindrical fibrin hydrogels (11 mm diameter x 3 mm thick) or the rectangular fibrin hydrogel constructs as described in Chapter 5.

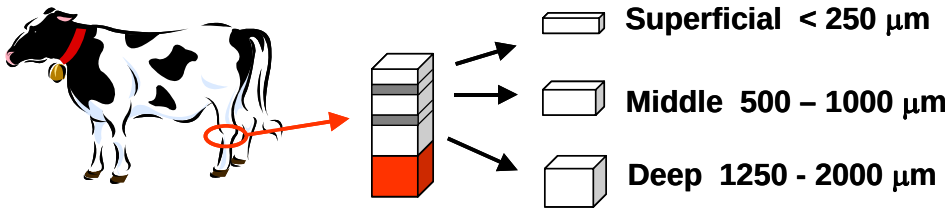

Figure 6.1 Schematic of zone-specific articular chondrocyte harvest procedure

Intact medial and lateral menisci were aseptically excised from up to 6 joints and thoroughly rinsed with PBS supplemented with antibiotic/antimycotic. All connective

tissue was carefully removed including the fibrous attachments located at the anterior and posterior horns. The boundary for the inner zone of the meniscus was determined visually as the point where the tissue transitioned from blue-white and partially translucent to more opaque and solid white in appearance (Figure 6.2).

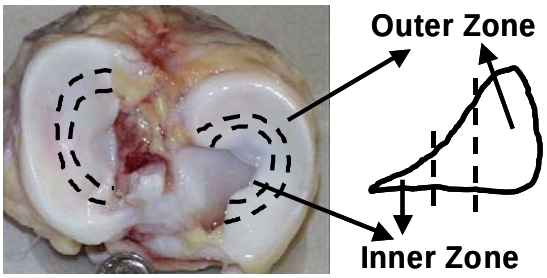

Figure 6.2 Schematic of zone-specific meniscal fibrochondrocyte harvest procedure

This inner portion consisted of approximately 25% of the total radial length of the meniscus. The inner zone was carefully separated from the bulk of the meniscus using a sterile scalpel and transferred to PBS. Progressing radially toward the outer edge of the tissue, the next 3-4 mm was dissected away and discarded. The remaining tissue was taken as the outer zone and transferred to PBS. All tissue was then minced and fibrochondrocytes were enzymatically isolated using a sequential protocol of trypsin and 0.4% collagenase as previously described in Chapter 5. Tissue from medial and lateral menisci was kept separate throughout the harvest and cell isolation procedures. Cell suspensions were processed as described above and equal numbers of cells derived from medial and lateral menisci were pooled after counting. This procedure left two distinct

populations of inner zone and outer zone meniscal fibrochondrocytes. These populations were suspended in fresh DMEM and seeded into rectangular fibrin hydrogel constructs as described in Chapter 5.

In addition, aliquots containing approximately 2 million cells from each zonal population were removed for gene expression analysis using real time RT-PCR prior to construct seeding. Cells in these aliquots were pelleted, the supernatant was replaced with cell lysis buffer plus β-mercaptoethanol, and the suspensions were frozen at -80°C. The Qiagen RNeasy RNA isolation procedure was used according to the manufacturer's instructions to isolate RNA. Total RNA isolated was quantified and equal amounts of RNA were reverse transcribed to cDNA using the Promega Reverse Transcription System (see Appendix C for additional details). Custom primers (Table 6.1) were used to amplify cDNA, and SYBR green was used to measure amplification in real time on an ABI Prism Sequence Detector 7700.

Table 6.1 Primer sequences for bovine genes used in real time RT-PCR

Gene	GenBank Accession #	Primer Sequence 5' – 3'	Amplicon
Type II Collagen	*X02420*		
Forward		GCA TTG CCT ACC TGG ACG AA	83 bp
Reverse		CGT TGG AGC CCT GGA TGA	
Aggrecan	*NM_173981*		
Forward		CCT CAG GGT TTC CTG ACA TTA	82 bp
Reverse		TAA GCT CAG TCA CGC CAG ATA	
Type I Collagen	*AB008683*		
Forward		AAG AAC CCA GCT CGC ACA TG	107 bp
Reverse		GGT TAG GGT CAA TCC AGT AGT AAC CA	
Decorin	*NM_173906*		
Forward		ACT GAA GGA ATT GCC AGA GAA	119 bp
Reverse		CTA CGA CGA TCA TCT GGT TCA	
Biglycan	*S82652*		
Forward		GGT CCT CGT GAA CAA CAA GAT	85 bp
Reverse		GGA TCT CAC ACA GGT GGT TCT	

6.2.2 Fibrin Hydrogel Construct Culture

Free Swelling Culture

Zone-specific chondrocytes in cylindrical fibrin hydrogels were cultured in 24-well tissue culture plates for up to 15 days and medium was changed every two days. The serum supplemented DMEM formulation described previously (Table 5.2) was used for all studies presented in this chapter, although the gentamicin and Fungizone were replaced with antibiotic/antimycotic. On the final day of culture for each time point (days 3, 8, or 15), medium was additionally supplemented with 10 μCi/mL L-5-^{3}H-proline and 5 μCi/mL ^{35}S-sodium sulfate. Additionally, the antibiotic/antimycotic

solution was withheld from the culture medium during the radiolabeling procedure. Upon removal from culture, hydrogels were washed 4 times for 30 minutes each at 4°C in PBS with 1.0 mM L-proline and 0.8 mM sodium sulfate to remove unincorporated radioactive precursors. The total wet mass of each hydrogel was then measured and the hydrogels were frozen at -20°C.

Oscillatory Tensile Loading

Rectangular fibrin hydrogel constructs, containing either zone-specific chondrocytes or fibrochondrocytes, were treated identically throughout the culture and tensile loading periods. Constructs were cultured in free swelling conditions using rectangular 8-well tissue culture plates in an incubator held at 37°C and 5.0% CO_2 for 6 days with media changed every 2 days. On the 6^{th} day, constructs were randomly assigned to the unloaded or tension culture chambers (see Section 4.3) and allowed to culture without any loading for one additional day. Thus, the total preculture time for these studies was 7 days. The antibiotic/antimycotic solution was only added to the culture medium during the first 6 days of culture.

On the following day, an intermittent oscillatory tensile loading protocol was used to stimulate the fibrin hydrogel constructs. Constructs were stretched using a 1.0 Hz sinusoidal wave form with a 5% ± 5% amplitude. This protocol was applied for 12 hours followed by a 12 hour recovery period where constructs were held at 0% displacement. This loading regime was repeated 3 times, yielding a total culture duration of 10 days (7 days unloaded, 3 days tension). Culture medium was changed everyday during the final hour of the recovery period, and a portion of the conditioned culture medium was collected at each media change throughout the studies. Parallel constructs in the

unloaded culture chambers served as controls. Culture medium was additionally supplemented with 10 μCi/mL L-5-^{3}H-proline and 5 μCi/mL ^{35}S-sodium sulfate on the final day of culture. Upon removal from culture, constructs were washed as described above, end blocks were removed, total construct mass was recorded, and samples were frozen at -20°C. In addition, a set of constructs from each group was randomly selected after only two days of free swelling culture, and the medium for these constructs was supplemented with radioactive precursors for an additional 24 hours. This set of constructs served as an early time point control and was designated "3 Day."

Table 6.2 Summary of culture conditions for zone-specific chondrocyte and fibrochondrocyte studies

Group Name	Preculture Duration	Loading Duration	Total Culture Time
3 Day	3 days	N/A	3 days
Unloaded	7 days	3 days, unloaded	10 days
Tension	7 days	3 days, tension	10 days

6.2.3 Biochemical Composition Analyses

For each study described here, the frozen hydrogel constructs were lyophilized to dryness, measured for solid mass, and digested overnight at 60°C using proteinase K in 100 mM ammonium acetate. ^{3}H-proline and ^{35}S-sulfate incorporation rates (indicators of total protein and proteoglycan synthesis, respectively) were assessed using a liquid

scintillation counter. Total DNA and sulfated glycosaminoglycan (sGAG) contents were measured using the Hoechst dye[168] and the 1,9-DMMB dye[169] assays, respectively.

For the zone-specific chondrocyte tensile loading study only, total sGAG released into the culture medium was also assessed using the DMMB assay. Further characterization of the proteoglycans released into the medium for this study was performed using size exclusion liquid chromatography and Western blot analysis. Portions of the conditioned media from the final day of culture were first processed using a Hi-Trap Sephadex G-25 Superfine column to remove radioactive precursors not incorporated into macromolecular structures. 7M Urea plus 50 mM Tris acetate was used to equilibrate the columns, and 8M Urea plus 50 mM Tris acetate was used as the elutent. Fractions in the excluded volume of this column were pooled and concentrated using Amicon Ultra-4 10 kDa centrifugal filters. Samples were then run on a 30 x 1 cm Econo-Column packed with Sepharose CL-4B and equilibrated with 4M Guanidine HCl plus 50 mM sodium acetate. 500 μL fractions were collected at a flow rate of 0.35 mL/minute and analyzed for ^{35}S and ^{3}H content with a liquid scintillation counter.

A quantitative assessment of liquid scintillation counter data from the size exclusion column chromatography was undertaken to determine the fraction of ^{35}S-sulfate incorporated into large proteoglycans (*i.e.* intact aggrecan) versus small proteoglycans (*i.e.* decorin, biglycan, or aggrecan fragments). The fractions representing these two proteoglycan populations were determined from examining data from all samples. It was important to subtract off the background level in this data, because some sample readings were only 2-3 times higher than the average background intensity readings. An appropriate method for estimating the background of each sample was to

use the average reading of the final 8 fractions of each column run. A Newton-Cotes integration method was used to approximate the area under each peak, which is equivalent to the total ^{35}S found in each peak.

$$A = \frac{h}{2} \cdot \left[\left(f_1 + f_n + 2\sum_{i=2}^{n-1} f_i \right) - B_{avg} \cdot (2n-2) \right]$$

where A = area under each peak, *i.e.* total ^{35}S in the peak

h = volume collected in each fraction

f_i = CPM reading from each fraction

n = number of fractions in each peak

B_{avg} = average background reading

The total macromolecular ^{35}S was calculated by adding the areas for the two peaks in each sample, and finally the percentage of the ^{35}S in each peak was determined.

Finally, fractions corresponding to peaks containing large proteoglycans (intact aggrecan) and to small proteoglycans (decorin, biglycan, aggrecan fragments, *etc.*) were each pooled and concentrated using the 10 kDa centrifugal filters. Proteoglycans from portions of the pooled samples were precipitated overnight at 4°C by adding 3 volumes of ice cold 100% ethanol plus 50 mM sodium acetate. The protocol for Western blot analysis found in Appendix C was followed to detect the presence of biglycan, decorin, and the G3 domain of aggrecan.

6.2.4 Statistical Analyses

Chondrocyte size data were analyzed using a two-sided paired student's t-test, and all other data were analyzed using a general linear model and Tukey's test for post hoc analysis with significance set at $p < 0.05$. The study investigating zone-specific chondrocytes in free swelling culture was analyzed with a multifactor model using cartilage zone and culture time as factors. The studies investigating the effects of tensile loading on zone-specific chondrocytes or fibrochondrocytes were analyzed with single factor models (cartilage zone or loading condition), evaluating each group separately. Column chromatography data were transformed using an arcsine function to ensure normality[185] and then analyzed using a multifactor model with cartilage zone and loading condition as factors. In all cases, interaction terms were included in the models when appropriate and the criterion for significance was satisfied. Unless otherwise noted, the sample size was 6 for all groups analyzed in these studies.

6.3 Results

6.3.1 Zone-Specific Chondrocytes: Free Swelling Culture

Consistent with published data[22,29,181,186], chondrocyte cell size was significantly larger with increasing distance from the tissue surface as indicated by shifts in the cell size distributions (Figure 6.3A, $p < 0.001$). Superficial zone cells were smaller than middle zone cells, which were in turn smaller than deep zone cells. Between 3800 and 6600 cells were measured in each zonal group for this analysis. Additionally, gene expression data generally agreed with previous published reports[30,187] (Figure 6.3B).

Type II collagen gene expression in middle and deep zone chondrocytes was approximately 4-fold higher than in superficial zone cells. Deep zone cells also had an approximately 3-fold higher level of aggrecan gene expression compared with superficial and middle zone cells. Finally, type I collagen gene expression was several orders of magnitude lower relative to type II collagen in all zones, and type I collagen expression in middle and deep zone chondrocyte was approximately 5- and 9-fold higher, respectively, compared with superficial zone cells.

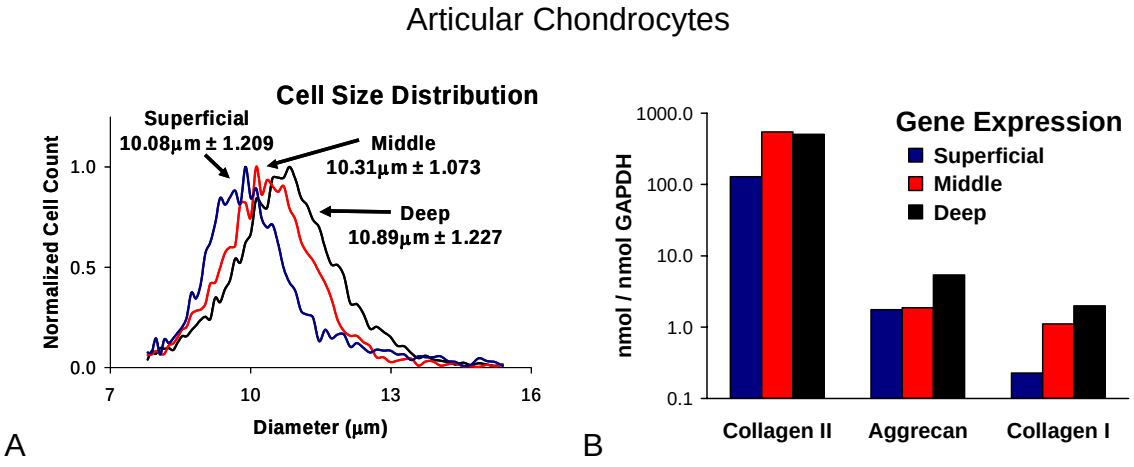

Figure 6.3 Characterization of zone-specific chondrocytes prior to seeding in fibrin hydrogel constructs. (A) Cell diameter distribution; mean ± standard deviation. (B) Gene expression for type II collagen, aggrecan, and type I collagen.

Data presented for free swelling culture using zone-specific chondrocytes are from one of two independent experiments yielding similar results. Fibrin hydrogel DNA content increased with time in culture for chondrocytes from all zones (Figure 6.4A, $p < 0.001$). Additionally, hydrogels containing chondrocytes from the superficial and

middle zones had a significantly higher cell density than those with deep zone chondrocytes after 15 days in culture (Figure 6.4A, $p < 0.002$). DNA data are presented as normalized to the average hydrogel DNA contents after 3 days in culture for each zonal group to account for small differences in initial hydrogel seeding density (differences were typically less than 10%). Total sGAG content also increased significantly with time in culture for hydrogels containing cells from all zones (Figure 6.4B, $p < 0.001$). After 8 days in culture, deep zone hydrogels contained a greater amount of sGAG than superficial zone hydrogels ($p < 0.001$). This trend persisted through 15 days of culture, where middle zone hydrogels also contained more sGAG than superficial zone hydrogels ($p < 0.001$).

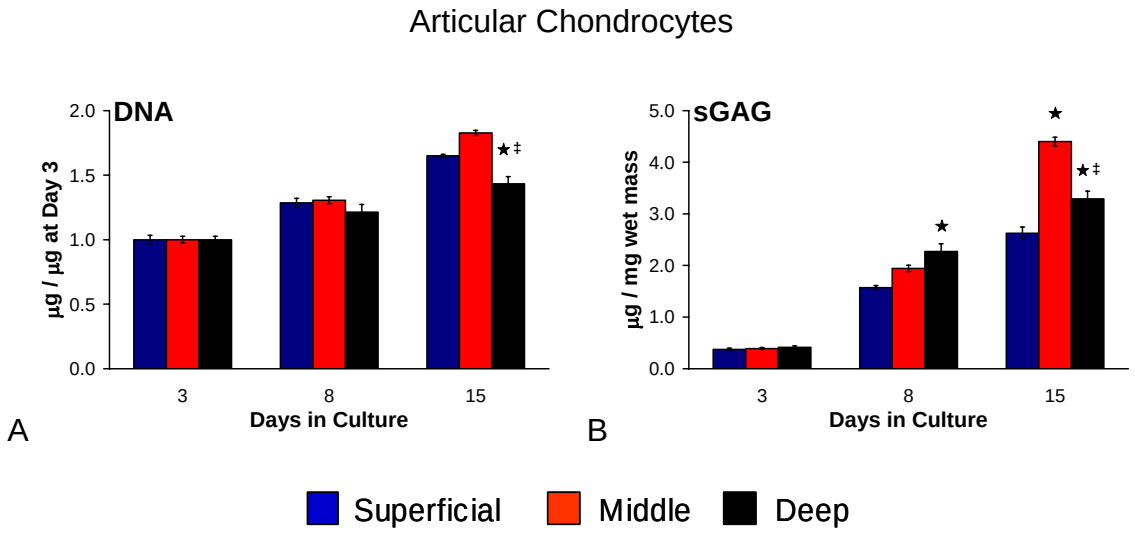

Figure 6.4 Biochemical content of fibrin hydrogels seeded with zone-specific chondrocytes cultured in free swelling conditions. (A) Hydrogel DNA content and (B) hydrogel sGAG content. ★ indicates significant difference from Superficial; ‡ indicates significant difference from Middle.

Data from the analysis of radiolabeled precursor incorporation were consistent with gross biochemical content and revealed interesting differences among chondrocytes with different zonal origins. ^{3}H-proline incorporation rates decreased with time in culture for superficial zone hydrogels (Figure 6.5A, $p < 0.001$). However, ^{3}H incorporation was stable through 8 days of culture in middle and deep hydrogels before significantly dropping off after 15 days of culture ($p < 0.001$). Additionally, ^{3}H incorporation was higher in middle and deep zone hydrogels compared to superficial zone hydrogels after both 3 and 8 days of culture ($p < 0.001$). On day 15 of culture, ^{3}H incorporation levels for all zones were comparable.

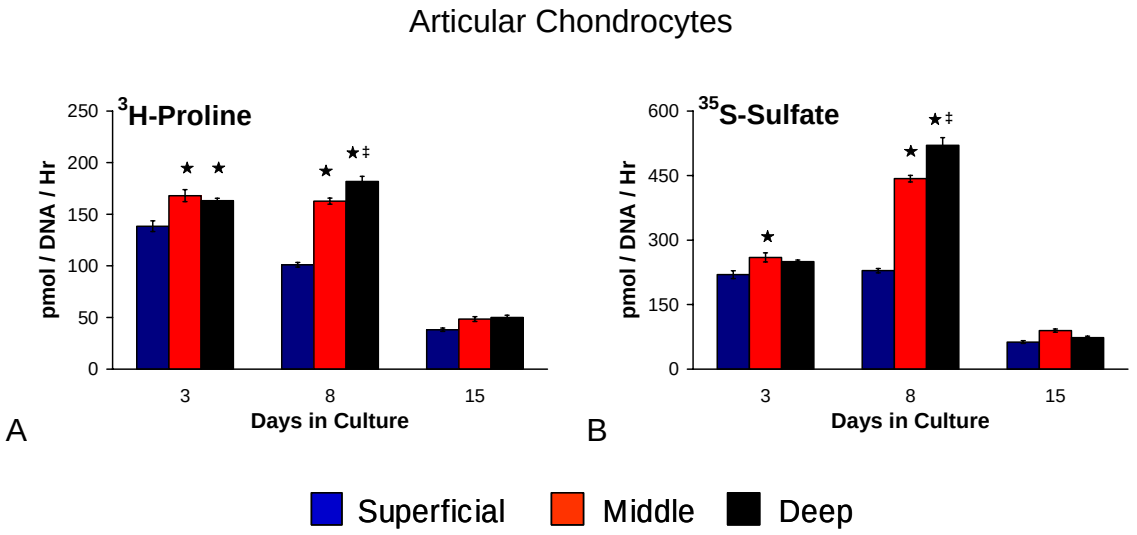

Figure 6.5 Biosynthesis rates of zone-specific chondrocytes in fibrin hydrogels cultured in free swelling conditions. (A) 3H-proline incorporation as a measure of total protein synthesis. (B) 35S-sulfate incorporation as a measure of proteoglycan synthesis. ★ indicates significant difference from Superficial; ‡ indicates significant difference from Middle.

The incorporation rate of ^{35}S-sulfate was not different between 3 and 8 days in culture for superficial zone hydrogels, but then was significantly decreased by 15 days in culture (Figure 6.5B, $p < 0.001$). In contrast, ^{35}S incorporation increased in middle and deep zone hydrogels from days 3 to 8 of culture, but had significantly declined by 15 days in culture ($p < 0.001$). Additionally, after 3 days of culture ^{35}S incorporation in middle zone hydrogels was higher than in superficial zone hydrogels ($p < 0.05$). After 8 days in culture, however, ^{35}S incorporation in both middle and deep zone hydrogels was significantly higher than in superficial zone hydrogels ($p < 0.001$). Finally, there were no significant differences in ^{35}S incorporation among any of the zones after 15 days in culture. Taken together, these results indicated that the phenotypic differences among zone-specific chondrocytes were largely maintained in three-dimensional fibrin hydrogel culture.

6.3.2 Zone-Specific Articular Chondrocytes: Oscillatory Tensile Loading

Having established that fibrin hydrogels were suitable for preserving phenotypic distinctions in zone-specific chondrocytes, the effects of intermittent oscillatory tensile loading on chondrocytes derived from specific tissue zones were explored. Constructs were precultured for 7 days in free swelling conditions and then subjected to 3 days of intermittent oscillatory tensile loading. Additional constructs were only cultured for a total of 3 days in free swelling conditions, serving as an early time point control. Culture and loading times for all remaining studies presented in this chapter are summarized in Table 6.2

Consistent with previous studies, chondrocytes from all zones proliferated from days 3 to 10 in culture (Figure 6.6, $p < 0.001$). DNA data are again presented as

normalized to the mean value of the "3 Day" constructs from each zonal group. Additionally, superficial zone constructs had a higher cell density compared to constructs containing cells from either the middle or deep zones (Figure 6.6, $p < 0.05$), but there were no differences between constructs containing chondrocytes from the middle and deep zones. Finally, no effect of tensile loading was found on cell density for constructs containing chondrocytes from any of the three zones.

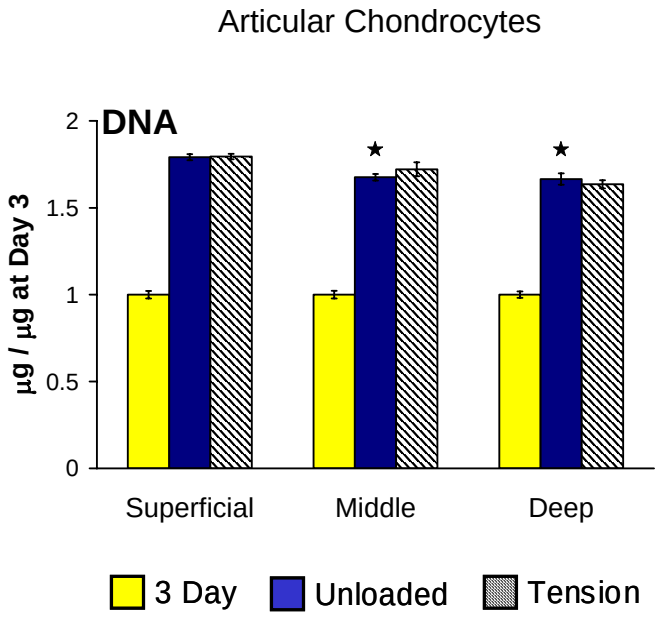

Figure 6.6 DNA content of fibrin hydrogel constructs seeded with zone-specific chondrocytes and subjected to intermittent oscillatory tensile loading. ★ indicates significant difference from Superficial.

Extracellular matrix synthesis rates, as indicated by ^{3}H-proline and ^{35}S-sulfate incorporation, varied (1) over time in culture, (2) with tissue zone, and (3) with the application of oscillatory tensile loading (Figure 6.7). As seen in the previous studies,

^{3}H-proline incorporation decreased with time in culture in superficial zone constructs, but increased with time in culture for middle and deep zone constructs (Figure 6.7A, $p < 0.005$). Additionally, deep zone constructs had higher ^{3}H incorporation compared to superficial zone constructs after 3 days of culture (Figure 6.7A, $p < 0.002$). After 10 days in culture ("Unloaded" group), deep zone constructs had elevated ^{3}H incorporation rates compared to both superficial and middle zone constructs ($p < 0.001$), and middle zone constructs had higher a ^{3}H incorporation rate than superficial zone constructs ($p < 0.001$). Oscillatory tensile loading decreased ^{3}H-proline incorporation only for deep zone constructs ($p < 0.001$).

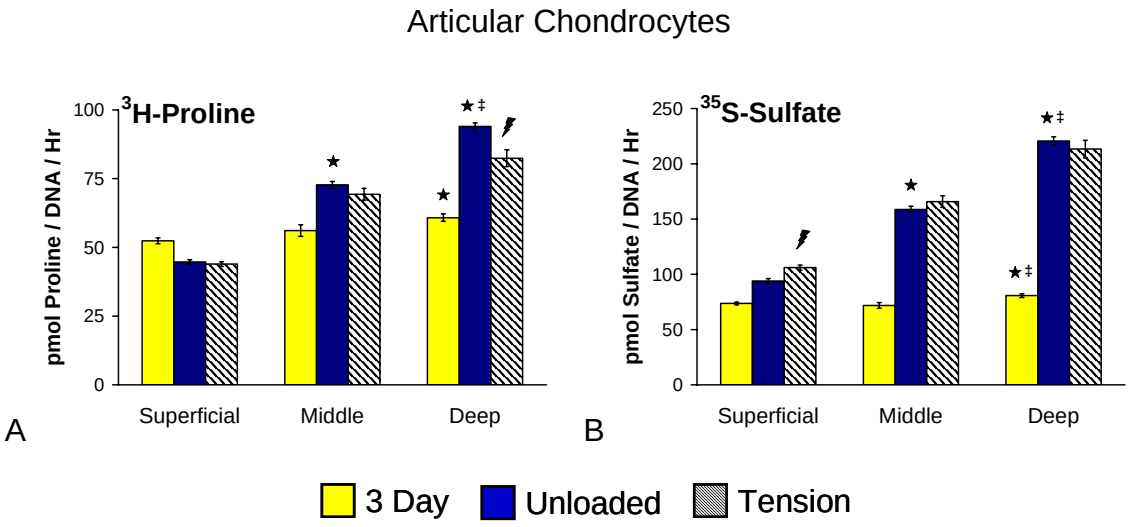

Figure 6.7 Biosynthesis rates of zone-specific chondrocytes in fibrin hydrogel constructs subjected to intermittent oscillatory tensile loading. ★ indicates significant difference from Superficial; ‡ indicates significant difference from Middle; ϟ indicates tension significantly different from unloaded.

The incorporation rate of ^{35}S-sulfate increased from day 3 to day 10 in culture for constructs containing cells derived from each of the three tissue zones (Figure 6.7B, $p < 0.001$). After 3 days of culture, the ^{35}S incorporation rate in deep zone constructs was also higher compared to superficial and middle zone constructs ($p < 0.05$). However, by 10 days of culture ("Unloaded" group), ^{35}S incorporation in deep zone constructs was significantly higher than in either superficial or middle zone constructs ($p < 0.001$). Middle zone constructs also had a higher ^{35}S incorporation rate compared to superficial zone constructs after 10 days in culture ("Unloaded" group, $p < 0.001$). ^{35}S-sulfate incorporation was not affected by oscillatory tensile loading except in superficial zone constructs, where it was increased due to loading ($p < 0.005$).

The sGAG content of hydrogel constructs from all zones increased significantly with time in culture (Figure 6.8, colored bars, $p < 0.001$). Although after only 3 days of culture ("3 Day" group) no significant differences in construct sGAG content were found among constructs containing chondrocytes from different zones, after 10 days in culture ("Unloaded" group) deep zone constructs had accumulated a significantly higher amount of sGAG compared to superficial or middle zone constructs ($p < 0.001$). Additionally, over the course of the 10 day culture period superficial zone constructs released more sGAG into the culture medium than either middle or deep zone constructs (Figure 6.8, open bars, $p < 0.001$). Finally, total sGAG synthesis (retained in constructs + released to media) after 10 days of culture was significantly higher in deep zone constructs compared with middle or superficial zone constructs (Figure 6.8, colored + open bars, $p < 0.001$).

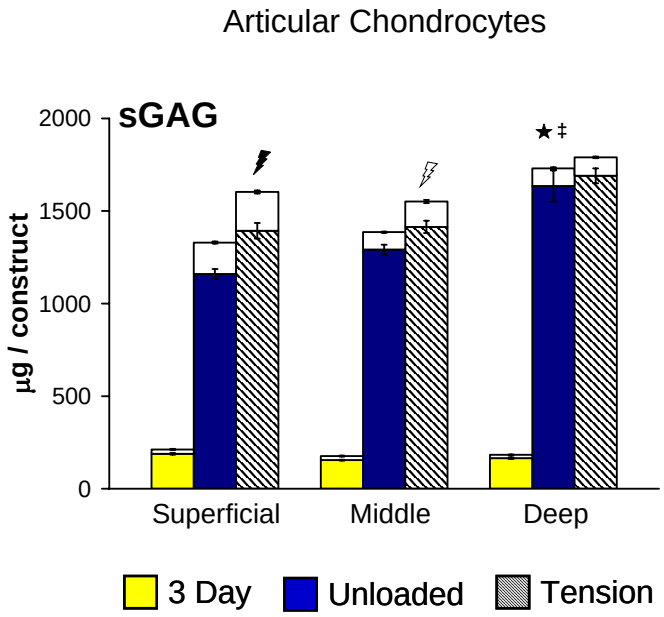

Figure 6.8 Total sGAG produced by zone-specific chondrocytes in fibrin hydrogel constructs subjected to intermittent oscillatory tensile loading. Colored bars represent sGAG accumulated in the constructs, while open bars represent sGAG released to the culture medium. ★ indicates significant difference from Superficial; ‡ indicates significant difference from Middle; ↯ indicates tension significantly different from unloaded in all cases (construct, media, and total); ↯ indicates tension significantly different from unloaded only for release to media.

The introduction of intermittent oscillatory tensile loading produced several intriguing results regarding sGAG accumulation in the constructs and release to the media. First, oscillatory tension significantly increased the amount of sGAG both retained in the construct (colored bars) and released to the media (open bars) only in superficial zone constructs (Figure 6.8, $p < 0.02$). Release of sGAG to the media was also increased by oscillatory tensile loading in the middle zone constructs ($p < 0.001$), but no effect of tension was observed for deep zone constructs. Intermittent oscillatory tensile loading increased total sGAG production (retained in construct + released to media) only in superficial zone constructs ($p < 0.003$). Interestingly, the total sGAG production in superficial zone constructs that were subjected to oscillatory tensile loading was equivalent to that in both the middle and deep zone constructs. Therefore, even though baseline levels of sGAG synthesis and ^{35}S-sulfate incorporation in superficial zone constructs were consistently lower than those of middle or deep zone constructs, intermittent oscillatory tensile loading stimulated proteoglycan production in superficial zone chondrocytes to such an extent that these seemingly inherent zone-dependent differences were overcome. Further characterization of the proteoglycans being produced and released to the culture medium by chondrocyte subpopulations was necessary to better understand the nature of the effects of intermittent oscillatory tensile loading.

Safranin-O staining on formalin fixed, paraffin embedded samples revealed that cells from all zonal groups were uniformly spread throughout the constructs (data not shown). Glycosaminoglycan accumulation, evidenced by red/orange stain, clearly increased with time in culture as small “pockets” of positive staining material were seen

to form around individual cells or cell clusters. No differences between superficial, middle, or deep zone cells or between loaded and unloaded constructs were readily apparent via Safranin-O staining.

Culture media collected on the final day of loading (day 10 of culture) were used to assess potential differences in the proteoglycans produced by zone-specific chondrocytes. These media samples contained proteoglycans that had been synthesized and released during the final 24 hours of culture as well as proteoglycans synthesized on previous days of culture, but not released to the medium until the final 24 hours. Proteoglycan characterization was focused on those both synthesized and released during the final 24 hours of culture. These proteoglycans would contain incorporated ^{35}S-sulfate and thus be readily detectable via liquid scintillation counting.

Proteoglycans in the culture medium collected from the final 24 hours of culture were separated into two populations based on hydrodynamic size, as evidenced by two peaks in the liquid chromatography data (Figure 6.9A,C,E). The Sepharose CL-4B used in the size exclusion chromatography columns has a fractionation range of 70 kDa to 20,000 kDa. The two proteoglycan populations were most clearly delineated in culture medium from the superficial zone hydrogel constructs. The first major peak, designated I in Figure 6.9, eluted near the void volume of the column and therefore corresponds to second peak, designated II, eluted much later and therefore corresponds to smaller macromolecules, perhaps small proteoglycans such as decorin and biglyan as well as aggrecan that has been processed via enzymatic cleavage.

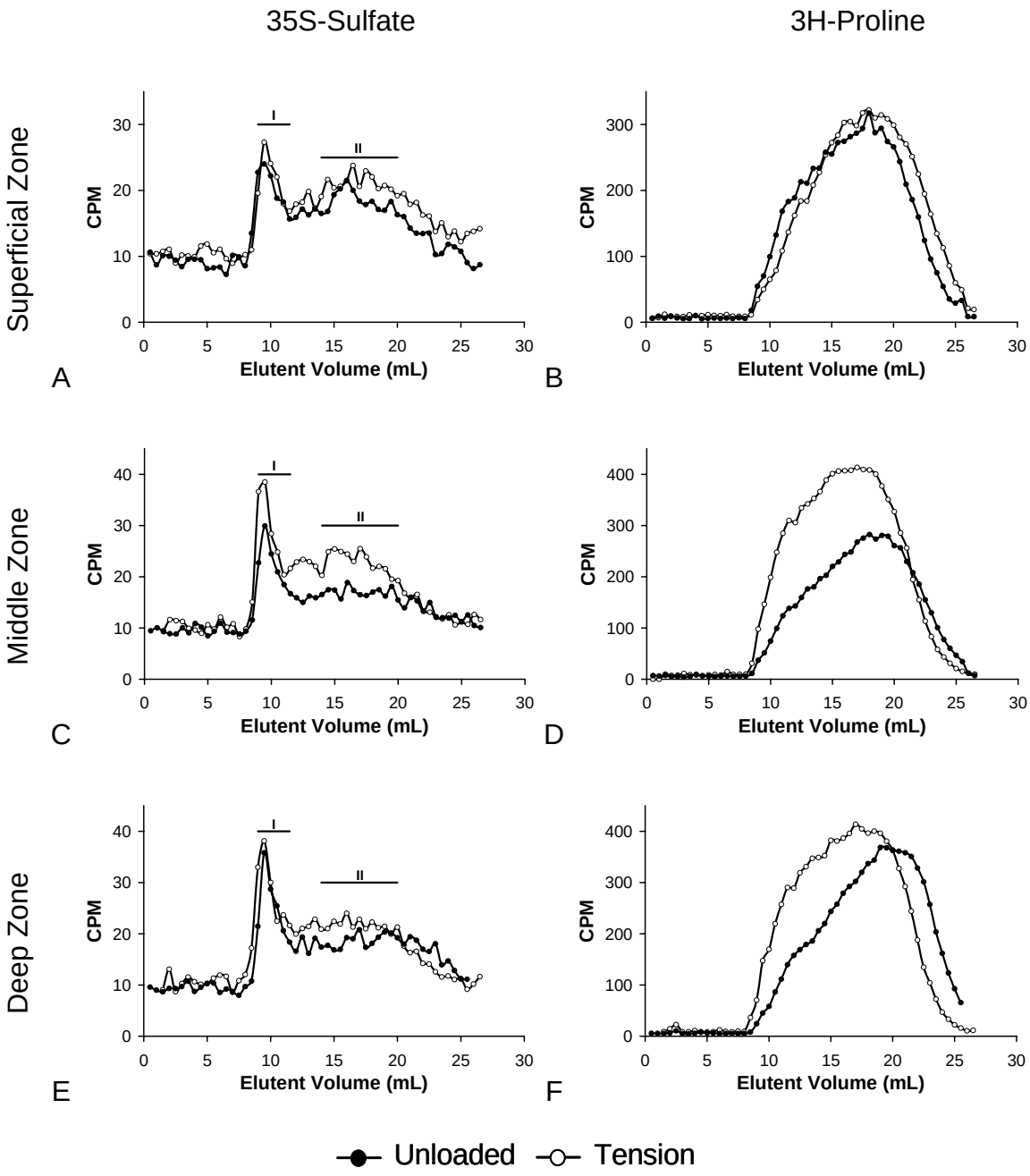

Figure 6.9 Analysis of proteoglycans and proteins released to the medium on the final day of culture using size exclusion liquid chromatography. (A, B) Superficial zone constructs. (C, D) Middle zone constructs. (E, F) Deep zone constructs. Lines labeled I and II (A, C, E) designate peaks corresponding to large and small proteoglycans, respectively. Data shown are the mean CPM values in each fraction for three replicates per group.

The percentage of ^{35}S-sulfate found in each of the two peaks was quantified. Chondrocytes from the deep zone incorporated a significantly larger amount of ^{35}S into large proteoglycans compared with chondrocytes from the middle (Figure 6.10, $p < 0.0419$) or superficial zones ($p < 0.001$). Interestingly, the application of oscillatory tensile loading tended to cause more ^{35}S to be incorporated into smaller proteoglycans, although this result was only statistically significant for deep zone chondrocytes ($p < 0.002$). From the column chromatography data alone, it is difficult to determine whether oscillatory tensile loading (1) decreased release of newly synthesized large proteoglycans relative to smaller proteoglycans, (2) preferentially increased the rate of synthesis and release of smaller proteoglycans, or (3) increased enzymatic activity leading to a higher release rate for smaller proteoglycan fragments.

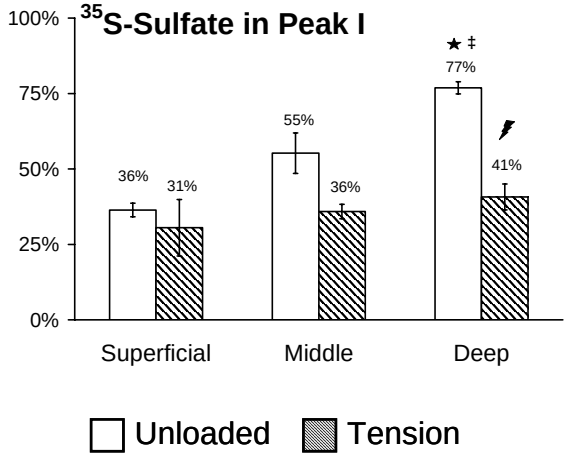

Figure 6.10 Quantification of proteoglycans released to the medium on the final day of culture. Data are shown as a percentage of ^{35}S-sulfate found in peak I, interpreted as intact aggrecan molecules. Data represent the mean percentage values for three replicates from each group. ★ indicates significant difference from Superficial; ‡ indicates significant difference from Middle; ↯ indicates tension significantly different from unloaded.

Following size exclusion chromatography, fractions from each peak were pooled and concentrated. Portions of three replicates from each group were pooled and proteoglycans were ethanol precipitated, separated via electrophoresis on Novex 4-12% gradient gels, and probed with antisera to various proteoglycans. Lanes containing peak I fractions from each group were negative for the G1 (N-terminal of the core protein) and G3 (C-terminal of the core protein) domains of aggrecan as well as decorin and biglycan (Figure 6.11A-D, lanes corresponding to Peak 1). This result was surprising considering DMMB analysis of the pooled fractions prior to ethanol precipitation indicated sufficient quantities for Western blotting and was comparable to (and in some cases greater than) values obtained for peak II fractions. Unfortunately, the limited quantity of pooled material was exhausted performing the Western blot analyses shown in Figure 6.11. Therefore, we cannot positively confirm the presence of large proteoglycan molecules (*i.e.* intact aggrecan) in the fractions that eluted in peak I, but this may be due to complications with the precipitation or gel loading procedures rather than due to the sample contents themselves.

Intact aggrecan was absent from lanes containing peak II fractions as no signal for either the G1 or G3 domains of aggrecan was found at molecular weights above approximately 100 kDa (Figure 6.11A,B). Intact deglycosylated aggrecan core protein would be expected to migrate to ~350 kDa and react with both G1 and G3 antisera (Figure 6.11B, lane corresponding to AC, >250 kDa). Conversely, decorin (Figure 6.11C, ~ 70 kDa) and biglycan (Figure 6.11D, ~70 kDa) were readily detected in lanes comprised of peak II fractions. The smear in the bands positive for biglycan may be the

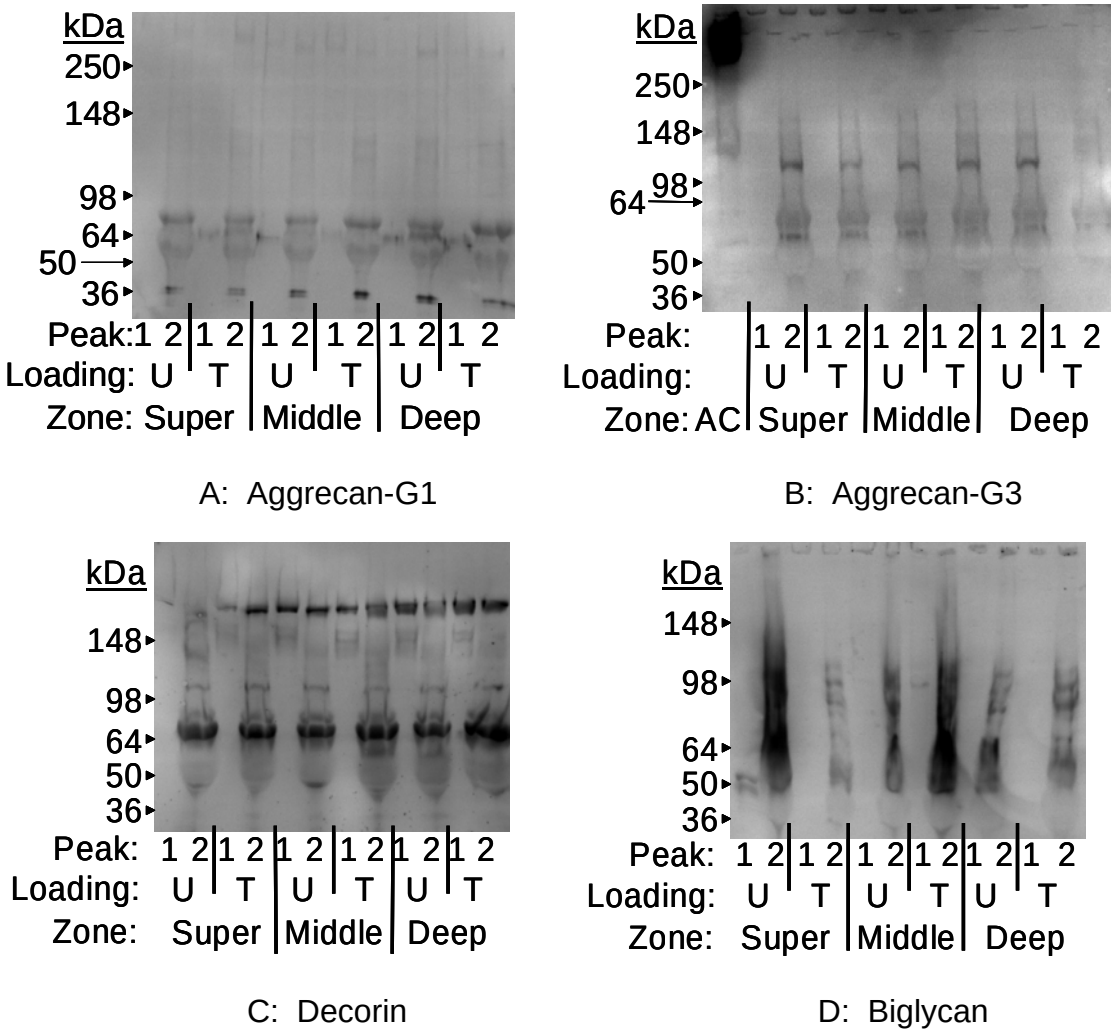

Figure 6.11 Western blot analysis of proteoglycans released to the culture medium on the final day of culture and separated using size exclusion liquid chromatography. All samples were deglycosylated with chondroitinase ABC and keratinase I and II prior to loading. (A) Aggrecan-G1 domain, ~65 and ~90 kDa. (B) Aggrecan-G3 domain, ~60 and ~110 kDa. (C) Decorin, ~75 kDa. (D) Biglycan, ~75 kDa. "AC" in (B) indicates extract from articular cartilage tissue as a positive control.

result of incomplete deglycosylation prior to sample loading. In addition, the G1 and G3 domains of aggrecan were found at positions corresponding to known aggrecan cleavage fragments in peak II fractions (Figure 6.11A, ~90 and ~65 kDa and Figure 6.11B, ~110 and ~60 kDa). Although an equal volume of each sample (as opposed to an equal quantity of precipitated proteoglycans) was loaded into each lane of the gel, differences between samples from the three tissue zones or between unloaded and loaded samples were difficult to assess using Western blot data. This is not surprising since differences among groups found via the size exclusion chromatography analysis were subtle.

Finally, the chromatography elution profiles for proteins containing ^{3}H-proline that were synthesized and released during the final 24 hours of culture also revealed interesting results (Figure 6.9B,D,F). Regardless of loading, cells from the superficial zone synthesized proteins that were similar in size and elution profile (Figure 6.9B). In contrast, proteins synthesized by cells from the middle and deep zones were affected by oscillatory tensile loading. Shifts in both the quantity and size of proteins released to the culture medium were seen with tensile loading (Figure 6.9D,F). Culture media from middle and deep zone hydrogel constructs exposed to oscillatory tensile loading contained higher amounts of larger proteins compared to unloaded constructs. Interestingly, this effect of loading was not seen as simply a shift in the mean hydrodynamic size of proteins, but a change in the elution profile. Therefore not only was the mean size of the proteins released to the medium increased by tensile loading, but also the proportion of larger to smaller proteins was increased.

6.3.3 Zone-Specific Meniscal Fibrochondrocytes: Oscillatory Tensile Loading

Distinct subpopulations from the inner and outer regions of the meniscus were successfully isolated as evidenced by gene expression data (Figure 6.12). Type II collagen gene expression levels in fibrochondrocytes from the inner zone were approximately 30-fold higher than in cells from the outer zone. In contrast, type I collagen gene expression was similar for the two cell populations. Aggrecan expression levels were slightly higher (nearly 2-fold) for inner zone fibrochondrocytes. Conversely, decorin gene expression was approximately 2-fold higher in outer zone cells. Finally, biglycan gene expression was approximately 5-fold higher for inner zone fibrochondrocytes compared with outer zone cells. These data are consistent with previous data from our laboratory[124]. Cell size, determined during cell viability and quantity assessments, was similar for the two subpopulations.

As seen in previous studies[164], a trend for decreasing cellular content with time in culture was evident in the fibrochondrocyte seeded hydrogel constructs. Additionally, after 10 days in culture ("Unloaded" group), outer zone constructs contained significantly fewer cells than inner zone constructs (Figure 6.13A, $p < 0.001$). Total sGAG content increased from 3 to 10 days in culture for inner zone constructs, but decreased over time in outer zone constructs (Figure 6.13B, $p < 0.005$). Additionally, the total sGAG content was significantly higher in inner zone constructs compared to outer zone constructs after 10 days in culture ($p < 0.001$). Intermittent oscillatory tensile loading had no apparent effect on construct sGAG content for cells from either tissue zone.

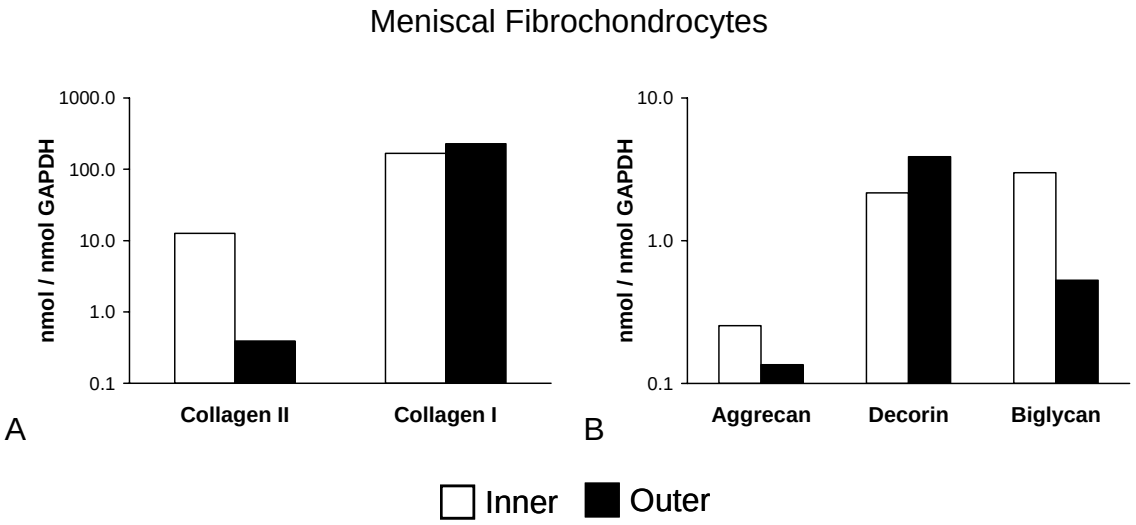

Figure 6.12 Zone-specific meniscal fibrochondrocyte collagen (A) and proteoglycan (B) gene expression prior to seeding into fibrin hydrogel constructs.

^{3}H-proline incorporation increased over time in culture ($p < 0.001$), but was similar for constructs containing either inner zone or outer zone fibrochondrocytes (Figure 6.13C). No differences were found in ^{3}H incorporation into hydrogel constructs containing either cell subpopulation with the application of oscillatory tensile loading. ^{35}S-sulfate incorporation decreased with time in culture ($p < 0.006$), but was not affected by tissue zone or oscillatory tensile loading (Figure 6.13D). Although the ^{3}H incorporation levels were comparable between the meniscal fibrochondrocytes and the zone-specific articular chondrocytes, as expected ^{35}S incorporation was much lower in the fibrochondrocyte hydrogel constructs.

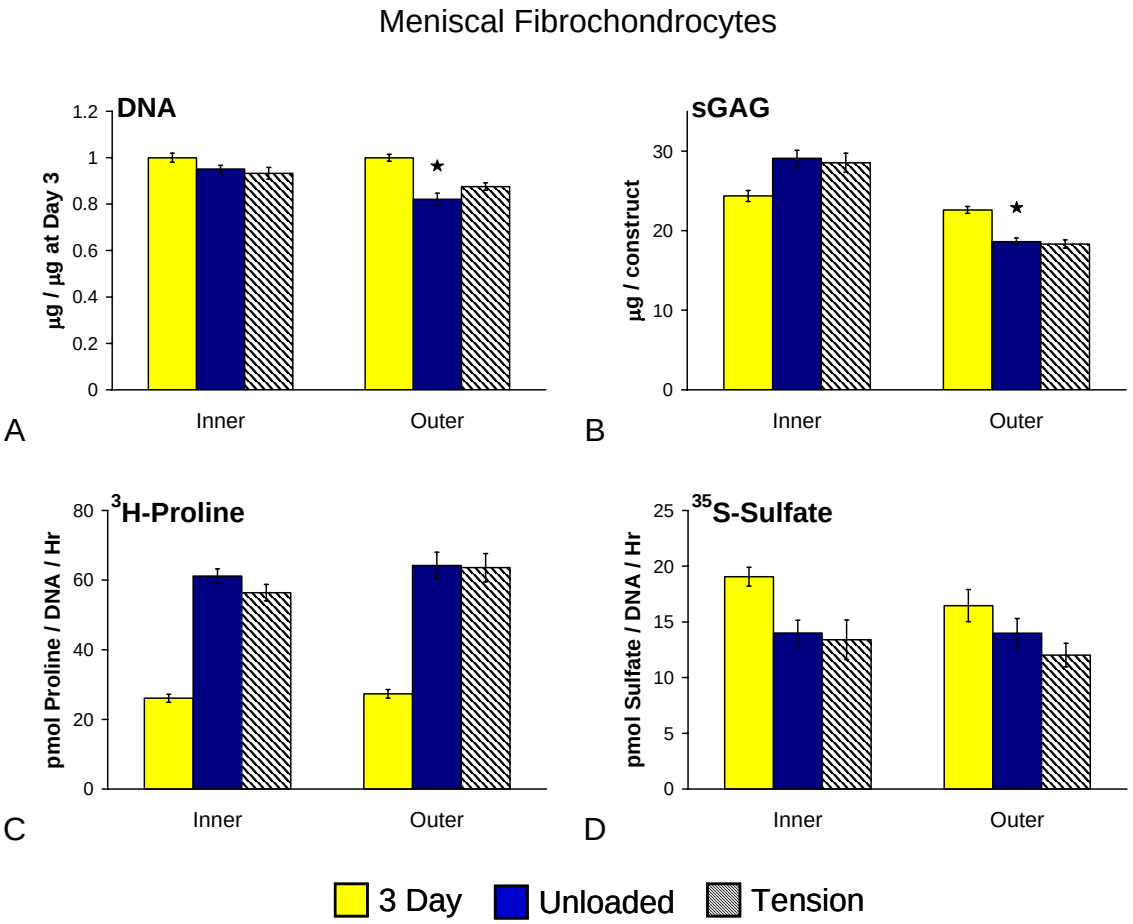

Figure 6.13 Biochemical analyses of fibrin hydrogel constructs seeded with zone-specific fibrochondrocytes and subjected to intermittent oscillatory tensile loading. Construct (A) DNA content and (B) sGAG content. Construct (C) ^{3}H-proline and (D) ^{35}S-sulfate incorporation indicate total protein and proteoglycan synthesis, respectively. ★ indicates significant difference from Inner.

6.4 Discussion

The series of studies presented in this chapter investigated potential phenotypic differences among cells isolated from distinct zones of articular cartilage or meniscal fibrocartilage and their responses to intermittent oscillatory tensile loading. Analysis of cell size demonstrated that chondrocyte diameter increased with increasing distance from the joint surface in immature bovine articular cartilage. This result has been consistently seen in numerous species of various ages including adult and immature bovine[22,181,182,187], adult porcine[29], and adult human[186]. Cell size *in situ* or immediately after enzymatic isolation appears to be a fairly universal indicator of zonal origin, although the differences in size between superficial and deep zones chondrocytes become less pronounced with time in culture[29,181] and with age[186,187]. Additionally, chondrocytes from both superficial and deep zones were shown to increase in size over 3 days of agarose culture[181]. Cell size immediately after isolation provides a simple and reliable method of delineating chondrocyte subpopulations based on zonal origin.

Chondrocytes from all three tissue zones proliferated over time in fibrin hydrogel culture, but to different degrees. In all studies, the cell density of hydrogels containing superficial zone chondrocytes increased at a higher rate than deep zone hydrogels. This finding is in contrast to Lee *et al.*[181], who observed that deep zone chondrocytes proliferated significantly faster in three-dimensional agarose culture compared to superficial zone cells. Several potential explanations exist for this difference. First, the aforementioned agarose study used chondrocytes from mature bovine metacarpophalangeal joints, whereas in our studies chondrocytes from immature bovine stifle joints were used. Mature chondrocytes are known to be less metabolically active

than cells from immature animals, so it is conceivable that age could differentially influence the proliferative capacity of chondrocyte subpopulations. Second, Lee *et al.* assessed proliferation only over the first 72 hours of culture using ^{3}H-thymidine incorporation, but our study focused on longer culture times, up to 15 days, and assessed cellular content via measuring total DNA. Therefore, a potential explanation is that deep zone chondrocytes proliferate more rapidly in the first few days of culture, but over time the proliferation rate of superficial zone chondrocytes increases.

A final possible cause for the differences seen in zone-specific chondrocyte proliferation is the different scaffold materials used. Agarose is essentially inert and provides no mechanism for cells to directly interact with the matrix. In contrast, fibrin has multiple cell binding sites and therefore enables direct cell-matrix interactions. Interestingly, total cellular content of micromass cultures of superficial zone chondrocytes from immature bovines was found to significantly increase from days 4 to 7 of culture, but no changes were seen in deep zone chondrocytes or cells from mature animals[187]. Micromass culture is essentially high density (*i.e.* $50x10^{6}$ cells/mL), pellet-like cell culture providing abundant direct cell-cell contact and potentially cell-matrix interactions. Scaffold environment has been demonstrated to significantly influence chondrocyte proliferation and matrix synthesis during *in vitro* culture[152]; therefore chondrocytes of distinct zonal origin could be differentially affected by scaffold materials with different cellular interaction motifs. In our fibrin hydrogel culture system cell density in hydrogels with superficial zone chondrocytes increased more rapidly than in hydrogel with deep zone chondrocytes, perhaps due to specific integrin or non-integrin cell-matrix interactions triggering cell cycle entry.

Chondrocytes from distinct tissue zones exhibited different extracellular matrix synthesis profiles over time in culture. Both ^{3}H-proline and ^{35}S-sulfate incorporation rates were higher in middle and deep zones cells compared to chondrocytes from the superficial zone for up to 8 days in culture. The finding that chondrocytes from the deeper regions of the tissue produced more extracellular matrix than cells from nearer to the surface is consistent with numerous published studies investigating zone-specific chondrocytes from many different species in various culture conditions[13,22,26,29,180-182,186,187]. After 15 days in culture, however, ^{3}H and ^{35}S incorporation rates in constructs containing chondrocytes from any of the three zones had dropped significantly and were no longer significantly different from one another. This dramatic decrease in the extracellular matrix synthesis rates at 15 days in culture was also seen in a previous study in our system, although to a somewhat lesser degree. Matrix synthesis rates for chondrocytes in agarose culture have been shown to decrease over time, which may be due to increased matrix accumulation in the pericellular space[89,188]. Thus, a similar mechanism may have contributed to the decline in ^{3}H and ^{35}S incorporation rates in our studies. However, some zone-dependent differences in proteoglycan synthesis must have persisted past 8 days of culture since the sGAG content in middle zone hydrogels was highest after 15 days in culture. Interestingly, this pattern is consistent with the proteoglycan distribution found in native tissue[7].

Over time in culture, rectangular fibrin hydrogel constructs seeded with zone-specific chondrocytes and used to investigate the effects of intermittent oscillatory tensile loading exhibited similar cellular proliferation and extracellular matrix synthesis characteristics to the hydrogels in our studies described above. Thus, we could be

confident that the zone-specific chondrocyte isolation procedure as well as fibrin hydrogel culture yielded consistent and repeatable results.

Three days of intermittent oscillatory tensile loading did not affect ^{3}H-proline incorporation rates for superficial or middle zone constructs, but did cause a significant decrease in ^{3}H incorporation into deep zone constructs. When the conditioned culture medium of deep zone constructs was analyzed via size exclusion chromatography, it was observed that medium from samples subjected to tension contained higher levels of proteins with incorporated ^{3}H-proline compared to medium from unloaded samples ($p < 0.03$). It is difficult to directly compare ^{3}H incorporated into proteins retained in the constructs and those released to the culture medium due to differences in construct and medium processing and analysis, but the increased ^{3}H incorporation seen in the media may have offset the decreased incorporation found in the constructs. The net effect produced would be an increase in protein release to the culture medium, but potentially no significant change in overall protein synthesis in response to tensile loading.

An interesting finding regarding the proteins synthesized and released to the media during the final day of culture was that intermittent oscillatory tension altered the elution profile of these proteins in the middle and deep zone chondrocytes, but not in the superficial zone chondrocytes. Elution profiles for proteins released to the culture medium from middle and deep zone constructs exhibited a shift toward larger proteins as well as higher quantities of total protein released. It is reasonable to assume that loading would cause an overall increase in the proteins released to the culture medium based on increased fluid flow through the constructs elevating transport rates. However, if increased transport was the only mechanism governing changes in protein release to the

media following oscillatory tensile loading, a shift in the magnitude, but not necessarily the shape, of the elution profile would be expected. Therefore oscillatory tensile loading may have promoted the synthesis of larger protein molecules, presumable collagens, by middle and deep zone chondrocytes, but not by superficial zone chondrocytes. Alternatively, oscillatory tensile loading could have induced enzymatic activity in middle and deep zone chondrocytes that facilitated the release of larger protein molecules to the culture medium. Additional studies specifically investigating the characteristics of the proteins synthesized by chondrocytes from each tissue zone would be necessary to ascertain if either of these proposed mechanisms would account for the differences seen in our studies.

In native cartilage tissue, the collagen content is denser and the ratio of collagen to proteoglycans is higher near the joint surface compared with deeper regions[7]. As a result, the tensile mechanical properties of the superficial zone in articular cartilage are greater than the rest of the tissue[8,58,184]. The unique structure of the superficial zone of articular cartilage is thought to be a functional adaptation to the shear and tensile forces induced during normal joint motion[7]. In our studies, proteins synthesized and released by superficial zone cells were not affected by oscillatory tensile loading and were essentially uniformly distributed across the entire column volume during size exclusion chromatography. When chondrocytes from the middle and deep zones of the tissue were exposed to oscillatory tensile loading, the elution profile of proteins released to the culture medium became quite similar to that of the superficial zone chondrocytes. This apparent shift in the size distribution of synthesized proteins may represent an adaptation

to a tensile mechanical environment and reveal subtle cellular changes in response to loading that are not apparent when measuring total protein production.

Intermittent oscillatory tensile loading increased ^{35}S-sulfate incorporation in superficial zone constructs, but did not affect ^{35}S incorporation in middle or deep zone constructs. In addition, total sGAG accumulation in the superficial zone constructs as well as sGAG release to the culture medium by superficial zone chondrocytes were also increased by oscillatory tensile loading. Thus, tension seemed to be a potent stimulus for proteoglycan production in superficial zone cells. In contrast, both 15% static compression as well as dynamic compression at several frequencies were found to inhibit glycosaminoglycan synthesis by superficial zone chondrocytes in three-dimensional agarose culture[181]. This difference is significant because it indicates that the effect on zone-specific chondrocyte extracellular matrix synthesis may be dependent on a specific mechanical environment. Superficial zone chondrocytes may respond to tensile loading in a fundamentally different manner compared to compressive loading. Since different scaffolding materials were used in these studies (fibrin versus agarose), it is difficult to make strong assertions regarding potential differences in mechanotransduction pathways involved in the tensile versus compressive loading. However, both static and dynamic compression suppressed proteoglycan synthesis and accumulation by full thickness chondrocytes in fibrin hydrogels when applied continuously for up to 20 days[140]. Therefore, it is possible that compressive loading triggers cellular signaling pathways distinct from those potentially activated by tensile loading in superficial zone chondrocytes.

Also of note was the observation that although oscillatory tensile loading increased proteoglycan synthesis and release to the culture medium in superficial zone constructs, the nature of these proteoglycans did not seem to be affected. Regardless of loading, conditioned medium from superficial zone constructs contained a larger proportion of smaller proteoglycans and processed aggrecan fragments relative to large proteoglycans. Therefore, the rate of proteoglycan synthesis of the superficial zone chondrocytes was increased by oscillatory tensile loading, but the nature of the proteoglycans being synthesized was unchanged. This is in contrast to chondrocytes from the middle and deep zones, where a more substantial percentage of incorporated ^{35}S was found in smaller proteoglycans and aggrecan fragments after the application of oscillatory tensile loading compared to unloaded controls. Thus, oscillatory tensile loading differentially affected proteoglycan synthesis in zone-specific chondrocytes in a more intricate manner than simply modulating total production. Functionally this difference implies that chondrocytes from the middle and deep tissue zones are more susceptible to phenotypic alterations induced by tensile loading than are superficial zone chondrocytes. Since tension is not a significant component of the mechanical environment in the deeper regions of articular cartilage during physiologic loading, perhaps chondrocytes from these regions respond more dramatically when tensile loading is introduced. However, superficial zone chondrocytes, which may experience more tensile loading *in vivo*, may be stimulated by oscillatory tension, but not necessarily induced to significantly alter the nature of extracellular matrix molecules produced or the degree to which those molecules are subsequently modified.

Differences in the initial gene expression profiles and glycosaminoglycan accumulation over time in culture were evident between fibrochondrocytes from the inner and outer zones, but no significant differences were found in either ^{3}H-proline or ^{35}S-sulfate incorporation rates. Contrary to our initial hypothesis, oscillatory tensile loading did not significantly affect meniscal fibrochondrocytes from specific tissue zones. Extracellular matrix synthesis levels and general cellular metabolic activity is much lower in fibrochondrocytes compared with articular chondrocytes, and consequently the outcome measures used in this study (*i.e.* indicators of cellular proliferation and extracellular matrix synthesis) may not be sensitive enough or even appropriate for detecting the potential effects of tensile loading. Analysis of gene expression or a more detailed investigation of the structural characteristics of extracellular matrix molecules produced in response to tensile loading may reveal more subtle features of zone-specific meniscal fibrochondrocytes.

The studies presented in this chapter revealed interesting and important differences in zone-specific chondrocytes; specifically how these subpopulations responded to intermittent oscillatory tensile loading. Many of the results shown here were consistent with previous work investigating chondrocytes from distinct tissue zones in a variety of culture models. However, some interesting differences were found that indicated zone-specific chondrocytes may respond to oscillatory tensile loading in a fundamentally different manner compared to compressive loading. Additionally, chondrocytes from the deep zone, and to a lesser extent those from the middle zone, were induced to change the characteristics of extracellular matrix molecules synthesized in response to oscillatory tensile loading. The overall protein and proteoglycan synthesis

rates in these chondrocyte subpopulations were not affected by tensile loading, but more subtle effects on the size distributions of extracellular matrix molecules were evident. Hence, chondrocytes from deeper regions in the tissue may be inherently more sensitive to an altered mechanical environment such as tension. Consequently, engineered cartilage tissues using predominantly deep zone chondrocytes may behave quite differently during culture and after implantation compared to those using superficial zone chondrocytes. Stratified tissue constructs that attempt to recapitulate the zonal inhomogeneities of native cartilage may also be subject to differential developmental patterns determined by the zonal origins of the cells used and the environment to which the constructs are exposed. Understanding differential behaviors of zone-specific chondrocytes and fibrochondrocytes in a variety of mechanical and biochemical environments will be important to the successful development of functional tissue engineered cartilage and fibrocartilage replacements.

CHAPTER 7

LONG TERM OSCILLATORY TENSILE LOADING OF ENGINEERED CARTILAGINOUS TISSUES

7.1 Introduction

A fundamental component to successful tissue engineering is the ability to produce tissue constructs with sufficient mechanical properties to function properly once implanted into a patient. This characteristic is especially important for tissues such as cartilage and fibrocartilage whose primary function is to provide mechanical support. Many factors can influence the mechanical properties of tissue engineered constructs, including the quantity and structural organization (*i.e.* directional orientation or degree of cross-linking) of the extracellular matrix produced by the cells during *in vitro* culture. Strategies to increase extracellular matrix accumulation during *in vitro* culture have been explored in an effort to generate constructs with superior mechanical properties. Techniques such as using dynamic mechanical stimulation[5,173], biochemical stimulation, or combinations of these two[189] have yielded some successes, but producing tissue engineered cartilage with equivalent mechanical characteristics to native tissue is still beyond reach.

As demonstrated in the preceding chapters, oscillatory tensile loading, when applied for relatively short periods of time (*e.g.* ≤ 3 days), affected both chondrocyte and fibrochondrocyte matrix synthesis rates. However, total extracellular matrix accumulation was not typically influenced by oscillatory tensile loading over these short

intervals. To evaluate the potential of oscillatory tensile loading to stimulate total extracellular matrix deposition and accumulation, longer time periods of *in vitro* culture may be necessary. Therefore, studies were undertaken to assess the effects of extended culture durations on matrix accumulation and the mechanical properties of the rectangular fibrin hydrogel construct system.

Initially it was important to characterize the changes in mechanical properties of the fibrin hydrogel constructs after extended culture in free swelling conditions. Although we hypothesized that the hydrogel constructs would remain viable, continue to accumulate extracellular matrix, and have improved mechanical characteristics after extended culture times, this free swelling study would determine the feasibility of using the fibrin hydrogel construct system over extended culture periods.

A subsequent study was designed to determine the effects of extended durations of *in vitro* culture coupled with oscillatory tensile loading. The primary outcome measures were the construct mechanical properties both in tension and compression, but extracellular matrix synthesis and degradation were also investigated. Previous work described in Chapter 5, indicated that longer durations of sustained oscillatory tensile loading may adversely affect extracellular matrix accumulation. Therefore, an intermittent loading protocol, also detailed in Chapter 5, was chosen for the longer term loading study. We hypothesized that extended durations of intermittent oscillatory tensile loading would result in hydrogel constructs with enhanced tensile and compressive mechanical properties. Additionally, we proposed that this outcome would result from an increase in extracellular matrix accumulation as well as a directional orientation of the newly synthesized matrix.

7.2 Materials and Methods

7.2.1 Tissue Harvest and Cell Isolation

Articular chondrocytes were obtained from 2 - 4 week old bovine stifle joints as previously described. Briefly, articular cartilage was aseptically removed from the femoral-patellar groove and femoral condyles. Cartilage from the full depth of the tissue was excised, although care was taken to exclude tissue from the deepest zones that may have included some calcified cartilage. Tissue was minced and chondrocytes were isolated using 0.2% collagenase in DMEM supplemented with antibiotics at 37°C for approximately 40 hours. The cell suspension was then passed through a sterile 74 μm mesh and concentrated via several centrifugation and wash steps. Finally, chondrocytes were counted using a Beckman Coulter Vi-Cell XR, suspended in fresh DMEM, and seeded into rectangular fibrin hydrogel constructs as described in Chapter 5.

7.2.2 Free Swelling Culture

Fibrin hydrogel constructs were cultured in free swelling conditions using rectangular 8-well tissue culture plates in an incubator held at 37°C and 5% CO_2. Medium was changed every two days and the fully supplemented formulation described in Chapter 5 was used (Table 5.2). The gentamicin and Fungizone were withdrawn from the culture medium after the third media change. After 9, 18, or 27 days of culture, 6 samples were randomly chosen for tensile mechanical testing. The specimens were washed in sterile PBS and maintained at 37°C until shortly before testing.

7.2.3 Intermittent Oscillatory Tensile Loading

Fibrin hydrogel constructs were initially cultured for 6 days in free swelling conditions, as described in Section 7.2.2. On the 6th day, constructs were randomly assigned to the unloaded or tension culture chambers (see Section 4.3) and allowed to culture without any loading for one additional day. Thus, the total preculture time for this study was 7 days. On the following day, an intermittent oscillatory tensile loading protocol was used to stimulate the fibrin hydrogel constructs. Constructs were stretched using a 1.0 Hz sinusoidal wave form with a 5% ± 5% amplitude. This protocol was applied for 12 hours followed by a 12 hour recovery period where constructs were held at 0% displacement. Culture medium was changed every day during the final hour of the recovery period. A modified formulation of the fully supplemented culture medium described previously (Table 5.2) with gentamicin and Fungizone replaced with antibiotic/antimycotic was used for these studies. The antibiotic/antimycotic solution was included in the medium during the first 7 days of culture and then only on days 14 and 21 of the remaining culture period. On these days, constructs were removed from the oscillatory tensile loading device, increasing the risk of bacterial or fungal contamination, and therefore necessitating the inclusion of the antibiotic/antimycotic solution. Parallel constructs in the unloaded culture chambers served as controls at each time point.

After 2, 7, 14, 21, and 28 days of total culture, 8 constructs per group were removed from the oscillatory tensile loading device. A group of 6 constructs was transferred to PBS and maintained at 37°C until shortly before mechanical testing. The remaining two constructs were immediately fixed in 10% neutral buffered formalin for 25

minutes at 4°C, washed in PBS, and stored at 4°C until processing for cell morphology and extracellular matrix imaging.

7.2.4 Mechanical Testing Procedures and Analyses

Tensile Mechanical Tests

The dimensions of the fibrin hydrogel constructs were measured using a digital Vernier caliper (length and width) and a custom designed resistance micrometer (thickness). Length measurements were taken from the interface of the fibrin hydrogel and the end blocks, width measurements were taken at the narrowest location along the hydrogel, and thickness measurements were taken at three points across the width of the hydrogel and averaged. This method of determining the mean construct thickness was necessary because surface tension during casting caused the edges of the fibrin hydrogel to be thicker than the center region.

Custom designed aluminum adapters were used to interface the constructs with the EnduraTEC ELF 3200 testing frame and the load cell (Figure 7.1A). Engineering drawings of the adapters can be found in Appendix B. Once constructs were interfaced with the testing adapters, a small preload of approximately 0.05 N was applied to each construct to establish the start position for each test. Constructs were then subjected to 5 cycles of preconditioning (0.1 Hz frequency, 2.5% ± 2.5% amplitude sinusoid), returned to the start position for 2 minutes of equilibration, stretched 2 mm (~ 10% engineering strain) at a rate of 0.1 mm/sec, and then held at this position for 2 minutes to allow for stress relaxation. Time, position, and load data were collected during the ramp and stress relaxation portions of the tests at a sampling frequency of 100 Hz. Constructs were then

returned to initial position and allowed to re-equilibrate for several minutes until the value of the measured load reached the tare load prior to testing.

Next, dynamic tensile tests were performed using frequencies covering two decades. For the initial long term free swelling culture study, the dynamic tests were performed at 0.05, 0.1, 0.5, 1.0, and 5.0 Hz using a 10% ± 5% sinusoidal strain wave. However, to prevent damaging the fibrin hydrogels during testing, the amplitude of the sinusoidal waveform was reduced to 10% ± 1.5% for subsequent testing in the second study reported here. The same range of testing frequencies was used. The dynamic tension tests were begun by stretching constructs 0.1 mm/sec to a load value of 0.05 N. This position was designated as the new start position. A 0.1 mm/sec linear ramp was performed to 10% engineering strain, which was the mean value for dynamic testing. Additionally, constructs were held at this position for 2 minutes before initiating the frequency sweep. During the dynamic tests, 5 cycles were performed at each testing frequency, and data from the third cycle was collected for analysis. Upon completion of the dynamic tension tests, constructs were removed from the adapters and allowed to equilibrate in PBS at room temperature for a minimum of one hour. The EnduraTEC dynamic mechanical analysis (DMA) software was used to perform FFT analysis on the force and position data acquired during the dynamic frequency sweep. The ratio of the fundamental components from the FFT analysis of the measured force and the measured displacement was used to calculate the dynamic stiffness (K*). The dynamic modulus (E*) was then determined by multiplying K* by the ratio of the construct length to the construct cross-sectional area. These values were calculated for each frequency used during the tensile testing procedure.

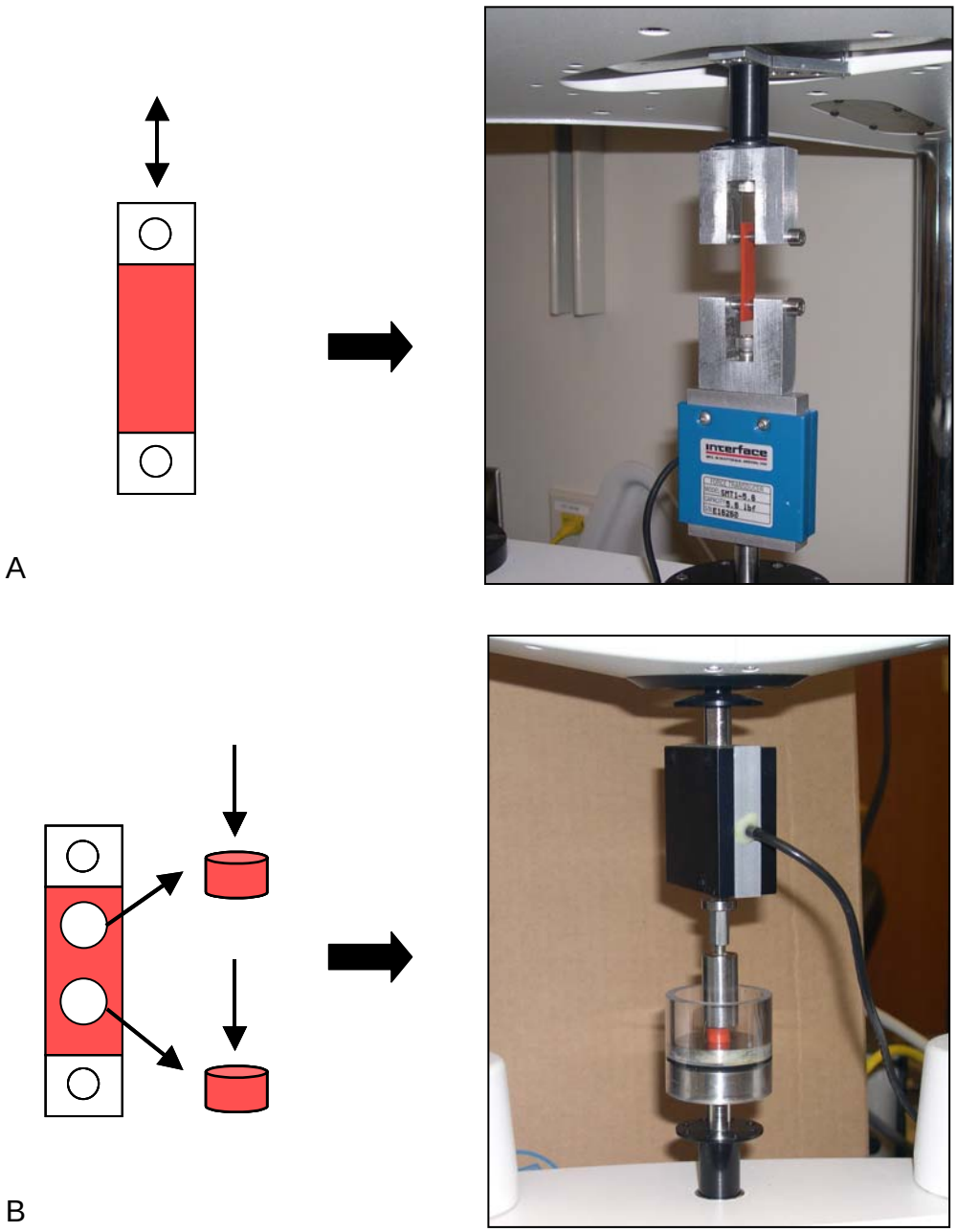

Figure 7.1 Mechanical testing of the fibrin hydrogel constructs in (A) the tension test configuration and (B) the compression test configuration.

Compressive Mechanical Tests

Only constructs from the long term intermittent oscillatory tensile loading study were tested in compression. Following equilibration in PBS for at least one hour after tension tests, two 6 mm diameter cylindrical cores were removed from each fibrin hydrogel construct using a dermal biopsy punch (Figure 7.1B). The diameter and thickness of each core were measured as described above. Cores were tested in unconfined compression by first positioning them in a cylindrical polycarbonate chamber interfaced with an EnduraTEC ELF 3100 testing device. The chamber was manually raised until the hydrogel core was within 2 mm of an impermeable stainless steel platen attached to a 1 N load cell and the actuator of the testing device. The platen was slowly lowered until a load value of 0.05 N was achieved. This position was recorded and used as the starting position for the test. Without moving the platen, the chamber was filled with room temperature PBS, and the load cell was tared to 0.0 N to compensate for any surface tension forces between the PBS and the platen. The platen was then lowered 10% of the hydrogel core thickness at 0.1 mm/sec, and held at this position for 10 minutes to allow for stress relaxation. Time, position, and load data were collected throughout the ramp and relaxation portions of the tests at a 100 Hz sampling frequency.

The compressive ramp modulus was calculated using the slope of the stress-strain curve during the linear ramp. An initial non linear region was observed up to approximately 5% strain. The linear portion of the stress-strain curve was found to be between 5% and 10% strain, and thus the ramp modulus was calculated using data from this range by least squares regression. The compressive equilibrium modulus was calculated by averaging the final 100 stress data points of the relaxation portion of the

test and then normalizing this value by the strain level (-0.10 in all cases). The mean rate of change for the stress at this time was less than 0.025% per second. Following compression tests, hydrogel cores were equilibrated in room temperature PBS for at least one hour before further processing.

7.2.5 Extracellular Matrix Composition and Degradation Analyses

Following mechanical testing, each fibrin hydrogel construct was allowed to equilibrate in room temperature PBS for at least one hour and then the end blocks were separated from the hydrogel and discarded. Constructs were measured for wet mass as three separate pieces: the two 6 mm hydrogel cores and the remaining material from the rectangular constructs. Samples were frozen, lyophilized to dryness, measured for solid mass, and stored at -20°C for further analysis.

Proteoglycans from one 6 mm diameter hydrogel core from each sample were extracted overnight with agitation at 4°C in 4M Guanidine HCl, 50mM sodium acetate, 10mM MES, and protease inhibitors (5mM EDTA, 5mM IAA, 1x Protease Inhibitor Cocktail Set I), pH 7.5. Vials were centrifuged for 30 minutes at 20,000 x g at 4°C to pellet insoluble material. The supernatants were transferred to fresh tubes and assayed for sulfated glycosaminoglycans (sGAG) using the 1,9-DMMB dye assay[169]. Equal volumes of extracted material were pooled in groups according to time in culture and loading condition. Next, 3 volumes of ice cold 100% ethanol with 50mM sodium acetate was added to each pooled sample, and proteoglycans were precipitated at 4°C overnight. Proteoglycans then were deglycosylated with chondroitinase ABC and keratinase I and II. The protocol for Western blot analysis found in Appendix C was followed to detect the G1 domain and the NITEGE fragment of aggrecan core protein. The NITEGE epitope is

revealed following enzymatic cleavage in the inter-globular domain of aggrecan core protein (Figure 7.2). Aggrecanases, including ADAM-TS4 and ADAM-TS5, are known to specifically act on this site.

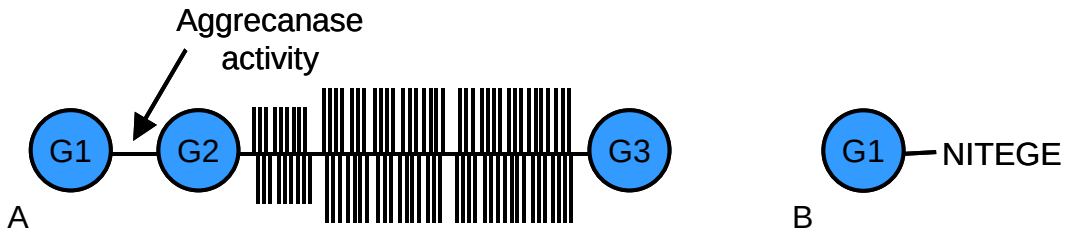

Figure 7.2 Diagram of enzymatic cleavage of aggrecan. (A) Intact aggrecan molecule depicting one site of aggrecanase activity. (B) Aggrecan fragment with exposed NITEGE neo-epitope.

Insoluble material remaining from guanidine extracts was soaked in 10 volumes of PBS overnight at room temperature. Excess PBS was removed and samples were then frozen, lyophilized to dryness, and digested using 0.25 mg/mL proteinase K in 100 mM ammonium acetate at 60°C. The DMMB dye assay was again used to determine the level of proteoglycan extraction.

7.2.6 Extracellular Matrix Imaging

Formalin fixed constructs were stored in sterile PBS at 4°C before processing. The polyethylene endblocks were removed and each construct was sliced in half lengthwise to yield two pieces approximately 20 mm long x 5 mm wide x 3 mm thick. One portion from each construct was transferred to an embedding cassette and

maintained in 70% ethanol for at least 24 hours. Samples were processed for paraffin embedding using graded alcohol dehydration followed by paraffin infiltration. 4 μm thick sections were cut from paraffin blocks and mounted on microscope slides. Sections were obtained from regions near the construct surface as well as from the midsubstance.

Samples were deparaffinized and rehydrated in deionized water. Proteoglycan accumulation and distribution in the construct sections were assessed using Safranin-O staining (see Appendix C for detailed protocol). Cell nuclei were counterstained with hematoxylin. Parallel samples were stained with Picrosirius Red to assess the collagen content and orientation in the constructs (protocol also found in Appendix C), and cell nuclei were again counterstained with hematoxylin. Images were captured using conventional or polarized light microscopy on a Nikon E600 microscope and QCapture Pro software.

7.2.7 Statistical Analyses

Data were analyzed using a general linear model and Tukey's test for post hoc analyses with significance set at $p < 0.05$. A multifactor model (loading and loading duration) was used for data from tensile mechanical testing and biochemical analyses. Interaction terms were included in the models as appropriate where the criterion for significance was satisfied. Statistical significance represented in figures by the combination of connecting lines and symbols indicates the interaction term was not significant, whereas symbols alone indicate a significant interaction term and therefore statistical significance only in the associated treatment groups.

As described in Section 7.2.4, two cylindrical punches were taken from each fibrin hydrogel construct for mechanical testing in compression yielding a total of 12

samples. Since the two samples from each construct were not independent, their data values were averaged and then treated as a single sample, yielding a sample size of 6. A multifactor model (loading and loading duration) was initially used to analyze data from compression testing. Additionally, the effects of tensile loading on construct compressive mechanical properties were analyzed with pairwise t-tests treating each loading duration group separately.

7.3 Results

7.3.1 Free Swelling Culture

Fibrin hydrogel constructs seeded with chondrocytes obtained from full thickness articular cartilage were cultured in free swelling conditions for up to 27 days. The measured length and thickness of the hydrogel constructs decreased over time in culture, indicating compaction of the hydrogels (Table 7.1). Measurements of the width of the hydrogels were not recorded, but only one sample (Day 27 group) exhibited any visibly noticeable contraction in this direction.

Table 7.1 Compaction of fibrin hydrogel constructs over time in free swelling culture

Culture Time (days)	Change in Length (from nominal 20 mm)	Change in Thickness (from nominal 3.0 mm)
9	-1.58% ± 0.51%	+4.56% ± 2.80%
18	-2.71% ± 0.38%	-7.33% ± 1.78% ★
27	-6.44% ± 0.33% ★ ‡	-14.2% ± 1.50% ★

values are mean ± standard error of the mean
★ indicates significant difference from Day 9, $p < 0.005$
‡ indicates significant difference from Day 18, $p < 0.001$

The results of the dynamic tensile tests indicated that the fibrin hydrogel constructs became stiffer over time (Figure 7.3). Both the dynamic stiffness (K*) and the dynamic modulus (E*) increased significantly from day 9 to day 18 ($p < 0.001$) and again from day 18 to day 27 ($p < 0.001$). This trend was consistent for each frequency tested, but only the results at 1.0 Hz are shown.

These two measures are not independent, but do provide complementary information. For rectangular test specimens, the relationship between K* and E* is:

$$E^* = \frac{K^* \cdot length}{width \cdot thickness}$$

The increase in E* over time in culture indicated the modulus of the hydrogel constructs was increasing, but a reduction in cross sectional area with no concurrent increase in stiffness could also yield this result. However, since K* is independent of the cross sectional area, the increase in K* over time in culture indicated that the stiffness of the hydrogel constructs was increasing independent of dimensional changes. Additionally, the dramatic increases in the tensile mechanical properties (~69% and ~94% from days 9 to 27 for K* and E*, respectively) far outweigh the modest changes in

the construct dimensions (Table 7.1). The results of this study indicated that three dimensional fibrin hydrogel constructs seeded with articular chondrocytes exhibited enhanced mechanical characteristics following extended periods of *in vitro* culture.

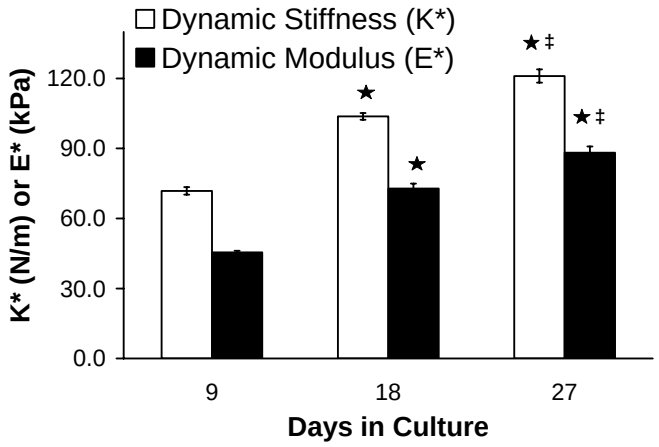

Figure 7.3 Dynamic tensile properties of fibrin hydrogel constructs in long term free swelling culture. Both the dynamic stiffness and the dynamic modulus increased significantly with culture time. ★ indicates significant difference from Day 9; ‡ indicates significant difference from Day 18.

7.3.2 Intermittent Oscillatory Tensile Loading

Fibrin hydrogel constructs were seeded with chondrocytes obtained from full thickness articular cartilage, cultured for 7 days in free swelling conditions and then cultured for up to 21 additional days using an intermittent oscillatory tensile loading protocol. In all subsequent figures and discussion, groups are denoted by their time in free swelling culture and the time subjected to loading. For example, "7 + 7" indicates 7

days of free swelling culture plus 7 additional days of culture either unloaded or with intermittent oscillatory tensile loading.

Construct Mechanical Properties

The percentage of solid matrix in the constructs increased with time in culture (Figure 7.4A, $p < 0.001$). Intermittent oscillatory tensile loading further increased the percentage of solid matrix in the constructs (Figure 7.4A, $p < 0.004$). Much of this effect was due to a decrease in overall construct mass as evidenced by the concurrent reduction in construct cross sectional area induced by tensile loading (Figure 7.4B, $p < 0.001$). The total amount of solid matrix, however, did increase over time for all groups. Interestingly, unloaded constructs showed no signs of compaction over time in culture. Digital images of the hydrogel constructs taken prior to mechanical testing further illustrated the dimensional changes induced by tensile loading (Figure 7.5).

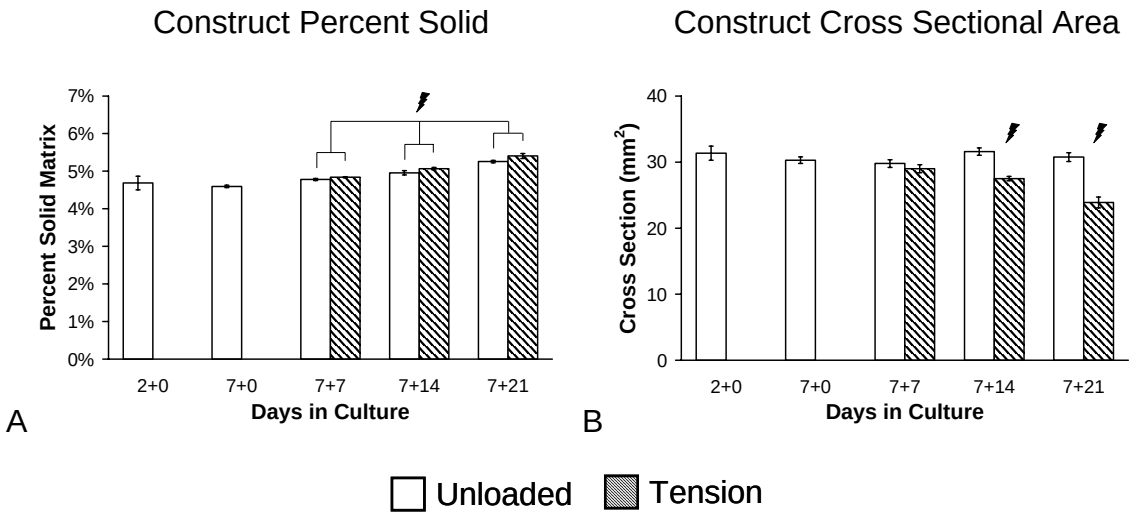

Figure 7.4 Long term intermittent oscillatory tensile loading induced matrix compaction in fibrin hydrogel constructs. (A) The percentage of solid matrix in the constructs increased with time in culture and tensile loading. (B) The cross sectional area of the constructs remained constant over time in culture, but decreased with tension. ↯ indicates tension significantly different from unloaded.

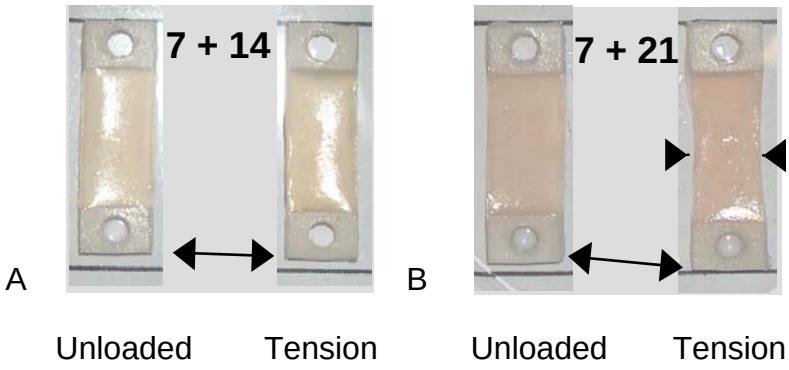

Figure 7.5 Images of fibrin hydrogel constructs after (A) 7 days of preculture plus 14 days loading or (B) 7 days of preculture plus 21 days loading. Note the subtle change in construct length after 14 days of intermittent oscillatory tensile loading (A, double arrow) and the noticeable decrease in construct width (B, arrow heads) and increase in construct length (B, double arrow) after 21 days of intermittent oscillatory tensile loading.

Dynamic tension tests revealed results consistent with those seen in the long term free swelling culture study. The dynamic tensile stiffness (K*) significantly increased with time in culture for unloaded constructs (Figure 7.6A, $p < 0.001$) as well as constructs subjected to oscillatory tensile loading ($p < 0.01$). K* was not affected by tensile loading except after 21 days of loading where it was significantly decreased compared to unloaded controls (Figure 7.6A, $p < 0.01$). In contrast, the dynamic tensile modulus significantly increased both with time in culture (Figure 7.6B, $p < 0.001$) and the application of intermittent oscillatory tensile loading ($p < 0.001$). As discussed in Section 7.3.1, the differences in K* and E* resulted from changes in the overall construct dimensions.

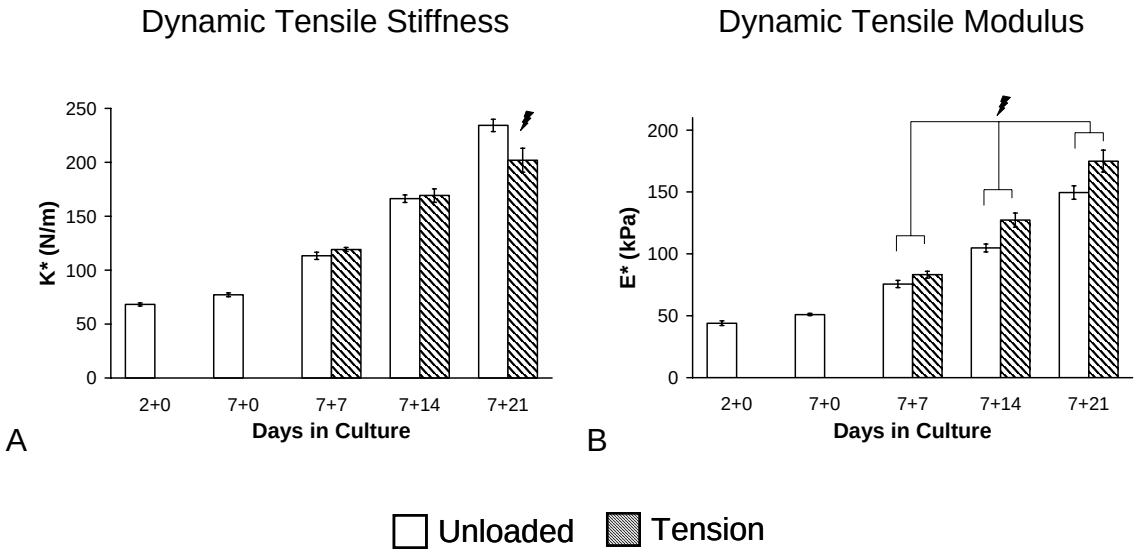

Figure 7.6 Dynamic tensile mechanical properties of fibrin hydrogel constructs. (A) Dynamic tensile stiffness (K*) increased significantly with time in culture, but did not change in response to tension except in the 7+21 group. (B) Dynamic tensile modulus (E*) significantly increased with time in culture and with intermittent oscillatory tensile loading. ↯ indicates tension significantly different from unloaded.

Mechanical tests conducted in unconfined compression also revealed interesting characteristics regarding the development of the hydrogel constructs. The results of the multifactor ANOVA indicated that the compressive ramp modulus, calculated as the ratio of stress to strain during the linear portion of the ramp to a 10% strain, increased from day 14 (7+7) to day 28 (7+21) for unloaded constructs (Figure 7.7A, $p < 0.034$), however p-values for comparisons between unloaded and tension groups were not significant. In contrast, when data were analyzed with pairwise t-tests 7 or 14 days of intermittent oscillatory tensile loading was found to significantly enhance the construct compressive ramp modulus ($p < 0.01$). After 21 days of loading, however, the compressive ramp modulus was not significantly different compared to unloaded controls. The equilibrium compressive modulus, measured after 10 minutes of stress relaxation, also significantly increased with time in culture for unloaded constructs (Figure 7.7B, $p < 0.001$) according to ANOVA analysis. However, pairwise t-tests indicated the equilibrium modulus was only affected by tensile loading in the 7+14 group where it was significantly elevated compared to unloaded controls (Figure 7.7B, $p < 0.001$). Since all samples for compression testing had similar cross-sectional areas, the trends for the peak and equilibrium compressive loads, which were not normalized by the sample cross-sectional area, were consistent with data presented here.

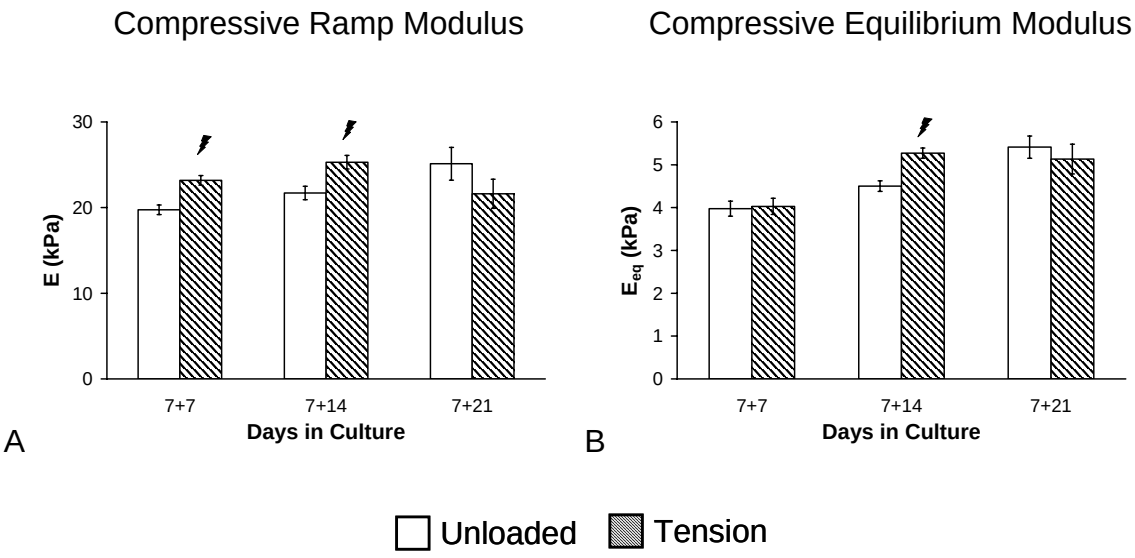

Figure 7.7 Compressive mechanical properties of the fibrin hydrogel constructs. (A) The compressive ramp modulus increased with time in culture and further increased with 7 or 14 days of intermittent oscillatory tensile loading (7+7 and 7+14 groups). (B) The compressive equilibrium modulus also increased with time in culture and additionally increased with 14 days of intermittent oscillatory tensile loading. ↯ indicates tension significantly different from unloaded by pairwise t-tests.

Construct Extracellular Matrix Content

The sGAG contents of the fibrin hydrogel constructs significantly increased with time in culture regardless of loading condition (Figure 7.8, $p < 0.001$), ultimately accounting for approximately 0.45% of the total construct mass and nearly 10% of the construct solid content after 28 days in culture. Oscillatory tensile loading, however, did not have a significant effect on sGAG accumulation at any time point. Data shown are the total sGAG content from one cylindrical core used for compressive mechanical

testing and are normalized to the wet mass of the core. Data for non-normalized sGAG and sGAG normalized by dry mass had similar trends as data shown in Figure 7.8.

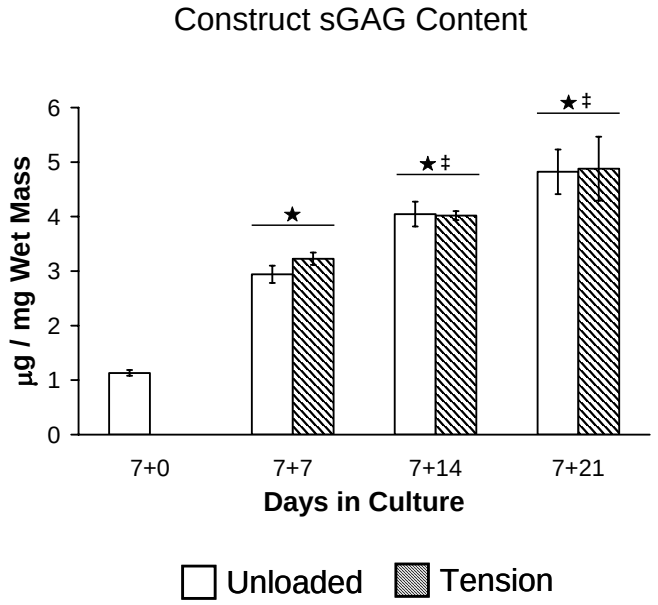

Figure 7.8 sGAG content of the fibrin hydrogel constructs normalized to wet mass. sGAG content increased with time in culture, but was not affected by tensile loading. ★ indicates significant difference from 7+0; ‡ indicates significant difference from 7+7.

Thin sections of paraffin embedded constructs were stained with Safranin-O to show glycosaminoglycan distribution and accumulation over the course of this study. Images of sections from constructs only cultured for 2 days revealed that chondrocytes were uniformly distributed throughout the constructs, but as expected, sGAG was virtually undetectable at this early time point. Images from later culture times, however, clearly demonstrated an increase in sGAG accumulation over time in culture (Figure 7.9). Heaviest staining was seen immediately surrounding cells and cell clusters, but the

overall sGAG distribution was uniform within each construct. Sections were obtained both from regions near the surface and at a depth of least 100 μm (5-8 cell diameters) into the constructs, and sGAG distribution and accumulation were similar in both locations. Higher magnification images revealed that sGAG was evenly distributed in the pericellular space of individual cells as well as around larger cell clusters (Figure 7.10). No substantial differences in sGAG accumulation or distribution were readily apparent between unloaded controls and constructs subjected to oscillatory tensile loading at any time point imaged.

Adjacent construct sections were stained with Picrosirius Red to investigate collagen deposition and organization within the constructs. Collagen accumulation was found in similar patterns as sGAG. Little collagen accumulation was found after 14 days in culture (Figure 7.11A, 7+7 group). However, the pericellular space readily stained positive for collagen with increased time in culture (Figure 7.11B, 7+21 group). Differences in collagen staining between unloaded controls and constructs subjected to tension were not evident (images in Figure 7.11 were taken from unloaded constructs). The fibrillar structure of fibrin is similar to collagen, which caused high background staining in all images. Finally, polarized light was used to assess collagen orientation in the constructs. Images appeared similar to those of the midsubstance of articular cartilage samples used as positive controls. Collagen fibers were found to be more well organized, and therefore more brightly colored in polarized light, in circumferential patterns around chondrocytes, but no linear collagen orientation was found in either unload constructs or those subjected to oscillatory tensile loading.

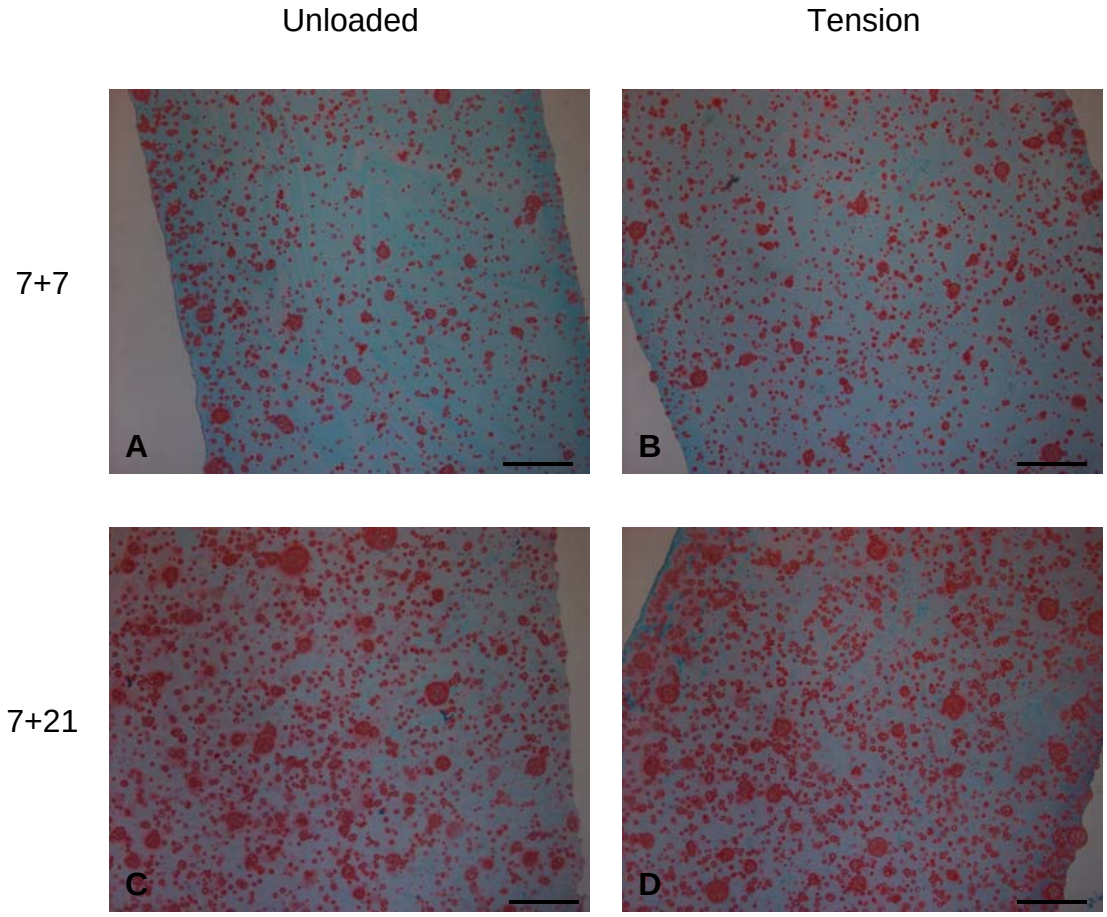

Figure 7.9 Safranin-O staining demonstrates proteoglycan accumulation in fibrin hydrogel constructs during long term intermittent oscillatory tensile loading culture. Scale bars are 500 μm.

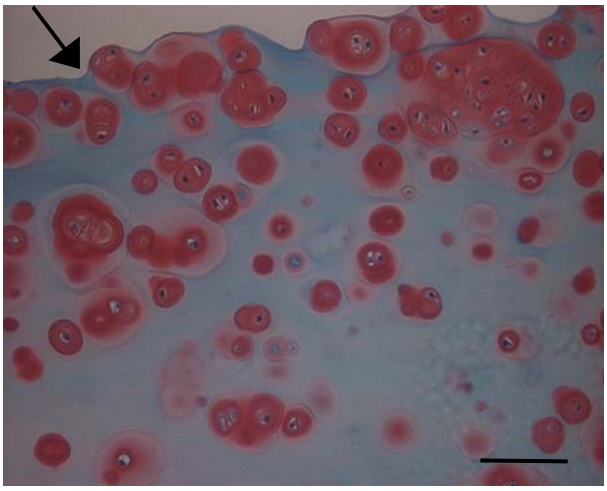

7+21 Unloaded

Figure 7.10 Higher magnification image of Safranin-O staining in a construct subjected to oscillatory tensile loading (7+21 culture group). The interface between the fibrin hydrogel and the polyethylene end block is shown along the upper edge of this image (arrow). Scale bar is 100 μm.

7+7 Unloaded

7+21 Unloaded

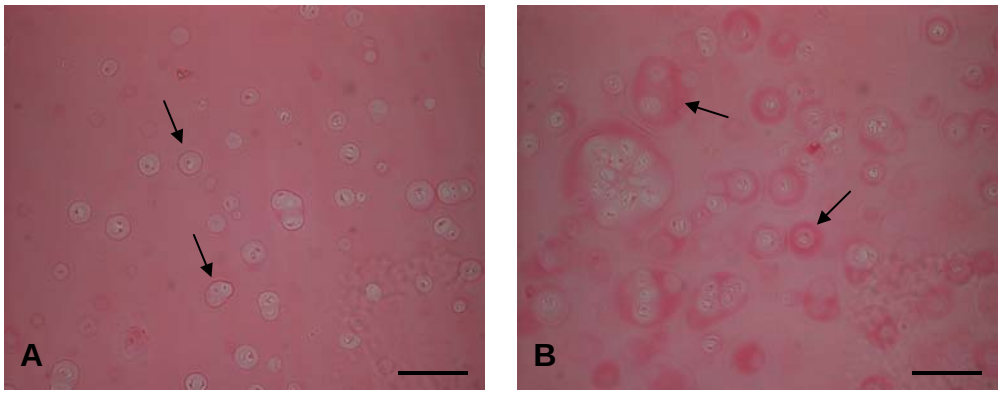

Figure 7.11 Picrosirius Red staining indicates collagen accumulation in unloaded fibrin hydrogel constructs. (A) Little collagen was visible in the 7+7 constructs, but areas surrounding cells had some positive staining (arrows). (B) Collagen accumulation was apparent in the 7+21 constructs as heavier staining was found around individual cells and cell clusters (arrows). Scale bars are 500 μm.

Extracellular Matrix Degradation

To assess potential extracellular matrix degradation in our fibrin hydrogel construct system, proteoglycans were extracted from the 6 mm diameter cores used for compressive mechanical testing, and immunoblots for the G1 domain of aggrecan and a specific aggrecan cleavage fragment were performed. Aggrecan G1 positive bands were detected in all construct extracts and migrated to positions corresponding to molecular weights greater than 250kDa, representing predominately intact aggrecan molecules (Figure 7.12A). Much less intense band staining was seen at a variety of lower molecular weight positions in all groups. Band intensity for the large aggrecan molecules appeared to increase with time in culture, correlating to the increases found in sGAG content described above. Additionally, migration of these bands also increased with time in culture, indicating the presence of smaller aggrecan molecules likely due to C-terminal enzymatic cleavage in a process also seen in aging native tissue. The increased aggrecan-G1 band migration also appeared in samples from constructs subjected tensile loading. This effect was more pronounced in the 7+14 and 7+21 groups (Figure 7.12A, lanes 4-7). Thus, aggrecan processing may be triggered by longer periods of culture in three dimensional fibrin hydrogel constructs and accelerated by extended duration of tensile loading.

An antibody specific to the aggrecan-NITEGE cleavage fragment, known to be generated by aggrecanases such as ADAM-TS4 and ADAM-TS5 in cartilage tissues, was used in a subsequent immunoblot (Figure 7.12B, approximately 65 kDa). Band intensity for aggrecan-NITEGE increased with time in culture. The aggrecan-NITEGE positive band corresponding to constructs in the 7+21 group subjected to intermittent oscillatory

tensile loading also was more intense compared to the corresponding unloaded control group (Figure 7.12B, lanes 6-7). Adobe Photoshop 5.5 (Adobe Systems) was used to analyze pixel intensity levels in regions encompassing individual bands. Uniform rectangular areas were analyzed for each lane and the average pixel intensities were compared. This analysis confirmed the observations that band intensity for aggrecan-G1 increased with time in culture and band intensity for aggrecan-NITEGE increased with time in culture and with tensile loading in the 7+21 constructs. The pixel intensity measurements for the NITEGE bands were also normalized by the measurements from the corresponding G1 bands, yielding results consistent with those discussed above.

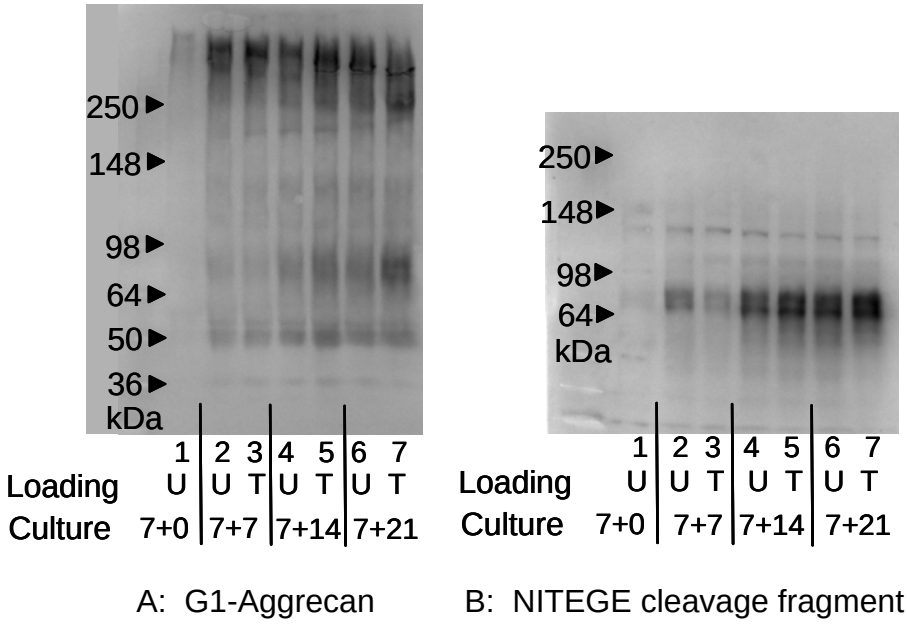

Figure 7.12 Western blot analysis of guanidine extracts indicated significant accumulation of aggrecan and its degradation products in the fibrin hydrogel constructs. Proteoglycans were deglycosylated prior to loading. (A) Aggrecan processing increased over time in culture and with tension as indicated by the increasing migration of G1-aggrecan band positions. (B) Accumulation of NITEGE epitope increased with time in culture and further increased after 21 days of tensile loading (B, lanes 6-7 ~65 kDa).

Thin sections from paraffin embedded constructs were also processed for immuno-fluorescence detection of the aggrecan-NITEGE cleavage fragment. Intense staining was found near the cell surface in all samples, however, no differences were apparent with time in culture or between loading groups. Representative images of unloaded constructs from the 7+7 and 7+21 groups are shown in Figure 7.13.

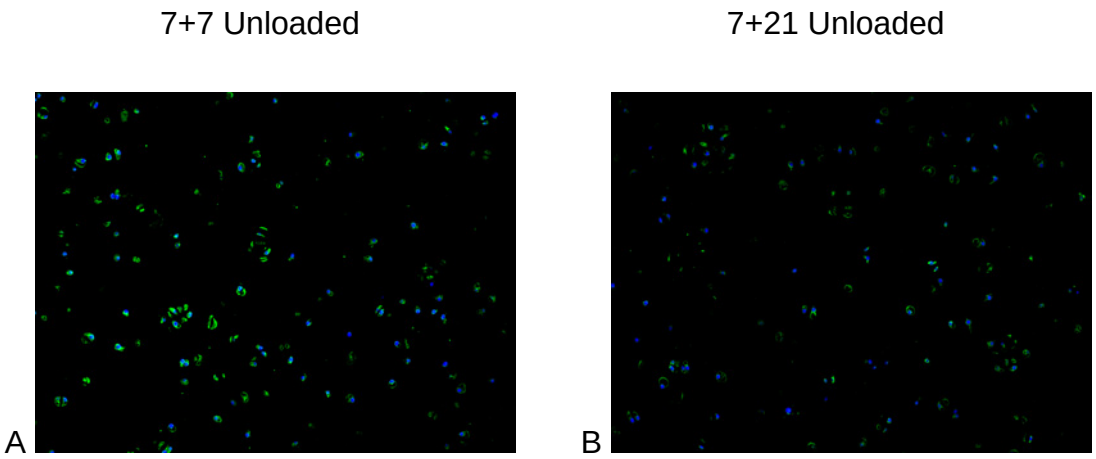

Figure 7.13 Immunofluorescence images of the aggrecan G1–NITEGE cleavage fragment in unloaded fibrin hydrogel constructs cultured for either 14 days (A, 7+7) or 28 days (B, 7+21). Staining for the –NITEGE fragment (green) was localized at the cell periphery. Blue is DNA. Original magnification 100x.

7.4 Discussion

The studies presented in this chapter were designed to investigate the effects of intermittently applied long term oscillatory tensile loading on chondrocyte seeded three dimensional fibrin hydrogel constructs. Extended periods of intermittent mechanical

stimulation have been shown to enhance the mechanical properties of tissue engineered constructs[5,102,173,190]. Therefore, we hypothesized that oscillatory tensile loading could also be an effective stimulus for producing engineered cartilaginous tissues with enhanced mechanical characteristics.

The percentage of solid mass of the fibrin hydrogel constructs increased with time in culture in both studies presented in this chapter. As previously discussed, a portion of this effect was due to a decrease in the overall mass of the constructs. Consistent with this decrease in construct mass were changes in construct dimensions. These dimensional changes were presumably due to cell-mediated compaction of the fibrin matrix. Intermittent oscillatory tensile loading applied for 14 and 21 days significantly enhanced matrix compaction. Mechanical tension has been found to induce cell-mediated matrix compaction in both fibrin and collagen scaffolds populated with several different cell types[165,174,191-194]. However, matrix compaction in many of these cited studies occurred more rapidly and to a greater degree than what was seen in our system. This difference could have resulted from the higher initial protein concentration used in our system (50 mg/mL fibrin versus typically < 5 mg/mL fibrin or collagen). Additionally, chondrocytes do not typically have a highly contractile phenotype, unlike the fibroblasts or smooth muscle cells used in the reports cited above. Thus, tensile loading may promote a more contractile phenotype in articular chondrocytes, similar to that seen in fibroblasts or meniscal fibrochondrocytes (see Chapter 5, section 5.3.1).

Both the tensile and compressive properties of the fibrin hydrogel constructs increased with time in culture. This result was consistent with the observation that extracellular matrix molecule accumulation also increased with culture time. Oscillatory

tensile loading further increased construct dynamic tensile modulus (E*), but it appears that this was due primarily to a reduction in cross-sectional area of the loaded constructs. However, modest increases in the compressive mechanical properties were caused by up to 14 days of tensile loading. This finding is consistent with previous studies that have reported increases in the mechanical properties of tissue engineered cartilage constructs following 4 weeks of intermittently applied compressive loading[5,173]. Interestingly, although these reports described more substantial increases in construct mechanical properties after loading than what were found in our studies, longer culture times were needed before any differences were seen. After 21 days of intermittent oscillatory tensile loading, however, the mechanical properties of constructs in our system were either not significantly different or decreased compared to unloaded controls.

The large increase in matrix compaction along with the decreasing trends in the mechanical properties of constructs subjected to 21 days of intermittent oscillatory tensile loading indicated that increasing levels of extracellular matrix degradation may have been triggered. During development, engineered tissues probably require some level of extracellular matrix degradation and turnover for proper tissue maturation. If matrix degradation exceeds synthesis, however, then the growth and the potential for success of these tissues may be compromised. Analyses of proteoglycans extracted from the fibrin hydrogel constructs indicated that a basal level of matrix degradation was occurring in all samples, and this level was increasing with time in culture. Additionally, constructs subjected to 21 days of tensile loading appeared to contain increased levels of enzyme generated aggrecan fragments. Hence, durations of this intermittent oscillatory tensile loading protocol longer than 14 days may increase enzyme activity in fibrin hydrogel

constructs thereby promoting extracellular matrix degradation and reducing mechanical integrity. Additionally, cyclic tensile loading has been shown to increase the susceptibility of devitalized[195] or glutaraldehyde crosslinked[196] pericardium tissue to enzymatic degradation via exogenous bacterial collagenase. The mechanism responsible is unknown, but this phenomenon could have resulted from conformational changes in matrix molecules thereby enhancing access to cleavage sites for proteolytic enzymes or simply from increased enzyme and proteolytic byproduct transport through the tissue. Oscillatory tensile loading in our system could have similarly enhanced degradation via extracellular matrix molecule deformation once a sufficient pool of proteolytic enzymes had accumulated within the constructs (*i.e.* after 21 days of loading).

The studies presented in this chapter demonstrated that our fibrin hydrogel construct system can be used for long-term *in vitro* culture of articular chondrocytes. Cells within the constructs appeared to maintain their chondrocytic phenotype and continued to produce proteoglycans for up to 28 days in culture. Constructs accumulated newly synthesized extracellular matrix over time in culture, resulting in increased levels of stiffness in both tension and compression. The intermittent oscillatory tensile loading protocol chosen for these studies also transiently enhanced construct mechanical properties. This protocol utilized a 50% duty cycle consisting of 12 hours of oscillatory tensile loading followed by 12 hours of recovery each day. Although this loading protocol was found to increase total glycosaminoglycan production over 7 days in earlier studies, it may not have been optimal for promoting extracellular matrix synthesis and retention over longer culture periods. Further work could clearly be done optimizing the system in an effort to improve a number of outcome measures, such as matrix

accumulation and/or organization, construct mechanical properties, the suppression of excessive enzymatic activity, *etc*. However, these studies have demonstrated that oscillatory tensile loading, when applied in intermittent bouts, can modulate chondrocyte behavior in fibrin hydrogel constructs and has the potential to enhance important characteristics of tissue engineered constructs. Although tensile stresses and strains are not typically a dominant component of the mechanical environment in articular cartilage, understanding how chondrocytes respond to tension can lead to new insights regarding cartilage development, maintenance, degeneration, and strategies for repair.

CHAPTER 8

CONCLUSIONS AND RECOMMENDATIONS

8.1 Summary

Disease and degeneration of orthopedic tissues such as articular cartilage and fibrocartilage severely impacts the quality of life for millions of patients. Unfortunately, current surgical repair techniques do not adequately treat osteoarthritis and other degenerative joint diseases. Thus, novel tissue engineering strategies may be necessary to combat disease progression and replace damaged tissue. Both articular cartilage and the meniscal fibrocartilage in the knee joint are subjected to a complex mechanical environment consisting of compressive, shear, and tensile forces. Therefore, engineered replacement tissues must be mechanically competent to successfully function after implantation into a joint. Although mechanical integrity is crucial, engineered tissues must also perform biological functions (*i.e.* synthesis and maintenance of extracellular matrix molecules) that will be affected by the local mechanical and biochemical environment. Understanding how these engineered tissues respond to applied mechanical stimuli will offer insights into improving techniques used in their development as well as how they may perform post implantation. The work presented in this dissertation investigated the effects of oscillatory tensile loading on three dimensional engineered cartilaginous tissues in an effort to elucidate important aspects of mechanotranduction.

The series of studies presented in Chapter 3 provided detailed images of the cellular and extracellular matrix morphology in immature bovine meniscus tissues.

Cellular cytoskeletal organization was rounded and chondrocyte-like in the inner region of the tissue but gradually transitioned to a stellate morphology in the middle and outer regions. These results agreed with a published study on rabbit menisci[74]. Additionally, the distribution and organization of proteoglycan and collagen extracellular matrix molecules varied throughout the tissue. The inner region of the meniscus was composed of a more diffuse matrix with larger aggrecan and type II collagen contents. In contrast, both collagen and aggrecan were highly organized in the middle and outer regions of the tissue. Large, circumferentially oriented type I collagen bundles dominated the extracellular matrix in the outer region with types II and VI collagen located near the periphery of these large fiber bundles. Simultaneous imaging of multiple collagen species yielded results similar to those recently reported for types I and II collagen[64], but also provided a unique view of the spatial relationship between types I and VI collagen. Type VI collagen was located at the periphery of large type I collagen fiber bundles with intense colocalization often found at fiber junctions. Detailed investigations of native meniscal extracellular matrix structure not only offer insights into the functions of specific matrix components, but also can assist in developing design criteria for engineered replacement tissues.

The Oscillatory Tensile Loading Device, the custom designed bioreactor used in many of the studies presented in this dissertation, represented a novel contribution to the field of tissue engineering. This versatile device was capable of imparting a well defined and repeatable oscillatory tensile displacement to hydrogel constructs. The design of the construct interface ensured that the strain field generated in the constructs during loading was highly uniform. In addition to being useful for investigating specific cellular

responses to tensile loading (as was the goal in this work), this device could also be used for conditioning large numbers of tissue engineered constructs for future *in vivo* studies.

The series of studies described in Chapter 5 explored the effects of a wide variety of oscillatory tensile loading protocols on articular chondrocytes and meniscal fibrochondrocytes seeded in three dimensional fibrin hydrogel constructs. Longer durations of sustained loading inhibited the matrix synthesis of both cell types and increased chondrocyte proliferation; however, these effects were not found for shorter loading durations. This result suggested that shorter durations of tensile loading may be able to stimulate extracellular matrix metabolism. Chondrocyte gene expression levels for types I and II collagen and aggrecan, however, were not substantially influenced by short durations (1, 4 or 8 hours) of oscillatory tensile loading. Therefore, repeated bouts of short durations of loading were applied in an intermittent protocol in an effort to enhance the chondrocyte response. Three days of intermittent oscillatory tensile loading using the "3 Hour" protocol inhibited extracellular matrix synthesis, but three days of the "12 Hour" protocol stimulated proteoglycan synthesis. Finally, longer durations of these intermittent protocols were found to enhance overall sGAG production, but much of this synthesized matrix was lost to the culture medium and not retained in the construct. This set of studies provided evidence that oscillatory tensile loading could be used to modulate chondrocyte metabolism, and to a lesser extent fibrochondrocyte metabolism, during *in vitro* culture. Specifically, the "12 Hour" intermittent protocol was selected for future studies because this loading regime showed potential for stimulating chondrocyte extracellular matrix synthesis.

The effects of oscillatory tensile loading on constructs containing cells derived from the entire articular cartilage or meniscus were often subtle. Therefore studies were undertaken to isolate the responses of chondrocytes and fibrochondrocytes derived from distinct regions of the tissues. Zone-specific chondrocytes seeded into fibrin hydrogels exhibited similar matrix biosynthesis trends as found in native tissue[22] and other *in vitro* culture environments[26,29,183]. Additionally, zone dependent differences were found in response to intermittent oscillatory tensile loading. Tensile loading significantly enhanced proteoglycan synthesis in chondrocytes from the superficial zone. This difference was more striking for the total sGAG produced, (retained in the constructs plus released to the culture medium). Additionally, protein synthesis was only inhibited in deep zone cells by tension. To better characterize the proteoglycans and proteins released to the culture medium, column chromatography was used to separate them based on hydrodynamic size. Consistent with previously published reports[26], superficial zone chondrocytes incorporated a lower proportion of ^{35}S-sulfate into larger proteoglycans compared to cells from the deep zone. Additionally, tensile loading significantly decreased the proportion of ^{35}S-sulfate incorporated into large proteoglycans only in deep zone chondrocytes. Decorin, biglycan, and both N-terminal and C-terminal aggrecan fragments were detected in all samples containing small proteoglycans. Tensile loading also induced an increasing shift in the size of proteins synthesized by middle and deep zone chondrocytes. Finally, tensile loading did not significantly affect the matrix metabolism of meniscal fibrochondrocytes isolated from either the inner or outer zone of the tissue. These studies demonstrated that chondrocytes from distinct cartilage zones differentially respond to tensile loading.

Chapter 7 described studies investigating the effects of extended durations of oscillatory tensile loading on fibrin hydrogel constructs seeded with articular chondrocytes. Modest levels of hydrogel compaction were seen after 4 weeks of free swelling culture, and the mechanical characteristics of the constructs were significantly enhanced over this time. Up to 3 weeks of the "12 Hour" intermittent oscillatory loading protocol substantially increased hydrogel compaction compared to unloaded controls, as evidenced by a reduction in cross sectional area. Additionally, tensile loading did not significantly alter construct dynamic tensile stiffness (K*) compared to unloaded controls except after 21 days of loading where K* was decreased. In contrast, construct dynamic tensile modulus (E*), which was normalized by the construct cross sectional area, was significantly enhanced by tensile loading. Construct compressive mechanical properties were also enhanced by up to 14 days of tensile loading. Extracellular matrix molecules accumulated in all constructs over time in culture, but these levels were not affected by tensile loading. Western blot analyses indicated that increased enzymatic cleavage of aggrecan occurred over time in culture and was further increased by 3 weeks of tensile loading. These studies demonstrated that some mechanical characteristics of chondrocyte seeded fibrin hydrogel constructs were enhanced with oscillatory tensile loading; however, extended durations of loading triggered increased enzymatic activity, resulting in extracellular matrix degradation.

8.2 Conclusions

The studies presented in this dissertation provided the first extensive set of investigations into the effects of oscillatory tensile loading on articular chondrocytes and

meniscal fibrochondrocytes cultured in a three dimensional tissue engineered scaffold system. The results of these studies provide insights into cartilage mechanobiology and may be useful for cartilage and meniscus tissue engineering applications. Oscillatory tensile loading was found to modulate chondrocyte and fibrochondrocyte metabolism in a protocol dependent manner. Longer durations of sustained loading inhibited extracellular matrix synthesis, whereas shorter durations and intermittent loading could stimulate matrix production. A variety of different loading protocols were explored to determine important characteristics for stimulating chondrocyte extracellular matrix synthesis. Our results along with data available in the literature suggest that effective stimuli for chondrocyte metabolism may result from shorter loading durations applied for a few hours per day. Alternatively, employing a protocol where loading is only applied every other day may additionally enhance this effect[197]. A single cycle of compressive loading has been shown to enhance chondrocyte matrix production over a 4 week culture period[178]. Minimal mechanical stimulation in this manner could serve to trigger mechanotransduction signaling pathways, thereby increasing extracellular matrix production. Concurrently, the increase loss of matrix molecules to the culture medium that results from subsequent cycles of mechanical deformation could be reduced by the extended recovery periods used in this loading regime.

Much of the work presented in this dissertation was originally motivated by the clinical need to address the inadequate reparative capacity of meniscal fibrocartilage following injury. Stimulating meniscal fibrochondrocytes with oscillatory tensile loading is a promising approach because the mechanical environment in the meniscus has a large tensile component. Thus, we designed a custom bioreactor capable of applying well-

defined oscillatory tensile strains to tissue engineered constructs in a controlled *in vitro* environment. Although fibrochondrocyte protein synthesis levels *in vitro* are comparable to those of articular chondrocytes, fibrochondrocyte proteoglycan metabolism was found to be quite low compared to articular chondrocytes. However, it should be noted that many of the analysis techniques used in these studies were developed to evaluate articular cartilage explants or isolated chondrocytes during *in vitro* culture. Although fibrocartilage shares much in common with articular cartilage, these outcome measures may not be optimal for investigating fibrochondrocyte behavior. Fibrochondrocyte total proteoglycan and protein synthesis levels were not typically affected by tensile loading in our system, but these measures only reflect gross matrix production. More specific molecular biochemical evaluations of the matrix molecules produced by fibrochondrocytes might be necessary to resolve potential differences in subtle structural features or functional characteristics. Alternatively, fibrochondrocyte metabolism could be enhanced using growth factor supplementation to augment the responsiveness of these cells to mechanical or other modes of stimulation, as has been explored in our laboratory[108,198]. Finally, it is important to bear in mind that certain limitations exist in all *in vitro* model systems. To achieve a well defined and controlled system, many of the growth factors, cytokines, and chemotactic or haptotactic factors found in an *in vivo* environment are not present in a model system. Therefore, it is important to keep the results presented here regarding the metabolic inactivity of meniscal fibrochondrocytes in this context of an *in vitro* model system. However, the above experimental outcomes, combined with the higher metabolic activity of articular chondrocytes, led us to primarily

focus our remaining studies on the responses of articular chondrocytes to oscillatory tensile loading.

Elucidating various aspects of meniscal fibrochondrocyte biology provides important information regarding how fibrocartilage tissues develop, are maintained, and can be repaired. However, using primary fibrochondrocytes is not necessarily a requirement for a successful engineered fibrocartilage tissue. Early studies in our laboratory demonstrated that oscillatory tensile loading could induce a morphological change in articular chondrocytes cultured in fibrin hydrogel constructs[164]. Chondrocytes in unloaded constructs remained rounded with peripheral F-actin filaments, but a significant subpopulation of chondrocytes subjected to tensile loading developed a stellate morphology with extensive cytoskeletal projections containing both vimentin and vinculin proteins. This new morphology was strikingly similar to the morphology meniscal fibrochondrocytes spontaneously developed in the same culture conditions indicating this chondrocyte population may have the potential to adopt more fibrochondrocyte-like characteristics when stimulated with tension. These results suggested that since articular chondrocytes are inherently more metabolically active than fibrochondrocytes, inducing a phenotypic shift in chondrocytes may be beneficial for fibrocartilage tissue engineering applications. In addition to the potential of chondrocytes as a fibrocartilage tissue engineering cell source, investigating their responses to oscillatory tensile loading is interesting from a mechanobiology perspective.

Although it is well established that chondrocyte morphology and phenotype vary throughout the tissue depth, relatively few efforts have been made to understand how these different cell populations respond to exogenous mechanical stimuli. We report here

that chondrocytes from the superficial zone of articular cartilage increased proteoglycan production in response to a three day intermittent oscillatory tensile loading protocol. The molecular characteristics of the PGs being produced and released to the culture medium were found to be similar to unloaded controls. In essence, oscillatory tensile loading stimulated proteoglycan synthesis in superficial zone chondrocytes, but did not structurally alter those synthesized molecules. This zone-specific response of articular chondrocytes to tensile loading may be related to zone dependent differences found in the mechanical environment of native tissue. As discussed previously, the surface of articular cartilage experiences some tensile strain during normal joint articulation. The combination of compression and a sliding motion as two cartilage surfaces move past one another will produce shear strain at the surface and therefore local tensile strain will also be present. Thus, chondrocytes resident in the superficial zone of articular cartilage may experience tension as part of their normal mechanical environment. Moderate levels of appropriate mechanical stimulation increase cartilage metabolism at both the cell and tissue levels. Therefore, a reasonable hypothesis is that tensile stimulation could increase metabolism in chondrocytes that are accustomed to mechanical tension, *i.e.* cells near the articular surface. This idea is also consistent with our observation that the nature of the proteoglycans being produced by superficial zone chondrocytes did not change, and therefore tensile loading simply stimulated metabolism without altering the synthesis product. Furthermore, a specific protein that may have a role in this response is proteoglycan-4 (PRG4, a.k.a. superficial zone protein). PRG4 is an intermediate sized proteoglycan (~345 kDa MW) with only a few chondroitin sulfate and keratin sulfate GAG chains[199]. Found exclusively at cartilage surfaces and in synovial fluid, it has been

implicated in maintaining the frictional properties of the articular surface. A recent report described an upregulation of PRG4 mRNA and protein synthesis in response to combined compression and sliding stimuli not found when only compressive loading was applied[200]. Although we did not specifically investigate whether tensile loading increased PRG4 synthesis in superficial zone chondrocytes, it is reasonable to suggest that PRG4 production could be influenced by tensile loading and that the substantial increase in proteoglycan production in our system was at least partially due to PRG4 production. Assessing the extent that tensile loading may modulate PRG4 synthesis could elucidate an interesting aspect of cartilage mechanobiology: whether tensile loading generally enhances proteoglycan metabolism in superficial zone chondrocytes or specifically stimulates particular molecules such as PRG4.

As previously stated, our results suggest that tensile loading stimulated metabolism in superficial zone chondrocytes without altering the synthesis products; however, this was not the case for chondrocytes from the middle and deep zones. For deep zone chondrocytes oscillatory tensile loading increased the proportion of lower molecular weight proteoglycans. This trend was also found for middle zone cells, but further experiments are needed to confirm this result. Chondrocytes from the middle and deep zones would typically experience little mechanical tension *in situ*; therefore tensile loading can be considered a more abnormal mechanical environment for these cells. Thus, the change in the characteristics of the proteoglycans synthesized by middle and deep zone chondrocytes in response to tensile loading may indicate an adaptation to the altered mechanical environment. This response could have been the result of middle and deep zone cells synthesizing a larger proportion of the smaller, dermatin sulfate PGs

(decorin and biglycan) or generating more aggrecan fragments through increased enzyme activity.

In addition to the differences found in the proteoglycans, oscillatory tensile loading applied to middle and deep zone chondrocytes induced a shift in the size distribution of proteins with incorporated ^{3}H-proline. Chondrocytes typically incorporate the majority of ^{3}H-proline into newly synthesized collagen molecules. Therefore, this shift in the size of proteins containing ^{3}H in response to tensile loading most likely represents an increase in the size of collagen molecules being assembled and released to the culture medium. This response may also be an adaptation to the altered mechanical environment. A tempting speculation is that tensile loading induced middle and deep zone chondrocytes to produce larger collagen molecules to better accommodate the new local mechanical environment. Further characterization, such as an ELISA, could determine what portion of these proteins are in fact collagens, and column chromatography in combination with specific degradative enzymes may serve to more precisely assess the size and composition of these proteins.

These studies are the first to demonstrate differential responses of zone-specific chondrocytes to oscillatory tensile loading in three dimensional *in vitro* culture and have important implications for cartilage tissue engineering and mechanobiology. Our findings of differential proteoglycan and protein synthesis characteristics between chondrocytes obtained from the superficial zone and the middle and deep zones of articular cartilage suggest that chondrocyte origin is an important consideration when developing strategies for cartilage tissue engineering. Often chondrocytes from the entire thickness of articular cartilage are pooled to generate tissue engineered constructs, but

cellular subpopulations may respond in very different ways to the same exogenous stimuli. Specifically, in response to tensile loading, chondrocytes from the middle and deep zones exhibited proteoglycan synthesis characteristics that may not be beneficial for the development of tissue engineered cartilage replacements. Therefore, it is important to recognize differences in zone-specific chondrocyte mechanobiology when employing exogenous mechanical stimuli. Engineered cartilaginous tissues implanted into a defect site will most likely experience some tensile strain as the deformation of the construct and the surrounding cartilage tissue will differ due to their mismatch in material properties. Hence, understanding the effects of tensile loading on chondrocyte subpopulations can help direct strategies for conditioning engineered tissues prior to implantation as well as promoting successful integration, healing, and ultimately cartilage restoration.

Long term *in vitro* culture using intermittent mechanical stimulation has been demonstrated to be an effective means of generating engineered tissues with enhanced mechanical characteristics[5,173]. We found that modest increases in the mechanical properties of chondrocyte seeded fibrin hydrogel constructs could be achieved with up to 14 days of intermittent oscillatory tensile loading. However, beyond this time point, both tensile and compressive mechanical properties were adversely affected by tensile loading. Evidence of increased aggrecanase activity was also found in constructs subjected to 21 days of tensile loading. These results indicate that extended durations of tensile loading, even when applied intermittently, may trigger a degradatory response from chondrocytes. Enhancement of matrix degrading enzyme activity was also seen in chondrocytes subjected to sustained dynamic compression[140] and fibroblasts subjected to sustained

dynamic stretch[165]. In each of these studies, only 8-10 days of sustained loading were necessary to induce changes in enzyme activity, whereas 21 days of intermittent tensile loading, but not shorter loading durations, increased levels of aggrecan fragments in our system. The total number of cycles during 8-10 days of sustained loading is roughly equivalent to the number of cycles in 21 days of our "12 Hour" intermittent loading protocol (1 Hz frequency in all cases). Potentially a threshold for the total number of deformation cycles (or # cycles per unit time) exists that delineates stimulatory from degradatory loading regimes. Hence, our intermittent loading protocol may have had stimulatory effects at earlier time points, but was akin to an "over use" regime at longer times inducing an increased in matrix degrading enzyme activity. Identifying a threshold for metabolic stimulation could greatly assist in developing mechanical loading protocols by optimizing stimulatory effects while avoiding regimes where detrimental catabolic processes are prominent.

Unexpectedly, substantial quantities of aggrecan cleavage fragments were produced after long term culture in the fibrin hydrogel constructs regardless of loading condition. In contrast, few aggrecan fragments were released to the culture medium during *in vitro* culture of untreated articular cartilage tissue explants[201], and the majority of aggrecan synthesized by chondrocytes and retained in alginate constructs over 21 days of culture had full-length core protein[202]. Additionally, fibrin has been found to activate gelatinase activity in glomerular endothelial cells[203]. In normal physiologic wound healing, fibrin clots rapidly form at injury sites and possess many factors that recruit cells to initiate repair processes. Wound healing involves both anabolic and catabolic responses as cells remodel the extracellular matrix at the site of injury. Hence, although

fibrin clots are typically only found in articular cartilage following penetration of the underlying subchondral bone, extended chondrocyte culture in a fibrin matrix may induce aspects of a wound healing response such as enhanced enzyme activity. This characteristic may be unique to fibrin hydrogels and limit their potential for use in the long term development of engineered tissues. However, if the catabolic side of the wound healing response could be controlled and the anabolic side exploited, then such a response could be advantageous for construct development. Selective enzyme inhibitors could be used to investigate this idea. Since aggrecan molecules were clearly being degraded in these studies, selective aggrecanase inhibitors may be able to reduce or eliminate undesirable aggrecan cleavage. Studies in our laboratory have shown that these inhibitors can reduce or delay the effects of interleukin-1α induced degradation in articular cartilage and meniscus tissue explants[201,204]; therefore, appropriately administered aggrecanase inhibitors may also be beneficial for promoting growth in engineered tissue constructs.

8.3 Future Recommendations

The work completed for this dissertation provided novel contributions to the understanding of chondrocyte mechanobiology and may prove useful in developing engineered cartilaginous tissues for both articular cartilage and meniscal fibrocartilage repair. Additionally, many of the immunofluorescence imaging techniques as well as the bioreactor developed for this research can be used for numerous future investigations. Many avenues for further exploration could be pursued based on this work, and a few specific recommendations for future developments are provided here.

The Oscillatory Tensile Loading Device was designed for maximum adaptability, allowing for future modifications as needed. The device is currently controlled using closed loop position feedback, but is not capable of measuring forces applied to constructs during operation. Incorporating force monitoring into the system would provide valuable additional information during construct loading. A simple means to achieve this goal would be to place a force transducer in line with the mobile tension rake. However, this would only provide a global force measurement that included the sum of the forces generated by each construct plus the inertia of the system. Although technically challenging, placing micro pressure transducers on each stationary pin of the culture chambers could yield individual force measurements for each construct. The tensile mechanical characteristics of each construct could then be monitored longitudinally over the course of an experiment, which would be a significantly improvement over destructive end point testing currently used. This modification will enhance the capabilities and overall utility of the Oscillatory Tensile Loading Device for future applications.

The depth of knowledge regarding cellular responses to tensile mechanical stimuli could be enhanced by using varied cell sources. All of the studies presented here employed an immature bovine cell source. This cell type is well characterized in the articular cartilage literature and thus was an excellent choice for these studies. However, when using an animal cell source, questions always arise regarding the applicability of the results to humans. Additionally, most patients in need of cartilage repair are older adults. Chondrocyte extracellular matrix metabolism and sensitivity to growth factor stimulation are known to decrease with age; therefore cells from older animals (or older

humans) may not respond in the same manner as the immature cells used here. Related to this concern is that cells from different animal species can also respond differently to exogenous stimuli. As was discussed in Chapter 3, variations exist in the patterns of extracellular matrix molecule distribution in menisci from different species. Conducting additional studies using either human cells or at least cells from another animal species would be beneficial for understanding if the results presented here are more universal or highly age and species dependent. Additionally, bone marrow stromal cells (BMSCs) have the potential to differentiate down chondrocytic or fibrochondrocytic pathways and therefore make an attractive cell source for tissue engineering. Using the Oscillatory Tensile Loading Device developed at part of this dissertation research, on-going work in our laboratory is investigating the combination of loading and growth factor supplementation to differentiate BMSCs into cells that produce a fibrocartilage matrix[205,206].

Local mechanical, biochemical, and cellular interaction characteristics are extremely important influences on cellular behaviors. The three dimension culture system used throughout this dissertation work employed a homogeneous fibrin hydrogel scaffold material. Numerous studies have shown that cellular responses to a variety of stimuli are dependent on the local environment, and therefore observations regarding specific cellular behaviors in one scaffold system may not necessarily translate to another. Thus, conducting similar studies using another material, preferably with different cellular adhesion characteristics, would help determine if the results presented here are more broadly applicable. Fibrin has many cellular adhesion sites as well as regions that can bind other adhesion molecules, such as fibronectin. Presumably

chondrocytes and fibrochondrocyte can interact with this matrix using a number of different receptors. Studies with more inert hydrogel materials such as alginate or poly(ethylene glycol), which do not contain cell receptor binding sites, could help isolate the effects of direct tensile strain on the cell membrane from indirect mechanical stimulation caused by macroscopic deformation of the construct. Synthetic self assembling peptide materials are also an ideal choice, because they can often be thermally, photochemically, or ionically crosslinked on demand. Additionally, specific molecules can be tethered to these materials generating custom designed cell-scaffold interface regimes. Adhesion molecules, such as RGD peptides, could be used to promote specific integrin interactions that initiate desirable signaling cascades. Growth factors or cytokines could be immobilized on the scaffold material to provide a homogeneous distribution of these signaling molecules. Studies using materials with well defined cell-scaffold interface regimes could be used for more in depth investigations into mechanotransduction signaling pathways as well as specific synergistic effects between mechanical and biochemical stimuli.

In addition to exploring scaffolds with diverse cell-matrix interaction regimes, the organization of the scaffold matrix itself may prove important. Both articular cartilage and fibrocartilage tissues are highly inhomogeneous and anistropic, but the vast majority of tissue engineering studies, including those presented here, have utilized a homogenous scaffold material. In our studies, uniaxial tensile loading did not induce either cellular or extracellular matrix directionality. Therefore, employing a scaffold material with a predefined orientation, perhaps to mimic the outer zone of the meniscus, could be advantageous in generating a replacement tissue with enhanced mechanical

characteristics or growth potential. The haptotactic factors of an organized scaffold matrix environment could promote the development of a newly synthesized extracellular matrix with preferential directionality. Used in combination with mechanical stimulation this technique could further enhance tissue construct growth, ideally leading to the development of a biologically and mechanically functional extracellular matrix.

The ability to generate a functional extracellular matrix is fundamental to the success of tissue engineering and regenerative medicine therapies. Our major motivation for performing the detailed immunofluorescence imaging of meniscus tissue was to gain an understanding of the spatial relationships of various matrix molecules *in situ*. During *in vitro* culture, chondrocytes and fibrochondrocytes synthesize and organize a new extracellular matrix in a time dependent manner. Many researchers have found ways to augment matrix synthesis via exogenous stimuli, but few have been able to accomplish this while also controlling the organization of this developing matrix. Applying the imaging techniques presented in Chapter 3 to tissue constructs early in their development would provide useful insights important growth and maturation characteristics of repair tissue. For example, examining specific matrix molecules produced by meniscal fibrochondrocytes as well as their organization in the first several days of culture would be useful for understanding the initial events in fibrochondrocyte-mediated tissue repair. Additionally, comparisons of developmental patterns among various scaffolding materials would also be useful in determining whether early extracellular matrix deposition and organization are dependent on specific cell-scaffold interactions. Knowledge acquired from these types of imaging studies could then be used to develop

strategies that can either promote or repress specific extracellular matrix synthesis patterns observed during construct maturation.

In summary, along with the specific findings regarding articular chondrocyte and meniscal fibrochondrocyte responses to oscillatory tensile loading, this dissertation explored ideas that can propel future research in a number of areas. The Oscillatory Tensile Loading Device is a robust bioreactor currently used for tissue engineering and mechanobiology investigations in cartilage and meniscus but also has the potential to be used with other tissue such as tendons and ligaments. Exploring differences in chondrocytes derived from specific zones of articular cartilage is becoming an area of increasing research interest, and identifying zone-specific characteristics that can be exploited in developing cartilage tissue replacements represents an exciting opportunity. Finally, immunofluorescence imaging techniques developed in this work for native tissues are powerful tools that can be used to identify key relationships between molecules and assess how well those relationships are being emulated in engineered tissues.

APPENDIX A

OSCILLATORY TENSILE LOADING DEVICE

A.1 List of Device Components

Table A.1: Components purchased for the oscillatory tensile loading device

Part Number	**Description**	**Vendor**
0150-1208	PS01-23X80-M20 Linear Motor Stator, with IP67 connector	LinMot
0150-1301	PL01-12X170/120 Linear Motor Slider	LinMot
0150-1901	Mounting Flange 23x5mm	LinMot
0150-1981	KS01-D/M-04 4 meter IP67 cable	LinMot
0150-1651	E110-VF LinMot Amplifier/Controller	LinMot
0150-1944	24V/150W Power Supply	LinMot
0150-1941	48V/300W Power Supply	LinMot
P165	MC202 Trio Motion Controller	Trio Motion Technology
P350	RS232 Serial Cable	Trio Motion Technology
RGH24Z30F00A	0.5 Micron encoder with reference switch	Renishaw
A-9541-0037	RGM245S 90 degree mount reference	Renishaw
A-9541-0124	Scale installation tool	Renishaw
A-9523-6050	50 cm encoder tape	Renishaw
RSR9WZM-110	110mm mini block and rail assembly	THK Co.
all above components purchased through Dynamic Solutions (Lilburn, GA)		
LK-70	Linear misalignment coupling, G1/G2 = M5	R+W Coupling Technology

Table A.2: Components custom made for the oscillatory tensile loading device

Figure Reference	**Quantity**	**Description**	**Source**
Figure A.2A	4	Tension culture chamber	JM Machining
Figure A.2B	2	Unloaded culture chamber	JM Machining
Figure A.3	4	Mobile Tension rake	JM Machining
Figure A.3	48	Stainless steel pins for tension rake	JM Machining
Figure A.4	8	Polycarbonate construct mold	JM Machining
Figure A.5A	2	End block length spacer	JM Machining
Figure A.5B	2	End block width spacer	JM Machining
Figure A.6A	2	End block punch template (upper)	JM Machining
Figure A.6B	2	End block punch template (lower)	JM Machining
Figure A.7A,B	2	Polycarbonate base plate	Mech. Engr.
Figure A.8A	2	THK slide mount	Mech. Engr.
Figure A.8B	2	Optical encoder mount	Mech. Engr.
Figure A.8C	2	Linear motor bracket	Mech. Engr.
Figure A.9A	2	Rake connector plate	Mech. Engr.
Figure A.9B	2	Double rake interface plate	Mech. Engr.
Figure A.9C	2	Double chamber spacer block	Mech. Engr.
Figure A.10	4	Culture chamber shield	Mech. Engr.

* JM Machining (Lawrenceville, GA)

* Mech. Engr. = Georgia Tech School of Mechanical Engineering machine shop

A.2 Oscillatory Tensile Loading Device Engineering Drawings

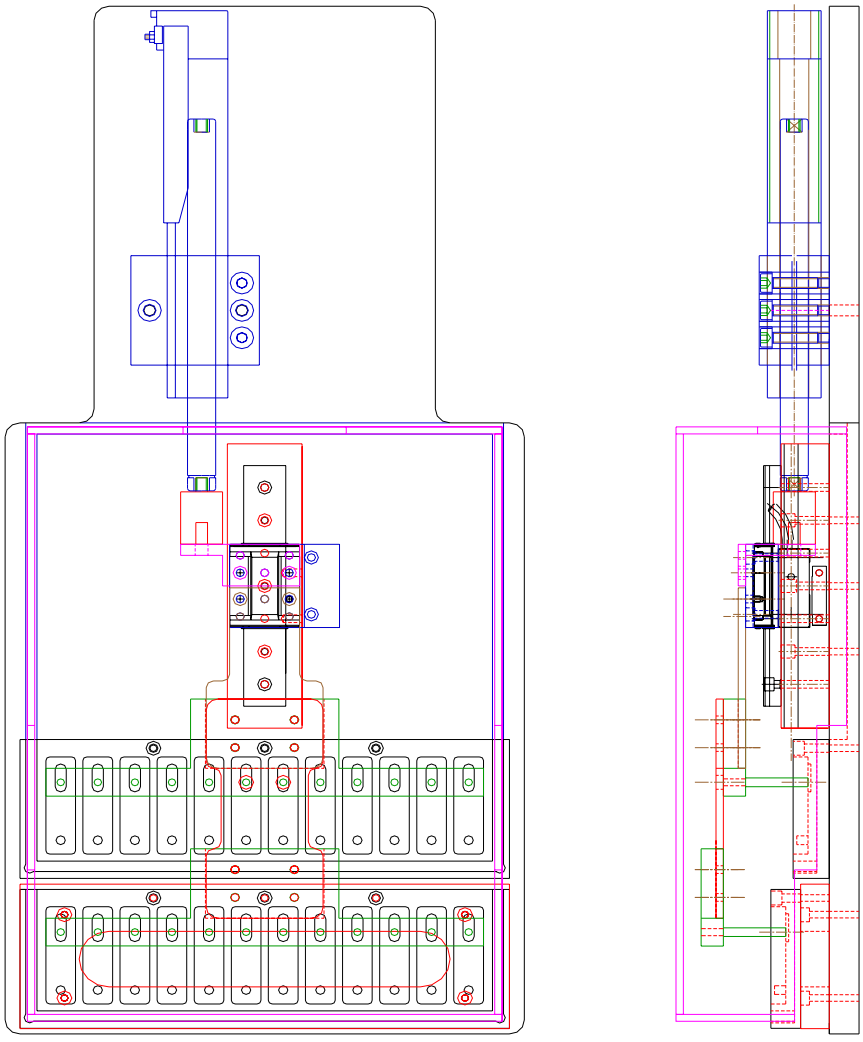

Figure A.1: Complete assembly of the oscillatory tensile loading device.

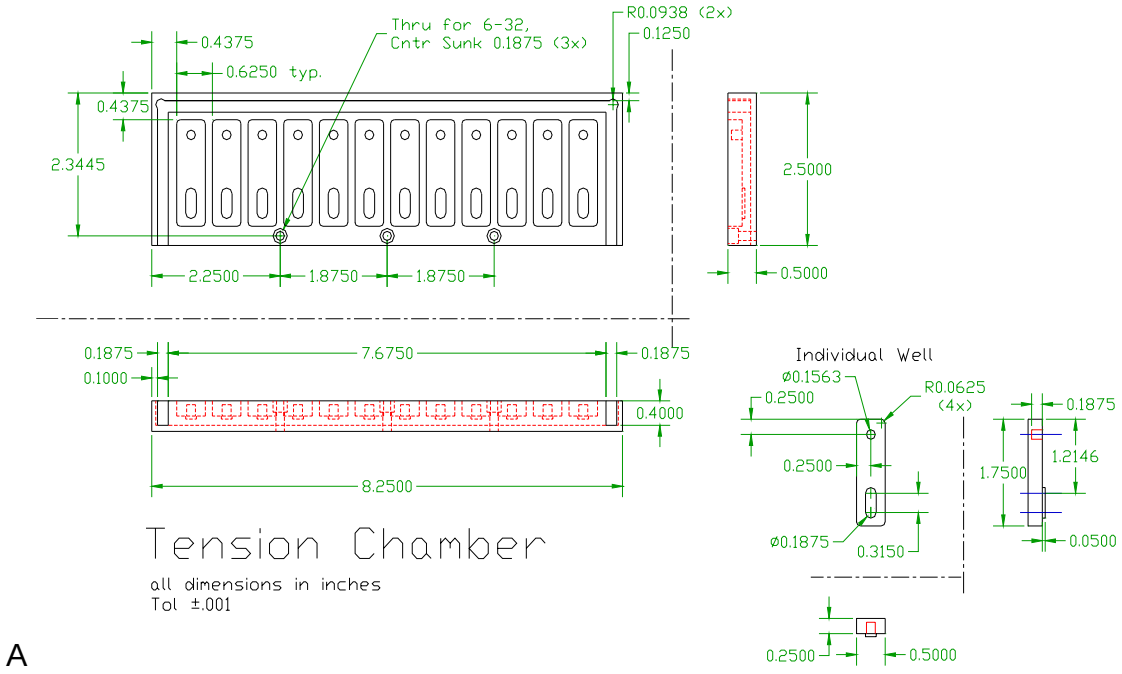

A

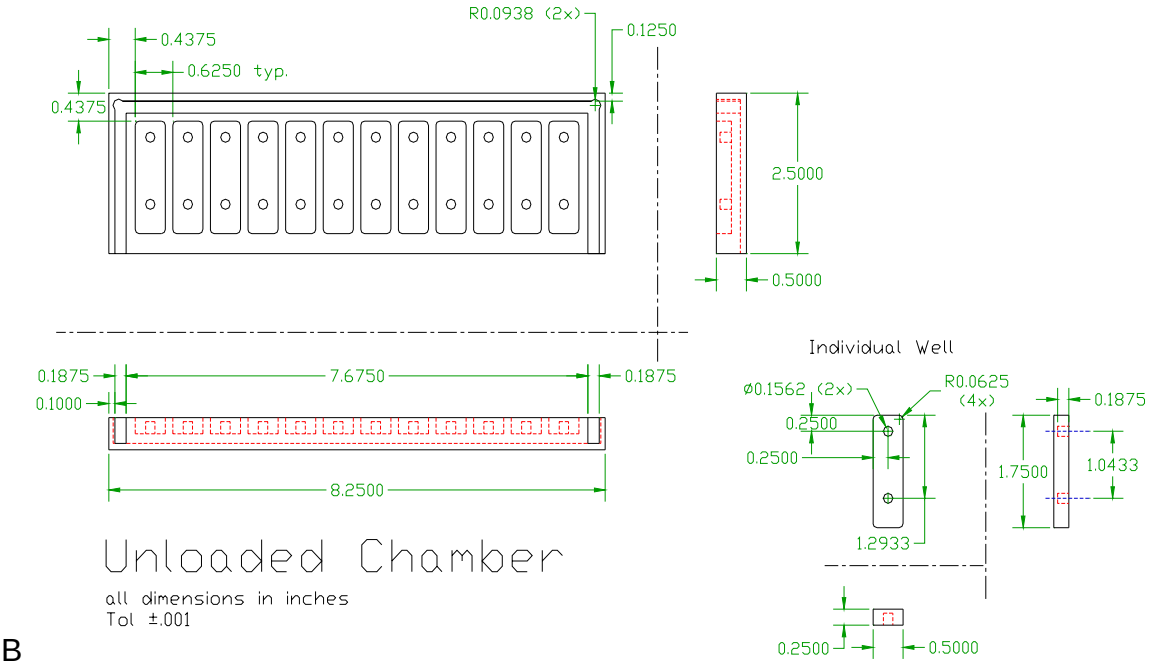

B

Figure A.2 Stationary culture chambers

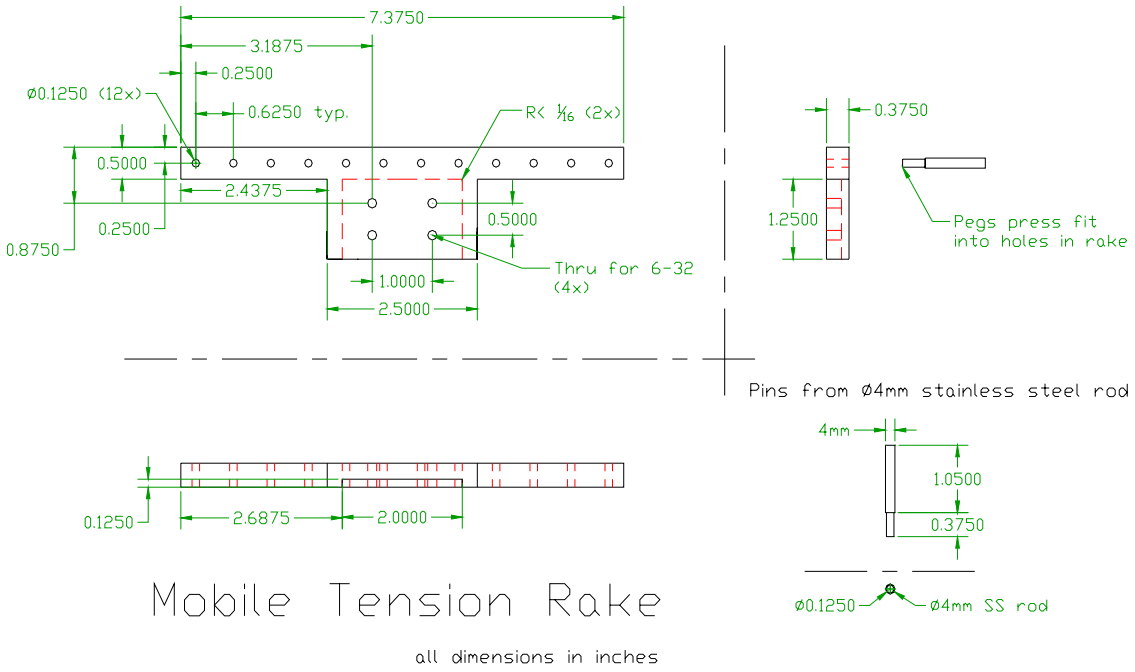

Figure A.3 Mobile tension rake and stainless steel pins

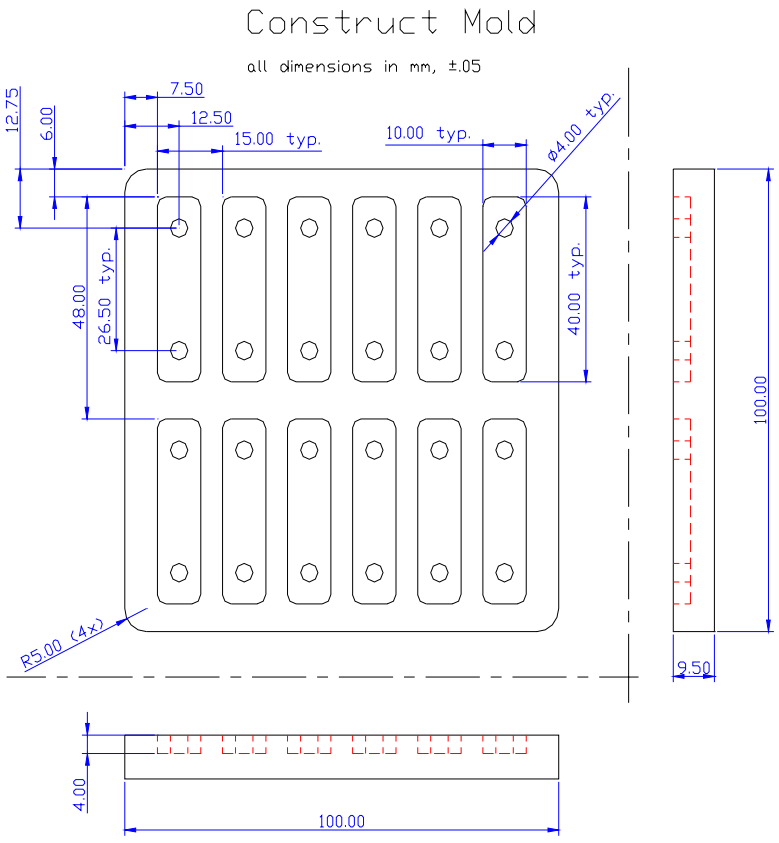

Figure A.4 Polycarbonate construct mold

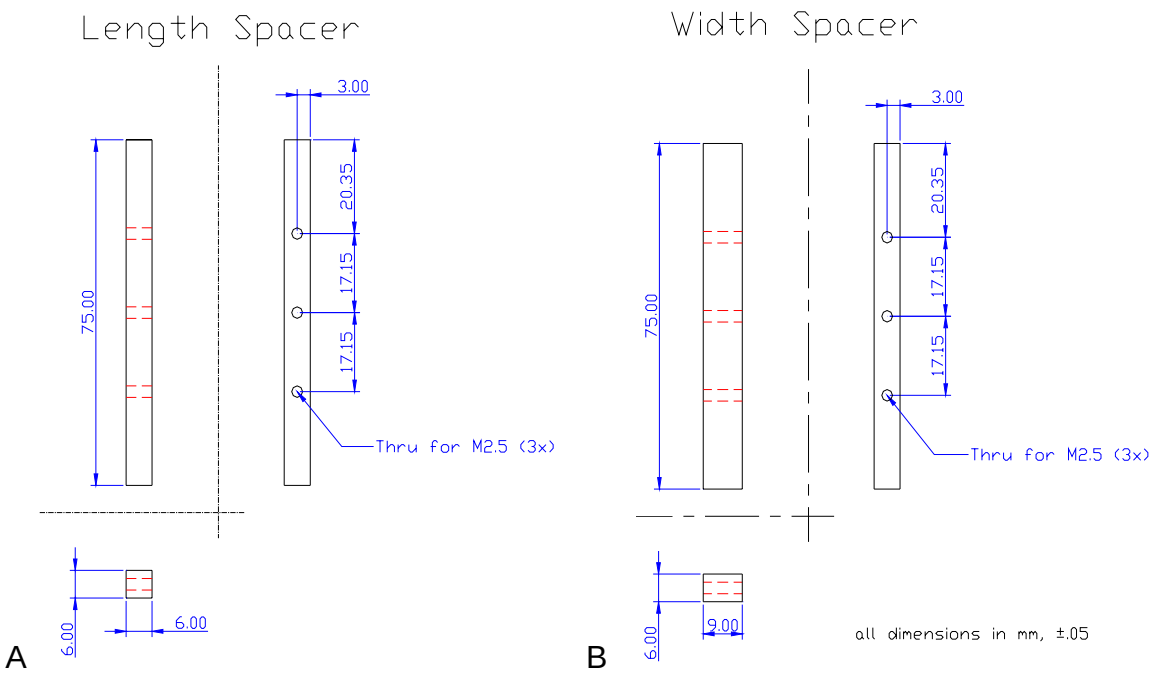

Figure A.5 End block length and width cutting tools

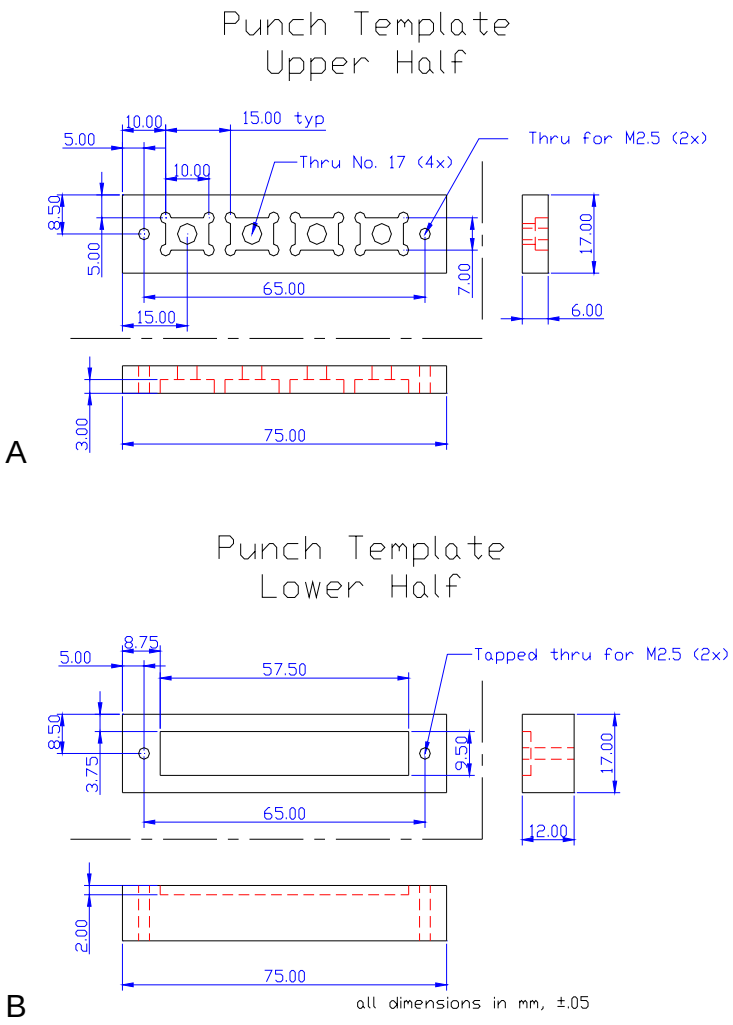

Figure A.6 End block punching templates

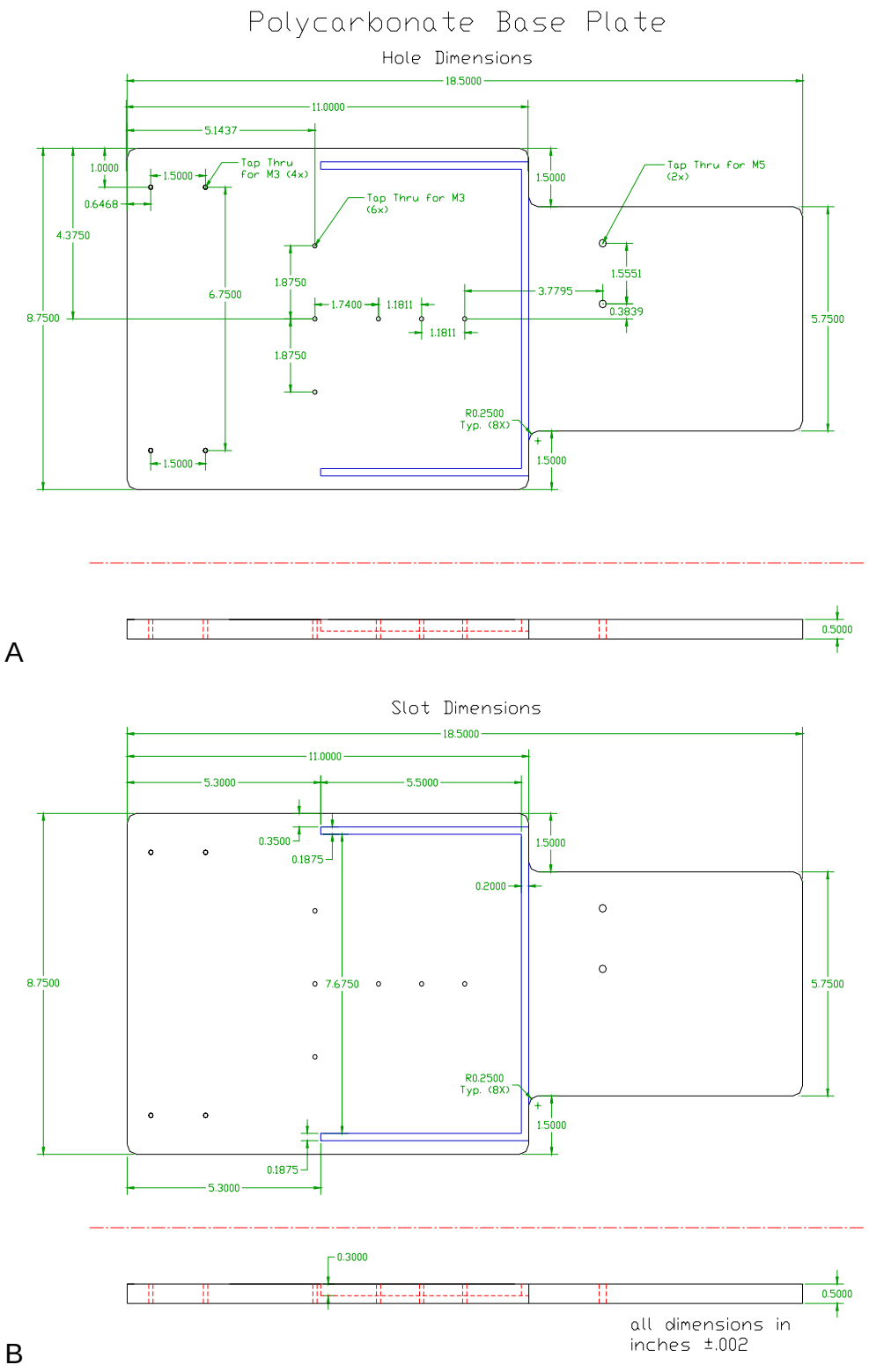

Figure A.7 Polycarbonate base plate

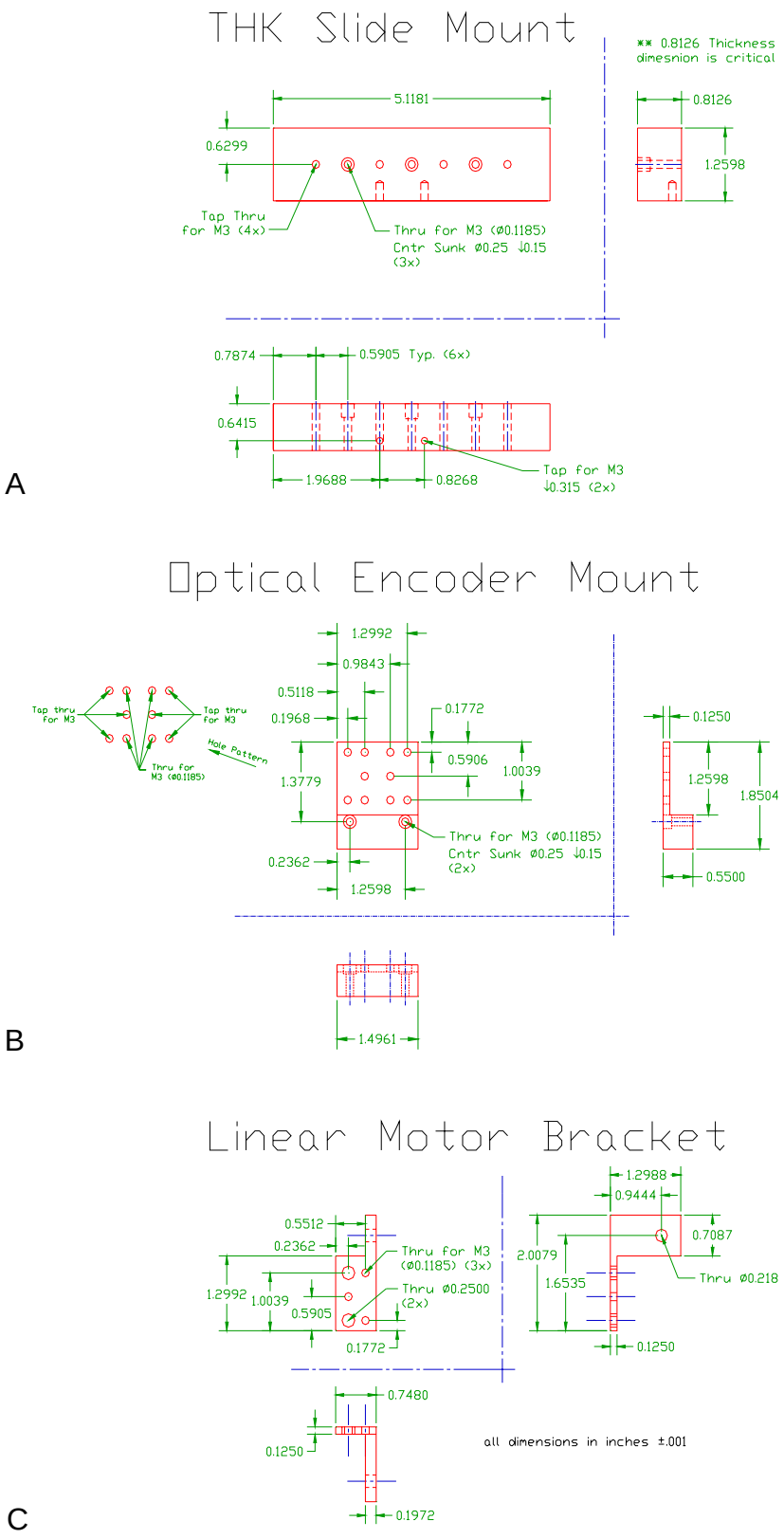

Figure A.8 Linear motor and linear slide bearing interface pieces

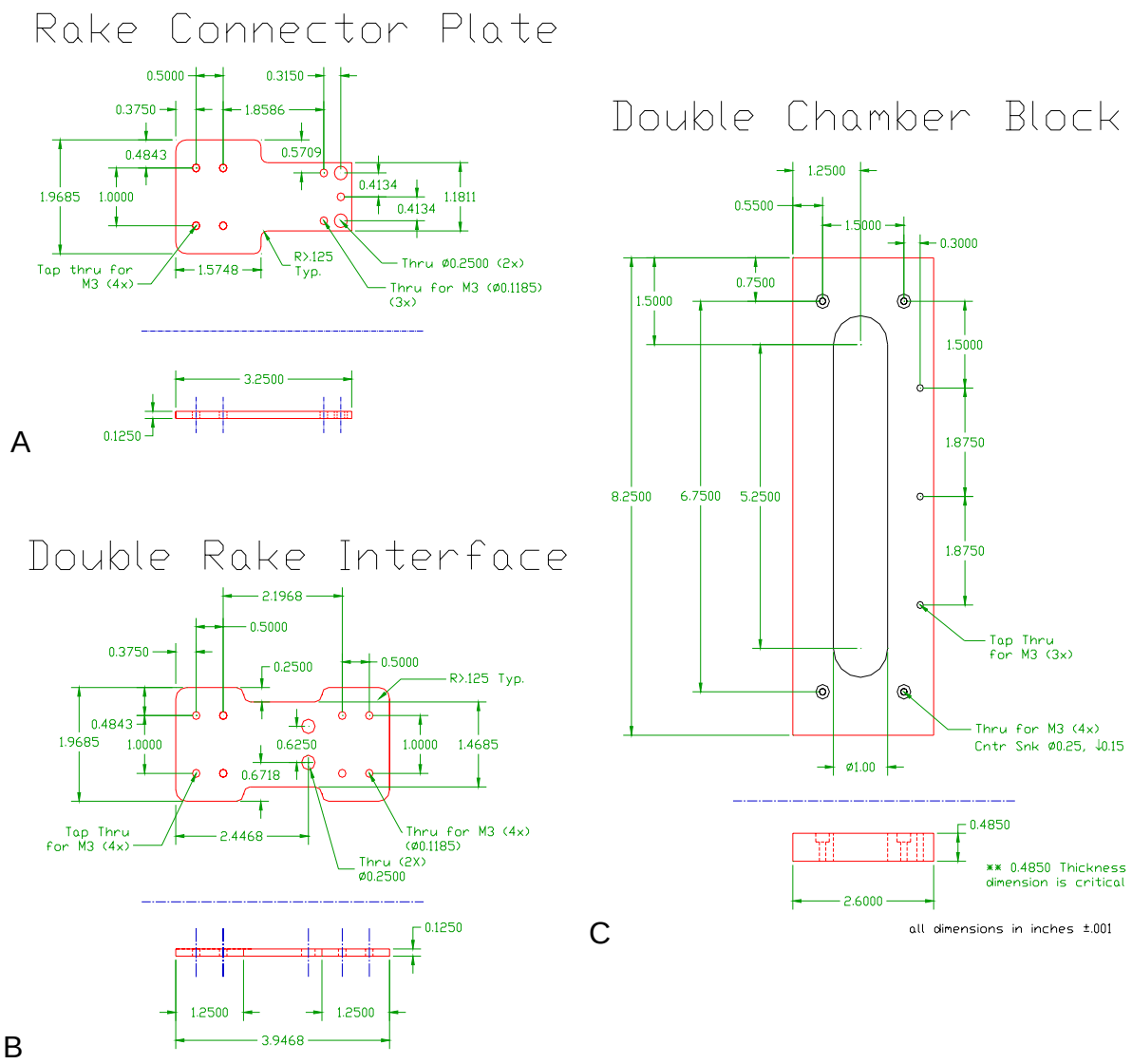

Figure A.9 Tension rake and culture chamber interface pieces

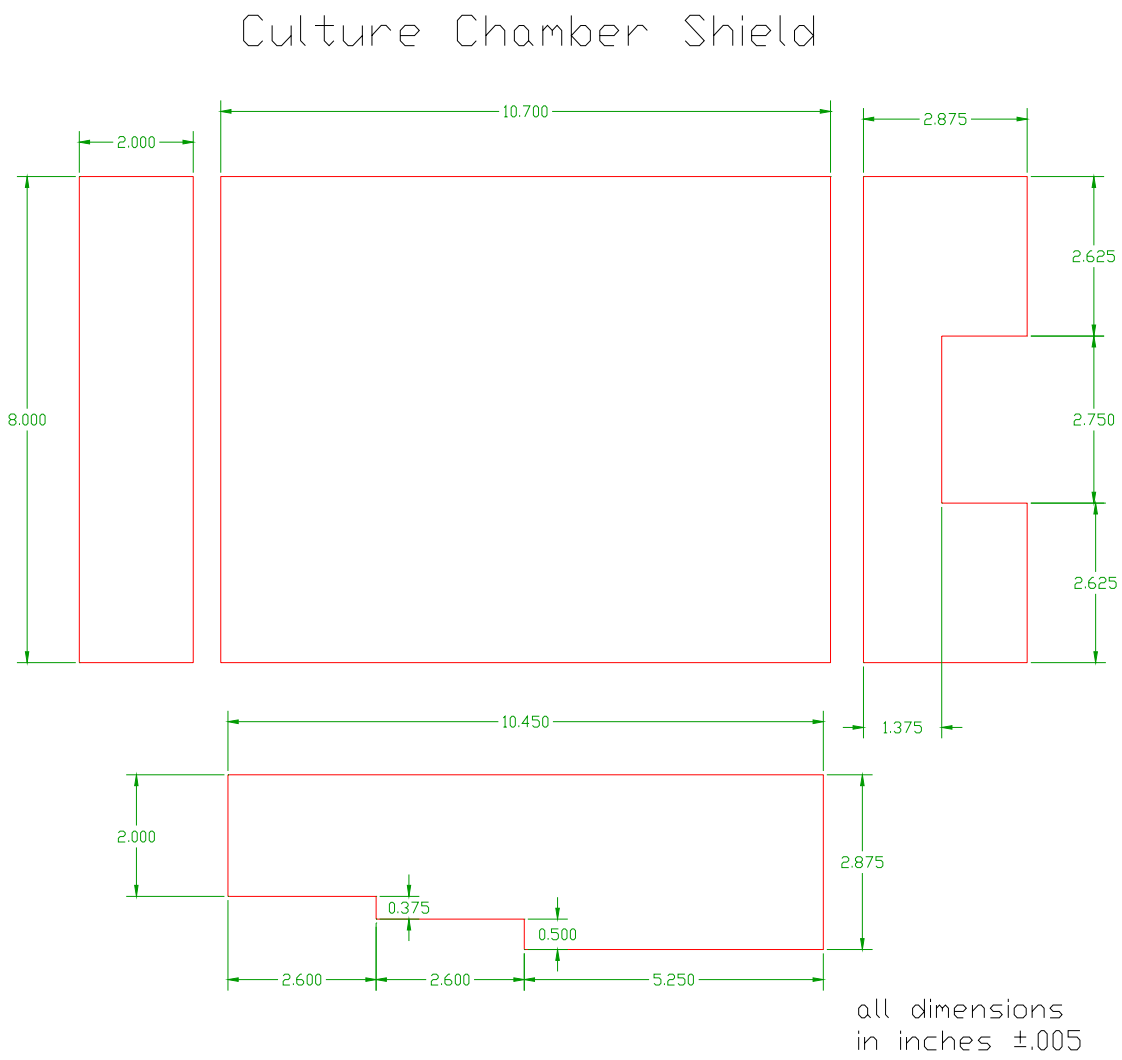

Figure A.10 Polycarbonate culture chamber shield

A.3 Device Operation Instructions

A.3.1 Device Startup

1. Culture chambers, tension rakes and rake interface pieces, and socket head cap screws should all be sterilized prior to beginning this procedure
2. Polycarbonate culture chamber shield should be thoroughly wiped with 70% ethanol before being transferred to the biosafety cabinet and again once they are inside the cabinet
3. Move the Oscillatory Tensile Loading Device into the biosafety cabinet
4. Ensure the device control box is in the off position and the computer is connected to the control box via the RS-232 cable
5. Connect the motor power/signal cable from the control box to the LinMot motor
6. Connect the optical encoder cable to the control box, and secure with back shell screws
7. Power on the control box using the power switch on the back of the unit
8. Open the Motion Perfect 2 software on the attached computer
9. Open the Terminal window and select COM 0

   Also open the Axis Parameters and Oscilloscope windows so that the motion of the device can be monitored during operation
10. Run the program called STARTUP_1

    ** IMPORTANT: the tension rake cannot be connected to the device while running this program
11. Follow the instructions and choose which controller is being used (1) or (2)
12. The device will move to a mechanical stop and then find the home position for the system being used. Wait for the program to finish. Now the motor will be positioned at the home position for 20 mm long constructs
13. Attach the Tension Culture Chamber to the Base Plate with at least 2 M6 socket head cap screws. Ideally, constructs should have been positioned in the culture chambers previously
14. Carefully insert the stainless steel pins on the Tension Rake into the holes in the construct end blocks. Start on one end of the chamber and work down to the opposite end. Be careful to minimize unnecessary deformation of the constructs
15. Attach the Tension Rake to the interface piece with 4 M6 socket head cap screws

    ** If two Tension Culture Chambers are being used simultaneously, the Double Rake Interface piece must also be attached at this point
16. Repeat steps 13-15 above for the second culture chamber if necessary

17. Ensure all screws are tight, but do not over tighten as this may damage the polysulfone pieces
18. Check the alignment of the device and ensure that the end blocks of all constructs are in line with the axis of tensile displacement
19. Fill each well in the culture chamber with 1.5 – 2.0 mL of culture medium
20. Position the polycarbonate culture chamber shield over the chambers and rake pieces
21. Before moving the system to the incubator, it is advisable to perform 15-30 cycles of oscillatory tensile loading to check that everything is functioning properly. See steps 24-26 below and choose the "input number of loading cycles option"
22. Carefully move the Oscillatory Tensile Loading Device to the tissue culture incubator keep it as level as possible during the transfer. The culture chambers should be positioned at the back of the incubator with the back of the motor facing the door of the incubator. Close the inner door to the incubator and position the cables such that the door can be latched closed
23. Collect the cables and secure them in a manner to keep them out of the way
24. Run the program INTERMITTENT in the Motion Perfect 2 software
25. Follow the instructions of the program

    Enter which controller and system is being used

    Enter the desired peak-to-peak amplitude if the sine wave in mm

    Enter the desired frequency of motion in Hz

    Choose the type of protocol to be performed: Intermittent, Continuous, or Input number of cycles

    * For the Input number of cycles option, enter the desired number of cycles as an integer

    * For the Intermittent option enter (1) how many minutes of loading are desired, (2) how many minutes are recovery are desired, and (3) how many repeats of this cycle are desired.

        Note: Minutes of loading and recovery must be entered as integers ≥ 1

        Note: Loading period + recovery period = 1 cycle
26. The program will instruct the device to begin automatically and the parameters selected will be outputted to the screen
27. Visually check the device to ensure it appears to the operating correctly. Also check the motion profile using the digital oscilloscope in the Motion Perfect 2 software to ensure that the following error is within tolerance limits

    ** Minor adjustments can be made to the device tuning parameters (in the Axis Parameters window) to adjust the motion of the device

    IMPORTANT: THIS SHOULD ONLY BE ATTEMPTED BY SOMEONE WITH INTIMATE KNOWLEDGE OF TUNING THE DEVICE AS

INCORRECT VALUES FOR THE TUNING PARAMETERS CAN LEAD TO SYSTEM INSTABILITY AND DAMAGE OR DESTROY THE OSCILLATRY TENSILE LOADING DEVICE

28. Periodically check the motion profile of the device using the digital oscilloscope
29. At any time during device operation the command "VR(1) = 0" can be entered into the Terminal window and the device will finish its current cycle, return to the home position, and the program will terminate

A.3.2 Device Takedown

1. Ensure the device is stopped or enter "VR(1) = 0" into the Terminal window to stop the device motion. The loading protocol parameters will be outputted to the screen
2. DO NOT turn off the control box at this point
3. Remove the device from the incubator and place on a wheeled cart
4. Move the cart to a nearby laboratory bench with adequate space
5. Carefully remove the culture chamber shield and the tension rake(s)
6. Transfer constructs to appropriate buffer solution depending on the specific experimental design of the study
7. Disable the drivers in the Motion Perfect 2 software (upper left corner of the screen)
8. Turn off power to the control box by the switch on the back
9. Wait at least 2 minutes before disconnecting the motor and encoder cables from the control box
10. All components of the Oscillatory Tensile Loading Device should be thoroughly cleaned with 70% ethanol after each use and before storing the device

Following these simple procedures will ensure that you maximize the performance of the Oscillatory Tensile Loading Device as well as your own productivity, safety, and enjoyment for many years to come.

A.4 Source Code for Operational Programs

A.4.1 Program STARTUP_1

```
'THIS PROGRAM WILL INITIALIZE THE CONTROLLER UPON STARTUP

'DETERMINE WHICH CONTROLLER IS BEING USED
controlcheck:
PRINT " "
PRINT "WHICH CONTROLLER IS BEING USED?"
PRINT "ENTER (1) FOR CONTROLLER #1 OR (2) OR CONTROLLER #2: ";
INPUT controller
IF (controller <> 1) AND (controller <> 2) THEN
   PRINT "INVALID ENTRY - RETRY"
   GOTO controlcheck
ENDIF
IF controller = 1 THEN
   offset = 2.9019
ELSE
   offset = 2.3850
ENDIF
PRINT " "
PRINT "OFFSET FOR CONTROLLER #";
PRINT controller[0];
PRINT " IS ";
PRINT offset[4];
PRINT " MM"

'INITIALIZE AXIS PARAMETERS
UNITS=2000
SPEED=.5
ACCEL=1000
DECEL=1000
FE_LIMIT=.1
CREEP=.5

'INITIALIZE CONTROL LOOP PARAMETERS
P_GAIN=2.75
I_GAIN=.5
D_GAIN=7
OV_GAIN=0
VFF_GAIN=80

DATUM (0)
SERVO=1
```

```
WDOG=1
WA (5000)
REVERSE
WAIT IDLE
WA (5000)
DATUM(0)
DEFPOS(0)
SERVO=1
WDOG=1
WA (5000)
DATUM (1)
WAIT IDLE
WA (2000)
MOVEABS(offset)
WAIT IDLE
DEFPOS(0)
PRINT "STARTUP PROGRAM COMPLETE ON CONTROLLER #";
PRINT controller[0]
STOP
```

A.4.2 Program INTERMITTENT

```
'THIS PROGRAM WILL USE THE CAM FUNCTION
'TO PERFORM A SINE WAVE MOTION
'THE OPTION FOR INTERMITTENT PROTOCOLS WILL BE INCLUDED

'INITIALIZE AXIS PARAMETERS
UNITS=2000
SPEED=1
ACCEL=2
DECEL=2
FE_LIMIT=1.0
'INITIALIZE CONTROL LOOP PARAMETERS
P_GAIN=.7
I_GAIN=.0035
D_GAIN=7
OV_GAIN=-3
VFF_GAIN=-28

VR(1)=0
VR(2)=0
VR(3)=0
```

```
SERVO=1
WDOG=1

'DETERMINE WHICH CONTROLLER IS BEING USED
controlcheck:
PRINT " "
PRINT "WHICH LOADING SYSTEM IS BEING USED?"
PRINT "ENTER (1) FOR SYSTEM #1 OR (2) FOR SYSTEM #2: ";
INPUT controller
IF (controller <> 1) AND (controller <> 2) THEN
   PRINT "INVALID ENTRY - RETRY"
   GOTO controlcheck
ENDIF
IF controller = 1 THEN
   P_GAIN=.7
   I_GAIN=.0029
   D_GAIN=7
   OV_GAIN=-3
   VFF_GAIN=-30
ELSE
   P_GAIN=.7
   I_GAIN=.025
   D_GAIN=.5
   OV_GAIN=-2
   VFF_GAIN=10
ENDIF

encchk:
amp = 0
freq = 0
cycles = 0
PRINT " "
PRINT "WHAT IS THE DESIRED SINE WAVE AMPLITUDE IN MM? ";
INPUT amp
PRINT "WHAT IS THE DESIRED FREQUENCY IN Hz? ";
INPUT freq
PRINT " "
PRINT "ENTER (2) FOR INTERMITTENT LOADING"
PRINT "ENTER (1) FOR CONTINUOUS LOADING"
PRINT "ENTER (0) TO INPUT NUMBER OF LOADING CYCLES: ";
INPUT VR(1)
PRINT " "
IF (VR(1) <> 0) AND (VR(1) <> 1) AND (VR(1) <> 2) THEN
   PRINT "ERROR, PLEASE RE-ENTER"
   GOTO encchk
```

```
ENDIF
IF VR(1)=0 THEN
   PRINT "HOW MANY CYCLES ARE DESIRED? ";
   INPUT cycles
ENDIF
IF VR(1)=2 THEN
   PRINT "HOW MANY MINUTES OF LOADING? ";
   INPUT loading
   PRINT "HOW MANY MINUTES OF RECOVERY? ";
   INPUT recovery
   PRINT "HOW MANY REPEATS OF THIS PATTERN? ";
   INPUT repeats
ENDIF
scale = amp * UNITS*1.0
num_p = 50
count = 0
incrcount = 0
waitcount = 0
repcount = 0
SPEED AXIS(0)= (2*amp)*freq
ACCEL AXIS(0) = SPEED AXIS(0)*10
DECEL AXIS(0) = SPEED AXIS(0)*10
WAIT IDLE
MOVEABS (0.0)
WAIT IDLE
MOVE (-amp*1.0)
WAIT IDLE
SPEED AXIS(0) = (num_p * freq)*1.0
ACCEL AXIS(0) = SPEED AXIS (0)* 1000
DECEL AXIS(0) = SPEED AXIS (0)* 1000
dist = num_p
FOR p= 0 TO num_p
   TABLE(p,((-SIN(PI*2*p/num_p)/(PI*2))+p/num_p))
NEXT p
FOR i= 1 TO num_p
   TABLE(num_p+i,TABLE(num_p-i))
NEXT i
IF (VR(1)=0) AND (cycles <>0) THEN
   PRINT " "
   PRINT "SPECIFIED CYCLES LOADING PROTOCOL:"
   PRINT amp[2];" MM DISPLACEMENT AT ";freq[2];" Hz FOR ";cycles[0];"
CYCLES."
   FOR j= 1 TO cycles
      'IF j=15 THEN
      'SCOPE (ON,1,1000,7000,MPOS,DPOS,FE)
      'TRIGGER
```

```
      'ENDIF
      CAM(0,2*num_p,scale,dist)
      count=count+1
      VR(2) = count
      WAIT IDLE
   NEXT j
ELSE
   IF (VR(1)=1) THEN
      PRINT " "
      PRINT "CONTINUOUS LOADING PROTOCOL:"
      PRINT amp[2];" MM DISPLACEMENT AT ";freq[2];" Hz."
      REPEAT
         CAM(0,2*num_p,scale,dist)
         count=count+1
         VR(2) = count
         WAIT IDLE
      UNTIL (VR(1) <> 1) OR (WDOG <> 1)
   ELSE
      IF (VR(1)=2) THEN
         PRINT " "
         PRINT "INTERMITTENT PROTOCOL:"
         PRINT amp[2];" MM DISPLACEMENT AT ";freq[2];" Hz."
         PRINT loading[0];" MIN LOADING, ";recovery[0];" MIN RECOVERY, ";
         PRINT "REPEATED "; repeats[0];" TIMES."
         REPEAT
            incrcount = 0
            waitcount = 0
            VR(4) = 0
            IF DPOS <> (-amp*1.0) THEN
               WAIT IDLE
               SPEED AXIS(0)= (2*amp)*freq
               ACCEL AXIS(0) = SPEED AXIS(0)*10
               DECEL AXIS(0) = SPEED AXIS(0)*10
               MOVE (-amp*1.0)
            ENDIF
            PRINT " "
            PRINT "LOADING FOR ";loading[0];
            PRINT " MINUTES IN REPEAT #";repcount+1[0];"..."
            REPEAT
               WAIT IDLE
               SPEED AXIS(0) = (num_p * freq)*1.0
               ACCEL AXIS(0) = SPEED AXIS (0)* 1000
               DECEL AXIS(0) = SPEED AXIS (0)* 1000
               CAM(0,2*num_p,scale,dist)
               incrcount = incrcount + 1
               VR(2) = incrcount
```

```
            UNTIL (VR(2)= freq*loading*60) OR (VR(1) <> 2) OR (WDOG <> 1)
            VR(3) = VR(3) + VR(2)
            WAIT IDLE
            SPEED AXIS(0)= (2*amp)*freq
            ACCEL AXIS(0) = SPEED AXIS(0)*10
            DECEL AXIS(0) = SPEED AXIS(0)*10
            MOVE (amp*1.0)
            PRINT VR(2)[0]; " CYCLES WERE RUN ";
            PRINT "IN ";VR(2)/(60*freq)[2];" MINUTES OF RUN TIME.";
            PRINT " (REPEAT #";repcount+1[0];")"
            IF (VR(1) = 2) AND (recovery > 0) THEN
               PRINT " "
               PRINT "WAITING FOR ";recovery[0];
               PRINT " MINUTES IN REPEAT #";repcount+1[0];"..."
               REPEAT
                  WA (60000)
                  waitcount = waitcount + 1
                  VR(4) = waitcount
               UNTIL (waitcount = recovery) OR (VR(1) <> 2)
               PRINT "WAITED ";VR(4)[0];" MINUTES OF RECOVERY TIME.";
               PRINT " (REPEAT #";repcount+1[0];")"
               repcount = repcount + 1
            ENDIF
         UNTIL (repcount = repeats) OR (VR(1) <> 2)
         WAIT IDLE
      ENDIF
   ENDIF
ENDIF
WAIT IDLE
IF DPOS <> 0 THEN
   SPEED AXIS(0)= (2*amp)*freq
   ACCEL AXIS(0) = SPEED AXIS(0)*10
   DECEL AXIS(0) = SPEED AXIS(0)*10
   MOVE (amp*1.0)
ENDIF
IF (VR(1) <> 2) AND (repcount = repeats) THEN
   PRINT " "
   PRINT VR(2)[0]; " CYCLES WERE RUN";
   PRINT " IN ";VR(2)/(60*freq)[2];" MINUTES OF RUN TIME."
ENDIF
PRINT " "
PRINT "LOADING PROTOCOL COMPLETE"
STOP
```

APPENDIX B

CUSTOM ADAPTERS FOR TENSILE MECHANICAL TESTS

B.1 Tensile Mechanical Testing Adapters Engineering Drawings

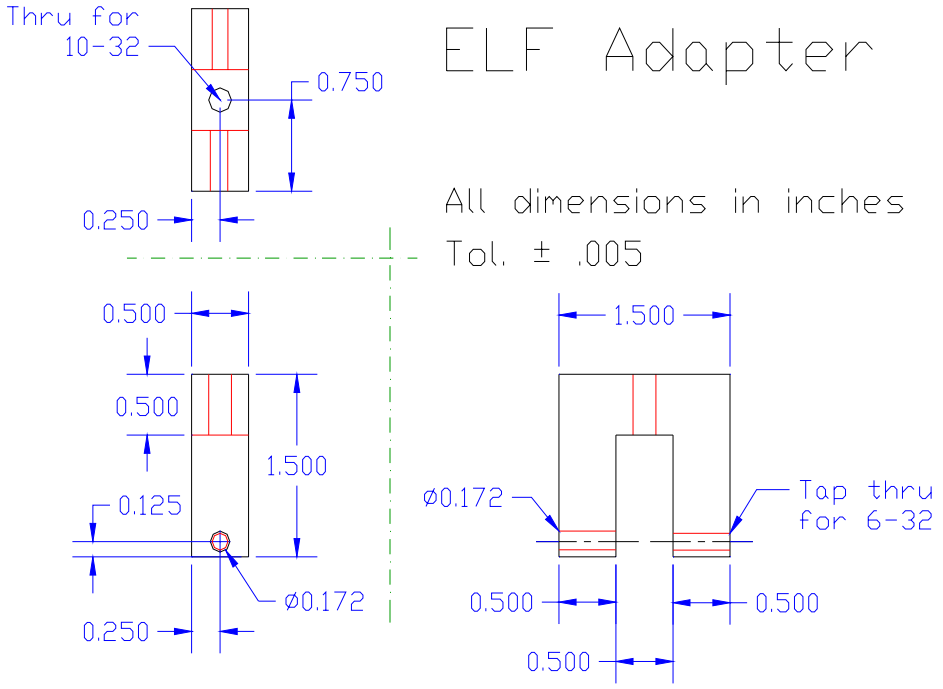

Figure B.1 Tensile mechanical test adapter to interface hydrogel constructs with the EnduraTEC ELF 3200 testing frame.

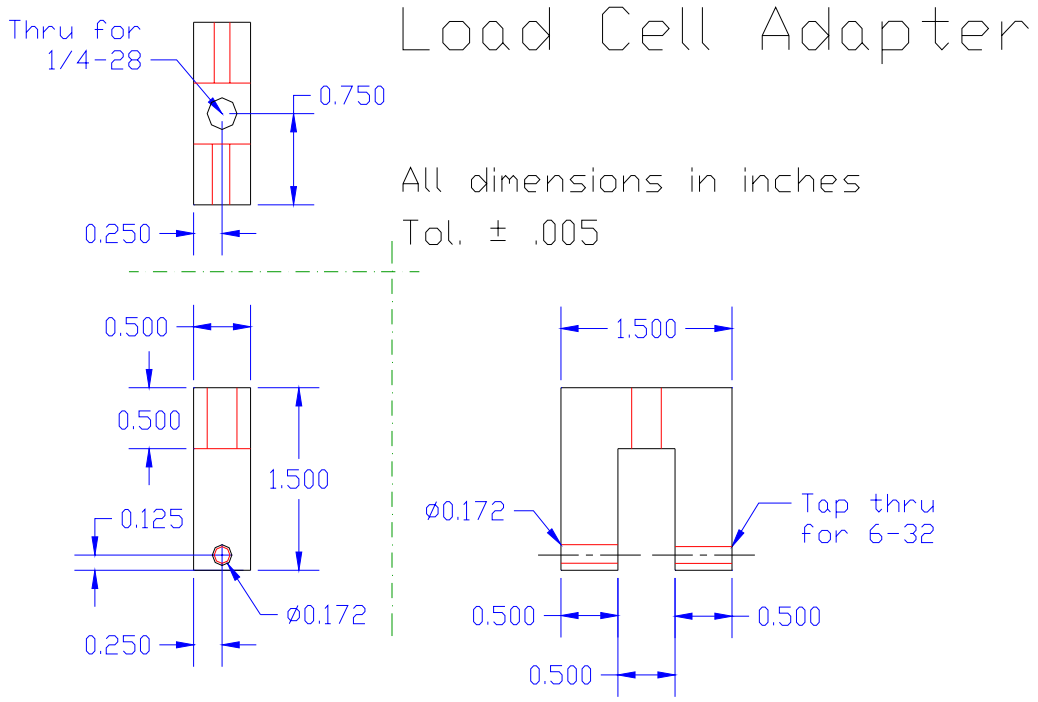

Figure B.2 Tensile mechanical test adapter to interface hydrogel constructs with the Interface SMT load cell.

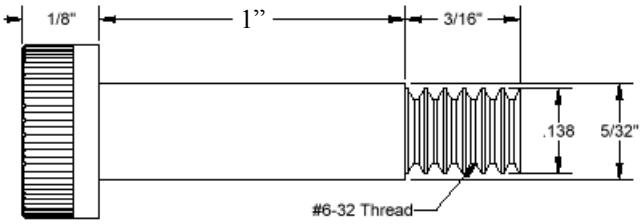

Figure B.3 Custom shoulder screws to interface the hydrogel constructs with the tensile mechanical test adapters. Drawing adapted from McMaster-Carr.

B.2 Tensile Mechanical Test Adapters Use Procedures

Custom designed adapters for the tensile mechanical tests were necessary because commercially available "grip" adapters did not allow for accurate or repeatable positioning of the hydrogel constructs in the EnduraTEC ELF 3200 testing frame. Using the "grip" adapters would have introduced a greater degree of experimental error due to the potential for misalignment of the hydrogel construct as well as the need to adjust the grips for each individual test. Therefore, simple yet highly practical adapters were designed, manufactured, and used for all tensile mechanical tests described in Chapter 7.

The ELF interface adapter (Figure B.1) was attached to the actuator of the ELF 3200 test frame with a single 10-32 stainless steel socket head cap screw via the through hole in the base of the adapter. The Load Cell interface adapter (Figure B.2) was attached to the Interface SMT series load cell using a 1/4-20 stainless steel socket head cap screw via the through hole in the base of the adapter. Attaching the adapters using a single screw was an important design feature, because it allowed the adapters to be properly aligned with respect to one another. The screws were first hand tightened and then secured with an Allen wrench, being carefully not to over-tighten and potentially damage the load cell.

Two custom shoulder screws were used to interface the hydrogel constructs with the tensile mechanical test adapters (Figure B.3). These shoulder screws had a 6-32 thread and a 1-inch long shoulder. To attach the hydrogel construct, one shoulder screw was slid into the through hole of the ELF adapter, through the hole in the end block of a hydrogel construct, and then tightened into the threaded hole in the ELF adapter. The hydrogel construct was then centered and positioned vertically in the adapter. The load

cell and Load Cell adapter were attached to a mechanical stroke adapter, which was positioned to align the through and threaded holes in the Load Cell adapter with the hole in the lower end block of the hydrogel construct. The second shoulder screw was then fed through the adapter, the end block, and secured into the threaded hole in the Load Cell adapter. Finally, the actuator on the ELF 3200 was positioned such that the hydrogel construct was in a zero deformation state prior to the start of the test.

APPENDIX C

LABORATORY PROTOCOLS

C.1 Western Blotting Procedure

C.1.1 Sample Preparation

1. Either media samples or tissue extracts in 4M Guandine-HCl can be used in this procedure
2. Add 3 volumes of ice cold absolute ethanol with 5mM sodium acetate to portions of the samples containing at least 100 μg GAG by DMMB assay
3. Let samples stand at 4°C for at least 16 hours to precipitate proteoglycans
4. Centrifuge samples at 4°C at maximum speed
5. Remove and discard the ethanol supernatant, dry the pellet, and resuspend in chondroitinase buffer with protease inhibitors (typically 100 μL)
6. Remove the CS chains by digesting samples with 5 μL Chondroitinase ABC at 37 °C for 2-3 hours
7. Add 3 μL each of Keratinase I (endobetagalactosidase) and Keratinase II and incubate for at least another 2 hours at 37 °C (can be left overnight)
8. SpeedVac dry a portion of each sample that is equivalent to 10 μg of GAG according to the previous DMMB assay
9. Dissolve samples in electrophoresis sample buffer (Tris-Glycine, 3M Urea, DTT)

C.1.2 Gel Electrophoresis and Western Blotting Procedure

1. Boil samples for 4 minutes to separate structures prior to loading
2. Load samples into the lanes of a Novex 4-12% gel in electrode buffer at 200 volts for 40 minutes at room temperature
3. Transfer proteins to nitrocellulose membrane in transfer buffer at 30 volts for 90 minutes on ice
4. Rinse in TBS-TWEEN for 5 minutes on rocker plate

5. Block membrane for 30 minutes at room temperature on rocker plate in blocking buffer (800 mg non-fat dry mile in 80 mL TBS-TWEEN)
6. Incubate membranes with primary antibody solutions (1:1000 dilution in Blotto with TWEEN) overnight at 4 °C on rocker plate
7. Wash 3 x 5 minutes in TBS-TWEEN at room temperature
8. Incubate for 1 hour at room temperature in secondary antibody solution (1:10,000 in Blotto with TWEEN) on rocker plate
9. Wash 3 x 5 minutes in TBS-TWEEN
10. Develop membrane with ECF for 5 minutes
11. Scan on Fuji Phosphoimager

C.2 RT-PCR Procedures

C.2.1 RNA Isolation from Fibrin Hydrogels

1. Dissociate fibrin hydrogels in a small volume of RLT buffer plus β-mercaptoethanol (~300 μL) at 60°C for 10-15 minutes
2. Either proceed with RNA isolation below or store samples at -80°C
3. Add 1 mL Trizol reagent and incubate at room temperature for 15 minutes
4. Centrifuge at 12000 x g for 10 minutes
5. Transfer the supernatant to a new tube and discard the pellet
6. Add 200 μL of chloroform and vortex well
7. Centrifuge at 12000 x g for 15 minutes. The mixture will separate into a red organic phase, a white interphase, and a clear aqueous phase, containing the nucleic acids.
8. Pipette the aqueous phase to a new tube being careful not to mix the phases.
9. Precipitate the RNA with 500 μL of isopropyl alcohol
10. Incubate at room temperature for 10 minutes
11. Centrifuge at 12000 x g for 10 minutes
12. Discard the supernatant and resuspend the pellet in 350 μL of RLT buffer
13. Continue with the RNeasy isolation protocol for animal tissues, including homogenization with the QIAshredder

Qiagen RNeasy Isolation Protocol

1. Pipette cell lysate directly onto a QIAshredder spin column placed in a 2 mL collection tube, and centrifuge for 2 minutes at maximum speed
2. Add one volume (usually 350 or 600 μL) of 70% ethanol to the homogenized lysate, and mix well by pipetting. Do not centrifuge
3. Apply up to 700 μL of the sample, including any precipitate that may have formed, to an RNeasy mini column placed in a 2 mL collection tube. Close the tube gently, and centrifuge for 15 seconds at ≥8000 x g. Discard the flow-through
4. Add 700 μL Buffer RW1 to the RNeasy column. Close the tube gently, and centrifuge for 15 seconds at ≥8000 x g to wash the column. Discard the flow-through and collection tube
5. Transfer the RNeasy column into a new 2 mL collection tube. Pipette 500 μL Buffer RPE onto the TNeasy colun. Close the tube gently, and centrifuge for 15 seconds at ≥8000 x g to wash the column. Discard the flow-through
6. Add another 500 μL Buffer RPE to the RNeasy column. Close the tube gently, and centrifuge for 2 minutes at ≥8000 x g to dry the RNeasy silica-gel membrane
7. To elute, transfer the RNeasy column to a new 1.5 mL collection tube. Pipette 30 μL RNase-free water directly onto the RNeasy silica-gel membrane. Close the tube gently, and centrifuge for 1 minute at ≥8000 x g to elute.
8. Repeat the elution step as described with a second volume of RNase-free water. Elute into the same collection tube

Measuring RNA Quantity

1. After eluting the RNA from the RNeasy columns, take 5 μL and dilute 1:20 into 100 μL of RNase-free water in a fresh tube
2. Store the remaining RNA at -80°C
3. Read the absorbance of each sample at 260 and 280 nm with the UV spectrophotometer
4. Total RNA = OD_{260} * 43μg/mL/OD * 20 * 0.055 mL
5. The ideal 260:280 ratio is 1.8-2.0; lower ratios indicate protein contamination

C.2.2 Reverse Transcription to cDNA

1. Take a volume from each sample equal to 1 μg of total RNA and transfer to a new tube

2. If the volume is less than 9.75 μL, bring the volume up to 9.75 μL with RNase-free water. If the volume is great than 9.75 μL, speedvac the samples until all the volume has been evaporated and resuspend in 9.75 μL of water
3. Incubate the samples at 70°C for 10 minutes to remove secondary structures
4. While the samples are incubating, prepare the RT-master mix in a new tube

   Volumes per reaction:

$MgCl_2$	4 μL
RT 10x Buffer	2 μL
DNTPs	2 μL
Oligo dT primers	1 μL
RNasin	0.5 μL

   * make enough total volume for each sample plus 2 extra; keep everything on ice
5. Transfer the samples to room temperature for 2 minutes
6. While the vials are cooling add enough AMV reverse transcriptase to the master mix for 0.75 μL per reaction plus 2 extras
7. Add 10.25 μL to each sample and centrifuge briefly to collect the reaction mix
8. Incubate the samples at 42 °C for 60 minutes
9. Incubate the samples at 90 °C for 5 minutes
10. Transfer to ice for 5 minutes
11. Add 30 μL to each sample to bring the total volume to 50 μL
12. cDNA samples can be store at -20 °C

C.2.3 Real Time RT-PCR Procedure

1. Thaw cDNA samples, standards, and primers; pulse spin to collect material
2. Prepare qPCR reaction solution for a 50 μL reaction volume per sample

AP Biosystems Master Mix	25 μL
100 μM forward primer	0.125 μL
100 μM reverse primer	0.125 μL
Nuclease free water	23.75 μL

3. Arrange strip tubes in 96-well set up plate
4. Add 49 μL of reaction solution to each tube

5. Add 1 μL of each sample or standard to the tubes, being careful not to contact the reaction solution with the pipette tip (also add 1 μL water to at least 2 tubes for a no template control)
6. Close tubes with optical strip caps and ensure each cap fit securely
7. Briefly centrifuge plate to collect all solutions
8. Perform the real time RT-PCR reaction with ABI 7700 Sequence Detector

C.3 Histological Staining Procedures

C.3.1 Safranin-O Staining

1. Samples should be formalin-fixed, paraffin embedded, and sectioned to 4 μm
2. Deparaffinize and rehydrate samples in water
3. Rinse with deionized water for 1 minute
4. Incubate in Weigert's hematoxylin working solution (Sigma, HT10-79) for 5 seconds
5. Rinse in running tap water for 2 minutes
6. Dip once in 1% acid alcohol (glacial acetic acid in 70% ethanol)
7. Rinse in runner tap water for 2 minutes
8. Incubate in 0.2% aqueous fast green (Fast Green C.I. 42053 in distilled water) for 1 minute
9. Rinse in 1% acetic acid for 3 seconds
10. Incubate in 0.1% Safranin-O (Safranin-O C.I. 50240 in distilled water) for 5 minutes
11. Wash sections in 95% alcohol for 1 minute each
12. Dehydrate in reagent alcohol, 3 times for 1 minute each
13. Clear in xylene, twice for 1 minute each
14. Mount with synthetic resin and allow slides to dry in chemical fume hood

This procedure results in red-orange GAGs, black nuclei, and green cytoplasm

C.3.2 Picrosirius Red Staining

1. Samples should be formalin-fixed, paraffin embedded, and sectioned to 4 μm

2. Deparaffinize and rehydrate samples in water
3. Incubate in Weigert's hematoxylin working solution (Sigma, HT10-79) for 5 seconds
4. Rinse in running tap water for 10 minutes
5. Incubate in picro-sirius red (1mg/mL Sirius red F3B C.I. 35782 in saturated aqueous picric acid) for 60 minutes at room temperature
6. Wash in 2 changes of acidified water (5mL/L glacial acetic acid in distilled water)
7. Dehydrate in 3 changes of 100% ethanol, 1 minute each
8. Clear in xylene, twice for 1 minute each
9. Mount with synthetic resin and allow slides to dry in chemical fume hood

This procedure results in red collagen and black nuclei; under polarized light, larger more organized collagen fibers appear bright yellow/orange and thinner collagen fibers an reticulin appear green

APPENDIX D

MATERIALS AND SUPPLIES

Product	Vendor	Location
α-collagen I primary antibody	AbCam	Cambridge, MA
α-collagen II primary antibody	AbCam	Cambridge, MA
α-collagen VI primary antibody	AbCam	Cambridge, MA
SYBR Green Master Mix	Applied Biosystems	Foster City, CA
1.0 x 30 cm Econocolumns	BioRad	Hercules, CA
Chondroitinase ABC	Calbiochem	La Jolla, CA
Protease Inhibitor Cocktail Set I	Calbiochem	La Jolla, CA
T-75 Tissue culture flasks	Corning	Corning, NY
Proteinase K	EMD Chemicals	Gibbstown, NJ
β-Mercaptoethanol	EMD Chemicals	Gibbstown, NJ
24-well Tissue culture plates	Falcon	Franklin Lakes, CA
#22 Scalpel Blades	Fisher Scientific	Pittsburgh, PA
10% Neutral Buffered Formalin	Fisher Scientific	Pittsburgh, PA
Sodium Dodecyl Sulfate (SDS)	Fisher Scientific	Pittsburgh, PA
Sodium Sulfate	Fisher Scientific	Pittsburgh, PA
Tris Acetate	Fisher Scientific	Pittsburgh, PA
Triton X-100	Fisher Scientific	Pittsburgh, PA
Hi-Trap Sephadex G-25 Superfine Desalting Column	GE Healthcare	Piscataway, NJ
L-5-^{3}H-proline	GE Healthcare (Amersham)	Piscataway, NJ
Fetal Bovine Serum (FBS)	Hyclone	Logan, UT
Porous Polyethylene (POR-4898)	Interstate Specialty Products	Leicester, MA
4',6-Diamidino-2-phenylindole (DAPI)	Invitrogen (Molecular Probes)	Carlsbad, CA

Product	Vendor	Location
AlexaFluor 488 Goat α-Rabbit IgG secondary antibody	Invitrogen (Molecular Probes)	Carlsbad, CA
AlexaFluor 546 Phalliodin	Invitrogen (Molecular Probes)	Carlsbad, CA
AlexaFluor 594 Goat α-Mouse IgG secondary antibody	Invitrogen (Molecular Probes)	Carlsbad, CA
Antibiotic/Antimycotic	Invitrogen	Carlsbad, CA
Collagenase Type II	Invitrogen	Carlsbad, CA
Forward and Reverse PCR primers	Invitrogen	Carlsbad, CA
Fungizone (Amphotericin B)	Invitrogen	Carlsbad, CA
Gentamicin	Invitrogen	Carlsbad, CA
HEPES Buffer	Invitrogen	Carlsbad, CA
High Glucose Dulbecco's Modified Eagle's Medium (DMEM)	Invitrogen	Carlsbad, CA
Kanamycin Sulfate	Invitrogen	Carlsbad, CA
LIVE/DEAD Assay Kit	Invitrogen (Molecular Probes)	Carlsbad, CA
Non-essential amino acids (NEAA)	Invitrogen	Carlsbad, CA
Penicillin-Streptomycin-Neomycin	Invitrogen	Carlsbad, CA
Phosphate Buffered Saline (PBS)	Invitrogen	Carlsbad, CA
α-Aggrecan-G1 primary antibody	John D. Sandy, PhD	Tampa Bay, FL
α-Aggrecan-G3 primary antibody	John D. Sandy, PhD	Tampa Bay, FL
α-Aggrecan-NITEGE primary antibody	John D. Sandy, PhD	Tampa Bay, FL
Isopentane	JT Baker	Phillipsburg, NJ
Urea	JT Baker	Phillipsburg, NJ
α-Biglycan primary antibody	Larry W. Fisher, PhD	Bethesda, MD
α-Decorin primary antibody	Larry W. Fisher, PhD	Bethesda, MD
Red FDA rubber	McMaster Carr	Atlanta, GA
Amicon Ultra-4 Centrifugal Filter	Millipore	Billerica, MA
4 mm Dermal Biopsy Punch	Miltex	York, PA
6 mm Dermal Biopsy Punch	Miltex	York, PA
^{35}S-Sodium Sulfate	MP Biomedicals	Irvine, CA
Bovine Thrombin	MP Biomedicals	Irvine, CA
Ecolume	MP Biomedicals	Irvine, CA
Sucrose	MP Biomedicals	Irvine, CA
8-well Tissue culture plates	Nalgene Nunc	Rochester, NY

Product	Vendor	Location
Polystyrene Beads	Polysciences	Warrington, PA
Promega Reverse Transcription Kit	Promega	Madison, WI
Qiagen Qiashredders	Qiagen	Valencia, CA
Qiagen RNeasy Mini Kit	Qiagen	Valencia, CA
Immature Bovine Stifle Joints	Research 87	Marlborough, MA
Acetone	Richard-Allan Scientific	Kalamazoo, MI
Tissue Tec OCT Freezing Compound	Sakura	Tokyo, Japan
Keratinase II	Seikagaku Corporation	Tokyo, Japan
Guanidine-HCl	Shelton Scientific	Shelton, CT
1,9-Dimethylmethlyene Blue	Sigma	St. Louis, MO
Absolute Ethanol	Sigma	St. Louis, MO
Ammonium Acetate	Sigma	St. Louis, MO
Bovine Fibrinogen	Sigma	St. Louis, MO
Bovine Serum Albumin (BSA)	Sigma	St. Louis, MO
Calf Thymus DNA	Sigma	St. Louis, MO
Chondroitin Sulfate	Sigma	St. Louis, MO
Glycine	Sigma	St. Louis, MO
Hoechst 33258	Sigma	St. Louis, MO
Keratinase I	Sigma	St. Louis, MO
L-ascorbic acid	Sigma	St. Louis, MO
L-proline	Sigma	St. Louis, MO
Non-immune Mouse IgG	Sigma	St. Louis, MO
Non-immune Rabbit IgG	Sigma	St. Louis, MO
Normal Goat Serum	Sigma	St. Louis, MO
Safranin O	Sigma	St. Louis, MO
Sepharose CL-4B	Sigma	St. Louis, MO
Sirius Red F3B	Sigma	St. Louis, MO
Sodium Acetate	Sigma	St. Louis, MO
Sodium Chloride	Sigma	St. Louis, MO
Tris Base	Sigma	St. Louis, MO
TWEEN-20	Sigma	St. Louis, MO
ε-aminocaproic acid	Sigma	St. Louis, MO
74 μm Mesh Filter Paper	Small Parts, Inc.	Miami Lakes, FL

Product	Vendor	Location
Sequenza Staining Racks/Coverslips	Thermo Electron	Waltham, MA
No. 12 Razor Blades	VWR Scientific	West Chester, PA

REFERENCES

1. Buckwalter,J.A., Saltzman,C. & Brown,T. The impact of osteoarthritis: implications for research. *Clin. Orthop Relat Res.* S6-15 (2004).

2. Roos,H., Adalberth,T., Dahlberg,L. & Lohmander,L.S. Osteoarthritis of the knee after injury to the anterior cruciate ligament or meniscus: the influence of time and age. *Osteoarthritis. Cartilage.* 3, 261-267 (1995).

3. Hough,A.J., Jr. & Webber,R.J. Pathology of the meniscus. *Clin. Orthop.* 32-40 (1990).

4. Sweigart,M.A. & Athanasiou,K.A. Toward tissue engineering of the knee meniscus. *Tissue Eng* 7, 111-129 (2001).

5. Mauck,R.L., Soltz,M.A., Wang,C.C., Wong,D.D., Chao,P.H., Valhmu,W.B., Hung,C.T. & Ateshian,G.A. Functional tissue engineering of articular cartilage through dynamic loading of chondrocyte-seeded agarose gels. *J. Biomech. Eng* 122, 252-260 (2000).

6. Poole,A.R., Kojima,T., Yasuda,T., Mwale,F., Kobayashi,M. & Laverty,S. Composition and structure of articular cartilage: a template for tissue repair. *Clin. Orthop Relat Res.* S26-S33 (2001).

7. Buckwalter,J.A. & Mankin,H.J. Articular cartilage: tissue design and chondrocyte-matrix interactions. *Instr. Course Lect.* 47, 477-486 (1998).

8. Roth,V. & Mow,V.C. The intrinsic tensile behavior of the matrix of bovine articular cartilage and its variation with age. *J. Bone Joint Surg. Am.* 62, 1102-1117 (1980).

9. Akizuki,S., Mow,V.C., Muller,F., Pita,J.C., Howell,D.S. & Manicourt,D.H. Tensile properties of human knee joint cartilage: I. Influence of ionic conditions, weight bearing, and fibrillation on the tensile modulus. *J. Orthop Res.* 4, 379-392 (1986).

10. Kempson,G.E., Muir,H., Pollard,C. & Tuke,M. The tensile properties of the cartilage of human femoral condyles related to the content of collagen and glycosaminoglycans. *Biochim. Biophys. Acta* 297, 456-472 (1973).

11. Roughley,P.J. & Lee,E.R. Cartilage proteoglycans: structure and potential functions. *Microsc. Res. Tech.* 28, 385-397 (1994).

12. Hardingham,T.E. & Fosang,A.J. Proteoglycans: many forms and many functions. *FASEB J.* 6, 861-870 (1992).

13. Bayliss,M.T., Venn,M., Maroudas,A. & Ali,S.Y. Structure of proteoglycans from different layers of human articular cartilage. *Biochem. J.* 209, 387-400 (1983).

14. Bayliss,M.T., Osborne,D., Woodhouse,S. & Davidson,C. Sulfation of chondroitin sulfate in human articular cartilage. The effect of age, topographical position, and zone of cartilage on tissue composition. *J. Biol. Chem.* 274, 15892-15900 (1999).

15. Zanetti,M., Ratcliffe,A. & Watt,F.M. Two subpopulations of differentiated chondrocytes identified with a monoclonal antibody to keratan sulfate. *J. Cell Biol.* 101, 53-59 (1985).

16. Buckwalter,J.A. & Rosenberg,L.C. Electron microscopic studies of cartilage proteoglycans. Direct evidence for the variable length of the chondroitin sulfate-rich region of proteoglycan subunit core protein. *J. Biol. Chem.* 257, 9830-9839 (1982).

17. Buckwalter,J.A. & Rosenberg,L. Structural changes during development in bovine fetal epiphyseal cartilage. *Coll. Relat Res.* 3, 489-504 (1983).

18. Venn,M.F. Variation of chemical composition with age in human femoral head cartilage. *Ann. Rheum. Dis.* 37, 168-174 (1978).

19. Poole,A.R., Webber,C., Pidoux,I., Choi,H. & Rosenberg,L.C. Localization of a dermatan sulfate proteoglycan (DS-PGII) in cartilage and the presence of an immunologically related species in other tissues. *J. Histochem. Cytochem.* 34, 619-625 (1986).

20. Poole,A.R., Rosenberg,L.C., Reiner,A., Ionescu,M., Bogoch,E. & Roughley,P.J. Contents and distributions of the proteoglycans decorin and biglycan in normal and osteoarthritic human articular cartilage. *J. Orthop Res.* 14, 681-689 (1996).

21. Schinagl,R.M., Gurskis,D., Chen,A.C. & Sah,R.L. Depth-dependent confined compression modulus of full-thickness bovine articular cartilage. *J. Orthop Res.* 15, 499-506 (1997).

22. Wong,M., Wuethrich,P., Eggli,P. & Hunziker,E. Zone-specific cell biosynthetic activity in mature bovine articular cartilage: a new method using confocal microscopic stereology and quantitative autoradiography. *J. Orthop Res.* 14, 424-432 (1996).

23. Schumacher,B.L., Hughes,C.E., Kuettner,K.E., Caterson,B. & Aydelotte,M.B. Immunodetection and partial cDNA sequence of the proteoglycan, superficial zone protein, synthesized by cells lining synovial joints. *J. Orthop Res.* 17, 110-120 (1999).

24. Keene,D.R., Engvall,E. & Glanville,R.W. Ultrastructure of type VI collagen in human skin and cartilage suggests an anchoring function for this filamentous network. *J. Cell Biol.* 107, 1995-2006 (1988).

25. Bidanset,D.J., Guidry,C., Rosenberg,L.C., Choi,H.U., Timpl,R. & Hook,M. Binding of the proteoglycan decorin to collagen type VI. *J. Biol. Chem.* 267, 5250-5256 (1992).

26. Aydelotte,M.B., Greenhill,R.R. & Kuettner,K.E. Differences between sub-populations of cultured bovine articular chondrocytes. II. Proteoglycan metabolism. *Connect. Tissue Res.* 18, 223-234 (1988).

27. Schmidt,T.A., Schumacher,B.L., Klein,T.J., Voegtline,M.S. & Sah,R.L. Synthesis of proteoglycan 4 by chondrocyte subpopulations in cartilage explants, monolayer cultures, and resurfaced cartilage cultures. *Arthritis Rheum.* 50, 2849-2857 (2004).

28. Darling,E.M. & Athanasiou,K.A. Rapid phenotypic changes in passaged articular chondrocyte subpopulations. *J. Orthop Res.* 23, 425-432 (2005).

29. Siczkowski,M. & Watt,F.M. Subpopulations of chondrocytes from different zones of pig articular cartilage. Isolation, growth and proteoglycan synthesis in culture. *J. Cell Sci.* 97 (Pt 2), 349-360 (1990).

30. Darling,E.M., Hu,J.C. & Athanasiou,K.A. Zonal and topographical differences in articular cartilage gene expression. *J. Orthop Res.* 22, 1182-1187 (2004).

31. Sandy,J.D. & Verscharen,C. Analysis of aggrecan in human knee cartilage and synovial fluid indicates that aggrecanase (ADAMTS) activity is responsible for the catabolic turnover and loss of whole aggrecan whereas other protease activity is required for C-terminal processing in vivo. *Biochem. J.* 358, 615-626 (2001).

32. Felson,D.T., Zhang,Y., Hannan,M.T., Naimark,A., Weissman,B.N., Aliabadi,P. & Levy,D. The incidence and natural history of knee osteoarthritis in the elderly. The Framingham Osteoarthritis Study. *Arthritis Rheum.* 38, 1500-1505 (1995).

33. Oliveria,S.A., Felson,D.T., Reed,J.I., Cirillo,P.A. & Walker,A.M. Incidence of symptomatic hand, hip, and knee osteoarthritis among patients in a health maintenance organization. *Arthritis Rheum.* 38, 1134-1141 (1995).

34. Cooper,C., Inskip,H., Croft,P., Campbell,L., Smith,G., McLaren,M. & Coggon,D. Individual risk factors for hip osteoarthritis: obesity, hip injury, and physical activity. *Am. J. Epidemiol.* 147, 516-522 (1998).

35. Gelber,A.C., Hochberg,M.C., Mead,L.A., Wang,N.Y., Wigley,F.M. & Klag,M.J. Joint injury in young adults and risk for subsequent knee and hip osteoarthritis. *Ann. Intern. Med.* 133, 321-328 (2000).

36. Croft,P., Cooper,C., Wickham,C. & Coggon,D. Osteoarthritis of the hip and occupational activity. *Scand. J. Work Environ. Health* 18, 59-63 (1992).

37. Anderson,J.J. & Felson,D.T. Factors associated with osteoarthritis of the knee in the first national Health and Nutrition Examination Survey (HANES I). Evidence for an association with overweight, race, and physical demands of work. *Am. J. Epidemiol.* 128, 179-189 (1988).

38. Felson,D.T., Hannan,M.T., Naimark,A., Berkeley,J., Gordon,G., Wilson,P.W. & Anderson,J. Occupational physical demands, knee bending, and knee osteoarthritis: results from the Framingham Study. *J. Rheumatol.* 18, 1587-1592 (1991).

39. Buckwalter,J.A. Osteoarthritis and articular cartilage use, disuse, and abuse: experimental studies. *J. Rheumatol. Suppl* 43, 13-15 (1995).

40. Lohmander,L.S., Dahlberg,L., Ryd,L. & Heinegard,D. Increased levels of proteoglycan fragments in knee joint fluid after injury. *Arthritis Rheum.* 32, 1434-1442 (1989).

41. Sandy,J.D., Flannery,C.R., Neame,P.J. & Lohmander,L.S. The structure of aggrecan fragments in human synovial fluid. Evidence for the involvement in osteoarthritis of a novel proteinase which cleaves the Glu 373-Ala 374 bond of the interglobular domain. *J. Clin. Invest* 89, 1512-1516 (1992).

42. Alford,J.W. & Cole,B.J. Cartilage restoration, part 1: basic science, historical perspective, patient evaluation, and treatment options. *Am. J. Sports Med.* 33, 295-306 (2005).

43. Baumgaertner,M.R., Cannon,W.D., Jr., Vittori,J.M., Schmidt,E.S. & Maurer,R.C. Arthroscopic debridement of the arthritic knee. *Clin. Orthop Relat Res.* 197-202 (1990).

44. Moseley,J.B., O'Malley,K., Petersen,N.J., Menke,T.J., Brody,B.A., Kuykendall,D.H., Hollingsworth,J.C., Ashton,C.M. & Wray,N.P. A controlled trial of arthroscopic surgery for osteoarthritis of the knee. *N. Engl. J. Med.* 347, 81-88 (2002).

45. Goldberg,V.M. & Caplan,A.I. Biologic restoration of articular surfaces. *Instr. Course Lect.* 48, 623-627 (1999).

46. Steadman,J.R., Rodkey,W.G. & Rodrigo,J.J. Microfracture: surgical technique and rehabilitation to treat chondral defects. *Clin. Orthop Relat Res.* S362-S369 (2001).

47. Alford,J.W. & Cole,B.J. Cartilage restoration, part 2: techniques, outcomes, and future directions. *Am. J. Sports Med.* 33, 443-460 (2005).

48. Yamashita,F., Sakakida,K., Suzu,F. & Takai,S. The transplantation of an autogeneic osteochondral fragment for osteochondritis dissecans of the knee. *Clin. Orthop Relat Res.* 43-50 (1985).

49. Matsusue,Y., Yamamuro,T. & Hama,H. Arthroscopic multiple osteochondral transplantation to the chondral defect in the knee associated with anterior cruciate ligament disruption. *Arthroscopy* 9, 318-321 (1993).

50. Cain,E.L. & Clancy,W.G. Treatment algorithm for osteochondral injuries of the knee. *Clin. Sports Med.* 20, 321-342 (2001).

51. Brittberg,M., Lindahl,A., Nilsson,A., Ohlsson,C., Isaksson,O. & Peterson,L. Treatment of deep cartilage defects in the knee with autologous chondrocyte transplantation. *N. Engl. J. Med.* 331, 889-895 (1994).

52. Bentley,G., Biant,L.C., Carrington,R.W., Akmal,M., Goldberg,A., Williams,A.M., Skinner,J.A. & Pringle,J. A prospective, randomised comparison of autologous chondrocyte implantation versus mosaicplasty for osteochondral defects in the knee. *J. Bone Joint Surg. Br.* 85, 223-230 (2003).

53. Langer,R. & Vacanti,J.P. Tissue engineering. *Science* 260, 920-926 (1993).

54. Nerem,R.M. Cellular engineering. *Ann. Biomed. Eng* 19, 529-545 (1991).

55. Benjamin,M., Qin,S. & Ralphs,J.R. Fibrocartilage associated with human tendons and their pulleys. *J. Anat.* 187 (Pt 3), 625-633 (1995).

56. Shrive,N.G., O'Connor,J.J. & Goodfellow,J.W. Load-bearing in the knee joint. *Clin. Orthop* 279-287 (1978).

57. Ghosh,P. & Taylor,T.K. The knee joint meniscus. A fibrocartilage of some distinction. *Clin. Orthop.* 52-63 (1987).

58. Fithian,D.C., Kelly,M.A. & Mow,V.C. Material properties and structure-function relationships in the menisci. *Clin. Orthop.* 19-31 (1990).

59. Eyre,D.R. & Muir,H. The distribution of different molecular species of collagen in fibrous, elastic and hyaline cartilages of the pig. *Biochem. J.* 151, 595-602 (1975).

60. McDevitt,C.A. & Webber,R.J. The ultrastructure and biochemistry of meniscal cartilage. *Clin. Orthop.* 8-18 (1990).

61. Petersen,W. & Tillmann,B. Age-related blood and lymph supply of the knee menisci. A cadaver study. *Acta Orthop Scand.* 66, 308-312 (1995).

62. Petersen,W. & Tillmann,B. Collagenous fibril texture of the human knee joint menisci. *Anat. Embryol. (Berl)* 197, 317-324 (1998).

63. Skaggs,D.L., Warden,W.H. & Mow,V.C. Radial tie fibers influence the tensile properties of the bovine medial meniscus. *J. Orthop Res.* 12, 176-185 (1994).

64. Kambic,H.E. & McDevitt,C.A. Spatial organization of types I and II collagen in the canine meniscus. *J. Orthop Res.* 23, 142-149 (2005).

65. Wu,J.J., Eyre,D.R. & Slayter,H.S. Type VI collagen of the intervertebral disc. Biochemical and electron-microscopic characterization of the native protein. *Biochem. J.* 248, 373-381 (1987).

66. McNicol,D. & Roughley,P.J. Extraction and characterization of proteoglycan from human meniscus. *Biochem. J.* 185, 705-713 (1980).

67. Roughley,P.J., McNicol,D., Santer,V. & Buckwalter,J. The presence of a cartilage-like proteoglycan in the adult human meniscus. *Biochem. J.* 197, 77-83 (1981).

68. Roughley,P.J. & White,R.J. The dermatan sulfate proteoglycans of the adult human meniscus. *J. Orthop Res.* 10, 631-637 (1992).

69. Nakano,T., Dodd,C.M. & Scott,P.G. Glycosaminoglycans and proteoglycans from different zones of the porcine knee meniscus. *J. Orthop. Res.* 15, 213-220 (1997).

70. Tanaka,T., Fujii,K. & Kumagae,Y. Comparison of biochemical characteristics of cultured fibrochondrocytes isolated from the inner and outer regions of human meniscus. *Knee. Surg. Sports Traumatol. Arthrosc.* 7, 75-80 (1999).

71. Spindler,K.P., Miller,R.R., Andrish,J.T. & McDevitt,C.A. Comparison of collagen synthesis in the peripheral and central region of the canine meniscus. *Clin. Orthop.* 256-263 (1994).

72. Webber,R.J., Harris,M.G. & Hough,A.J., Jr. Cell culture of rabbit meniscal fibrochondrocytes: proliferative and synthetic response to growth factors and ascorbate. *J. Orthop Res.* 3, 36-42 (1985).

73. Ghadially,F.N., Thomas,I., Yong,N. & Lalonde,J.M. Ultrastructure of rabbit semilunar cartilages. *J. Anat.* 125, 499-517 (1978).

74. Hellio Le Graverand,M.P., Ou,Y., Schield-Yee,T., Barclay,L., Hart,D., Natsume,T. & Rattner,J.B. The cells of the rabbit meniscus: their arrangement, interrelationship, morphological variations and cytoarchitecture. *J. Anat.* 198, 525-535 (2001).

75. Binfield,P.M., Maffulli,N. & King,J.B. Patterns of meniscal tears associated with anterior cruciate ligament lesions in athletes. *Injury* 24, 557-561 (1993).

76. Baker,B.E., Peckham,A.C., Pupparo,F. & Sanborn,J.C. Review of meniscal injury and associated sports. *Am. J. Sports Med.* 13, 1-4 (1985).

77. King,D. The healing of semilunar cartilages. 1936. *Clin. Orthop Relat Res.* 4-7 (1990).

78. Arnoczky,S.P. & Warren,R.F. The microvasculature of the meniscus and its response to injury. An experimental study in the dog. *Am. J. Sports Med.* 11, 131-141 (1983).

79. Boyd,K.T. & Myers,P.T. Meniscus preservation; rationale, repair techniques and results. *Knee.* 10, 1-11 (2003).

80. Roos,H., Lauren,M., Adalberth,T., Roos,E.M., Jonsson,K. & Lohmander,L.S. Knee osteoarthritis after meniscectomy: prevalence of radiographic changes after twenty-one years, compared with matched controls. *Arthritis Rheum.* 41, 687-693 (1998).

81. Cicuttini,F.M., Forbes,A., Yuanyuan,W., Rush,G. & Stuckey,S.L. Rate of knee cartilage loss after partial meniscectomy. *J. Rheumatol.* 29, 1954-1956 (2002).

82. Kurz,B., Lemke,A.K., Fay,J., Pufe,T., Grodzinsky,A.J. & Schunke,M. Pathomechanisms of cartilage destruction by mechanical injury. *Ann. Anat.* 187, 473-485 (2005).

83. Verdonk,P.C., Verstraete,K.L., Almqvist,K.F., De Cuyper,K., Veys,E.M., Verbruggen,G. & Verdonk,R. Meniscal allograft transplantation: long-term clinical results with radiological and magnetic resonance imaging correlations. *Knee. Surg. Sports Traumatol. Arthrosc.* 1-13 (2006).

84. Roeddecker,K., Muennich,U. & Nagelschmidt,M. Meniscal healing: a biomechanical study. *J. Surg. Res.* 56, 20-27 (1994).

85. Cima,L.G., Vacanti,J.P., Vacanti,C., Ingber,D., Mooney,D. & Langer,R. Tissue engineering by cell transplantation using degradable polymer substrates. *J. Biomech. Eng* 113, 143-151 (1991).

86. Mow,V.C., Ratcliffe,A., Rosenwasser,M.P. & Buckwalter,J.A. Experimental studies on repair of large osteochondral defects at a high weight bearing area of the knee joint: a tissue engineering study. *J. Biomech. Eng* 113, 198-207 (1991).

87. von der,M.K., Gauss,V., von der,M.H. & Muller,P. Relationship between cell shape and type of collagen synthesised as chondrocytes lose their cartilage phenotype in culture. *Nature* 267, 531-532 (1977).

88. Benya,P.D. & Shaffer,J.D. Dedifferentiated chondrocytes reexpress the differentiated collagen phenotype when cultured in agarose gels. *Cell* 30, 215-224 (1982).

89. Buschmann,M.D., Gluzband,Y.A., Grodzinsky,A.J., Kimura,J.H. & Hunziker,E.B. Chondrocytes in agarose culture synthesize a mechanically functional extracellular matrix. *J. Orthop Res.* 10, 745-758 (1992).

90. Guo,J.F., Jourdian,G.W. & MacCallum,D.K. Culture and growth characteristics of chondrocytes encapsulated in alginate beads. *Connect. Tissue Res.* 19, 277-297 (1989).

91. van Susante,J.L., Buma,P., van Osch,G.J., Versleyen,D., van der Kraan,P.M., van der Berg,W.B. & Homminga,G.N. Culture of chondrocytes in alginate and collagen carrier gels. *Acta Orthop Scand.* 66, 549-556 (1995).

92. Homminga,G.N., Buma,P., Koot,H.W., van der Kraan,P.M. & van den Berg,W.B. Chondrocyte behavior in fibrin glue in vitro. *Acta Orthop Scand.* 64, 441-445 (1993).

93. Hendrickson,D.A., Nixon,A.J., Erb,H.N. & Lust,G. Phenotype and biological activity of neonatal equine chondrocytes cultured in a three-dimensional fibrin matrix. *Am. J. Vet. Res.* 55, 410-414 (1994).

94. Webber,R.J., Zitaglio,T. & Hough,A.J., Jr. In vitro cell proliferation and proteoglycan synthesis of rabbit meniscal fibrochondrocytes as a function of age and sex. *Arthritis Rheum.* 29, 1010-1016 (1986).

95. Webber,R.J. & Hough,A.J., Jr. Cell culture of rabbit meniscal fibrochondrocytes II. Sulfated proteoglycan synthesis. *Biochimie* 70, 193-204 (1988).

96. Webber,R.J. In vitro culture of meniscal tissue. *Clin. Orthop Relat Res.* 114-120 (1990).

97. Isoda,K. & Saito,S. In vitro and in vivo fibrochondrocyte growth behavior in fibrin gel: an immunohistochemical study in the rabbit. *Am. J. Knee. Surg.* 11, 209-216 (1998).

98. Pangborn,C.A. & Athanasiou,K.A. Growth factors and fibrochondrocytes in scaffolds. *J. Orthop Res.* 23, 1184-1190 (2005).

99. Collier,S. & Ghosh,P. Effects of transforming growth factor beta on proteoglycan synthesis by cell and explant cultures derived from the knee joint meniscus. *Osteoarthritis. Cartilage.* 3, 127-138 (1995).

100. Buschmann,M.D., Gluzband,Y.A., Grodzinsky,A.J. & Hunziker,E.B. Mechanical compression modulates matrix biosynthesis in chondrocyte/agarose culture. *J. Cell Sci.* 108 (Pt 4), 1497-1508 (1995).

101. Jin,M., Frank,E.H., Quinn,T.M., Hunziker,E.B. & Grodzinsky,A.J. Tissue shear deformation stimulates proteoglycan and protein biosynthesis in bovine cartilage explants. *Arch. Biochem. Biophys.* 395, 41-48 (2001).

102. Waldman,S.D., Spiteri,C.G., Grynpas,M.D., Pilliar,R.M. & Kandel,R.A. Long-term intermittent shear deformation improves the quality of cartilaginous tissue formed in vitro. *J. Orthop Res.* 21, 590-596 (2003).

103. Vunjak-Novakovic,G., Martin,I., Obradovic,B., Treppo,S., Grodzinsky,A.J., Langer,R. & Freed,L.E. Bioreactor cultivation conditions modulate the composition and mechanical properties of tissue-engineered cartilage. *J. Orthop Res.* 17, 130-138 (1999).

104. Vunjak-Novakovic,G., Meinel,L., Altman,G. & Kaplan,D. Bioreactor cultivation of osteochondral grafts. *Orthod. Craniofac. Res.* 8, 209-218 (2005).

105. Saini,S. & Wick,T.M. Concentric cylinder bioreactor for production of tissue engineered cartilage: effect of seeding density and hydrodynamic loading on construct development. *Biotechnol. Prog.* 19, 510-521 (2003).

106. Gemmiti,C.V. & Guldberg,R.E. Fluid Flow Increases Type II Collagen Deposition and Tensile Mechanical Properties in Bioreactor-Grown Tissue-Engineered Cartilage. *Tissue Eng* 12, 469-479 (2006).

107. Chen,J., Yan,W. & Setton,L.A. Static compression induces zonal-specific changes in gene expression for extracellular matrix and cytoskeletal proteins in intervertebral disc cells in vitro. *Matrix Biol.* 22, 573-583 (2004).

108. Imler,S.M., Doshi,A.N. & Levenston,M.E. Combined effects of growth factors and static mechanical compression on meniscus explant biosynthesis. *Osteoarthritis Cartilage* 12, 736-744 (2004).

109. Upton,M.L., Chen,J., Guilak,F. & Setton,L.A. Differential effects of static and dynamic compression on meniscal cell gene expression. *J. Orthop Res.* 21, 963-969 (2003).

110. Agarwal,S., Long,P., Gassner,R., Piesco,N.P. & Buckley,M.J. Cyclic tensile strain suppresses catabolic effects of interleukin-1beta in fibrochondrocytes from the temporomandibular joint. *Arthritis Rheum.* 44, 608-617 (2001).

111. Deschner,J., Rath-Deschner,B. & Agarwal,S. Regulation of matrix metalloproteinase expression by dynamic tensile strain in rat fibrochondrocytes. *Osteoarthritis Cartilage* 14, 264-272 (2006).

112. Murphy,C.L. & Sambanis,A. Effect of oxygen tension on chondrocyte extracellular matrix accumulation. *Connect. Tissue Res.* 42, 87-96 (2001).

113. Malda,J., van den,B.P., Meeuwse,P., Grojec,M., Martens,D.E., Tramper,J., Riesle,J. & van Blitterswijk,C.A. Effect of oxygen tension on adult articular chondrocytes in microcarrier bioreactor culture. *Tissue Eng* 10, 987-994 (2004).

114. Kurz,B., Domm,C., Jin,M., Sellckau,R. & Schunke,M. Tissue engineering of articular cartilage under the influence of collagen I/III membranes and low oxygen tension. *Tissue Eng* 10, 1277-1286 (2004).

115. Bonassar,L.J., Grodzinsky,A.J., Frank,E.H., Davila,S.G., Bhaktav,N.R. & Trippel,S.B. The effect of dynamic compression on the response of articular cartilage to insulin-like growth factor-I. *J. Orthop Res.* 19, 11-17 (2001).

116. Jin,M., Emkey,G.R., Siparsky,P., Trippel,S.B. & Grodzinsky,A.J. Combined effects of dynamic tissue shear deformation and insulin-like growth factor I on chondrocyte biosynthesis in cartilage explants. *Arch. Biochem. Biophys.* 414, 223-231 (2003).

117. Saini,S. & Wick,T.M. Effect of low oxygen tension on tissue-engineered cartilage construct development in the concentric cylinder bioreactor. *Tissue Eng* 10, 825-832 (2004).

118. Messner,K. & Gao,J. The menisci of the knee joint. Anatomical and functional characteristics, and a rationale for clinical treatment. *J. Anat.* 193 (Pt 2), 161-178 (1998).

119. Chen,J., Akyuz,U., Xu,L. & Pidaparti,R.M. Stress analysis of the human temporomandibular joint. *Med. Eng Phys.* 20, 565-572 (1998).

120. Valiyaveettil,M., Mort,J.S. & McDevitt,C.A. The concentration, gene expression, and spatial distribution of aggrecan in canine articular cartilage, meniscus, and anterior and posterior cruciate ligaments: a new molecular distinction between hyaline cartilage and fibrocartilage in the knee joint. *Connect. Tissue Res.* 46, 83-91 (2005).

121. Kavanagh,E. & Ashhurst,D.E. Distribution of biglycan and decorin in collateral and cruciate ligaments and menisci of the rabbit knee joint. *J. Histochem. Cytochem.* 49, 877-885 (2001).

122. Melrose,J., Smith,S., Cake,M., Read,R. & Whitelock,J. Comparative spatial and temporal localisation of perlecan, aggrecan and type I, II and IV collagen in the ovine meniscus: an ageing study. *Histochem. Cell Biol.* 124, 225-235 (2005).

123. Naumann,A., Dennis,J.E., Awadallah,A., Carrino,D.A., Mansour,J.M., Kastenbauer,E. & Caplan,A.I. Immunochemical and mechanical characterization of cartilage subtypes in rabbit. *J. Histochem. Cytochem.* 50, 1049-1058 (2002).

124. Imler, S. M., Vanderploeg E.J., & Levenston, M. E., Differential behavior of fibrochondrocytes from different regions of the meniscus. *Trans ORS*. Washington, D.C. (2005).

125. Walker,P.S. & Erkman,M.J. The role of the menisci in force transmission across the knee. *Clin. Orthop Relat Res.* 184-192 (1975).

126. Krause,W.R., Pope,M.H., Johnson,R.J. & Wilder,D.G. Mechanical changes in the knee after meniscectomy. *J. Bone Joint Surg. Am.* 58, 599-604 (1976).

127. Kurosawa,H., Fukubayashi,T. & Nakajima,H. Load-bearing mode of the knee joint: physical behavior of the knee joint with or without menisci. *Clin. Orthop Relat Res.* 283-290 (1980).

128. Adams,M.E., Billingham,M.E. & Muir,H. The glycosaminoglycans in menisci in experimental and natural osteoarthritis. *Arthritis Rheum.* 26, 69-76 (1983).

129. Eyre,D.R. & Wu,J.J. Collagen of fibrocartilage: a distinctive molecular phenotype in bovine meniscus. *FEBS Lett.* 158, 265-270 (1983).

130. Sztrolovics,R., Alini,M., Roughley,P.J. & Mort,J.S. Aggrecan degradation in human intervertebral disc and articular cartilage. *Biochem. J.* 326 (Pt 1), 235-241 (1997).

131. Lee,V., Chen,L., Paiwand,F., Cao,L., Wu,Y., Inman,R., Adams,M.E. & Yang,B.B. Cleavage of the carboxyl tail from the G3 domain of aggrecan but not versican and identification of the amino acids involved in the degradation. *J. Biol. Chem.* 277, 22279-22288 (2002).

132. Vogel,K.G. & Peters,J.A. Histochemistry defines a proteoglycan-rich layer in bovine flexor tendon subjected to bending. *J. Musculoskelet. Neuronal. Interact.* 5, 64-69 (2005).

133. Vogel,K.G., Sandy,J.D., Pogany,G. & Robbins,J.R. Aggrecan in bovine tendon. *Matrix Biol.* 14, 171-179 (1994).

134. Koob,T.J. & Vogel,K.G. Site-related variations in glycosaminoglycan content and swelling properties of bovine flexor tendon. *J. Orthop Res.* 5, 414-424 (1987).

135. Felisbino,S.L. & Carvalho,H.F. Identification and distribution of type VI collagen in tendon fibrocartilages. *J. Submicrosc. Cytol. Pathol.* 31, 187-195 (1999).

136. Marcelino,J. & McDevitt,C.A. Attachment of articular cartilage chondrocytes to the tissue form of type VI collagen. *Biochim. Biophys. Acta* 1249, 180-188 (1995).

137. McDevitt,C.A., Miller,R.R. & Spindler,K.P. The Cells and Cell Matrix Interactions of the Meniscus. In: Mow,V.C., Arnoczky,S.P. & Jackson,D.W., editors. Knee Meniscus: Basic and Clincial Foundations. New York: Raven Press, Ltd., (1992).

138. McDevitt,C.A., Marcelino,J. & Tucker,L. Interaction of intact type VI collagen with hyaluronan. *FEBS Lett.* 294, 167-170 (1991).

139. Sah,R.L., Kim,Y.J., Doong,J.Y., Grodzinsky,A.J., Plaas,A.H. & Sandy,J.D. Biosynthetic response of cartilage explants to dynamic compression. *J. Orthop Res.* 7, 619-636 (1989).

140. Hunter,C.J., Mouw,J.K. & Levenston,M.E. Dynamic compression of chondrocyte-seeded fibrin gels: effects on matrix accumulation and mechanical stiffness. *Osteoarthritis Cartilage* 12, 117-130 (2004).

141. Cartmell,S.H., Porter,B.D., Garcia,A.J. & Guldberg,R.E. Effects of medium perfusion rate on cell-seeded three-dimensional bone constructs in vitro. *Tissue Eng* 9, 1197-1203 (2003).

142. Banes,A.J., Gilbert,J., Taylor,D. & Monbureau,O. A new vacuum-operated stress-providing instrument that applies static or variable duration cyclic tension or compression to cells in vitro. *J. Cell Sci.* 75, 35-42 (1985).

143. Cacou,C., Palmer,D., Lee,D.A., Bader,D.L. & Shelton,J.C. A system for monitoring the response of uniaxial strain on cell seeded collagen gels. *Med. Eng Phys.* 22, 327-333 (2000).

144. Eastwood,M., Mudera,V.C., McGrouther,D.A. & Brown,R.A. Effect of precise mechanical loading on fibroblast populated collagen lattices: morphological changes. *Cell Motil. Cytoskeleton* 40, 13-21 (1998).

145. Connelly,J.T., Vanderploeg,E.J. & Levenston,M.E. The influence of cyclic tension amplitude on chondrocyte matrix synthesis: experimental and finite element analyses. *Biorheology* 41, 377-387 (2004).

146. Andreatta,R.H., Liem,R.K. & Scheraga,H.A. Mechanism of action of thrombin on fibrinogen. I. Synthesis of fibrinogen-like peptides, and their proteolysis by thrombin and trypsin. *Proc. Natl. Acad. Sci. U. S. A* 68, 253-256 (1971).

147. Berg,J.M., Tymoczko,J.L. & Stryer,L. Biochemistry. W.H. Freeman and Company, New York (2002).

148. Grassl,E.D., Oegema,T.R. & Tranquillo,R.T. Fibrin as an alternative biopolymer to type-I collagen for the fabrication of a media equivalent. *J. Biomed. Mater. Res.* 60, 607-612 (2002).

149. Herbert,C.B., Bittner,G.D. & Hubbell,J.A. Effects of fibinolysis on neurite growth from dorsal root ganglia cultured in two- and three-dimensional fibrin gels. *J. Comp Neurol.* 365, 380-391 (1996).

150. Ye,Q., Zund,G., Benedikt,P., Jockenhoevel,S., Hoerstrup,S.P., Sakyama,S., Hubbell,J.A. & Turina,M. Fibrin gel as a three dimensional matrix in cardiovascular tissue engineering. *Eur. J. Cardiothorac. Surg.* 17, 587-591 (2000).

151. Cox,S., Cole,M. & Tawil,B. Behavior of human dermal fibroblasts in three-dimensional fibrin clots: dependence on fibrinogen and thrombin concentration. *Tissue Eng* 10, 942-954 (2004).

152. Mouw,J.K., Case,N.D., Guldberg,R.E., Plaas,A.H. & Levenston,M.E. Variations in matrix composition and GAG fine structure among scaffolds for cartilage tissue engineering. *Osteoarthritis Cartilage* 13, 828-836 (2005).

153. Ameer,G.A., Mahmood,T.A. & Langer,R. A biodegradable composite scaffold for cell transplantation. *J. Orthop. Res.* 20, 16-19 (2002).

154. van Susante,J.L., Buma,P., Schuman,L., Homminga,G.N., van den Berg,W.B. & Veth,R.P. Resurfacing potential of heterologous chondrocytes suspended in fibrin glue in large full-thickness defects of femoral articular cartilage: an experimental study in the goat. *Biomaterials* 20, 1167-1175 (1999).

155. Clark,R.A., Nielsen,L.D., Welch,M.P. & McPherson,J.M. Collagen matrices attenuate the collagen-synthetic response of cultured fibroblasts to TGF-beta. *J. Cell Sci.* 108 (Pt 3), 1251-1261 (1995).

156. Yee,K.O., Rooney,M.M., Giachelli,C.M., Lord,S.T. & Schwartz,S.M. Role of beta1 and beta3 integrins in human smooth muscle cell adhesion to and contraction of fibrin clots in vitro. *Circ. Res.* 83, 241-251 (1998).

157. Tuszynski,G.P., Kornecki,E., Cierniewski,C., Knight,L.C., Koshy,A., Srivastava,S., Niewiarowski,S. & Walsh,P.N. Association of fibrin with the platelet cytoskeleton. *J. Biol. Chem.* 259, 5247-5254 (1984).

158. Sierra,D.H., Eberhardt,A.W. & Lemons,J.E. Failure characteristics of multiple-component fibrin-based adhesives. *J. Biomed. Mater. Res.* 59, 1-11 (2002).

159. Ariens,R.A., Lai,T.S., Weisel,J.W., Greenberg,C.S. & Grant,P.J. Role of factor XIII in fibrin clot formation and effects of genetic polymorphisms. *Blood* 100, 743-754 (2002).

160. Kim,Y.J., Sah,R.L., Grodzinsky,A.J., Plaas,A.H. & Sandy,J.D. Mechanical regulation of cartilage biosynthetic behavior: physical stimuli. *Arch. Biochem. Biophys.* 311, 1-12 (1994).

161. Parkkinen,J.J., Lammi,M.J., Helminen,H.J. & Tammi,M. Local stimulation of proteoglycan synthesis in articular cartilage explants by dynamic compression in vitro. *J. Orthop Res.* 10, 610-620 (1992).

162. Lee,D.A. & Bader,D.L. Compressive strains at physiological frequencies influence the metabolism of chondrocytes seeded in agarose. *J. Orthop Res.* 15, 181-188 (1997).

163. Hunter,C.J., Imler,S.M., Malaviya,P., Nerem,R.M. & Levenston,M.E. Mechanical compression alters gene expression and extracellular matrix synthesis by chondrocytes cultured in collagen I gels. *Biomaterials* 23, 1249-1259 (2002).

164. Vanderploeg,E.J., Imler,S.M., Brodkin,K.R., Garcia,A.J. & Levenston,M.E. Oscillatory tension differentially modulates matrix metabolism and cytoskeletal organization in chondrocytes and fibrochondrocytes. *J. Biomech.* 37, 1941-1952 (2004).

165. Seliktar,D., Nerem,R.M. & Galis,Z.S. Mechanical strain-stimulated remodeling of tissue-engineered blood vessel constructs. *Tissue Eng* 9, 657-666 (2003).

166. Reno,C., Marchuk,L., Sciore,P., Frank,C.B. & Hart,D.A. Rapid isolation of total RNA from small samples of hypocellular, dense connective tissues. *Biotechniques* 22, 1082-1086 (1997).

167. Hellio Le Graverand,M.P., Reno,C. & Hart,D.A. Influence of pregnancy on gene expression in rabbit articular cartilage. *Osteoarthritis Cartilage* 6, 341-350 (1998).

168. Kim,Y.J., Sah,R.L., Doong,J.Y. & Grodzinsky,A.J. Fluorometric assay of DNA in cartilage explants using Hoechst 33258. *Anal. Biochem.* 174, 168-176 (1988).

169. Farndale,R.W., Sayers,C.A. & Barrett,A.J. A direct spectrophotometric microassay for sulfated glycosaminoglycans in cartilage cultures. *Connect. Tissue Res.* 9, 247-248 (1982).

170. Chowdhury,T.T., Bader,D.L., Shelton,J.C. & Lee,D.A. Temporal regulation of chondrocyte metabolism in agarose constructs subjected to dynamic compression. *Arch. Biochem. Biophys.* 417, 105-111 (2003).

171. Wong,M., Siegrist,M. & Goodwin,K. Cyclic tensile strain and cyclic hydrostatic pressure differentially regulate expression of hypertrophic markers in primary chondrocytes. *Bone* 33, 685-693 (2003).

172. Davisson,T., Kunig,S., Chen,A., Sah,R. & Ratcliffe,A. Static and dynamic compression modulate matrix metabolism in tissue engineered cartilage. *J. Orthop. Res.* 20, 842-848 (2002).

173. Waldman,S.D., Spiteri,C.G., Grynpas,M.D., Pilliar,R.M. & Kandel,R.A. Long-term intermittent compressive stimulation improves the composition and mechanical properties of tissue-engineered cartilage. *Tissue Eng* 10, 1323-1331 (2004).

174. Balestrini,J.L. & Billiar,K.L. Equibiaxial cyclic stretch stimulates fibroblasts to rapidly remodel fibrin. *J. Biomech.* (2005).

175. Ikenoue,T., Trindade,M.C., Lee,M.S., Lin,E.Y., Schurman,D.J., Goodman,S.B. & Smith,R.L. Mechanoregulation of human articular chondrocyte aggrecan and type II collagen expression by intermittent hydrostatic pressure in vitro. *J. Orthop Res.* 21, 110-116 (2003).

176. Lee,C.R., Grad,S., Gorna,K., Gogolewski,S., Goessl,A. & Alini,M. Fibrin-polyurethane composites for articular cartilage tissue engineering: a preliminary analysis. *Tissue Eng* 11, 1562-1573 (2005).

177. Ragan,P.M., Badger,A.M., Cook,M., Chin,V.I., Gowen,M., Grodzinsky,A.J. & Lark,M.W. Down-regulation of chondrocyte aggrecan and type-II collagen gene expression correlates with increases in static compression magnitude and duration. *J. Orthop Res.* 17, 836-842 (1999).

178. Waldman,S.D., Couto,D.C., Grynpas,M.D., Pilliar,R.M. & Kandel,R.A. A single application of cyclic loading can accelerate matrix deposition and enhance the properties of tissue-engineered cartilage. *Osteoarthritis Cartilage* (2005).

179. Aydelotte,M.B. & Kuettner,K.E. Differences between sub-populations of cultured bovine articular chondrocytes. I. Morphology and cartilage matrix production. *Connect. Tissue Res.* 18, 205-222 (1988).

180. Klein,T.J., Schumacher,B.L., Schmidt,T.A., Li,K.W., Voegtline,M.S., Masuda,K., Thonar,E.J. & Sah,R.L. Tissue engineering of stratified articular cartilage from chondrocyte subpopulations. *Osteoarthritis Cartilage* 11, 595-602 (2003).

181. Lee,D.A., Noguchi,T., Knight,M.M., O'Donnell,L., Bentley,G. & Bader,D.L. Response of chondrocyte subpopulations cultured within unloaded and loaded agarose. *J. Orthop Res.* 16, 726-733 (1998).

182. Kim,T.K., Sharma,B., Williams,C.G., Ruffner,M.A., Malik,A., McFarland,E.G. & Elisseeff,J.H. Experimental model for cartilage tissue engineering to regenerate the zonal organization of articular cartilage. *Osteoarthritis Cartilage* 11, 653-664 (2003).

183. Waldman,S.D., Grynpas,M.D., Pilliar,R.M. & Kandel,R.A. The use of specific chondrocyte populations to modulate the properties of tissue-engineered cartilage. *J. Orthop Res.* 21, 132-138 (2003).

184. Mow,V.C. & Ratcliffe,A. Structure and Function of Articular Cartilage and Meniscus. In: Mow,V.C. & Hayes,W.C., editors. Basic Orthopaedic Biomechanics. Philadelphia: Lippincott-Raven Publications, (1997).

185. Sokal,R.R. & Rohlf,F.J. Biometry. W.H. Freeman and Company, New York, NY (1981).

186. Archer,C.W., McDowell,J., Bayliss,M.T., Stephens,M.D. & Bentley,G. Phenotypic modulation in sub-populations of human articular chondrocytes in vitro. *J. Cell Sci.* 97 (Pt 2), 361-371 (1990).

187. Hidaka,C., Cheng,C., Alexandre,D., Bhargava,M. & Torzilli,P.A. Maturational differences in superficial and deep zone articular chondrocytes. *Cell Tissue Res.* 323, 127-135 (2006).

188. Wilson,C.G., Bonassar,L.J. & Kohles,S.S. Modeling the dynamic composition of engineered cartilage. *Arch. Biochem. Biophys.* 408, 246-254 (2002).

189. Mauck,R.L., Nicoll,S.B., Seyhan,S.L., Ateshian,G.A. & Hung,C.T. Synergistic action of growth factors and dynamic loading for articular cartilage tissue engineering. *Tissue Eng* 9, 597-611 (2003).

190. Isenberg,B.C. & Tranquillo,R.T. Long-term cyclic distention enhances the mechanical properties of collagen-based media-equivalents. *Ann. Biomed. Eng* 31, 937-949 (2003).

191. Seliktar,D., Nerem,R.M. & Galis,Z.S. The role of matrix metalloproteinase-2 in the remodeling of cell-seeded vascular constructs subjected to cyclic strain. *Ann. Biomed. Eng* 29, 923-934 (2001).

192. Grinnell,F. Fibroblast biology in three-dimensional collagen matrices. *Trends Cell Biol.* 13, 264-269 (2003).

193. Tranquillo,R.T. Self-organization of tissue-equivalents: the nature and role of contact guidance. *Biochem. Soc. Symp.* 65, 27-42 (1999).

194. Cummings,C.L., Gawlitta,D., Nerem,R.M. & Stegemann,J.P. Properties of engineered vascular constructs made from collagen, fibrin, and collagen-fibrin mixtures. *Biomaterials* 25, 3699-3706 (2004).

195. Ellsmere,J.C., Khanna,R.A. & Lee,J.M. Mechanical loading of bovine pericardium accelerates enzymatic degradation. *Biomaterials* 20, 1143-1150 (1999).

196. Margueratt,S.D. & Lee,J.M. Stress state during fixation determines susceptibility to fatigue-linked biodegradation in bioprosthetic heart valve materials. *Biomed. Sci. Instrum.* 38, 145-150 (2002).

197. Kisiday,J.D., Jin,M., DiMicco,M.A., Kurz,B. & Grodzinsky,A.J. Effects of dynamic compressive loading on chondrocyte biosynthesis in self-assembling peptide scaffolds. *J. Biomech.* 37, 595-604 (2004).

198. Imler, S. M. & Levenston, M. E., Biosynthetic differences in chondrocyte and fibrochondrocyte behavior in agarose. *Trans ORS*. Chicago, IL (2006).

199. Schumacher,B.L., Block,J.A., Schmid,T.M., Aydelotte,M.B. & Kuettner,K.E. A novel proteoglycan synthesized and secreted by chondrocytes of the superficial zone of articular cartilage. *Arch. Biochem. Biophys.* 311, 144-152 (1994).

200. Grad,S., Lee,C.R., Gorna,K., Gogolewski,S., Wimmer,M.A. & Alini,M. Surface motion upregulates superficial zone protein and hyaluronan production in chondrocyte-seeded three-dimensional scaffolds. *Tissue Eng* 11, 249-256 (2005).

201. Wilson, C. G., Palmer, A. W., Zuo, F., Eugui, E., Machenzie, R., Sandy, J. D., & Levenston, M. E., Selective and non-selective protease inhibitors reduce IL-1 induced cartilage degradation and loss of material properties. *Trans ORS*. Washington, D.C. (2005).

202. Ragan,P.M., Chin,V.I., Hung,H.H., Masuda,K., Thonar,E.J., Arner,E.C., Grodzinsky,A.J. & Sandy,J.D. Chondrocyte extracellular matrix synthesis and turnover are influenced by static compression in a new alginate disk culture system. *Arch. Biochem. Biophys.* 383, 256-264 (2000).

203. Cai,G., Chen,X., Fu,B. & Lu,Y. Activation of gelatinases by fibrin is PA/plasmin system-dependent in human glomerular endothelial cells. *Mol. Cell Biochem.* 277, 171-179 (2005).

204. Wilson, C. G., Zuo, F., Sandy, J. D., & Levenston, M. E., Inhibition of MMPs, but not of ADAMTS-4 and 5, Reduces IL-1 Stimulated Fibrocartilage Degradation. *Trans ORS*. Chicago, IL (2006).

205. Connelly, J. T., Mouw, J. K., Vanderploeg E.J., & Levenston, M. E., Cyclic tensile loading influences differentiaion of bovine bone marrow stromal cells in a TGF-beta dependent manner. *Trans ORS*. San Fransisco, CA (2005).

206. Connelly, J. T., Mouw, J. K., Vanderploeg E.J., & Levenston, M. E., Cyclic tensile loading alters gene expression and matrix synthesis of bone marrow stromal cells. *Trans ORS*. Chicago, IL (2006).

VITA

Eric James Vanderploeg was born in Keflavik, Iceland in the fall of 1976 at the U.S. Naval Air Station hospital to James and Sandra Vanderploeg. After a brief stint in Iowa City, Iowa, they settled near Houston, Texas and became part of the NASA community. Growing up only minutes from Johnson Space Center and being surrounded by the science and technology of the space program, no doubt influenced Eric's decision to pursue a career in science and engineering. Following graduation from Clear Lake High School in 1995, he attended Calvin College in Grand Rapids, Michigan earning a Bachelor's degree in engineering (BSE) with a concentration in mechanical engineering. During this time he had several summer internships with two different NASA contractors, which were tremendous learning experiences and ultimately led him to the field of bioengineering. Eric arrived at the Georgia Institute of Technology in Atlanta, Georgia in the fall of 1999 and began graduate studies in the School of Mechanical Engineering with a focus in bioengineering and orthopedics. In addition to activities directed related to the doctoral degree program, he was heavily involved in the student leadership council for the Georgia Tech-Emory Center for the Engineering of Living Tissues (GTEC), co-chairing both the Education and Outreach committee as well as the overall council. Following graduation, Eric plans to pursue a post-doctoral research position with the ultimate goal of becoming a faculty member where he can continue scientific research as well as teach and mentor undergraduate and graduate students.